Expression of Phospholipase C zeta (PLCζ) in a mammalian cell line

Sally Victoria Phillips

A thesis submitted in candidature for the degree of Philosophiae Doctor

SEPTEMBER 2009

Department of Obstetrics and Gynaecology

School of Medicine

Cardiff University

Supervisors:

Professor Karl Swann

Mr Nazar Amso

coleg meddygaeth cymru
wales college of medicine

ProQuest LLC
789 East Eisenhower Parkway
P.O. Box 1346
Ann Arbor, MI 48106-1346

DECLARATION

This work has not been accepted in substance for any degree and is not concurrently submitted in candidature for any degree.

Signed ...S V Phillips..... (candidate) Date ...7/4/10.....

STATEMENT 1

This thesis is being submitted in partial fulfilment of the requirements for the degree of PhD

Signed ...S V Phillips..... (candidate) Date ...7/4/10.....

STATEMENT 2

This thesis is the result of my own independent work/investigations, except where otherwise stated. Other sources are acknowledged by explicit references.

Signed ...S V Phillips..... (candidate) Date ...7/4/10.....

STATEMENT 3

I hereby give consent for my thesis, If accepted, to be available for photocopying and inter-library loan, and for the title and summary to be made available to outside organisations.

Signed ...S V Phillips..... (candidate) Date ...7/4/10.....

STATEMENT 4

I hereby give consent for my thesis, if accepted, to be available for photocopying and for inter-library loans **after expiry of a bar on access previously approved by the Graduate Development Committee**

Signed ..... (candidate) Date .....

Dedicated to Mr Pee & Bean

Acknowledgements

I would like to thank my supervisor Professor Karl Swann for giving me the opportunity to work in his lab and for being my source of inspiration. Thanks also to Professor Tony Lai for permitting me to work as part of his group at the Wales Heart Research Institute.

I am especially thankful to Dr Christopher George to whom I am indebted for his guidance, support and the broadening of my horizons by introducing me to a plethora of invaluable techniques.

I am grateful to Dr Andreas Rossbach and Dr Yuansong Yu for their help and practical assistance. I would like to express my gratitude to Liz for all her help in flow cytometry and for being a good friend and sounding board.Thanks to Karen and Katherine for their friendship and support during the early years; to Deb for taking me under her wing when I moved to the WHRI and to Steve for being a computer genius.

I should like to thank Kirsten for being a great friend over many years. I wouldn't have made it this far without her advice and support.

Thanks to my family for their patience , understanding and for always believing in me.

A special thank you to Mr Pee and Bean. Here's to the next chapter! Xxx

Summary

Phospholipase C zeta (PLCζ) is a sperm specific isoform of phospholipase C. It has been shown to produce a long lasting series of calcium oscillations and triggers the activation of development when introduced into mammalian eggs. It is not known how PLCζ is regulated or if its effects are specific to eggs. Here Chinese Hamster Ovary (CHO) cells were transfected with cDNA encoding PLCζ tagged with enhanced yellow fluorescent protein (eYFP) or luciferase (LUC). Comparisons were made between these cells and cells transfected with the catalytically inactive PLCζ, the corresponding reporter gene, or nontransfected cells. PLCζ exhibited variable levels of nuclear localisation in a manner that depended upon time after transfection. Analysis of resting intracellular calcium levels in transfected CHO cells produced no evidence that PLCζ expression has a significant effect upon calcium homeostasis. The calcium response to ATP receptor stimulation also remained unchanged after PLCζ expression. A lack of any clear effect on cell viability enabled the generation of a stably transfected PLCζ cell line. Individual cells were estimated to be expressing PLCζ within and above the range required to initiate calcium transients in eggs, and are therefore considered to be expressing at levels comparable with that of sperm. Despite the lack of effect on calcium in CHO cells, the injection of either cytosolic extracts, or whole cells, from the PLCζ transfected cell line were able to cause calcium oscillations in mouse eggs. Such an effect was not seen with control CHO cells. These data suggest that PLCζ is inactive when expressed in CHO cells and yet active when subsequently introduced into an egg. The results imply that the enzymatic activity of PLCζ may be reversibly inhibited in somatic cells, or else specifically stimulated by factors in the egg cytoplasm.

TABLE OF CONTENTS

LIST OF FIGURES

LIST OF ABBREVIATIONS

AM	Acetoxymethyl
AMP	Adenosine monophosphate
AP-1	Adaptor Protein 1
APH	Aminoglycoside Phosphotransferase
ATP	Adenosine triphosphate
BAPTA	1,2-Bis(2-aminophenoxy)ethane-N,N,N',N'-tetraacetic acid
Bp	Base pair
BSA	Bovine Serum Albumin
C2	PKC-homology type 2
Ca^{2+}	Calcium
Ca^{2+}_i	Intracellular calcium
$[Ca^{2+}]$	Calcium concentration
cADPR	Cyclic Adenosine Diphosphate Ribose
CamKII	Calmodulin Dependent Protein Kinase II
CBR	Calcium binding region
CCE	Capacitative Calcium Entry
CDC25	Cell division cycle 25
cDNA	Complementary Deoxyribonucleic acid
CHO	Chinese Hamster Ovary
CICR	Calcium Induced Calcium Release
CLSM	Confocal Laser Scanning Microscopy
CMV	Cytomegalovirus
CO_2	Carbon dioxide
CoV	Coefficient of Variance
Cps	Counts per second
CRAC	Calcium release activated calcium channel
cRNA	Complimentary Ribonucleic acid
DAG	Diacylglycerol
EDTA	Ethylenediaminetetraacetic acid
EGF	Epidermal Growth Factor
eGFP	Enhanced Green Fluorescent Protein
ER	Endoplasmic Reticulum
EST	Expressed Sequence Tag
EtBr	Ethidium Bromide
eYFP	Enhanced Yellow Fluorescent Protein
FACS	Fluorescence Activated Cell Sorting
FAPP	Four Phosphate Adaptor Protein
FBS	Foetal Bovine Serum
FITC	Fluorescein isothiocynate acid
FSC	Forward Scatter
FYVE	Fab1p-YOPB-Vps27p-EEA1
GDP	Guanosine diphosphate

GFP	Green Fluorescent Protein
GPCR	G-Protein Coupled Receptors
GTP	Guanosine triphosphate
GV	Germinal Vesicle
H_2O	Water
HBS	Hepes Buffered Saline
HBSS	Hepes Buffered Salt Solution
Hepes	4-(2-hydoxyethyl)-1-piperazineethanesulfonic acid
HKSOM	Hepes buffered potassium simplex optimised medium
ICCD	Intensified Charge-Coupled Device
ICSI	Intra-Cytoplasmic Sperm Injection
ING2	Inhibitor of growth protein 2
$InsP_3$	Inositol 1,4,5-trisphosphate
KCl	Potassium Chloride
Kd	Dissociation Constant
KRH	Krebs Ringer Hepes
LB	Luria Bertani
LH_2	Luciferin
LUC	Luciferase
MARCKS	Myristoylated Alanine Rich C Kinase Substrate
MCP	Microchannel Plate
$MgCl_2$	Magensium Chloride
MII	Second Metaphase
mPLCζ	Mouse Phospholipase C zeta
Na^{2+}	Sodium
NAADP	Nicotinic Acid Adenine Dinucleotide
NAD	Nicotinamide Adenine Dinucleotide
NCKX	Potassium-dependent Sodium/Calcium Exchanger
NCX	Sodium/Calcium Exchanger
NES	Nuclear Export Signal
Ni^{2+}	Nickel
NLS	Nuclear Translocation Signal
NO	Nitric oxide
NPC	Nuclear Pore Complex
O_2	Oxygen
OGBD	Oregon Green Bapta Dextran
PB	Polar Body
PBS	Phosphate Buffered Saline
Pc	Compensation pressure
PESDA	Perfluorocarbon-Exposed Sonicated Dextrose Albumin
PH	Plecktrin Homology
PHD	Plant Homeodomain
Pi	Injection pressure
PI	Phosphatidylinositol
PKA	Protein kinase A
PKC	Protein Kinase C

PLC	Phospholipase C
PLCβ	Phospholipase C beta
PLCγ	Phospholipase C gamma
PLCδ	Phospholipase C delta
PLCε	Phospholipase C epsilon
PLCζ	Phospholipase C zeta
PLCη	Phospholipase C eta
PM	Plasma membrane
PMCA	Plasma membrane calcium ATPase
PMT	Photomultiplier tube
PN	Pronucleus
PtdIns3,4,5P3	Phosphatidylinositol 3,4,5 triphosphate
PtdIns3,4P2	Phosphatidylinositol 3,4 bisphosphate
PtdIns3,5P2	Phosphatidylinositol 3,5 bisphosphate
PtdIns3P	Phosphatidylinositol 3 phosphate
PtdIns4,5P2 / PIP_2	Phosphatidylinositol 4,5 bisphosphate
PtdIns4P	Phosphatidylinositol 4 phosphate
PtdIns5P	Phosphatidylinositol 5 phosphate
PTK	Protein Tyrosine Kinase
RA	Ras Associating
REM	Ras exchanger motif
RNAi	Ribonucleic acid interference
ROC	Reactive Oxygen Species
ROCC	Receptor Operated Calcium Channel
ROI	Region Of Interest
RT-PCR	Reverse Transcriptase polymerase chain reaction
SD	Standard Deviation
SDM	Site Directed Mutagenesis
SDS	Sodium dodecyl sulfate
SEM	Standard Error Mean
SERCA	Sarco(endo)plasmic reticulum ATPase
SH	Scr homology
SOCC	Store operated calcium channel
SR	Sarcoplasmic Reticulum
SSC	Side Scatter
SV	Signal Variability
TAPP	Tumour suppressor protein
TGN	Trans Golgi Network
Ti	Injection time
TPC	Two pore channel
tr-kit	Truncated form of the c-kit receptor
TRPC	C type transient receptor potential
USW	Ultrasonic Standing Wave
UV	Ultraviolet
VOCC	Voltage operated calcium channel
WT	Wild Type

ZP	Zona Pellucida

CHAPTER 1
INTRODUCTION

CHAPTER 1 INTRODUCTION

1.1 Calcium (Ca^{2+}) Signalling

1.1.1 A fundamental ionic messenger

Calcium is an ubiquitous intracellular messenger that regulates a wide range of cellular processes, including muscle contraction, neurotransmission, gene transcription, cellular proliferation, apoptosis and fertilization (Berridge *et al.*, 2003; Bootman *et al.*, 2001a; Clapham, 1995; Jayaraman *et al.*, 1997). Resting cytosolic free Ca^{2+} levels are typically ~100nM (Berridge, 1997; Bootman *et al.*, 2001a). This level can increase to more than 1-10μM in response to various stimuli such as depolarisation, mechanical deformation, hormonal activation or exposure to a Ca^{2+} ionophore (Bootman *et al.*, 2001a). Elevation of the intracellular calcium, either via influx from the extracellular environment or release from intracellular stores acts as a trigger to switch "on" various cellular processes. The subsequent removal of cytosolic Ca^{2+} then acts to switch them "off". This simplistic theory is in fact dependent on a complex interplay between several channels, pumps and exchangers as illustrated in Figure 1.1 (Berridge *et al.*, 2000).

1.1.2 Calcium Influx

Ca^{2+} influx occurs via Ca^{2+} entry channels located at the plasma membrane (PM). The various Ca^{2+} entry channels are grouped according to their mechanism of activation (Bootman *et al.*, 2001a). Receptor-operated Ca^{2+} channels (ROCCs) are found primarily on the PM of nerve terminals and secretory cells.

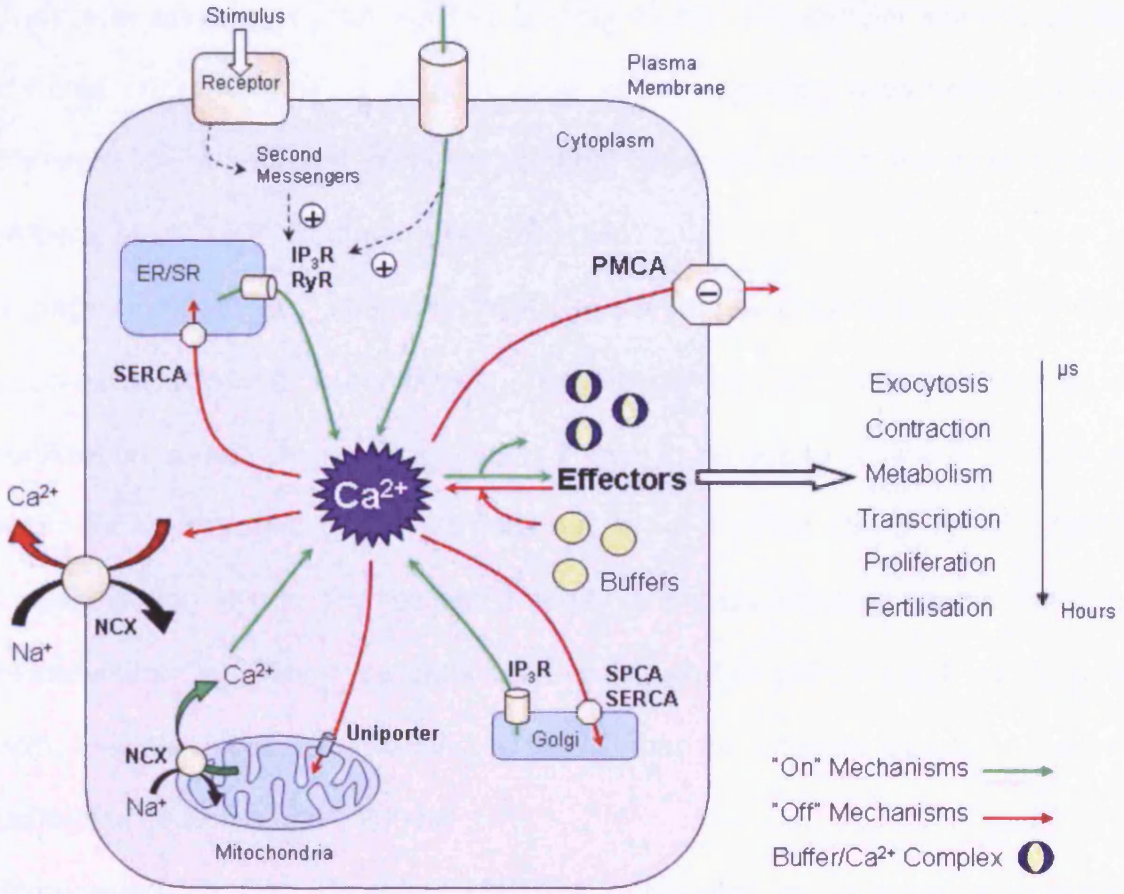

Figure 1.1 The Ca^{2+} signalling network

Figure based upon Berridge *et al.*, (2003).
Calcium can enter the cell via activation of receptor; voltage or store operated Ca^{2+} channels (ROCCs, VOCCs, SOCCs) located on the plasma membrane (PM). (For simplicity only one Ca^{2+} channel type is indicated at the PM). External stimuli also give rise to the formation of second messengers that release stored Ca^{2+} from within the endoplasmic/sarcoplasmic reticulum (ER/SR) via the inositol-1,4,5-trisphosphate ($InsP_3R$) or the ryanodine receptor (RyR). The majority of Ca^{2+} within the cytoplasm remains bound to buffers (shown as yellow circles), while a small amount binds to effectors that activate various cellular processes that operate over a broad temporal spectrum (shown to the right of the figure). The intracellular effectors and buffers release Ca^{2+} prior to its removal from the cell via a range of exchangers and pumps. Ca^{2+} is extruded from the cell via the Na^+/Ca^{2+} exchanger (NCX) and the plasma membrane Ca^{2+} ATPase (PMCA), or it can be sequestered back into the ER/SR via the sarco(endo)plasmic reticulum Ca^{2+} ATPase (SERCA). Mitochondria play a role in the sequestration of Ca^{2+} via a uniporter, this Ca^{2+} is then released slowly into the cytoplasm through a mitochondrial NCX. The golgi apparatus has been shown to contribute to elevations in cytosolic Ca^{2+} levels through $InsP_3R$ activation present on the golgi membrane. The Golgi also has the ability to sequester Ca^{2+} via the secretory pathway Ca^{2+} ATPase (SPCA) and a Ca^{2+} ATPase belonging to the SERCA family. Cell survival is dependant on Ca^{2+} homeostasis, whereby Ca^{2+} fluxes during the "off" reactions (red arrows) exactly match those during the "on" reactions (green arrows).

They are activated by an agonist binding to the extracellular domain of the channel. Acetylcholine is a commonly known agonist, responsible for the transmission of neuronal impulses at nerve terminals through the synaptic cleft (Alberts *et al.*, 1997; Bootman *et al.*, 2001a).

Voltage operated Ca^{2+} channels (VOCCs) are largely present in excitable cells such as muscle and neuronal cells. Interestingly the Ca^{2+} increase observed at fertilisation in many types of oocytes is known to be due to activation of VOCCs, such as in the sea urchin (Chambers *et al.*, 1979; David *et al.*, 1988). Depolarisation of the PM activates these channels resulting in the influx of extracellular Ca^{2+}. They are composed of five protein subunits (α1, α2, β, γ, δ) with multiple isoforms, resulting in a number of different possible channel isoforms (Bootman *et al.*, 2001a).

Store operated Ca^{2+} channels (SOCCs) are gated by a poorly understood mechanism triggered by the depletion of intracellular Ca^{2+} stores (Bootman *et al.*, 2001a). The most studied and best characterised SOCCs are the Ca^{2+} release-activated Ca^{2+} (CRAC) channels, which were first identified in human T cells and mast cells (Hoth *et al.*, 1992; Lewis *et al.*, 1989). The search for the genes that code for the CRAC channel lead to the discovery of two proteins, Orai1 and STIM1, which are now considered to play obligatory roles in the activation of SOCCs. Orai1 is a four transmembrane protein present in the PM with intracellular N- and C- termini. Stim1 is a type1 transmembrane protein located primarily on the ER. Upon store depletion Stim1 have been shown to translocate into puncta that accumulate in ER regions closely associated with the PM (Liou

et al., 2005). The redistribution of Stim1 is believed to be the initiator of SOC entry as puncta formation has been shown to preceed CRAC channel activation by 6-10s (Wu *et al.*, 2006). Furthermore, live cell imaging has revealed that Stim1 forms oligomers within 5s after store depletion prior to its translocation (Liou *et al.*, 2007). Studies have shown that Stim1 interacts functionally with Orai1 to activate SOC entry (Potier *et al.*, 2008), however the precise mechanism by which Stim 1 conveys information regarding store depletion to Orai1 channels remains to be determined. Accumulating evidence indicates that STIM1 acts as a sensor of Ca^{2+} store content, while Orai1 is believed to be a pore-forming CRAC channel subunit (Gwack *et al.*, 2007; Mignen *et al.*, 2007). The C-type transient receptor potential class of ion channels (TRPCs) have also been suggested as candidates for forming SOCCs (Birnbaumer *et al.*, 1996; Hardie *et al.*, 1993; Selinger *et al.*, 1993), however their activity is believed to be distinct from CRAC channels (Smyth *et al.*, 2006).

1.1.3 Intracellular stores and Ca^{2+} releasing agents

1.1.3.1 Phosphoinositides and inositol 1,4,5-trisphosphate ($InsP_3$)

Phosphatidylinositol (PI) is a ubiquitous eukaryotic lipid whose phosphorylated derivatives (collectively known as phosphoinositides) have been implicated in a number of important cell signalling events including cell survival, cell division and membrane trafficking (Cullen *et al.*, 2001). The structure of PI consists of a myo-inositol headgroup connected to a diacylglycerol via a phosphodiester linkage (Figure 1.2). The 3, 4 and 5 hydroxyl groups of the inositol head group can be

phosphorylated by a variety of kinases (Figure 1.3). To date, seven phosphoinositides have been identified; three phosphatidylinositol monophosphates [phosphatidylinositol 3-phosphate (PtdIns3P), phosphatidylinositol 4-phosphate (PtdIns4P) and phosphatidylinositol 5-phosphate (PtdIns5P)], three phosphatidylinositol bisphosphates [(phosphatidylinositol 3,4-bisphosphate (PtdIns3,4P_2), phosphatidylinositol 3,5-bisphosphate (PtdIns3,5P_2) and phosphatidylinositol 4,5-bisphosphate (PtdIns4,5P_2)], and phosphatidylinositol 3,4,5 trisphosphate (PtdIns3,4,5P_3).

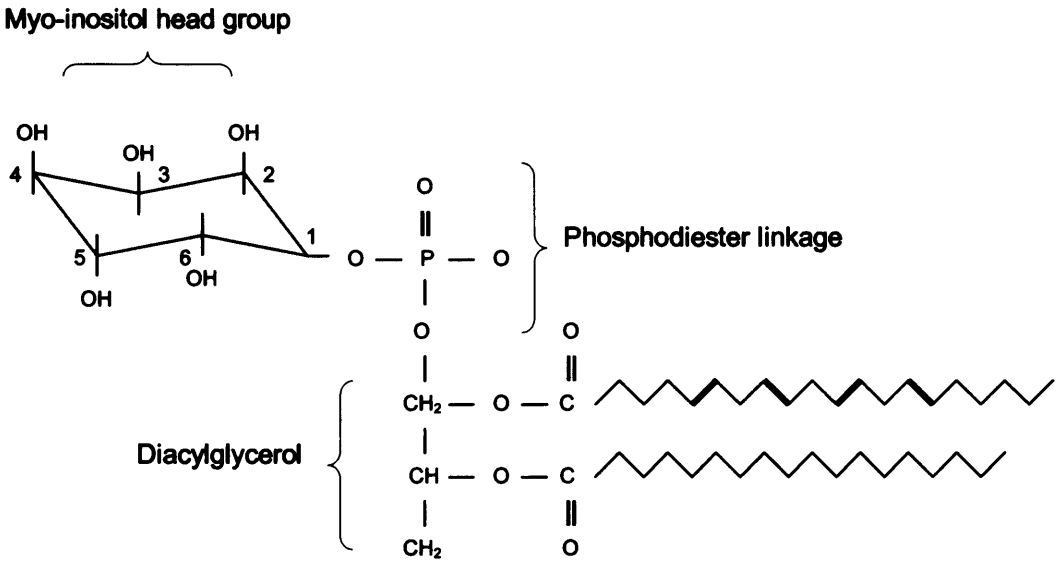

Figure 1.2 Phosphatidylinositol (PI)
The structure of Phosphoinositol (PI) contains a myo-inositol head group connected to a diacylglycerol via a phosphodiester linkage. In mammalian cells the fatty acid moiety is typically stearoyl-arachidonyl. The inositol head group can be phosphorylated at one of three currently identified positions, 3OH, 4OH and 5OH for a total of one, two or three times by a variety of kinases.

The reversible production of phosphoinositides is catalyzed through the combined actions of a number of specific phosphatases and phosphoinositide kinases which have not been fully identified. In the canonical phosphoinositide pathway PtdIns acts as a substrate for PI 4-Kinases, generating PtIns(4)P which in turn acts as a substrate for PI 5-Kinases to produce $PtIns(4,5)P_2$. PI 5-Kinases are found at the PM, at focal adhesions, in the nucleus and the golgi. PI 4-Kinases are found in the cytosol, nucleus and associated with the ER, but are not strongly associated with the PM (Doughman *et al.*, 2003). $PtIns(4,5)P_2$ is hydrolysed by activated phospholipase C (PLC) proteins resulting in the synthesis of two second messengers, diacylglycerol (DAG), which activates protein kinase C (PKC), and inositol-1,4,5-trisphosphate ($InsP_3$). $InsP_3$ binds to $InsP_3$ receptors ($InsP_3R$) stimulating Ca^{2+} release from the endoplasmic reticulum. The localisation of $PtIns(4,5)P_2$ in mammalian eggs is unknown. Experiments involving the glutathione S-transferase tagged PH domain of PLCδ1 have revealed the distribution of $PtIns(4,5)P_2$ in somatic cells (Watt *et al.*, 2002). $PtIns(4,5)P_2$ was labelled in the plasma membrane and also in intracellular membranes including Golgi, endosomes and ER, as well as electron dense structures within the nucleus. Mammalian sperm PLC activity has been shown to induce Ca^{2+} dependent $InsP_3$ formation in a cytoplasmic sea urchin egg preparation (Rice *et al.*, 2000). This data suggests that the Ca^{2+} wave in both mammals and sea urchin eggs could be generated via Ca^{2+} induced $InsP_3$ made in the cytoplasm.

Recent work has uncovered a role for PtdIns(3)P and PtdIns(3,5)P_2 in the regulation of vesicular trafficking through the recruitment of Fab1p-YOPB-Vps27p-EEA1 (FYVE) domain-containing proteins (Wurmser *et al.*, 1999). The sole function of PtdIns(4)P was previously considered to be acting as a substrate for the generation of PtdIns(3,4)P_2 and PtdIns(4,5)P_2. However, recent studies have demonstrated a role in the recruitment of proteins that are involved in vesicular trafficking from the trans-Golgi network (TGN) to the plasma membrane, including adaptor-protein (AP)-1 (Wang *et al.*, 2003) and the four phosphate adaptor protein (FAPP) 1 and 2 (Godi *et al.*, 2004). PtdIns(5)P was recently discovered to bind to the plant homeodomain (PHD) finger of inhibitor of growth protein-2 (ING2), a candidate tumor suppressor protein (Gozani *et al.*, 2003). Tandem PH domain containing protein-1 (TAPP-1) and TAPP-2 have been found to selectively bind PtdIns(3,4)P_2. The biological significance of this interaction remains elusive, however it suggests a more specific role other than simply a by-product of PtdIns(3,4,5)P_3 breakdown (Sasaki *et al.*, 2007). PtdIns(3,4,5)P_3 is an important second messenger in numerous signalling pathways involved in the control of cell growth, survival, metabolism, motility and immune responses. Proteins that bind PtdIns(3,4,5)P_3 are diverse in nature and include adaptor molecules, protein kinases and exchange factors for the small G proteins Arf (Cantley, 2002; Stephens *et al.*, 2005; Vanhaesebroeck *et al.*, 2005).

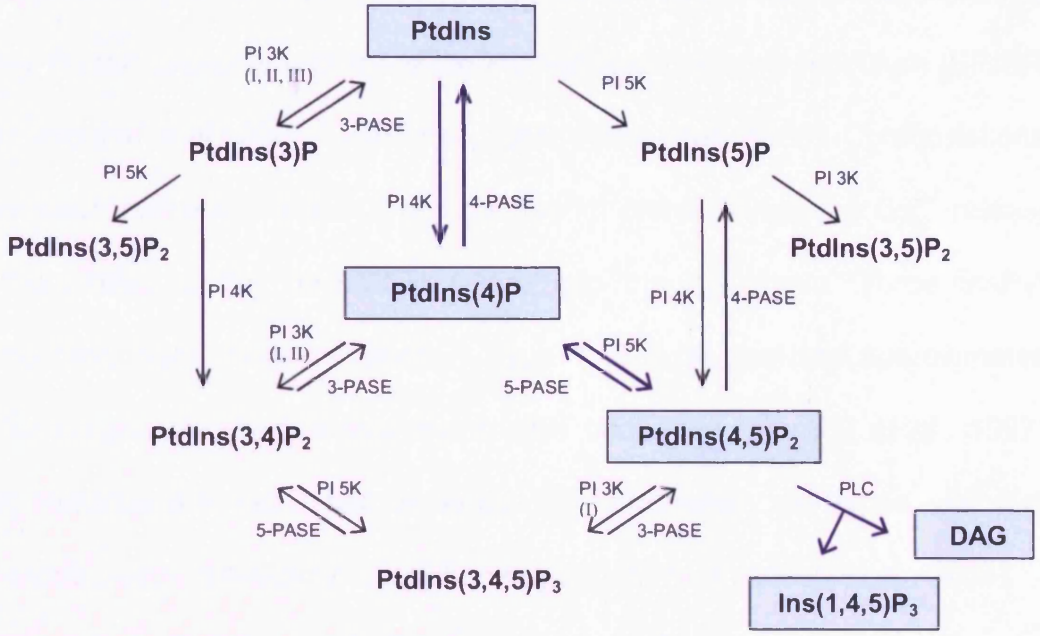

Figure 1.3 Phosphoinositide metabolism

The figure shows the main pathways of phosphoinositide synthesis in mammalian cells. The combined action of phosphoinositide kinases (PIxKs) and phosphatases (X-Pases) generates multiple phosphoinositides phosphorylated at the 3, 4 and 5 positions either alone or in combination. Some of the reactions have been established in vitro but not yet in vivo. For the sake of clarity, only the enzymatic activity (3-,4-, or 5- kinase/phosphatase) is indicated and in some cases the identification of the enzyme is mentioned (Types I, II and III PI 3-kinases). The figure also shows the turnover of PtdIns(4,5)P_2 by phospholipase C (PLC) to yield soluble inositol-1,4,5P_3 and membrane-embedded diacylglycerol (DAG). The canonical phosphoinositide pathway is highlighted in blue. (Adapted from (Payrastre *et al.*, 2001)

1.1.3.2. The inositol 1,4,5-trisphosphate receptor ($InsP_3R$)

The activation of Phospholipase C (PLC) by a variety of stimuli including ligand interaction with G protein linked receptors is a common mechanism for modulating the intracellular Ca^{2+} concentration $[Ca^{2+}]_i$. Activation of PLC leads to the hydrolysis of the membrane lipid phosphatidylinositol 4,5 bisphosphate (PIP_2), generating inositol 1,4,5 trisphosphate ($InsP_3$) and diacylglycerol (DAG) (Berridge, 1993; Putney *et al.*, 1993). $InsP_3$ diffuses freely throughout the cytoplasm and binds to its receptor ($InsP_3Rs$), which is a ligand-gated Ca^{2+}

release channel (Ferris *et al.*, 1989; Maeda *et al.*, 1991). $InsP_3Rs$ are situated primarily on the membrane of the endoplasmic/ sarcoplasmic reticulum (ER/SR) (Ferreri-Jacobia *et al.*, 2005; Otsu *et al.*, 1990; Ross *et al.*, 1989). Conformational change upon activation of this receptor/channel complex induces Ca^{2+} release from the lumen of the intracellular store into the cytoplasm. Three $InsP_3R$ isoforms have been identified ($InsP_3R$ Type 1, 2 & 3), that are approximately 70% homologous in their overall amino acid sequence (Mackrill *et al.*, 1997). $InsP_3R$ isoforms are expressed in almost all mammalian cell types and their relative distribution is tissue type/function dependant (Vermassen *et al.*, 2004).

The Type 1 isoform is the most widely studied $InsP_3R$ subtype, and is expressed predominantly in cerebellar Purkinje neurons (Furuichi *et al.*, 1993). Genetic knockout of the Type 1 isoform in the mouse has been shown to cause neurological defects (Matsumoto *et al.*, 1996). The Type 1 isoform is also expressed in relatively high amounts in smooth muscles (Nixon *et al.*, 1994) and is the predominant isoform found in oocytes (Kume *et al.*, 1993). The role of Type 1 $InsP_3Rs$ in fertilization was demonstrated in hamster eggs using the $InsP_3R$-specific function blocking antibody 18A10, which blocked the Ca^{2+} oscillations induced by $InsP_3$ at fertilization (Miyazaki *et al.*, 1992). The Type 2 isoform is expressed primarily in cardiac myocytes (Perez *et al.*, 1997), and genetic deletion of the mouse $InsP_3R2$ has been shown to abolish the arrhythmogenic effect of endothelin in this cell type (Li *et al.*, 2005). The Type 3 isoform is expressed in the brain, kidney, gastrointestinal epithelium, and pancreatic islets (Blondel *et al.*, 1993; Taylor *et al.*, 1999).

Each $InsP_3R$ comprises four subunits of approximately 300KDa (Bootman *et al.*, 2001a). Each $InsP_3R$ subunit has a ligand binding domain located towards the end of a large cytoplasmic NH_2-terminus, six transmembrane (TM) spanning domains which contribute to the formation of the channel pore, and a relatively short COOH-terminus as illustrated in Figure 1.4 (Foskett *et al.*, 2007). $InsP_3Rs$ also contain another functionally distinct region termed the modulatory domain which is located between the pore domain and the $InsP_3$ binding domain. The modulatory domain contains binding sites for Ca^{2+} and ATP. In addition to $InsP_3$, Ca^{2+} also regulates $InsP_3R$ activation (Berridge, 1997; Bootman *et al.*, 1999). $InsP_3R$ function is stimulated by cytosolic Ca^{2+} concentrations of 0.5-1μM, unlike concentrations >1μM which inhibit their opening (Bootman *et al.*, 1999). Binding of Ca^{2+} to $InsP_3R$ Type 1 has been shown to induce structural changes in the receptor, indicating that Ca^{2+} regulates $InsP_3R$ gating activity through the rearrangement of functional domains (Hamada *et al.*, 2002). In the presence of $InsP_3$, ATP increases activity of $InsP_3Rs$ by binding to high affinity binding sites located within the modulatory domain (Maes *et al.*, 2000).

Phosphorylation and dephosphorylation modulates $InsP_3R$ function (DeSouza *et al.*, 2002; Jayaraman *et al.*, 1996), and numerous consensus phosphorylation sites have been identified (Patel *et al.*, 1999). $InsP_3Rs$ are regulated by phosphorylation by numerous kinases, including protein kinase A (PKA), protein kinase G (PKG), protein kinase C (PKC), protein tyrosine kinases (PTKs) and CaMKII (Foskett *et al.*, 2007; Patel *et al.*, 1999; Thrower *et al.*, 2001). A large number of protein interactions with the $InsP_3R$ have been described (for review

see (Patterson *et al.*, 2004), many of which involve allosteric modulation of channel gating which may contribute to the diversity of spatially and temporally distinct $InsP_3R$ signalling properties.

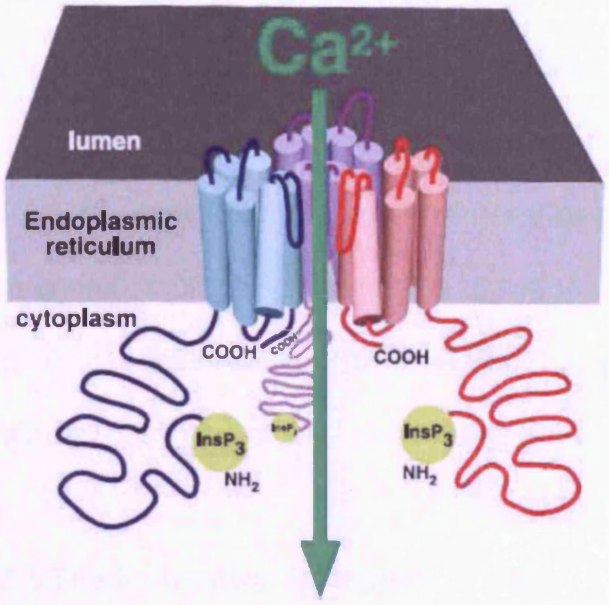

Figure 1.4 The Inositol 1,4,5-trisphosphate receptor (IP_3R)

(From (Foskett *et al.*, 2007)
Schematic representation of three of the four subunits (in different colours) of a single tetrameric IP_3R ligand gated Ca^{2+} channel. $InsP_3$ binds to the NH_2-terminus which elicts a conformational change that activates the channel. Part of the loop connecting the 5th and 6th transmembranes helices contributes to the formation of the channel pore which enables Ca^{2+} efflux from the lumen of the ER

1.1.3.2.1 $InsP_3R$ Downregulation

One of the mechanisms by which cells adapt during long term exposure to an agonist is by down-regulation of cell surface receptors, characterised by a reduction in the cellular content of these proteins. It has been found that chronic stimulation of receptors linked to $InsP_3$ formation leads to a decrease in the number of $InsP_3Rs$ and a decrease in sensitivity of the intracellular Ca^{2+} stores to $InsP_3$ (Wojcikiewicz *et al.*, 1991; Wojcikiewicz *et al.*, 1992). The large conformational changes that occur as a result of $InsP_3$ binding to its receptor appears to be the essential trigger for receptor degradation (Zhu *et al.*, 1999). The precise proteolytic mechanism responsible for $InsP_3R$ degradation has yet to

be identified, but has been proposed to involve the ubiquitin/ proteasome pathway (Oberdorf *et al.*, 1999). Activation of Phosphoinositide C linked receptors has been shown to cause $InsP_3R$ ubiquitination in a range of cell types (Oberdorf *et al.*, 1999). The cystein protease and proteasomal inhibitor ALLN and the highly specific proteasome inhibitor Lactacystin prevented $InsP_3R$ downregulation induced by activation of these receptors (Bokkala *et al.*, 1997). This suggests that InsP3Rs can be degraded by the proteasome, a cytosolic 26S multi protein complex that recognises and degrades poly-ubiquitinated proteins. Downregulation of $InsP_3R$ has been shown to inhibit Ca^{2+} release in mouse eggs (Brind *et al.*, 2000; Jellerette *et al.*, 2000), and has been proposed to partly explain the cessation of Ca^{2+} oscillations 3-4 hours after fertilisation.

1.1.3.3 The Ryanodine Receptor

Another ligand gated Ca^{2+} release channel that is structurally and functionally similar to the $InsP_3R$ is the Ryanodine receptor (RyR). RyRs are the largest known ion channel with a total molecular mass of ~2.2MDa and around twice the conductance of $InsP_3Rs$ (Franzini-Armstrong *et al.*, 1997). They are present on the ER/SR membranes of muscle and non-muscle cells (Fleischer *et al.*, 1989; Lai *et al.*, 1988). Each subunit of its tetrameric protein structure is comprised of ~5000 amino acids, ~90% of which constitutes a large cytoplasmic NH_2-terminus that is essential for the regulation of the channel pore (Franzini-Armstrong *et al.*, 1997; Mackrill, 1999). The three RyR isoforms that have been identified (RyR1, RyR2 and RyR3) have different physiological functions which are reflected by

their tissue specific expression. RyR1 is expressed primarily in skeletal muscle whilst RyR2 fulfils the same function in cardiac muscle and in brain cells (Berridge, 1997). RyR3 is expressed in the central nervous system and in smooth muscle (Berridge, 1997; Liu *et al.*, 2001). The RyR channels are activated by low Ca^{2+} concentrations (1-10μM), reaching a broad maximum near 100μM and inhibited by high Ca^{2+} concentrations (1-10mM) (Chen *et al.*, 1997; Chu *et al.*, 1993; Copello *et al.*, 1997; Laver *et al.*, 1995). Calcium induced calcium release (CICR) from RyR channels is stimulated by cyclic adenosine diphosphate ribose (cADPR). cADPR is produced from nicotinamide adenine dinucleotide (NAD) by ADP-ribosyl cyclase. It is unclear if cADPR acts a direct ligand for RyR channels, or whether it stimulates CICR by binding to an accessory protein. The Ca^{2+} wave observed at fertilisation is generally considered to be generated by $InsP_3Rs$. RyRs do not contribute to the fertilisation response in mouse eggs (Swann *et al.*, 2001), however they appear to make a substantial contribution to the mechanisms underlying the fertilisation Ca^{2+} wave in fish and echinoderm eggs (Fluck *et al.*, 1999; Galione *et al.*, 1993). Ruthenium Red, a RyR antagonist, has been shown to reduce the propagation velocity of the Ca^{2+} wave in sea urchin eggs (Galione *et al.*, 1993).

1.1.3.4 Nicotinic acid adenine dinucleotide phosphate (NAADP)

Nicotinic acid adenine dinucleotide phosphate (NAADP) has been identified an extremely potent Ca^{2+}-mobilizing messenger (Genazzani *et al.*, 1997; Lee *et al.*, 1995). Similar to cADPR, NAADP is also believed to be synthesized by members of the ADP-ribosyl cyclase family (Aarhus *et al.*, 1995; Lee *et al.*, 1991).

However, a recent study involving sea urchin sperm suggests the presence of a new NAADP synthase (Vasudevan *et al.*, 2008) which has raised questions regarding an already limited understanding of NAADP biosynthesis. Its Ca^{2+} releasing properties have been examined in a broad range of cell types from a variety of organisms including sea urchin and starfish oocytes (Chini *et al.*, 1995; Churchill *et al.*, 2002; Lee *et al.*, 1995; Lim *et al.*, 2001; Santella *et al.*, 2000), heart cells (Bak *et al.*, 2001) and pancreatic cells (Cancela *et al.*, 1999; Yamasaki *et al.*, 2004). Pharmacological experiments involving selective inhibitors of $InsP_3Rs$ and RyRs suggests that NAADP activates a distinct Ca^{2+} mobilising mechanism, involving a receptor/channel complex that has yet to be identified (Galione *et al.*, 2005). Recent evidence suggests that two-pore channels (TPCs) located within the endolysosomal system are involved in NAADP-induced Ca^{2+} mobilisation (Calcraft *et al.*, 2009; Galione *et al.*, 2009).

1.1.3.5 The Mitochondria as an intracellular Ca^{2+} store

Mitochondria may also be viewed as a Ca^{2+} store. If necessary, mitochondria can significantly buffer cytosolic Ca^{2+} increases (Bootman *et al.*, 2001b). Ca^{2+} is sequestered by a low affinity uniporter that operates at high speed that is driven by the mitochondria's membrane potential. Despite the low affinity of the uniporter, the mitochondria are able to modulate intracellular calcium due to their close proximity to other Ca^{2+} release sites which exposes them to increased local Ca^{2+} concentration $[Ca^{2+}]$ (Csordas *et al.*, 1999). Increasing the $[Ca^{2+}]$ within the mitochondria activates enzymes involved in the citric acid cycle, leading to

enhanced production of ATP (Bootman *et al.*, 2001b). Calcium is released slowly from the mitochondria via the Na^+ dependant exchanger, to then be dealt with by various pumps and exchangers which act to re set basal Ca^{2+} levels and ensure the replenishment of intracellular stores.

1.1.3.6 The Golgi apparatus as an intracellular Ca^{2+} store

The Golgi apparatus is involved in sorting and processing secretory and membrane proteins prior to them reaching their final destination within the cell. Golgi function is regulated by changes in Ca^{2+} levels either within the Golgi lumen or the adjacent cytoplasm (Burgoyne *et al.*, 2003; Wuytack *et al.*, 2003). The Golgi is recognized as a Ca^{2+} store containing both release and sequestration apparatus (Pinton *et al.*, 1998). The production of $InsP_3$ activates $InsP_3R$ located on the Golgi membrane resulting in Ca^{2+} release. The Golgi has been shown to act in unison with the ER to elevate cytoplasmic Ca^{2+} in response to agonist stimulation (Missiaen *et al.*, 2004b). Ca^{2+} release from the Golgi has been shown to contribute to the shaping of intracellular Ca^{2+} signals (Missiaen *et al.*, 2004b). Two types of Ca^{2+} ATPases are present on the Golgi membrane, one belonging to the secretory pathway calcium ATPase family (SPCA) and the other belonging to the sarco(endo)plasmic reticulum Ca^{2+}-ATPase (SERCA) family (Van Baelen *et al.*, 2004; Wuytack *et al.*, 2003). Altering the expression/ activity of the Golgi calcium ATPases, thus affecting their ability to sequester Ca^{2+}, has a profound effect on cellular function. Hailey-Hailey disease, an

autosomal dominant blistering skin disorder, is caused by mutations in the gene encoding Golgi localised SPCA1, demonstrating its important role in maintaining Ca^{2+} homeostasis (Missiaen *et al.*, 2004a; Sudbrak *et al.*, 2000).

1.1.4 Removal of cytoplasmic Ca^{2+}

The plasma membrane Ca^{2+}-ATPase (PMCA) utilises the energy generated by ATP hydrolysis to pump Ca^{2+} from the cytosol to the extracellular environment (Berridge *et al.*, 2003). Following a rise in cytoplasmic Ca^{2+}, the Na^{+}/ Ca^{2+} exchanger (NCX) rapidly extrudes Ca^{2+} from the cell in exchange for Na^{+} ions (Berridge *et al.*, 2000). Another mechanism by which Ca^{2+} is removed from the cytosol is via the sarco(endo)plasmic reticulum Ca^{2+}-ATPase (SERCA) which pumps Ca^{2+} into the lumenal spaces of the internal stores upon which they are located. It is critical for cell survival that the fluxes that switch "on" the Ca^{2+} reactions are counteracted by those that switch them "off" (Carafoli, 2002).

1.1.5 Ca^{2+} - Friend or Foe?

Ca^{2+} signals enable cells to function properly. However, it is vital that this cellular messenger is carefully regulated. Cells can tolerate a brief rise in cytosolic Ca^{2+}, however a sustained increase would result in persistent activation of Ca^{2+} controlled processes which would ultimately lead to necrotic cell death (Berridge *et al.*, 2000). Mitochondria act only as a temporary safety mechanism during periods of Ca^{2+} overload. Despite having a large capacity for Ca^{2+} uptake, the continuous pumping of Ca^{2+} into the mitochondrial matrix depletes the organelles energy reserve, thus depriving cells of the ATP necessary to remove Ca^{2+} out of

the cytoplasm through the pumps (Carafoli, 2002). Defects involving one or more component of the complex pathway involved in the generation, processing and control of Ca^{2+} signals have been implicated in a variety of disease states. Examples include cardiac and skeletal myopathies (Benkusky *et al.*, 2004; George *et al.*, 2005; Pogwizd *et al.*, 2001), liver, kidney and pancreatic dysfunction (Matsuda *et al.*, 2001; Shibao *et al.*, 2003; Vassilev *et al.*, 2001) and neuropathology (Mattson *et al.*, 1998; Tang *et al.*, 2003; Verkhratsky, 2005).

1.1.6 Spatio Temporal aspects of Ca^{2+} Signals

Cells protect themselves against the potentially harmful effects of Ca^{2+} by creating low amplitude Ca^{2+} signals or, more typically, by presenting the signals in a pulsatile manner. The up stroke of each transient is generated by the "ON" reactions that introduce Ca^{2+} into the cytoplasm, and the subsequent decline depends on the "OFF" reactions that pump Ca^{2+} out of the cell or back into the internal stores. Single transients that activate cellular processes such as muscle contraction and neurotransmitter release are generated in response to periodic stimulation (Berridge *et al.*, 2003). In contrast, many tissues receive continuous stimulation over a prolonged period, during which the Ca^{2+} signal is presented as brief transients that are produced rhythmically, giving rise to highly regular Ca^{2+} oscillations whose frequencies vary with the degree of stimulation. Cytosolic Ca^{2+} oscillations are a major feature of Ca^{2+} signalling in a wide range of cellular processes including oocyte activation at fertilisation (Ozil *et al.*, 1995), liver

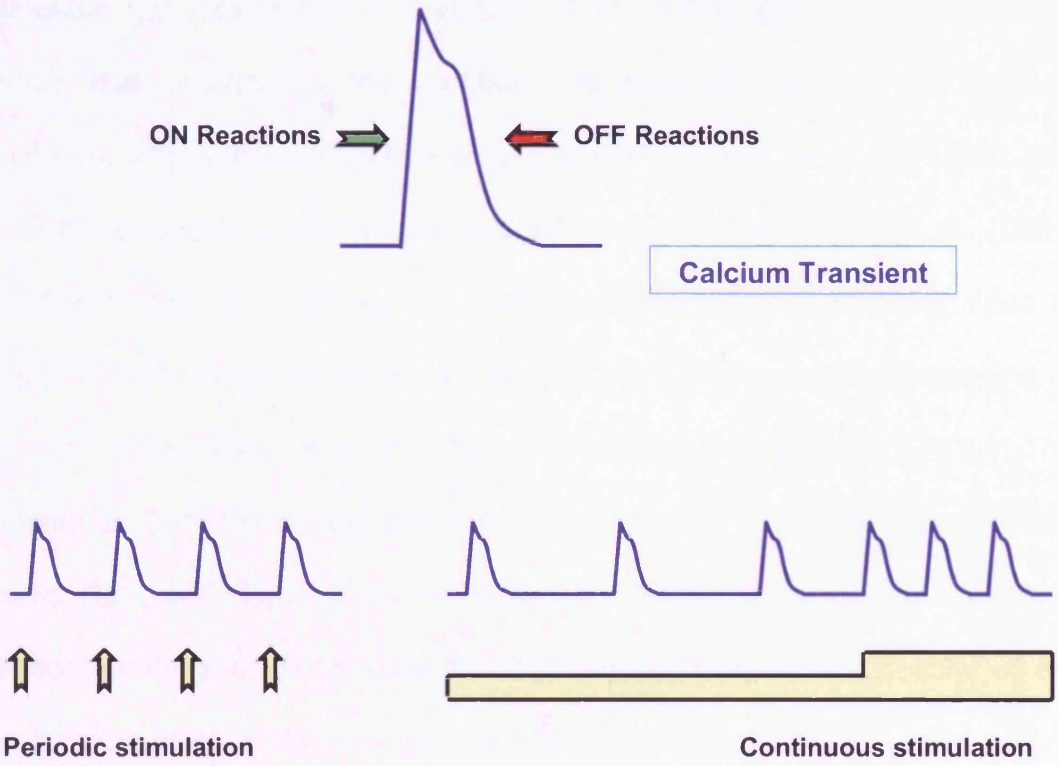

Figure 1.5 Temporal aspects of Ca^{2+} signalling

(Adapted from (Krebs *et al.*, 2007) The majority of Ca^{2+} signals appear as brief transients that can be utilized to set up complex temporal patters of Ca^{2+} signalling. The up stoke of each transient is generated by the "ON" reactions (green arrow) that introduce Ca^{2+} into the cytoplasm. The "OFF" reactions (red arrow) which are responsible for the removal of Ca^{2+} from the cytoplasm, prevent a sustained increase in Ca^{2+} levels and consequently protects the cell. In some cells these transients are produced in response to periodic stimulation (yellow arrows). Many other tissues receive continuous stimulation over a prolonged period (yellow bar), giving rise to highly regular Ca^{2+} oscillations whose frequency depends on the level of stimulation.

metabolism (Robb-Gaspers *et al.*, 1998), smooth muscle contraction (Filosa *et al.*, 2004), and lymphocyte activation (Feske, 2007).

Cells utilise highly sophisticated mechanisms which enable them to interpret changes in frequency of the Ca^{2+} oscillations. Such frequency modulation enable cells to regulate specific responses such as exocytosis (Tse *et al.*, 1993), mitochondrial ATP production (Hajnoczky *et al.*, 1995) and the control

ofdifferential gene transcription (Berridge *et al.*, 2003). Cells have developed decoders that respond to the duration and frequency of the Ca^{2+} signal, examples of which include protein kinase C (PKC) (Oancea *et al.*, 1998) and calmodulin dependent protein kinase II (CaM Kinase II) (De Koninck *et al.*, 1998). In addition to this temporal aspect, Ca^{2+} signals are also highly organized in space. Ca^{2+} microdomains are formed within cells as a result of brief opening of either Ca^{2+} entry channels in the PM or release channels in the ER/SR. The movement of Ca^{2+} throughout the cell is restricted by its limited diffusion and cytosolic Ca^{2+} buffering. These microdomains enable cells to perform highly localised signalling functions such as neurotransmitter release (Grosche *et al.*, 1999; Sharma *et al.*, 2003; Simkus *et al.*, 2002). These confined plumes of Ca^{2+} have been categorized according to the channels that produce them. Brief opening of VOCCs in the PM produces a sparklet (Wang *et al.*, 2001), and small groups of RyRs on the SR generate sparks (and syntillas) (Cheng *et al.*, 1993; De Crescenzo *et al.*, 2004), whereas the $InsP_3Rs$ produce puffs. Ca^{2+} sparks and puffs comprise the basic building blocks of global Ca^{2+} signalling. $InsP_3Rs$ and RyRs must be sufficiently sensitive enabling them to respond to the local Ca^{2+} puff or spark produced by their neighbours. These channels contribute to the positive feedback process of Ca^{2+}-induced Ca^{2+} release (CICR), whereby the Ca^{2+} signal is propagated throughout the cytoplasm as a regenerative wave (Berridge *et al.*, 2000). Ca^{2+} oscillations are generated by successive rounds of Ca^{2+} release and diffusion from small groups of $InsP_3Rs$ or RyRs located on the ER/SR. It has been proposed that Ca^{2+} oscillations are terminated by inactivation

of $InsP_3Rs$, allowing Ca^{2+} to be pumped back into the ER, thereby lowering the cytosolic calcium concentration before the $InsP_3Rs$ are resensitised to deliver the next pulse of Ca^{2+} (Berridge, 2007; Oancea *et al.*, 1996). A popular mechanism of Ca^{2+} oscillations involves positive and negative feedback loops of Ca^{2+} acting directly on the $InsP_3R$ (De Young *et al.*, 1992). At low Ca^{2+} concentrations the $InsP_3R$ is stimulated by Ca^{2+}, but at higher Ca^{2+} concentrations the $InsP_3R$ is closed by Ca^{2+} (Bezprozvanny *et al.*, 1991).

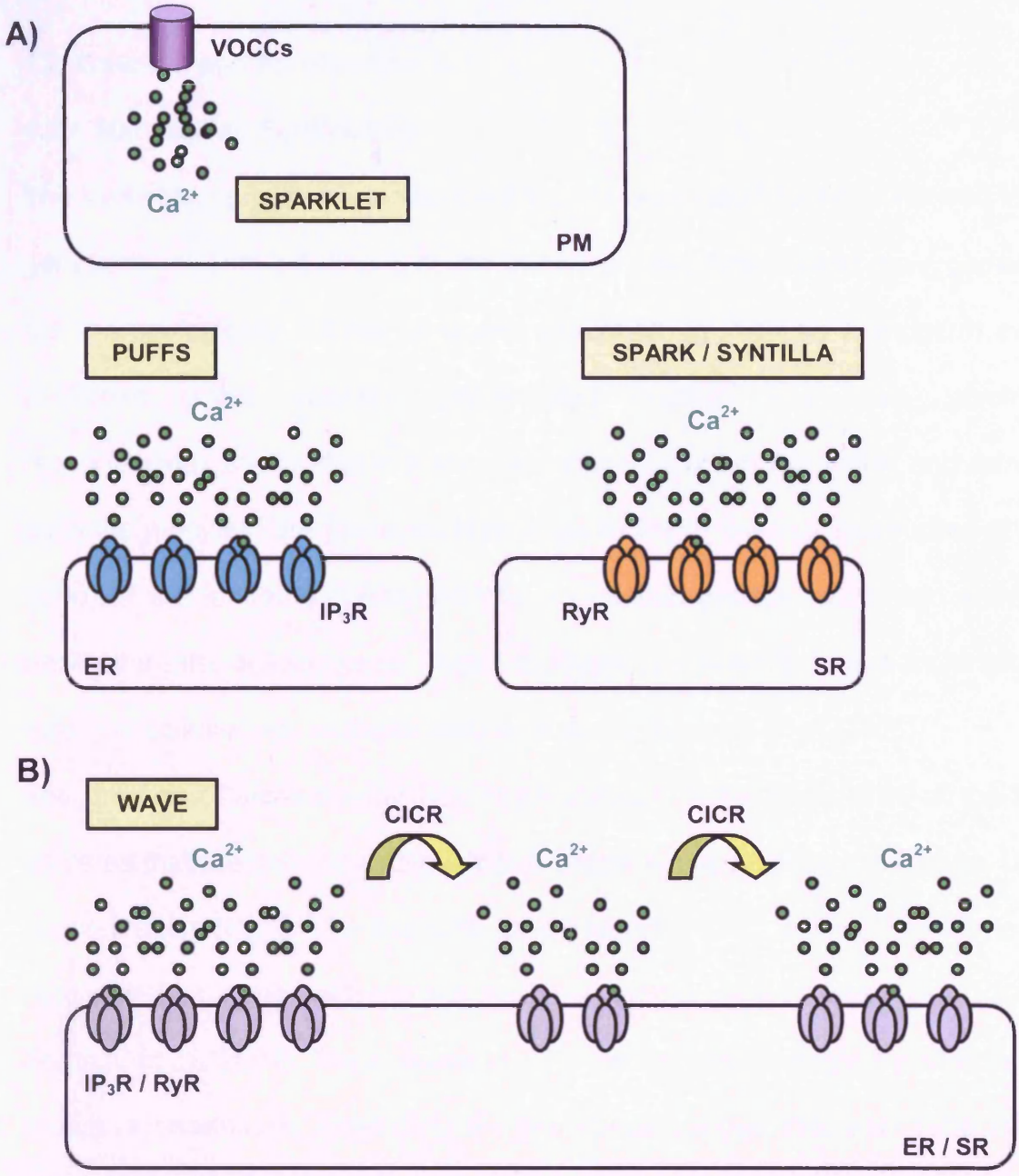

Figure 1.6 Spatial aspects of Ca^{2+} signalling.

Localised Ca^{2+} signals that arise from either individual or small groups of ion channels are depicted in panel A. Voltage operated Ca^{2+} channels (VOCCs) in the plasma membrane (PM) give rise to sparklets, and ryanodine receptors (RyRs) on the sarcoplasmic reticulum (SR) produce sparks (and syntillas), whereas the inositol 1,4,5-trisphosphate receptor ($InsP_3R$) produce puffs. Panel B illustrates the regenerative Ca^{2+} waves created by the process of Ca^{2+}-induced Ca^{2+} release (CICR), whereby $InsP_3Rs$ and RyRs with increase sensitivity become activated by the diffusion of Ca^{2+} from a neighbouring puff/spark and respond by releasing further Ca^{2+}. The receptors are sensitive enough to pass the signal over long distances (represented by the gaps) along the ER/SR membrane.

1.2. Calcium and Fertilisation

1.2.1 Mammalian Fertilisation

The fertilisation process relies on the fusion of two haploid gametes derived from genetically distinct individuals of the same species. Female and male gametes are morphologically distinct, and are generated by meiosis from germ cells contained within sexually differentiated organs. The male gametes (spermatozoa) are produced from spermatogonia within the testis, and female gametes (oocytes) are produced from oogonia within the ovaries (Kupker *et al.*, 1998). If the fertilizing sperm and the oocyte successfully locate and activate each other, the diploid zygote begins to divide by mitosis to form a multicellular organism (blastocyst), and ultimately an embryo (Florman *et al.*, 2006).

The process of activation involves large changes in the metabolism of the two gametes that are initiated by signals that trigger changes in the intracellular Ca^{2+} concentration $[Ca^{2+}]_i$. An increase in intracellular Ca^{2+} within the oocyte is recognised as a general feature of the fertilization process (Carafoli *et al.*, 2001; Santella *et al.*, 2004). The increase in Ca^{2+} can occur as a single transient or as repetitive oscillations, depending on the animal species (Stricker, 1999). The importance of Ca^{2+} in the regulation of oocyte physiology at fertilisation has been well documented, and it is generally accepted that in mammals, activation of $InsP_3Rs$ is responsible for the rise in Ca^{2+} (Runft *et al.*, 2002; Williams, 2002). More recently, information has began to emerge highlighting the importance of Ca^{2+} in the activation of sperm prior to fertilisation (Darszon *et al.*, 2005).

1.2.2 Oogenesis

Oogenesis, or female gametogenesis, is the mechanism by which the female gamete forms, grows and matures (Figure 1.7). This process begins during the early stages of female embryonic development, whereby primordial germ cells (oogonia) migrate to the embryonic ovaries and undergo several mitotic divisions. Approximately 7 million germ cells are formed during the second to seventh month of gestation. The majority of oogonia die following this period of rapid cellular division, while the remaining oogonia enter the first meiotic division (Pinkerton *et al.*, 1961). These latter cells, called the primary oocytes, are arrested during late prophase of the first meiotic division, at which point they are maintained until puberty (Edwards, 1965). Each primary oocyte is enveloped by a primordial follicle consisting of a single layer of epithelial granulosa (follicle) cells. With the onset of adolescence, groups of primary oocytes periodically resume meiosis when exposed to the correct hormonal stimulation. The primary follicle enters a stage of growth forming gravian follicles, during which the primary oocyte undergoes an increase in diameter from <20μm to 80μm or 120μm in mice and humans respectively (Grundzinskas *et al.*, 1995). Growing oocytes develop a large nucleus termed the germinal vesicle (GV), and a thick oligosaccharide based extracellular coat, the zona pellucida (ZP), which surrounds the plasma membrane. During the growth of the follicle, there is an increase in the number of granulosa cells which form concentric layers around the oocyte. In addition to this an antrum (cavity) forms, which is filled with secretions derived from follicular cells and the oocyte become surrounded by

several layers of granulosa cells known as the cumulus oophorus. These cells remain associated with the oocyte during ovulation, secreting hormones that are important for sperm capacitation and the acrosome reaction (discussed later) (Tesarik *et al.*, 1988) and act as a screen to remove abnormal sperm (Nottola *et al.*, 1998). Graafian follicles migrate towards the periphery of the ovary in preparation for final maturation and release of the oocyte (Grundzinskas *et al.*, 1995). Shortly after the initial follicle growth, the pituitary gland begins secreting luteinizing hormone (LH). In response to LH, the cell enters the first meiotic division whereby the germinal vesicle is broken down, and the spindle apparatus forms resulting in the segregation of the homologous chromosomes. One set of chromosomes is retained by the oocyte, while the other is extruded in a small daughter cell refered to as the first polar body (Donahue, 1968; Wassarman *et al.*, 1976). During the second meiotic cycle the oocyte is arrested in its second metaphase (MII) and at this point it is released from the ovary. Only oocytes arrested in the MII stage can be activated by sperm, and meiotic division is resumed in response to intracellular signals within the oocyte following activation. Fertilisation results in the extrusion of a second polar body, leading to degeneration of the 1st polar body, and pronuclear formation.

Figure 1.7: Oogenesis and fertilisation
Schematic representation of female gametogenesis and fertilisation of an MII oocyte (See text for details)

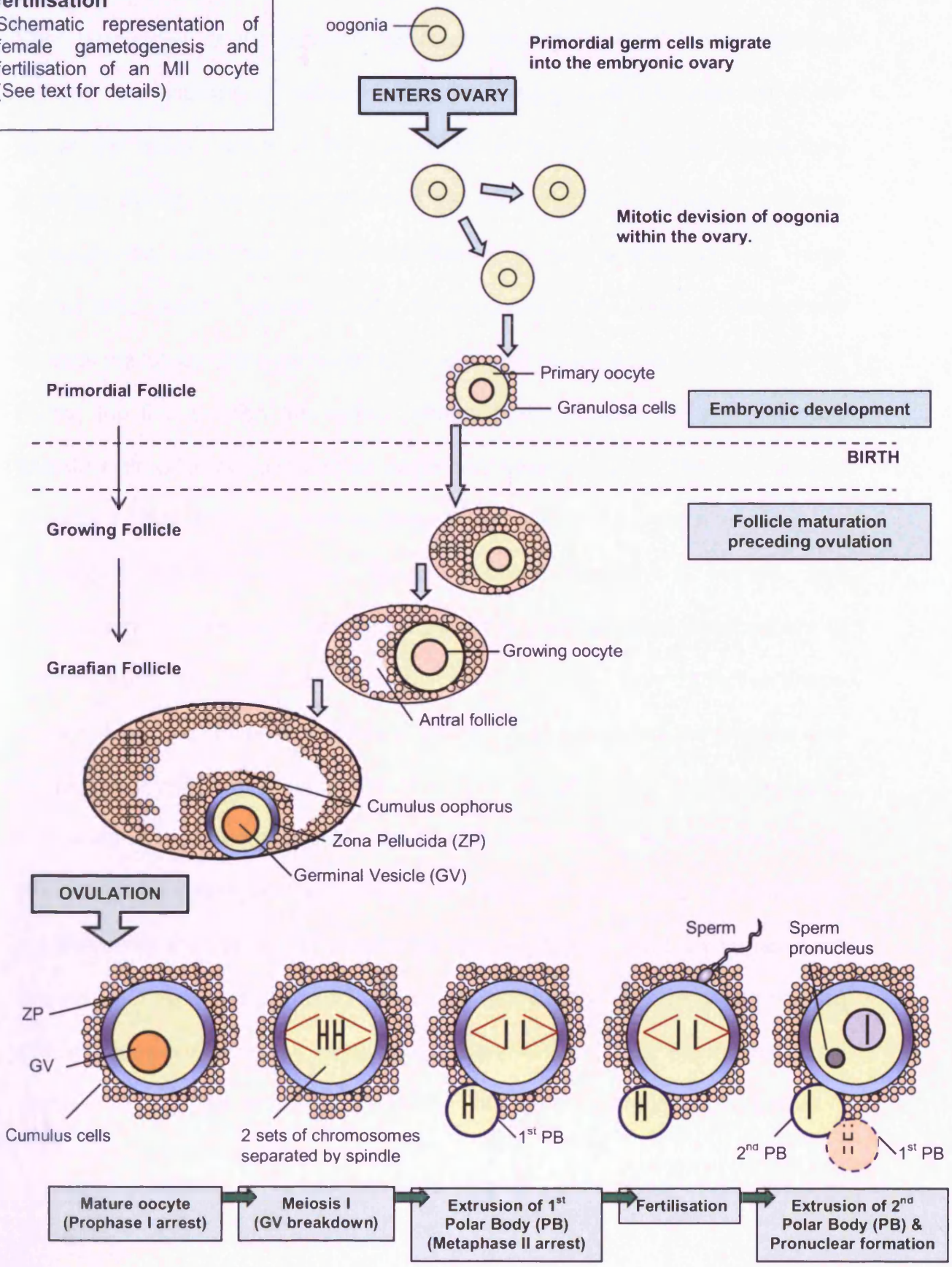

1.2.3 Spermatogenesis

Spermatogenesis is the process by which male germ cells (spermatogonia) develop into mature spermatozoa within the testis (Figure 1.8). Spermatogonia lie on the basal lamina of the convoluted seminiferous tubules where they undergo mitosis. This acts to maintain the spermatogonia population and also produces the cells that begin differentiation (primary spermatocytes). These diploid cells (46XY) migrate through the junctions at the base of Sertoli cells towards the lumen of the seminiferous tubules and undergo two meiotic divisions. During the first division the diploid primary spermatocytes separate into two haploid cells (23X or 23Y) termed secondary spermatocytes. The cells quickly proceed through this stage and undergo a second meiotic division whereby the chromatids separate forming spermatids that contain 23 single half chromosomes. Spermatids undergo a period of morphological development in vesicles within the sertoli cells during which they aquire their distinctive shape (Figure 1.8). This shape comprises a sperm head containing the nucleus and acrosome, a midpiece abundant in mitochondria and a long tail, or flagellum, containing a central complex of microtubules which form the axoneme that is responsible for sperm motility (Kupker *et al.*, 1998). These general characteristics are shared by the majority of mammalian species, though there are variations in the size and shape of the head, and in the lengths and relative amount of the different components of the flagellum (Roosen-Runge, 1977). Spermatozoa are extruded from the sertoli cells into the lumen of the seminiferous tubules before

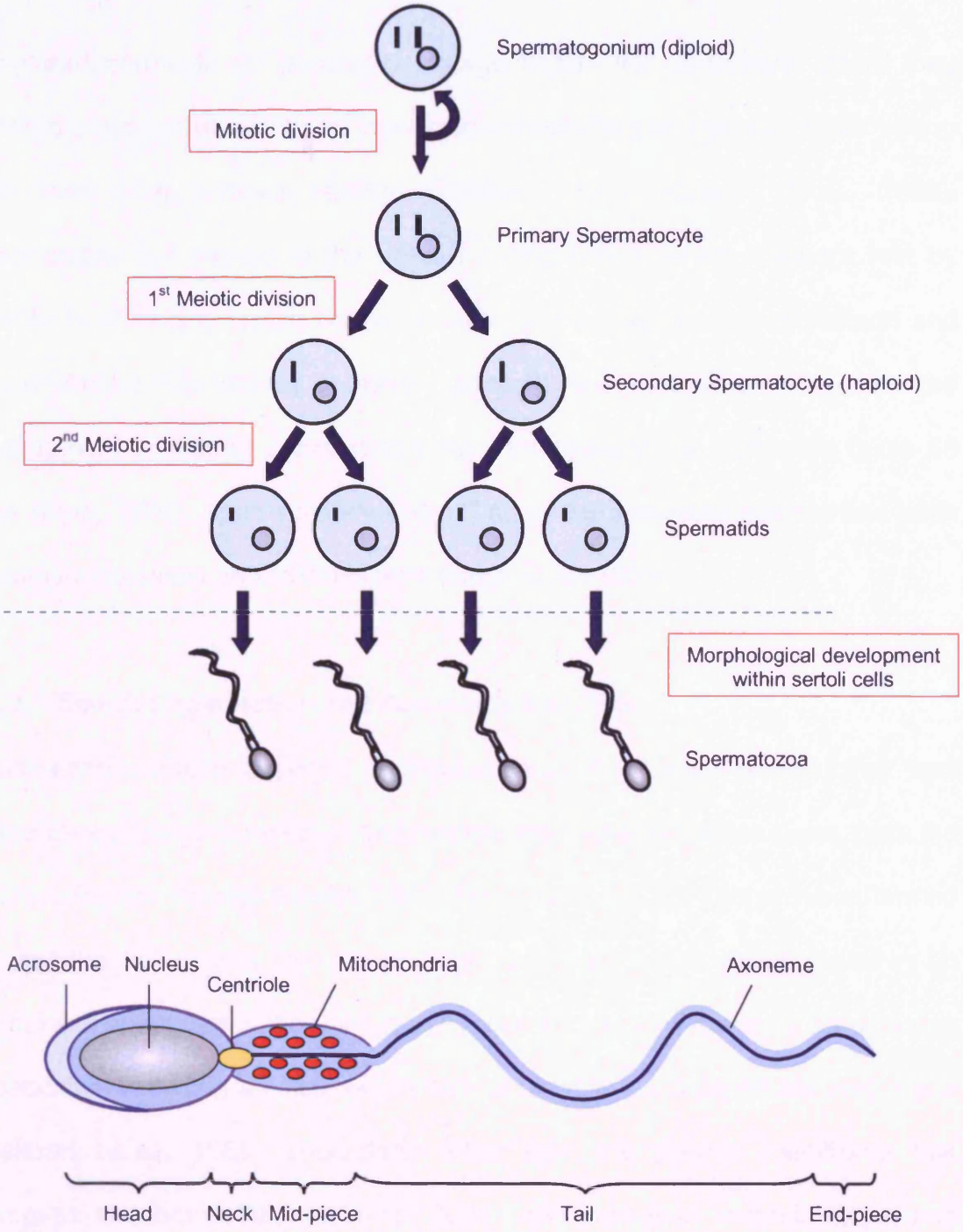

Figure 1.8 Spermatogenesis
Schematic representation of male gametogenesis (See text for details). The lower panel illustrates the characteristic shape of a single sperm cell. The head contains a large dense nucleus and a single large vesicle termed the acrosome. The midpiece contains numerous mitochondria which provide energy for sperm motility. The tail contains a complex of microtubules which form the axoneme, responsible for sperm motility. The tail is not shown to scale, and is typically 10-15 times larger than the remainder of the cell.

being transported to an accessory storage organ, the epididymis, where they undergo a period of functional development resulting in mature, motile sperm cells that have fertilising ability (Clermont, 1972; Kupker *et al.*, 1998). Spermatozoa are moved to the urethra during coitus, where they are met by secretions (including water, buffering salts, acid phosphatases, cholesterol and phospholipids) from various accessory glands prior to ejaculation. In humans the development of mature spermatozoa from spermatogonial stem cells takes 65 days (Dym, 1994). Approximately 100 million sperm are made per day and each ejaculation releases 200 million sperm (Reijo *et al.*, 1995).

1.2.3.1 Sperm Capacitation and Acrosome Reaction

Spermatozoa require a period of incubation in the female reproductive tract where they undergo a series of biochemical modifications, which gives them the ability to fertilize the egg (Austin, 1951; Austin *et al.*, 1952). This process, termed sperm capacitation, is a complex physiological event that is accompanied by an increase in sperm respiration and motility. Numerous cellular events occur during capacitation including an increase in intracellular Ca^{2+} and cAMP concentrations (Breitbart *et al.*, 1985), cholesterol efflux from the plasma membrane that increases membrane fluidity (Cross, 2004), and increased intracellular pH and tyrosine phosphorylation (Dorval *et al.*, 2002; Galantino-Homer *et al.*, 2004; Visconti *et al.*, 1999). Tyrosine phosphorylation of several sperm proteins play an important role in sperm capacitation (Visconti *et al.*, 1998), and it has been demonstrated for example that the inhibition of protein kinase A (PKA) can inhibit

the capacitation of spermatozoa (Visconti *et al.*, 1995). Reactive oxygen species (ROS) have been suggested to play an important role in capacitation-related phosphorylation of several proteins in human sperm (Aitken, 1989). Roles for Ca^{2+} and HCO_3^- have been suggested in the upregulation of adenyl cyclase in sperm (Visconti *et al.*, 1998). There is no direct evidence for a specific ligand which induces capacitation, however a role for epidermal growth factor (EGF) has been suggested, since its receptor tyrosine kinase EGFR has been identified in the head of bovine sperm (Lax *et al.*, 1994). Activation of EGFR results in tyrosine phosphorylation and activation of PLCγ; both of which are essential to the process of capacitation (Spungin *et al.*, 1995).

In order to reach the surface of the oocyte, the spermatozoa must penetrate both the cumulus matrix and the zona pellucida (ZP). The cumulus acts as a selective barrier, controlling the entry of sperm whose functional ability has been compromised, and only allows fully capacitated, acrosome intact sperm to reach the zona and the oocyte (Westphal *et al.*, 1993). Numerous observation suggest that PH20, a glycosyl-phosphatidylinositol-linked protein (expressed on the plasma membrane in response to capacitation), may be involved in the cumulus-dispersing activity of the sperm (Lin *et al.*, 1994). PH20 has hyaluronidase activity, which allows sperm with intact acrosomes to traverse the cumulus matrix (Myles *et al.*, 1997). Once contact has been made with the ZP, capacitated sperm undergo the acrosome reaction. This Ca^{2+} dependent mechanism enables the outer acrosomal membrane and the overlying plasma membrane to come into close proximity, to fuse, to secrete the acrosomal content, and to trigger the

opening of SOCCs in the plasma membrane. The release of the acrosomal contents, notably the enzymes hyaluronidase and acrosin, combined with vigorous sperm motility is required for the passage of the sperm through the zona (Talbot, 1985). This process enables the sperm to contact and fuse with the plasma membrane of the oocyte (Evans, 2002; Wassarman *et al.*, 2001).

1.2.3.2 Calcium signalling in sperm

Recent data has shown that Ca^{2+} signalling plays a major role in the important sperm functions that occur after ejaculation. Intracellular Ca^{2+} regulates sperm chemotaxis (Eisenbach, 1999), motility and hyperactivation (Carlson *et al.*, 2003; Suarez *et al.*, 2003), acrosome reaction (Kirkman-Brown *et al.*, 2002) and also plays a role in the process of capacitation. During fertilisation, the ability of the sperm to locate the egg is modulated by Ca^{2+} changes induced in the sperm by soluble components released by the outer layers of the egg. During chemotaxis, the swimming trajectory of sperm is dictated by Ca^{2+} spikes in the flagellum. Voltage gated Ca^{2+} channels as well as a cAMP-regulated Ca^{2+} transporter may be involved in the Ca^{2+} increase that gives rise to the asymmetry of flagellar movement (Cook *et al.*, 1994; Nishigaki *et al.*, 2004). The Ca^{2+} rise in the flagellum is followed by a Ca^{2+} rise in the sperm head, and the duration of the Ca^{2+} signal is regulated by two Ca^{2+} clearance mechanisms, a K^{+}-dependent Na^{+}/Ca^{2+} exchanger (NCKX) and a plasma membrane Ca^{2+}-ATPase (PMCA) pump. Mammalian sperm display hyperactivated motility prior to fertilisation. Hyperactivation is characterised by an increase in flagellar bend amplitude and

beat asymmetry, and is required for successful fertilisation as it increases the ability of the sperm to make contact with the egg and penetrate its extracellular coat. Recent data suggests that sperm hyperactivation may be regulated by the emptying of an $InsP_3$-dependent intracellular store (Ho *et al.*, 2001). The PMCA pump (isoform 4) is located almost exclusively in the tail of the sperm and is essential for extruding Ca^{2+} during hyperactivated motility. Recently, Catsper, a novel family of sperm cation channels, has been described. Catspers are distributed in the principal piece of the sperm tail, and mediate Ca^{2+} influx required for hyperactivated movement (Kirichok *et al.*, 2006). Immunolocalisation experiments have shown that the sperm acrosome appears to function as an $InsP_3R$ containing Ca^{2+} store activated by agonists linked to PLC. Mobilisation of acrosomal Ca^{2+} appears to play a direct role in activation of the acrosome reaction (De Blas *et al.*, 2002; Herrick *et al.*, 2005).

1.2.4. Calcium change at Fertilisation

One of the earliest and most important changes in the oocyte at fertilisation is a transient increase in Ca^{2+}, resulting from its release from intracellular stores, which stimulates the entire program of development. The suggestion that a Ca^{2+} increase plays a role in fertilisation dates back to the early 1920s when it was demonstrated that egg activation could be induced by promoting Ca^{2+} entry from the extracellular medium by pricking the egg with a needle (Jaffe, 1985; Loeb, 1921). One of the morphological changes that occur at egg activation includes the cortical reaction, where the content of the cortical granule is extruded into the

extracellular space (Jaffe *et al.*, 2001; Schuel, 1985). Experiments involving the use of the Ca^{2+} ionophore A23187 demonstrated that the triggering of the cortical reaction and activation of development is dependent upon the increase in intracellular Ca^{2+} (Steinhardt, 2006; Steinhardt *et al.*, 1974a). The observation that sperm interaction induces an increase in Ca^{2+} at the sperm entry site that then propagates to the opposite side of the egg was originally documented in medaka fish by experiments using injected aequorin (Ridgway *et al.*, 1977). It is now recognised that an increase in Ca^{2+} is a general feature of the fertilisation process, and is a crucial event in activation of plants, animals and non-mammalian species (Digonnet *et al.*, 1997; Jaffe, 1983; Zucker *et al.*, 1978). Depending on the animal species, the increase may occur as a single Ca^{2+} transient or as a series of repetitive oscillations (Stricker, 1999). In mammalian eggs a long lasting series of Ca^{2+} oscillations of constant amplitude continue at regular intervals (approximately every 7-20 minutes) for several hours after sperm-oocyte fusion, and persist until pronuclear (PN) formation (Carroll, 2001; Kline *et al.*, 1992; Marangos *et al.*, 2003; Miyazaki *et al.*, 1993) (Figure 1.9). The first transient is distinctively longer in duration and larger in amplitude (Swann *et al.*, 1994). The Ca^{2+} oscillations induced by sperm at fertilisation are both necessary and sufficient for the completion of the numerous events of egg activation, including membrane hyperpolarisation, changes in the pattern of protein synthesis, pronuclear formation and meiotic resumption (Kline *et al.*, 1992; Ozil *et al.*, 2005; Schultz *et al.*, 1995).

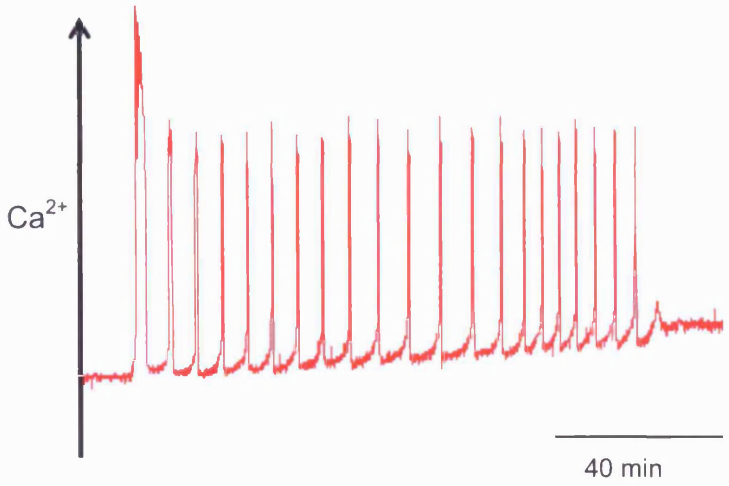

Figure 1.9 Ca^{2+} oscillations during mammalian egg activation

This figure shows a fluorescent trace of the long lasting series of Ca^{2+} oscillations that are initiated in a mouse egg by sperm. These oscillations persist until pronuclear (PN) formation. (Image courtesy of K.Swann)

1.3 The Sperm Factor

1.3.1 What signalling pathway is involved in the generation of Ca^{2+} oscillations during mammalian fertilisation?

A large body of evidence implicates the $InsP_3$ signalling pathway as the source of Ca^{2+} release from the ER during mammalian fertilisation. Early observations in sea urchin eggs showed a substantial increase the levels of polyphosphoinositide at fertilisation (Turner *et al.*, 1984), and $InsP_3$ generation was later found to coincide with the Ca^{2+} transient (Ciapa *et al.*, 1992). The critical role of $InsP_3$ and the $InsP_3Rs$ in the development of Ca^{2+} oscillations at fertilisation has been more recently illustrated in studies using mouse and hamster eggs, where Ca^{2+} oscillations are abolished by the microinjection of antibodies that inhibit $InsP_3Rs$ (Miyazaki *et al.*, 1992). Downregulation of $InsP_3Rs$ has also been found to inhibit Ca^{2+} transients in mouse eggs (Brind *et al.*, 2000; Jellerette *et al.*, 2000), a mechanism that has been proposed to partly explain the cessation of Ca^{2+} oscillations 3-4 hours after fertilisation.

Three main hypotheses have been proposed to explain the generation of Ca^{2+} oscillations in fertilised oocytes (Figure 1.10). All of which are consistent with the delay of several minutes observed between oocyte contact and the initiation of Ca^{2+} oscillations (Whitaker *et al.*, 1989). The conduit hypothesis, is an early hypothesis that involves a mechanism by which the sperm head, once fused with the oocyte, acts as a non-selective channel, allowing influx of extracellular Ca^{2+} via pores in the sperm membrane into the oocyte cytosol (Jaffe, 1991). The Ca^{2+} release from the ER was proposed to be a result of Ca^{2+} induced Ca^{2+} release (CICR). Injection of Ca^{2+} into fish and frog eggs has been shown to produce a Ca^{2+} wave (Nuccitelli, 1991), however this hypothesis fails to explain many features of Ca^{2+} changes in fertilised oocytes. It appears to be an unlikely mechanism for mammalian egg activation given the more recent observation that sperm is able to trigger repetitive Ca^{2+} transients in the absence of extracellular Ca^{2+} (Jones *et al.*, 1998; Swann, 1996).

The contact/receptor hypothesis suggests that upon sperm-oocyte contact, receptor-ligand interaction on the PM of the oocyte leads to the generation of intracellular messengers that trigger a series of signalling events that initiate Ca^{2+} release from the ER (Foltz *et al.*, 1993; Schultz *et al.*, 1995). There are surface proteins that play a role in sperm-egg interactions, however there is no evidence to suggest that they are linked to intracellular signalling (Runft *et al.*, 2002). According to this hypothesis, the generation of the Ca^{2+} increase might occur through several different routes, all ultimately leading to the activation of Phospholipase C (PLC) (Ciapa *et al.*, 2000). Ambiguous results with a number of

G-protein activators and inhibitors have significantly reduced the interest in conventional G-protein/PLC/$InsP_3$ involvement (Runft *et al.*, 2002). In echinoderms, it has become apparent that Ca^{2+} release may be triggered by a tyrosine kinase receptor that acts via a PLCγ-mediated pathway (Townley *et al.*, 2006).

The Content hypothesis has been proposed to explain the generation of Ca^{2+} oscillations at fertilisation (Swann, 1990; Swann *et al.*, 1994). It describes a mechanism by which a soluble sperm factor is released into the egg, capable of activating the $InsP_3$ signalling pathway and the subsequent Ca^{2+} release from the ER. Injection of hamster sperm extracts into mammalian eggs produced a series of Ca^{2+} oscillations much like those seen during in vitro fertilisation (Stricker, 1997; Swann, 1990; Swann *et al.*, 1994). Further support for this hypothesis comes from the clinical technique, intra-cytoplasmic sperm injection (ICSI) (Palermo *et al.*, 1992), which involves direct injection of intact sperm thus avoiding sperm-oocyte membrane contact. This technique has been shown to lead to normal activation and development of oocytes (Nakano *et al.*, 1997; Tesarik *et al.*, 1994). The sperm factor hypothesis appears to be consistent between species. Pig sperm extracts have been shown to generate Ca^{2+} oscillations in cow, mouse and hamster eggs (Swann, 1990; Wu *et al.*, 1997). Furthermore, fish sperm extracts were also able to induce oscillations in mouse eggs (Coward *et al.*, 2003).

Figure 1.10 Main hypotheses for intracellular Ca^{2+} increase at fertilisation

Schematic diagram showing the three main hypotheses to explain how sperm initiates the elevation in Ca^{2+} release from the ER of the oocyte during mammalian fertilisation.

A) Conduit Theory

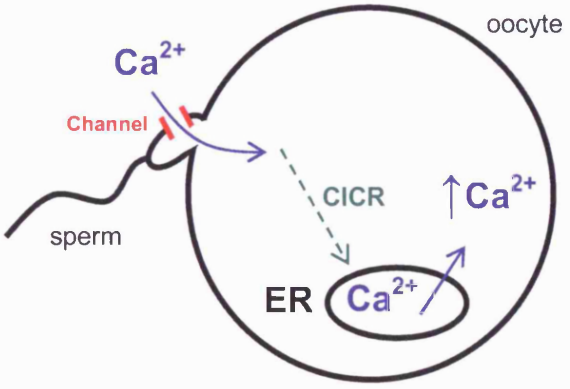

B) Contact/ Receptor Theory

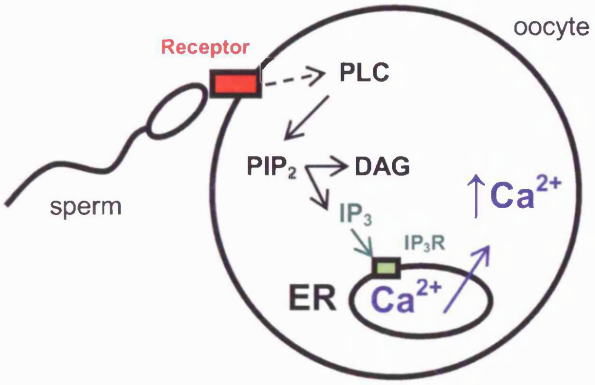

C) Content Theory

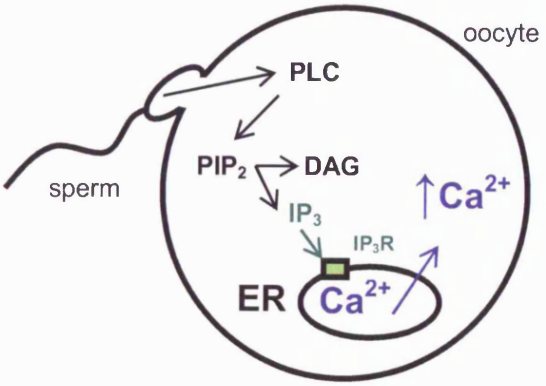

1.3.2. The sperm factor is a novel phospholipase C isoform

Early candidates for the sperm factor included small molecules such as $InsP_3$ (Tosti *et al.*, 1993), $NAADP^+$ (Lim *et al.*, 2001) and NO (Kuo *et al.*, 2000). Despite having the ability to generate intracellular Ca^{2+} release in non-mammalian species, none of these were capable of elicting a long period of Ca^{2+} oscillations observed during in vitro fertilisation in mammalian oocytes (Swann, 1994). Studies utilising various fractionation techniques suggested that the sperm factor was a protein (Stricker, 1997; Swann, 1996; Wu *et al.*, 1998), of ~30-100kDa in size (Parrington *et al.*, 2002; Rice *et al.*, 2000). Other potential candidates have included a 33kDa glucosamine-6-phosphate isomerase, termed Oscillin (Parrington *et al.*, 1996), and a truncated form of the c-kit receptor (tr-kit) (Sette *et al.*, 1997). None of these proteins however have been shown to be capable of generated fertilisation-like Ca^{2+} transients when injected into mammalian oocytes (Wolny *et al.*, 1999; Wolosker *et al.*, 1998; Wu *et al.*, 1998). The identification of the sperm factor has involved the isolation and purification of sperm extracts. In vitro PLC assays revealed that these extracts possessed a PLC activity, at least 100 times greater than that present in other tissues known to express PLC isoforms (Rice *et al.*, 2000). PLC became an obvious candidate for the sperm factor, not only due to the fact that the PI pathway is responsible for Ca^{2+} release at fertilisation, but also as several PLC isoforms have been shown to be expressed in mammalian sperm (Fukami, 2002). Despite this, microinjection of recombinant proteins corresponding to most of the known isoforms expressed in sperm, including PLCβ1, γ1, γ2 and δ1 failed to mimic the Ca^{2+} oscillations

observed at fertilisation (Jones *et al.*, 2000; Parrington *et al.*, 2002; Runft *et al.*, 2002), or only managed to initiate Ca^{2+} oscillations at non-physiological concentrations (Mehlmann *et al.*, 2001). Recent analysis of a mouse testis expressed sequence tag (EST) database revealed a novel PLC sequence. This led to the production of a full length cDNA encoding sperm protein, termed PLCζ (Saunders *et al.*, 2002). PLCζ was found to be smaller than the other PLC isoforms and its expression was found to be testis specific. Microinjection of complimentary RNA (cRNA) encoding mouse (Saunders *et al.*, 2002), human and monkey (Cox *et al.*, 2002) PLCζ into mouse eggs produced fertilisation-like Ca^{2+} responses. Furthermore, these Ca^{2+} oscillations were abolished when PLCζ was immunodepleted by an anti-PLCζ antibody, from native sperm extracts (Saunders *et al.*, 2002; Swann *et al.*, 2004). The amount of PLCζ required to initiate Ca^{2+} transients correlates with the approximate concentration of PLCζ in a single sperm (20-50fg) (Saunders *et al.*, 2002). Studies involving transgenic mice that generate RNAi to interfere with PLCζ expression in testis have shown that levels of PLCζ are half of those of normal mice, causing premature termination of Ca^{2+} oscillations during fertilisation (Knott *et al.*, 2005).

1.3.2.1 The Phospholipase C family

Mammalian phospholipases are an essential group of enzymes that play a central role in phosphatidylinositol metabolism and lipid signalling pathways in a Ca^{2+} dependent manner. Fourteen isoforms of PLC have been identified so far, grouped into six subfamilies that differ in mode of activation, catalytic regulation,

cellular localisation and membrane binding activity; β(1-4), γ(1,2), δ(1-4), ε, ζ and η(1,2) (Cockcroft *et al.*, 1992; Fukami, 2002; Hwang *et al.*, 2005; Kelley *et al.*, 2001; Nakahara *et al.*, 2005; Rhee, 2001; Rhee *et al.*, 1997; Saunders *et al.*, 2002; Song *et al.*, 2001). As described previously, these enzymes catalyse the hydrolysis of PIP_2 to generate the second messengers $InsP_3$ and DAG. The presence of distinct regulatory domains in PLC isoforms causes them to be susceptible to different modes of activation and allow them to participate in different signalling pathways (Rhee, 2001). The domain organisation of the six subfamilies of PLC are illustrated in Figure 1.11.

1.3.2.2 PLC Domain Functions

All PLC isoforms except PLCε and PLCζ possess a Pleckstrin Homology (PH) domain at the NH_2 terminal. The PH domain comprises approximately 120 amino acids is proposed to be essential for plasma membrane association of many proteins involved in intracellular signalling. This membrane association was first described in PLCδ1 (Rhee, 2001). Membrane binding is also regulated in a negative feedback by $InsP_3$, which binds to the PH domain, thus inactivating it (Williams, 1999). X-ray crystallography studies have indicated that the PH domains of all isoforms share a common architecture, consisting of a β-sandwich closed off at one end by a C-terminal α-helix (Ferguson *et al.*, 1995). The EF-hand domain consists of four helix-loop-helix motifs that are divided into pair-wise lobes. The loop region that links the two perpendicularly positioned α-helices possesses Ca^{2+} binding residues (Kretsinger *et al.*, 1973). EF hands always occur in pairs because one loop stabilises the other. The second lobe of the EF

hand domain interacts with the conserved (C2) domain, and its removal renders the enzyme inactive, probably due to tertiary structure destabilisation (Emori *et al.*, 1989; Nakashima *et al.*, 1995). All PLC isoforms have two regions of high sequence homology consisting of two building blocks, the X and Y domains.

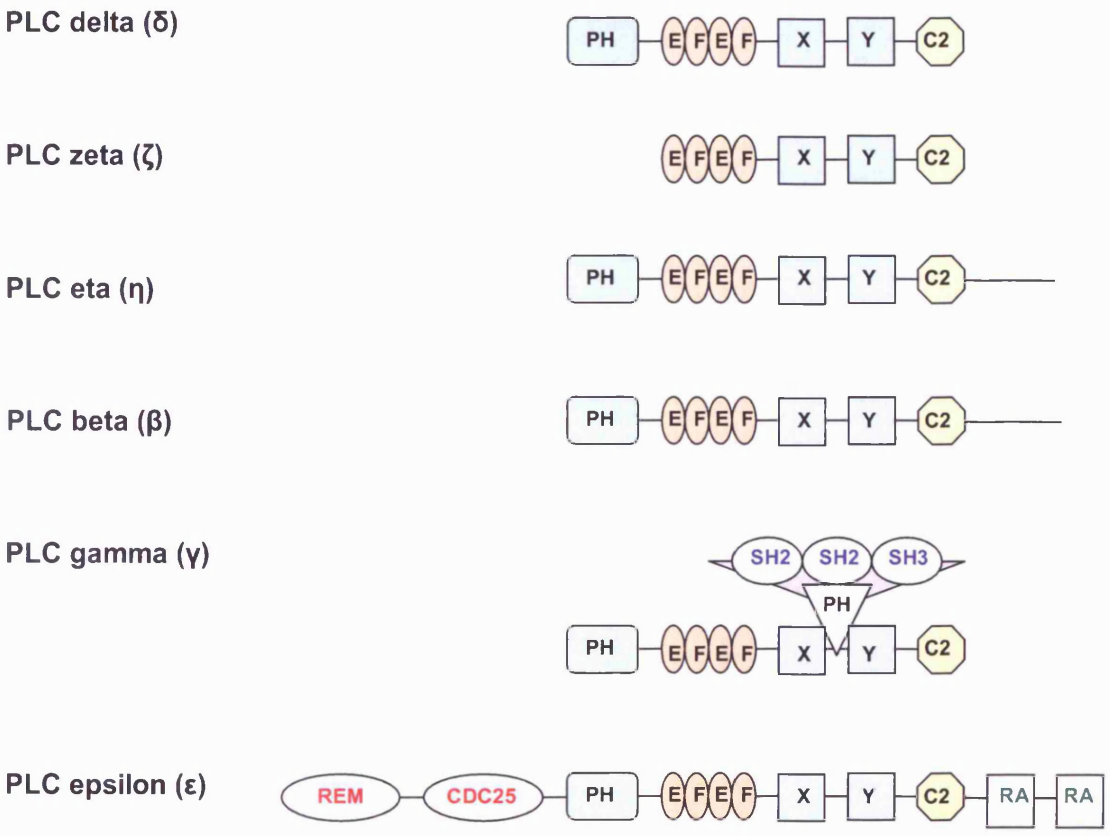

Figure 1.11 Domain topographies of the phospholipase C isoform families.

Schematic diagram of the domain organisation of the known PLC subfamilies, illustrating the plecktrin homology (PH) domains which target the PLC to membrane bound proteins, the EF-hands which bind Ca^{2+}, the X and Y catalytic domains, and the PKC-homology type II (C2) domain which binds lipids. The Scr homology (SH) domains bind to phosphorylated tyrosine residues in target proteins. The ras exchanger motif (REM) and cell division cycle 25 (CDC25) domains catalyse guanosine diphosphate (GDP) to guanosine triphosphate (GTP), an activity that is regulated by Ras associating (RA) domains.

X and Y are organised in eight repetitive beta sheet/alpha helix sequences, forming a distorted barrel (Ellis *et al.*, 1998; Williams, 1999). The catalytic mechanism involves a two step acid/base catalysis of the inositol 1-phosphate-glycerol bond that links the inositol headgroup to the DAG lipid anchor (Ellis *et al.*, 1998). There is an interruption strand between strands four and five of the catalytic domain, which forms a large loop, termed the X-Y linker sequence, which differs considerably between PLC isozymes. For example, in the PLCδ group, the X-Y linker is relatively short (46 amino acids). Proteolysis of this negatively charged region results in activation of the enzyme, and it is thought to play an important regulatory function (Rebecchi *et al.*, 2000; Williams, 1999). The PKC-homology type II (C2) domain is a protein structural motif, comprising ~120 amino acid residues, that is involved in targeting proteins to cell membranes. The secondary structure of the C2 domain comprises 8 β-sheets, forming an anti-parallel beta-sandwich motif (Williams, 1999). Membrane binding is facilitated by Ca^{2+} in three Ca^{2+} binding regions (CBR) which induces a conformational change in the domain. Ca^{2+} bound to CBRs does not take part in catalysis directly, but stabilises interactions with anionic phospholipids (Stahelin *et al.*, 2001).

1.3.2.3 PLCζ

PLCζ is a soluble protein of approximately 70KDa, the smallest of the PLC family identified to date, and is most closely related to PLCδ1 (Saunders *et al.*, 2002). Mouse PLCζ is comprised of a tandem pair of EF hands at the N-terminus,

followed by the catalytic XY domain and a C2 domain in the C-terminus. However, unlike other PLC isozymes, PLCζ lacks the pleckstrin homology (PH) domain. Despite this, PLCζ is similar to PLCδ1 sharing 38% identity and 49% sequence homology in 647 of its residues (Miyazaki *et al.*, 2006). The expression of PLCζ in mouse eggs following the microinjection of cRNA gives rise to a series of fertilisation like Ca^{2+} oscillations (Saunders *et al.*, 2002). The amount of PLCζ contained in a single sperm has been estimated to be around 20-50fg (Saunders *et al.*, 2002). Tagging PLCζ with Venus fluorescent protein, Myc epitope or luciferase has enabled the quantification of the amount of PLCζ protein produced following the microinjection of cRNA. The expression of levels comparable to that contained in a single sperm was shown to be sufficient to cause Ca^{2+} oscillations equivalent to those seen at fertilisation (Nomikos *et al.*, 2005; Saunders *et al.*, 2002; Yoda *et al.*, 2004). Recombinant PLCζ has also been found to generate Ca^{2+} oscillations when injected into mouse eggs, although a greater amount of protein is required (~300fg) (Kouchi *et al.*, 2004). The mechanism of action of PLCζ remains unknown. It is unclear how PLCζ targets its membrane bound substrate, PIP_2 or how the activity of this enzyme is regulated. PLCζ appears to be in an active state upon entry into the oocyte, however it remains uncertain how this protein maintains itself within the sperm and whether its effects are specific to eggs. Recent studies suggest that PLCζ expressed in cell lines can cause Ca^{2+} oscillations and alter phenotype (Coward *et al.*, 2006; Kuroda *et al.*, 2006). The transient expression of PLCζ tagged with eYFP was assessed in COS cells (derived from the kidney cell line of the African green monkey)(Coward

et al., 2006). Images taken of COS cells displaying expression of PLCζ-eYFP show the existence of two main patterns of fluorescence: either a grainy cytoplasmic distribution or a nuclear distribution. Kuroda *et al.* (2006) reported Ca^{2+} oscillations in somatic cells following the expression of PLCζ. The results show that 24 hours after transfection, repetitive Ca^{2+} spikes at intervals of ~3 minutes were observed in COS cells expressing venus tagged PLCζ. No Ca^{2+} oscillations were observed in any of the cells expressing the inactive D210R mutant or in non-transfected COS cells. This study also reports the nuclear accumulation of PLCζ in COS cells and its D210R mutant. In contrast to the observations of Coward *et al.*,(2006), the confocal images taken of cells 48 and 72 hours after transfection suggest an increase in active import into the nucleolus over time, with no report of cells displaying any other patterns of distribution. It is suggested that the less marked nucleolar accumulation observed in cells expressing the D210R mutant could be due to its inability to induce Ca^{2+} oscillations. Broad ectopic expression of PLCζ in transgenic mice appears to have no effect with the exception of ovarian abnormalities in females. This suggests that the activity of PLCζ is restricted to oocytes when low level expression is forced ectopically in multiple tissues, however the expression levels were not quantified (Yoshida *et al.*, 2007).

1.4 Aims of this study

In this study, the expression of PLCζ was examined in Chinese Hamster Ovary (CHO) cells in order to establish if it can trigger Ca^{2+} signals or compromise cell viability, and to determine if mammalian cell lines could otherwise be used for making recombinant PLCζ protein. Chapter 3 describes the first specific aim of this thesis, which includes the optimisation of recombinant PLCζ expression in CHO cells using different methods of nucleic acid delivery. This chapter also describes the cellular localisation of transiently expressed eYFP-PLCζ and examines the effects of PLCζ-LUC expression on intracellular Ca^{2+}. Chapter 4 describes a comprehensive analysis of the effects of PLCζ expression on basal Ca^{2+} handling and receptor induced Ca^{2+} mobilisation. Chapter 5 describes the generation of a CHO cell line stably expressing PLCζ, with the aim of obtaining relatively homogeneous cell populations where the vast majority of cells expressed the recombinant protein. This chapter also examines the activity of the PLCζ produced by this cell line in eggs. Chapter 6 will summarise the overall results from chapters 3 to 5 and provide a general discussion of the findings in this thesis.

CHAPTER 2
MATERIALS AND METHODS

Chapter 2 Materials and Methods

2.1 Materials

2.1.1 General laboratory reagents and chemicals

All chemicals and reagents were obtained from Sigma or Invitrogen unless otherwise stated. All reagents were dissolved in dH_2O and stored at room temperature unless otherwise stated. All filter sterilisation was through 0.2µm filters (Satorius).

2.1.2 Bacterial cell culture reagents

All growth media and antibiotics were obtained from Sigma, sterile plastic and glassware were obtained from Fisher or Greiner. All glassware was washed in detergent free water and autoclaved (135°C, 90min) prior to use. Growth media were autoclaved under the same conditions prior to the addition of antibiotics. Aseptic technique was used in all protocols and surfaces were swabbed with 70% (v/v) methanol before and after use.

Listed below are the reagents used for bacterial cell culture:

- Luria Bertani (LB) medium: 1% (w/v) tryptone, 0.5% (w/v) yeast extract, 0.5% (w/v) NaCl. Autoclaved. Medium cooled to <50°C before antibiotic addition. Stored at 4°C.
- LB-Agar medium: LB medium, 1.5% (w/v) agar. Autoclaved. Medium cooled to <50°C before antibiotic addition. Plates were freshly prepared before use.

- Ampicillin 100mg/ml stock: filter sterilised and stored at -20°C, used at a working concentration of 100µg/ml.
- S.O.C. medium (Invitrogen) Stored at 4°C.
- Bacterial cells: TOP10 chemically competent *Escherichia coli* (Invitrogen). Prepared by members of the WHRI laboratory using the $CaCl_2$ treatment method (Hanahan, 1983). Stored in 100µl aliquots at -80℃ for up to 6 months.

2.1.3 Molecular biology reagents

Listed below are the reagents used for molecular biology techniques:

- Wizard® Plus SV Miniprep DNA Purification system (Promega) comprising:
    - Cell Resuspension Solution
        - 50mM Tris-HCl, 10mM EDTA, 100µg/ml RNase A; pH 7.5
    - Cell Lysis Solution
        - 0.2M NaOH, 1% SDS (w/v)
    - Neutralisation Solution
        - 4.09M guanidine hydrochloride, 0.759M potassium acetate, 2.12M glacial acetic acid; pH4.2
    - Column Wash Solution
        - 60mM potassium acetate, 8.3M Tris-HCl, 40µM EDTA, 60% Ethanol; pH 7.5
- Plasmid Maxi kit (Qiagen®) comprising:

- Resuspension Buffer (Buffer P1)
  - 50mM Tris-Cl, 10mM EDTA, 100µg/ml Rnase A ; pH 8.0
- Cell Lysis Buffer (Buffer P2)
  - 200mM NaOH, 1% SDS (w/v)
- Neutralization Buffer (Buffer P3)
  - 3M potassium acetate; pH 5.5
- Equilibration Buffer (Buffer QBT)
  - 750mM NaCl, 50mM MOPS pH 7.0, 15% isopropanol (v/v), 0.15% Triton® X-100 (v/v)
- Column Wash Buffer (Buffer QC)
  - 1M NaCl, 50mM MOPS pH 7.0, 15% isopropanol (v/v)
- Elution Buffer (Buffer QF)
  - 1.25M NaCl, 50mM Tris-Cl pH 8.5, 15% isopropanol (v/v)

- Agarose powder (ultra pure, Eurogentec)
- TAE Buffer, 1x: 40mM Tris, 20mM acetic acid, 1mM EDTA.
- Ethidium bromide (EtBr), aqueous solution, 10mg/ml.
- DNA loading buffer, 2 x stock: 50% (v/v) TAE Buffer 1x, 50% (v/v) glycerol, 0.25% (w/v) orange G.
- DNA restriction enzymes: EcoRI and NcoI. Restriction enzymes and appropriate buffers were stored at -20°C.
- Molecular weight DNA marker: Hyperladder I (10Kb), obtained from Invitrogen. Stored at -20°C.

2.1.4 Plasmid vectors

2.1.4.1 pCR3 and pcDNA3.1

Vectors pCR3 and pcDNA3.1 (Invitrogen) contain a cytomegalovirus (CMV) promoter (P_{CMV}) that initiates transcription in mammalian cells. The vectors also contain the ampicillin resistance gene for selection in *E.coli,* and a T7 promoter upstream of the multiple cloning site for in vitro expression of recombinant proteins. These vectors were utilised in the production of the cDNA constructs used in this thesis (see methods section 2.2.1 for further details).

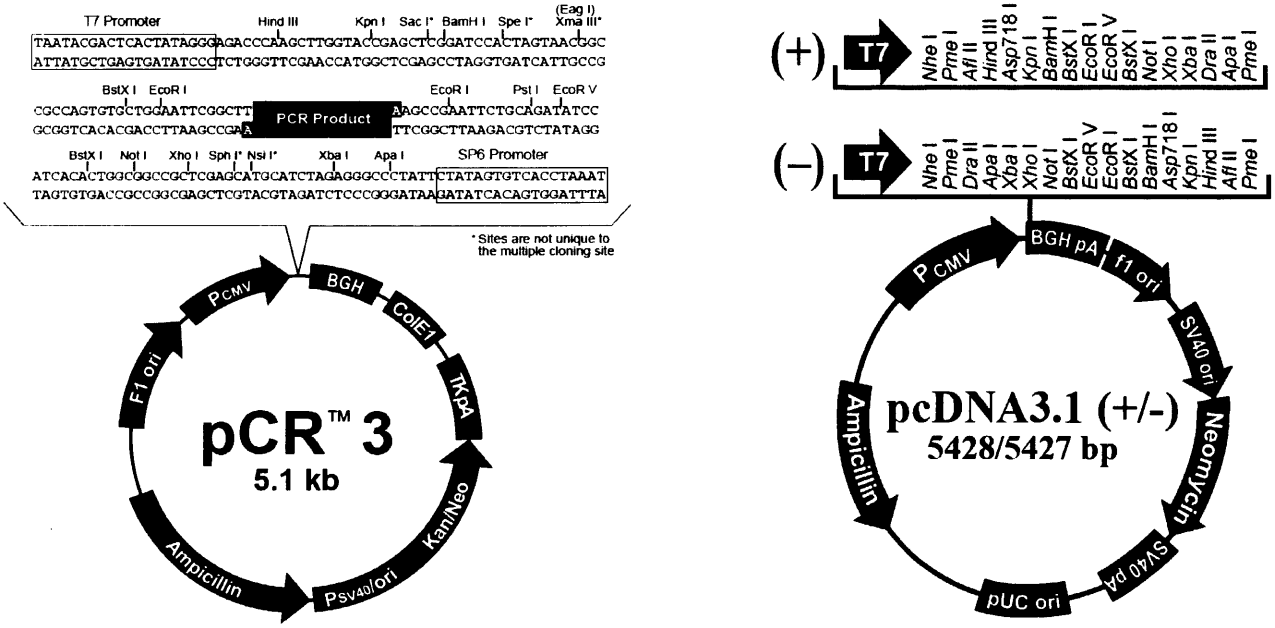

Figure 2.1 Mammalian expression vectors pCR3 and pcDNA3.1

PLCζ-LUC was constructed in the mammalian expression vector pCR3 (M.Nomikos). eYFP-PLCζ was constructed in the mammalian expression vector pcDNA3.1 (C.Saunders). See section 2.2.1 for further details. Expression was driven by a CMV promoter in all cDNA constructs. (Images from Invitrogen)

2.1.5 Chinese Hamster Ovary (CHO) cell line culture reagents

The CHO cell line was derived from a biopsy of an ovary of an adult Chinese hamster by T.T.Puck in 1957 (Puck *et al.*, 1958). They are adherent, and exhibit typical epithelial cell morphology. All growth media and reagents were supplied by Gibco/ Invitrogen and all chemicals were supplied by Sigma unless otherwise stated. Sterile culture flasks were supplied by Nunc (Fisher) or Greiner. Poly-D-lysine coated glass bottomed cell culture dishes were supplied by World precision instruments (WPI). Class I cell culture containment hoods were used for all procedures. Aseptic technique was used in all protocols and surfaces were swabbed with 70% ethanol before and after use.

Listed below are the reagents used for the culture of CHO cells:

- F-12 Nutrient Mixture (Ham) supplemented with filter sterilised 10% (v/v) foetal bovine serum (FBS) and 100µg/ml penicillin/streptomycin (supplemented media referred to as complete F-12). Stored at 4°C and warmed to 37°C prior to use.
- Trypsin-EDTA, 1x in hepes buffered salt solution (HBSS). Stored at -20°C.
- Saline solution, NaCl 0.9% (w/v) supplied by Baxter Medical Supplies.
- Cryopreservation medium: FBS containing 10% (v/v) dimethyl sulphoxide (DMSO), filter sterilized. Freshly prepared.
- Phosphate buffered saline (PBS): 137mM NaCl, 2.7mM KCl, 4.3mM Na_2HPO_4, 1.4mM KH_2PO_4, pH adjusted to 7.4 using HCL. Filter sterilised.

- Trypan Blue™ reagent (Sigma-Aldrich), 0.4%. Used as an addition of 100µl to a 0.5ml, 1 x 10^5 cell suspension in PBS pH 7.4.

2.1.6 DNA Transfection materials and reagents

Listed below are the materials and reagents used for the transfection of CHO cells and their subsequent analysis:

- Lipofectamine™ 2000 Tranfection reagent. Used as per manufacturers instructions. Stored at 4°C (Invitrogen)
- Hepes buffered saline (HBS) 2x: 280mM NaCl, 10mM KCl, 1.5mM Na_2HPO_4, 10mM glucose, 50mM Hepes, pH adjusted to 7.5 filter sterilised and stored at -20°C.
- Calcium Chloride, 2M stock. Filter sterilised and stored at -20°C.
- Pesda microbubbles: Perfluorobutane gas (F_2 Chemicals Ltd), 5% Glucose, 10% (w/v) BSA.
- FITC-dextran (10KDa), 10mg/ml stock stored at -20°C. For cell sonoporation this was dilued in KRH buffer to obtain a final concentration of 100µg/ml.
- Propidium Iodide, 1mg/ml stock stored at -20°C. Used at a working concentration of 20µg/ml.
- Femtotip® microinjection capillaries (Eppendorf)
- KCl Hepes Buffer: 100mM KCl, 20mM Hepes, pH adjusted to 7.2. Divalent metal ions were removed with the chelating resin Chelex 100 (Sigma). Filter sterilised and stored at 4°C.

- Cell extract buffer: KCl Hepes Buffer, 1mM EDTA, 200µM PMSF. Freshly prepared.
- Alexa Fluor® 594 10,000 MW Dextran conjugate was obtained from Invitrogen and dissolved in dH_2O to obtain a stock concentration of 5mg/ml, which was stored at -20°C. For use, this was then diluted 1 in 2 in KCL Hepes to obtain a working concentration of 2.5mg/ml
- Leibovitz's L-15 medium supplemented with 5% FBS and 100µg/ml penicillin/streptomycin (all filter sterilised). Stored at 4°C and warmed to 37°C prior to use.
- Luciferase assay buffer: 50mM Tris HCl, 5mM $MgCl_2$, 1mM EDTA, 1mM ATP, 0.5mM DTT, 1mg/ml BSA. Freshly prepared.
- Digitonin, 10mM stock.
- Luciferin, 2mM stock, stored at -20°C.
- Flow cytometry Buffer: 1x PBS, 1mM EDTA, 5% (v/v) FBS. Filter sterilised, freshly prepared.

2.1.7 Calcium (Ca^{2+}) imaging reagents

Listed below are the reagents used during Ca^{2+} imaging experiments:

- Krebs-Ringer-Hepes (KRH) buffer: 120mM NaCl, 25mM Hepes, 4.8mM KCl, 1.2mM KH_2PO_4, 1.2mM $MgSO_4$, 1.3mM $CaCl_2$, pH adjusted to 7.4. Filter sterilised and stored at 4°C.

- Ca^{2+} free KRH buffer: 120mM NaCl, 25mM Hepes, 4.8mM KCl, 1.2mM KH_2PO_4, 1.2mM $MgSO_4$, 1mM EGTA, pH adjusted to 7.4. Filter sterilised and stored at 4°C.
- Calcium dyes:
    - Oregon Green Bapta dextran (OGBD), 2mM stock. (Molecular Probes, Invitrogen). Stored at -20°C. For experiments this was injected at a pipette concentration of 0.5mM.
    - Fluo-3 and Fura Red™ acetoxymethyl (AM) esters were obtained from Molecular Probes (Invitrogen) and dissolved in a solution of 20% pluronic acid in DMSO to obtain a stock concentration of 1mM, which could be stored at -20°C but were usually freshly prepared. For use in CHO cell experiments, this was then diluted in serum free F-12 medium to obtain a working concentration of 10μM. For egg experiments Fura Red AM was used at a working concentration of 4μM.
    - Fura PE3 acetoxymethyl (AM) ester was obtained from Sigma. For egg experiments this was used at a working concentration of 4μM.
- Adenosine trisphosphate (ATP), 10mM stock solution freshly prepared and placed on ice. For use, this was then diluted in KRH to obtain a final concentration of 100μM.
- Ionomycin, 100μM stock, stored at -20°C. For use, this was then diluted in KRH to obtain a final concentration of 5μM.

2.1.8 Statistical analysis

Numerical data was stored in spreadsheets and plotted in graphical form using Excel (Microsoft) and GraphPad Prism. Data was expressed as mean ± standard error of the mean (SEM), where SEM is defined as standard deviation / $\sqrt{}$ (n-1) (n= number of observations). Unless stated all data in this thesis was derived from a minimum of three separate observations. Data sets of equal variance were analysed using One Way Analysis of Variance (ANOVA). In addition to the Bonferroni multiple comparisons post hoc test where applicable. Comparisons of two independent samples were analysed using an unpaired student's *t*-test. Data were considered statistically significant if $p<0.05$ (p value is the probability that any particular outcome would have arisen by chance).

2.1.9 Health and safety

All reagents were handled and stored as recommended by manufacturer's safety guidelines. All experiments were performed in accordance with COSHH regulations and local college regulations. All genetic manipulation was carried out in accordance with GMAG guidelines. All bacteria and mammalian cell culture waste was disinfected prior to disposal.

2.2 Methods

2.2.1 DNA Constructs

All DNA constructs shown in this thesis were kindly provided by Michail Nomikos (Luciferase tagged) or Christopher Saunders (enhanced yellow fluorescent protein (eYFP) tagged). The ezymatically inactive eYFP-^{D210R}PLCζ construct was derived from eYFP-PLCζ in collaboration with Andreas Rossbach. Diagramatic structural details of the DNA constructs are shown below (Figure 2.2). In addition to the PLCζ constructs, pCR3-LUC and pcDNA3.1-eYFP were used as controls in this thesis. Restriction digests with ECORI (Luciferase tagged constructs) or NcoI (eYFP tagged constructs) were performed to ensure successful ligation, and to confirm the presence and correct orientation of the insert (See Chapter 3).

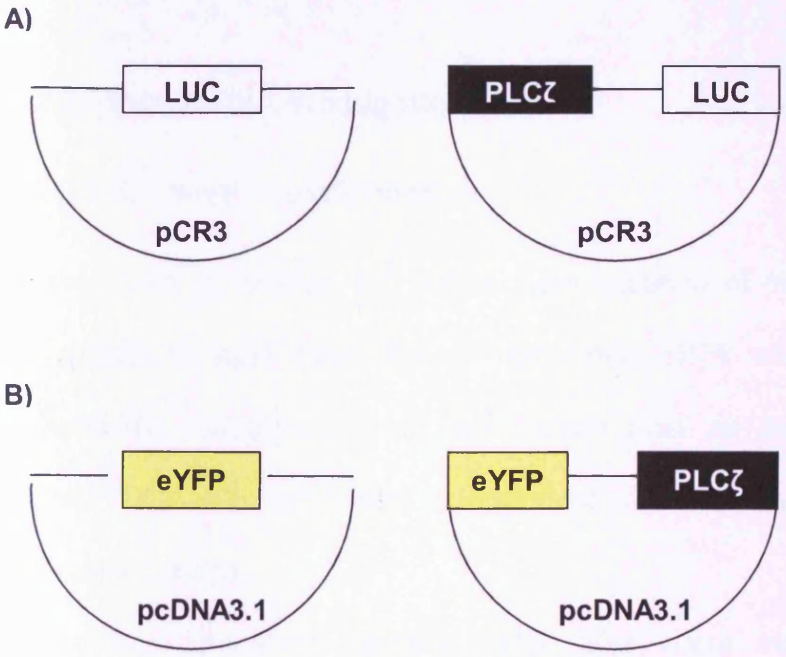

Figure 2.2:
Luciferase and eYFP tagged DNA constructs

Schematic diagrams showing the structural details of (A) the pCR3-LUC and PLCζ-LUC constructs (Courtesy of M.Nomikos), and (B) the pcDNA3.1-eYFP and eYFP-PLCζ constructs (Courtesy of C.Saunders)

2.2.2. In vitro site-directed mutagenesis

The eYFP tagged ^{D210R}PLCζ construct was created in collaboration with Andreas Rossbach using the eYFP-PLCζ construct (Christopher Saunders) and the method of in vitro site-directed mutagenesis (SDM). Mutagenesis of the aspartate residue at position 210 to arginine to produce ^{D210R}PLCζ was performed using the Stratagene Quikchange XL SDM kit. This technique utilises a dsDNA vector with an insert of interest and two synthetic oligonucleotide primers, both containing the desired mutation. The primers (complementary to opposite strands of the construct) are extended during temperature cycling by DNA polymerase, generating a mutated plasmid. Dpn I endonuclease treatment digests the parental DNA, whilst the mutation-containing synthesised DNA remains intact. The thermocycling reaction, digest of parental DNA and transformation were set up according to the manufacturer's instructions.

2.2.3 Plasmid DNA propagation

2.2.3.1 Bacterial Transformation

Bacterial transformation and subsequent isolation of plasmid DNA enables the production of large quantities of highly pure DNA suitable for eukaryotic cell transfection. Bacteria are an appropriate host as they replicate exogenous plasmid DNA with high fidelity independent of the bacterial genome, enabling it to be easily isolated.

Chemically competent bacterial cells (50µl) were inoculated with 100ng of plasmid DNA and incubated on ice for 15 minutes. The cells were subjected to a

heat shock at 42°C for 30 seconds in a water bath before being transferred immediately to ice for 2 minutes. The cells were placed into a 15ml snap cap tube containing SOC media (500µl) which was then incubated for 1 hour at 37°C with gentle rotary agitation at 225rpm. Two unequal volumes of the cell suspension were plated onto LB-Agar plates containing ampicillin (this ensures different densities of colony growth, avoiding lawn growth ensuring successful isolation of individual colonies). Plates were incubated overnight at 37°C until colonies were visible.

2.2.3.2 Small scale plasmid isolation (plasmid DNA miniprep)

Typically between 5-10 colonies were selected and screened for the presence of the plasmid using the following method; The 3mls of LB media supplemented with 100mg/ml Ampicillin were inoculated with a single colony and incubated overnight at 37°C with gentle rotary agitation at 225rpm. Subsequently 1ml of each culture was pelleted (14,000xg for 1 minute) and DNA isolation was performed by the alkaline lysis method employed by the Wizard SV Miniprep plasmid purification kit (Promega). The remaining culture was reserved for large scale plasmid isolation (section 2.2.3.4). Briefly, bacterial pellets were resuspended in 250µl of Resuspension solution (containing RNase A), prior to being lysed during a 3 minute incubation with 250µl Lysis solution. A high salt environment was created by the addition of 350µl Neutralisation solution, which results in the precipitation of all cell debris via the precipitation of potassium dodecyl sulphate (KDS) (co-precipitated in insoluble salt-detergent complexes).

The precipitate was subsequently removed by centrifugation at 14,000xg for 10min, and the cleared lysate was applied to a mini spin column containing a silica-gel DNA binding membrane. The column was centrifuged at 14,000xg for 2min, then was washed twice with an 80% ethanol buffer. DNA was eluted from the column in 30µl 10mM Tris pH 8.5. Recombinant plasmids were then analysed as in section 2.2.3.3 before being prepared on a larger scale (section 2.2.3.4).

2.2.3.3 Analysis of recombinant plasmids

Recombinant plasmids were verified by restriction enzyme mapping. Isolated DNA was digested using the EcoRI (luciferase tagged constructs) or NcoI (eYFP tagged constructs) restriction enzyme for 2 hours at 37°C, and the resulting fragments were analysed via agarose gel electrophoresis. An agarose gel was prepared by dissolving 1% agarose (Eurogentec) in TAE (1x) buffer and heating in a microwave oven. The solution was cooled to <50°C before the addition of ethidium bromide (0.2µg/ml final concentration), and poured into a pre-assembled gel tray (Bio-Rad). Once the gel was set, DNA samples in 30% (v/v) DNA loading buffer (1x) were loaded onto the gel alongside a DNA molecular weight marker (10Kb, Invitrogen). Electrophoresis was performed in a gel tank containing TAE (1x) with a constant voltage (typically 10v per cm of gel). The gel was visualized with UV transillumination and imaged using a gel documentation system (Bio-Rad) with Hamamatsu camera and Quantity One software. Typically 95-100% of colonies showed the correct pattern of DNA restriction fragment.

2.2.3.4 Large scale plasmid isolation (plasmid DNA maxi prep)

Large scale plasmid isolation (plasmid DNA maxi prep) was performed following observation of the correct restriction fragments. LB media (200ml, supplemented with 100mg/ml Ampicillin) was inoculated with 1ml of the mini prep transformant culture (see above) and grown overnight at 37°C with rotary agitation at 225rpm. Cultures were centrifuged (10,000xg, 10 minutes, 4°C, JLA16:250 fixed angle rotor, Avanti J-25, Beckman) and large scale plasmid isolation was carried out using the Qiagen Maxi Prep Kit which uses an ion-exchange resin method. Bacterial pellets were resuspended in 10ml of Buffer P1 (resuspension buffer, containing Rnase A), prior to the addition of 10ml of Buffer P2 (lysis buffer). Following a 5 minute incubation at room temperature, 10ml of Buffer P3 (neutralisation buffer) was added, and the samples were placed on ice for 30 minutes. The resulting precipitate was removed by centrifugation (20,000xg, 30 minutes, 4°C, JA25:50 fixed angle rotor, Avanti J-25, Beckman), and the supernatant was applied to a Qiagen-tip 500 silica gel column, which had been equilibrated using Buffer QBT (equilibration buffer). The plasmid DNA was washed twice with 30ml of Buffer QC (column wash buffer), then eluted with 15ml of Buffer QF (elution buffer). Plasmid DNA was precipitated using isopropanol (0.7 volumes), and harvested via centrifugation (20,000xg, 30min, 4°C). The DNA pellet was washed with 5ml of 70% ethanol and further centrifuged (20,000xg, 10min, 4°C). The plasmid DNA was dissolved in 700µl 10mM Tris pH 8.0. Plasmid DNA purity and concentration (µg/ml) was determined by UV spectrophotometry (Perkin-elmer MBA2000). Samples were diluted 1:50 and

measured in duplicate at an absorbance of 260nm (A_{260}). The DNA concentration was calculated using the following equation: A_{260} value of 1 = 50µg/ml of double stranded DNA. Plasmid purity was determined by measuring the ratio of A_{260}/A_{280}, with values ≥ 1.9 indicating high levels of purity. Plasmid DNA was then further analysed by restriction digest mapping and agarose gel elecrophoresis as described previously, before being stored at -20°C.

2.2.4 Chinese Hamster Ovary (CHO) cells

CHO cells were maintained in complete F-12 (cF-12) media (see section 2.1.5) in a humidified atmosphere of 5% CO_2 at 37°C. The culture media was changed every 2 days and cells were routinely passaged upon confluency (typically every 3-4 days) using the following method. Adherent cells were washed with saline and detached from the culture flasks using trypsin-EDTA for 3 minutes at 37°C. cF-12 (5mls) was added to the cell suspension prior to the cells being pelleted by centrifugation (1,200xg for 3 minutes), and re-suspended in fresh cF-12 (6mls). Subsequently 20µl of this cell suspension was removed for haemocytometric analysis (Neubauer haemocytometer), a method used to determine the correct volume of cells required to obtain the optimum seeding density (Typically 2.5 – 5 $x10^5$ cells per $75cm^2$ culture flask). In order to maintain cell stocks, cells (~5 x 10^6) were detached and pelleted as described above, and re-suspended in 1ml of cryopreservation medium (see section 2.1.5). Cell suspensions were placed in sealed screw top cryo-vials (NUNC), and gradually cooled to -80°C using insulating tissue paper, before being placed in liquid nitrogen for long term

storage. When required, cells were thawed rapidly by hand and gradually introduced to increasing volumes of pre-warmed cF-12 (to a maximum of 5ml) prior to centrifugation (1,200xg for 3min). Cells were re-suspended in cF-12, seeded into a 25cm^2 culture flask, and culture media was changed after 4 hours.

2.2.5 DNA Transfection

2.2.5.1 Calcium Phosphate mediated transfection

CHO cells were seeded in 6 well plates or in Poly Lysine coated glass bottomed culture dishes (WPI) 24 hours prior to transfection, and at ~70-80% confluency were transfected with high purity (A_{260}/A_{280} > 1.9) plasmid DNA using the calcium phosphate precipitation method (Chen *et al.*, 1987). Briefly, a mixture of plasmid DNA (2-8µg), 18.5µl of 2M $CaCl_2$ and sterile dH_2O (total volume of 150µl) was added dropwise (over a period of 30 seconds) to 150µl of pre-warmed 2x HBS with continuous mixing. Transfection complexes (125mM $CaCl_2$, 300µl final volume) were incubated at room temperature for no longer than 30 minutes. The mixture was vortexed briefly and added dropwise to the cells in cF-12 (3ml), before being mixed gently and incubated in a humidified atmosphere of 5% CO_2 at 37°C for 16-18 hours. Cells were washed twice with 0.9% w/v saline solution in order to remove precipitates, before incubation (humidified, 5% CO_2, 37°C) in cF-12 for a further 6 hours.

2.2.5.2 Lipid mediated transfection (Lipofectamine2000, Invitrogen)

CHO cells were seeded in 6 well plates or in Poly Lysine coated glass bottomed culture dishes (WPI) 24 hours prior to transfection, and at ~80-90% confluency were transfected with high purity (A_{260}/A_{280} > 1.9) plasmid DNA using cationic lipid mediated transfection (Lipofectamine2000, Invitrogen). This method was carried out according to manufacturer's instructions. Briefly, plasmid DNA (2-8µg) was diluted with F-12 medium (without FBS or antibiotics) to a total volume of 250µl. Lipofectamine2000 reagent (10µl) was also diluted with F-12 medium (240µl) and both mixtures were incubated at room temperature for 5 minutes. Lipid and DNA complexes were then combined (drop wise over a period of 30 seconds), prior to further incubation at room temperature for no longer than 20 minutes. During this time, cells were washed twice with 0.9% w/v saline solution before addition of the tranfection complexes in 2mls of F-12 medium, followed by incubation (humidified, 5% CO_2, 37°C) for 6 hours. Transfection complexes were removed, and the cells were incubated in complete F-12 for a further 16-18hours prior to testing for transgene expression.

2.2.5.3 Sonoporation

Sonoporation of cells using ultrasound (US) has recently gained interest for its potential as an alternative means of non-viral gene delivery (Bao *et al.*, 1997; Kim *et al.*, 1996; Taniyama *et al.*, 2002). Initial studies utilised devices operating at kilohertz (kHz) frequencies (Fechheimer *et al.*, 1987), however due to excessive cell damage, applications using megahertz (MHz) frequencies now

appear to be more prevalent (Huber *et al.*, 2000; Liang *et al.*, 2004). The application of US to a liquid causes the formation and implosion of vapour filled microbubbles, or cavities, in the solution. The energy release associated with this is believed to be sufficient to permeabilise adjacent cell membranes and lead to DNA delivery (Deng *et al.*, 2004; Unger *et al.*, 2001). This process is referred to as cavitation. Microbubble contrast agents (CA) are believed to lower the energy threshold for cavitation (Unger *et al.*, 2001), and have been shown to enhance gene delivery for applications using higher frequency US (1-3MHz) both *in vitro* and *in vivo* (Bao *et al.*, 1997; Lawrie *et al.*, 2000; Taniyama *et al.*, 2002). The ability of ultrasonic standing waves (USW) to suspend small particles and cells at MHz frequencies has been widely studied in recent years (Coakley, 1997; Lee *et al.*, 2005). Cells and particles in suspension exposed to an USW experience a force driving them towards the pressure node plane (Khanna *et al.*, 2003) as indicated schematically in the figure below. It has been noted that increasing the proximity between cavitating CA's and cells increases the probability of cell sonoporation (Ward *et al.*, 2000). Standing wave systems offer an advantage over travelling wave fields by encouraging this bubble cell interaction.

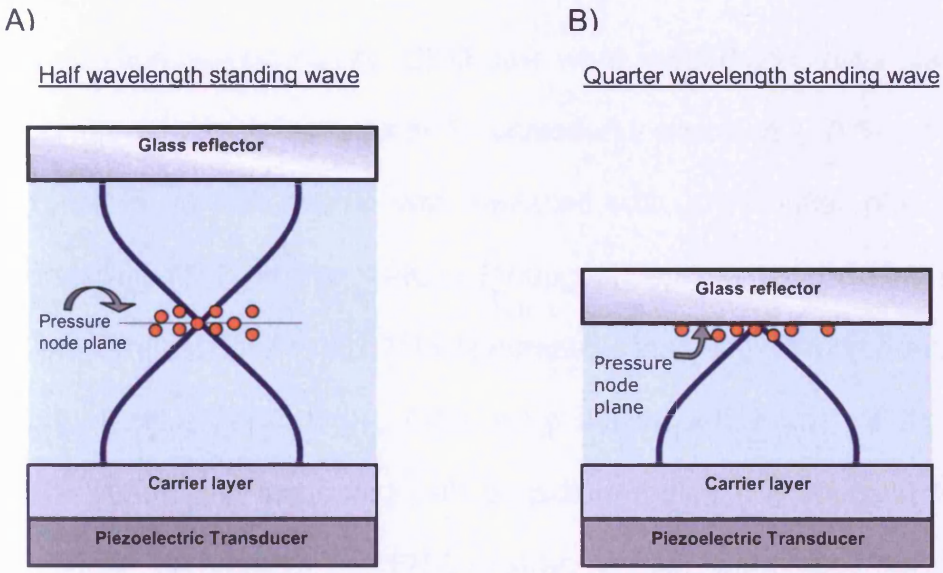

Figure 2.3: Particle movement towards the nodal plane of an USW

Current applications of this technology have focused on using devices that concentrate particles or suspensions of cells near the centre of the fluid cavity (Figure 2.3A). However, using a different combination of layer geometries, it is possible to focus particles up against the glass reflector (Figure 2.3B) (Harris *et al.*, 2004). This ¼λ mechanism has been utilised in the design of the novel USW minichamber used in this thesis (see figure 2.4). This presented us with the ability to expose adherent cells to cavitating CA's held in close proximity by an USW, thus enabling real time monitoring of the biological response to US exposure. The method of using USW fields has been examined in our laboratory for macromolecular uptake (Khanna *et al.*, 2006) and DNA transfection (unpublished observations) of cells in suspension. During this thesis an attempt was made to optimize sonoporation in a ¼ wavelength USW as a means of permeabilising and transfecting adherent cells, and to compare this with existing

transfection methodologies. CHO cells were seeded on circular glass cover slips (manufacturer) 24 hours prior to ultrasound exposure (~70% confluency upon exposure). Growth media was replaced with KRH buffer plus 4mg/ml BSA, containing FITC-dextran 10KDa (100µg/ml) and 2-10% PESDA microbubbles. Cells were exposed to a 1.72MHz ultrasonic standing wave at 40-80V for various pulse lengths (2sec-1min). Cells were subsequently washed three times with KRH buffer, and incubated with propidium iodide (PI; 20µg/ml) for 5 minutes. Optimum parameters for FITC-dextran uptake were used for plasmid DNA transfection experiments. Cells were exposed to USW at 40V in KRH buffer containing 100ng-10µg of plasmid DNA and 5% PESDA microbubbles. Fluorescence images were captured on a Nikon Diaphot 200 microscope equipped with a cooled CCD camera.

Figure 2.4 Design of the USW Quarter wavelength minichamber

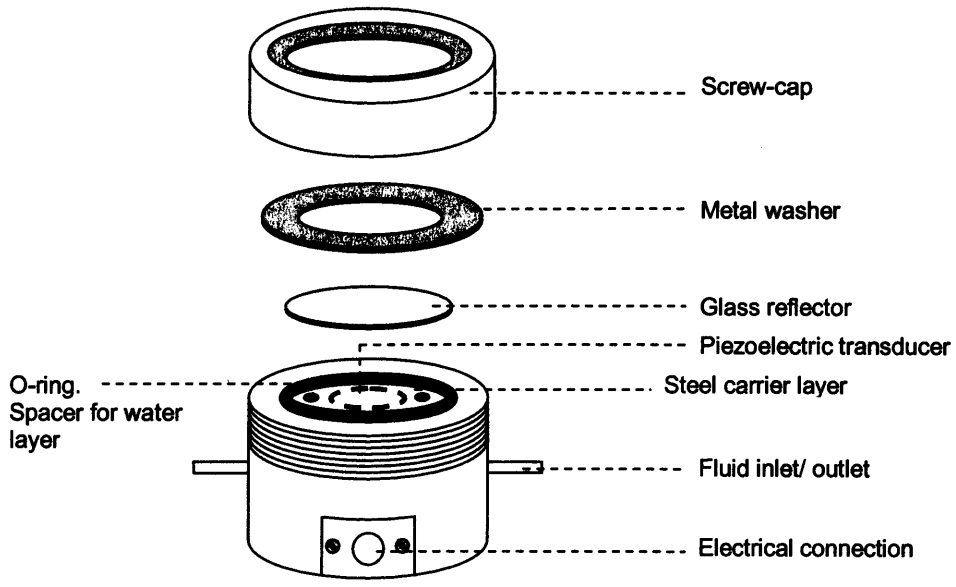

2.2.5.3.1 Perfluorocarbon-exposed sonicated dextrose albumin (PESDA) microbubbles

Perfluorocarbon-exposed sonicated dextrose albumin (PESDA) microbubbles were prepared by methods similar to those previously described (Porter *et al.*, 1995). Briefly, 5ml of perfluorobutane gas was hand agitated with a 3:1 mixture of 5% glucose and 10% BSA. This mixture then underwent sonication (Jencons Ltd) at 20kHz for 80 seconds, prior to a 30 minute incubation on ice.

2.2.5.4 Microinjection

Microinjection involves injecting DNA directly into cells, or even the cell nucleus using a very fine needle. CHO cells were seeded in Poly Lysine coated glass bottomed culture dishes (WPI) 24 hours prior to transfection, and at ~50-60 / 70-80% confluency were transfected with high purity (A_{260}/A_{280} > 1.9) plasmid DNA as follows. Plasmid DNA (100ng) was mixed with filter sterilised KCL Hepes buffer (section 2.1.6) and 2.5mg/ml Alexa 594-dextran (10,000 Mw), to a final volume of 12µl, prior to centrifugation at 14,000xg for 1 hour at 4°C. Alexa 594 was omitted from the injection solution for experiments involving the use of Fura Red. Microinjection was performed semi-automatically with a Femtojet (Eppendorf, Germany) attached to an InjectMan NI2 (Eppendorf) mounted on an Axiovert 200 inverted fluorescence microscope (Carl Zeiss). Femtotips (Eppendorf) with an inner diameter of 0.5µm and an outer diameter of 1.0µm were used for all injections. Injection capillaries were backfilled with 3µl of the injection solution using sterile microloaders (Ependorf). The injection angle was set at 45°, and each tip was used for the injection of 50-70 cells. The injection

time remained constant at 0.1s (lowest possible setting), and a constant compensation pressure of 80hPa was applied to the capillary. Cells were transferred to complete L-15 medium (section 2.1.5), and typically 50-100 cells were injected per culture dish over a period of 30-45 minutes with an injection pressure of 90hPa at 37°C. The medium was exchanged immediately for pre-warmed complete F-12, and cells were transferred to an incubator (humidified, 5% CO_2, 37°C) prior to imaging transgene expression 3-48 hours later.

2.2.6 Measurement of luciferase expression and intracellular Ca^{2+} in CHO cells

For experiments involving luciferase tagged constructs, CHO cells were microinjected as described in section 2.2.5.4 with 100ng of plasmid DNA mixed with 0.5mM Oregon Green BABTA dextran (Molecular Probes) in KCL Hepes buffer. Cells were transferred to an incubator (humidified, 5% CO_2, 37°C) for 3-48 hours in complete F-12 medium before being incubated with 100µM luciferin. Cells were imaged on a Zeiss Axiovert 100 microscope equipped with a cooled intensified charge-coupled device (ICCD) camera (Photek Ltd, UK), encased within a purpose built dark box. An ICCD is a charge-coupled device (CCD) that is optically connected to an image intensifier that is mounted in front of the CCD. The ICCD camera is depicted in Figure 2.5. Image intensifiers are comprised of three functional elements mounted in close proximity to one another in the following sequence: a photocathode, a microchannel plate (MCP) and a phosphor screen. Photons generated by the bioluminescent sample fall onto the photocathode and are converted to photoelectrons. The photoelectrons are

accelerated towards the MCP which amplifies the signal by generating a cascade of secondary electrons. The multiplied electrons are accelerated towards the phosphor screen which finally converts them back to photons which are guided to the CCD by a fibre optic taper. Cells were monitored for luminescence by integrating light emission for 20 minutes before Ca^{2+} was monitored in the same cells for 1 hour with low level excitation light from a halogen lamp.

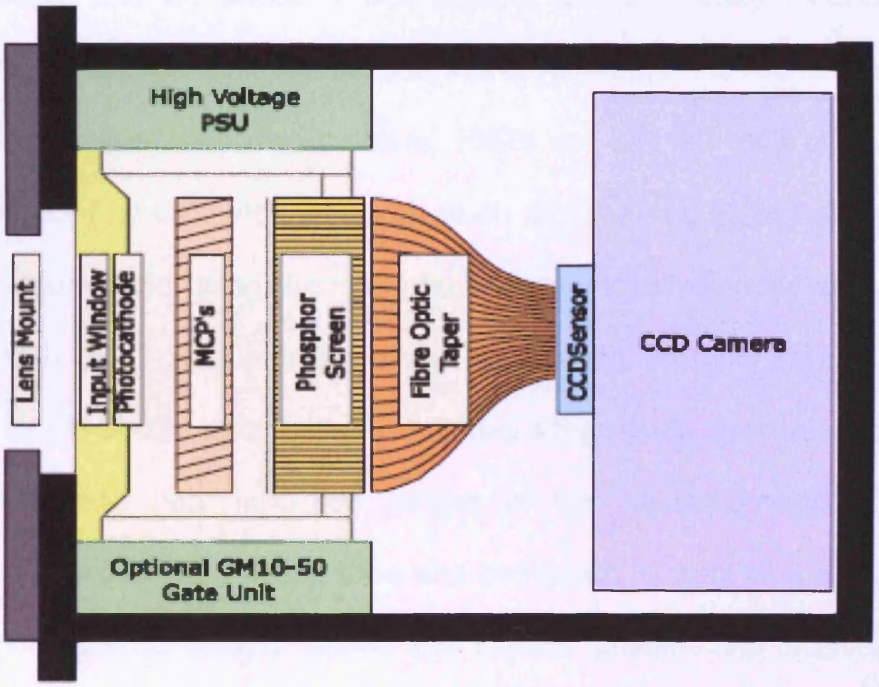

Figure 2.5 Intensified charge-coupled device (ICCD) camera (Photek)

A) Schematic representation of the ICCD camera from Photek Ltd. Light is collected onto the front of the camera before being intensified and imaged as described above (section 2.2.6).

2.2.7 Measurment of luminescence using a luminometer

Luminometers detect and measure light using an extremely sensitive photomultiplier tube (PMT). PMTs are comprised of a vacuum-tube containing a photocathode which converts the light to photoelectrons (made of a compound semiconductor, mostly consisting of alkali metals); one or more secondary-electron-emitting electrodes or dynodes which amplify the number of photoelectrons; and an anode which collects the secondary electrons and provides the electrical output signal. Due to the very large amplification provided by the secondary emission mechanism, PMTs are capable of multiplying the current produced by incident light by as much as 10^7 times. Experiments in this thesis were performed using a custom built luminometer equipped with an S20 PMT cooled to -20°C using a peltier cooler (Figure 2.6). The S20 PMT contains a multialkali (Na-K-Sb-Cs) photocathode that has a high, wide spectral response in the ultraviolet and near infra red ranges of the elecromagnetic spectrum. Samples were placed into a 5ml tube and positioned in front of the PMT. The injection port located directly above the sample enables the addition small volumes of reagents to the sample using a pressure controlled 50µl Syringe (Hamilton Ltd, Carnforth, U.K.). The output signal is connected to a current to voltage converter and photon counter, and is received by a computer in the form of photons per second. CHO cells (~1.5 x 10^6) transfected with luciferase tagged constructs were trypsinised and washed twice with 1x PBS, before being resuspended in luciferase assay buffer (section 2.1.6). Cells were lysed by the addition of 40µM digitonin and placed in the luminometer. Background light

emmision was recorded for each sample before the addition of 100µM luciferin. Luciferase activity was measured for 10 minutes, and expressed as counts per second.

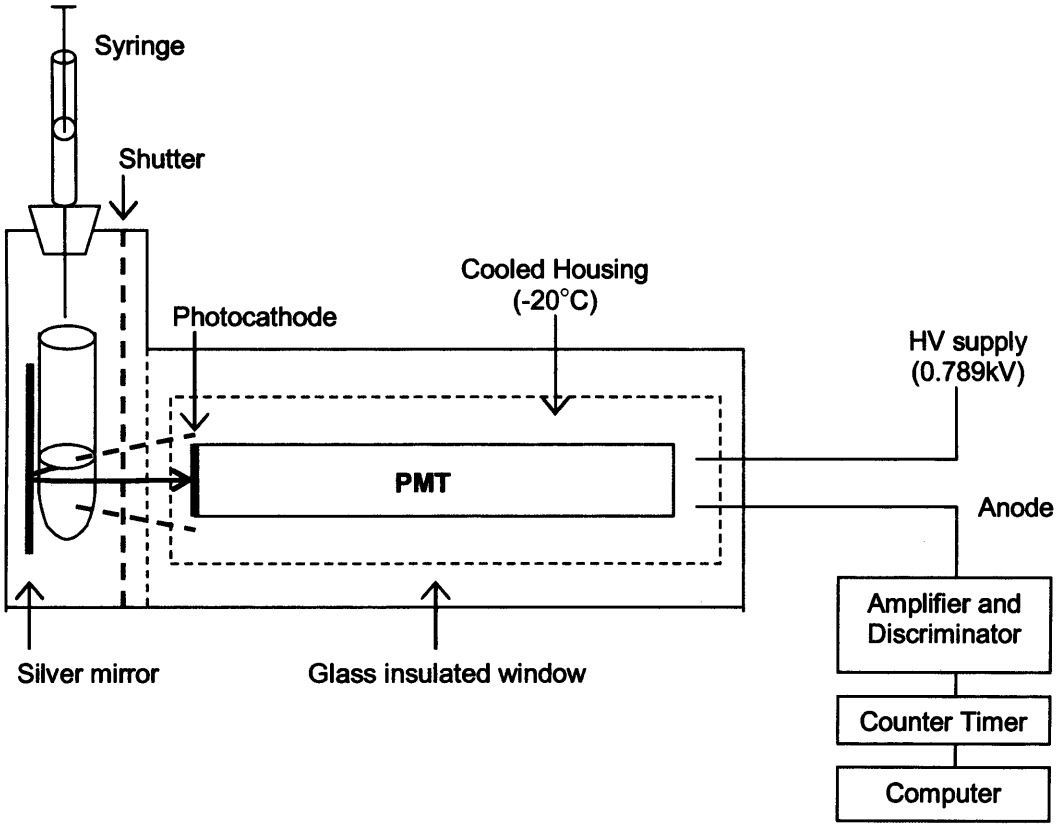

Figure 2.6 Luminometer

Schematic diagram of a custom built luminometer. The light emitted from the sample following the addition of lysis buffer is collected and amplified as described above (section 2.2.7).

2.2.8 Confocal laser scanning microscopy (CLSM)

Confocal laser scanning microscopy (CLSM) offers several advantages over conventional fluorescence microscopy, including controllable depth of field and elimination of image degrading out of focus fluorescent light. The acquisition of time resolved confocal image series (known as time series) provides the possilbility of visualizing and quantifying dynamic changes within living specimens, even in the range of microseconds. The Leica TCS SP5 (True confocal scanner equipped with 5 spectrophotometer channels) equipped with the Leica DMI 6000 inverted microscope (Figure 2.7) was used for experiments involving eYFP-tagged constructs, including live cell experiments and experiments using paraformaldehyde fixed cells. Cells were visualised using an oil immersion, 63x objective lens (numerical aperture = 1.23) and images were acquired at 512 x 512 pixel resolution. eYFP fluorescence (excitation and emission peaks at 514nm and 527nm respectively) was visualised using the 488nm laser line from an argon laser (set at 20% source power), with the PMT set to detect emission at 510-540nm. Alexa-594 fluorescence (excitation and emission peaks at 594nm and 617nm respectively) was visualised using the 561nm He:Ne laser line at 20% power, with the PMT set to detect emission at 600-630nm. Fluo 3 fluorescence (excitation and emission peaks at 506nm and 526nm respectively) was visualised using the 488nm laser line from an argon laser (set at 20% source power), with the PMT set to detect emission at 510-540nm. Fura Red fluorescence (excitation and emission peaks at 488nm and 597nm respectively) was visualised using the 488nm laser line from an argon

laser (set at 20% source power), with the PMT set to detect emission at 580-610nm.

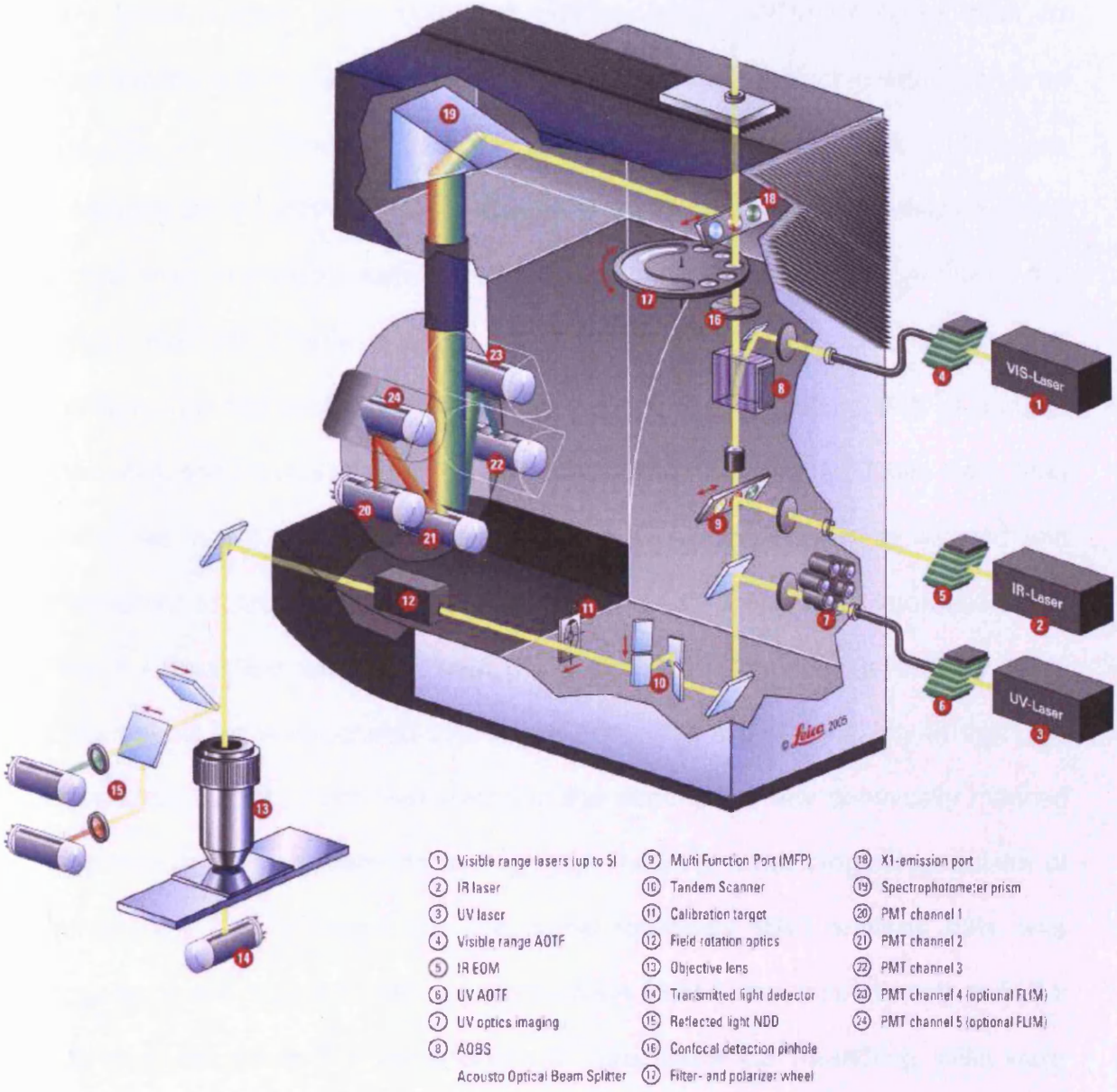

Figure 2.7 The Leica SP5 Confocal laser scanning microscope
The Leica SP5 uses an acousto-optical tunable filter (AOTF) to control the excitation laser light and an acousto-optical beam splitter (AOBS) instead of filter blocks to convey the excitation laser light to the sample and to reflect the emitted light from the sample to the scan head. The emitted light is passed through a pinhole that prevents the out of focus light from dectected by the photomultiplier tube (PMT). The PMT converts light into an electrical signal that is recorded by the computer equipped with Leica confocal software. Image taken from *www.zmb.uzh.ch/resources/download/CLSM.pdf*

2.2.8.1 Intracellular Ca^{2+} imaging

For experiments involving eYFP tagged constructs, CHO cells were seeded in poly lysine coated glass bottomed culture dishes (WPI) 24 hours prior to transfection, and at ~50-60 / 70-80% confluency were transfected with high purity (A_{260}/A_{280} > 1.9) plasmid DNA as described in section 2.2.5.4. Cells were visualized for intracellular Ca^{2+} between 3 to 48 hours after transfection using CLSM. Prior to imaging, cells were loaded with the Ca^{2+} indicator dye Fluo-3 AM / Fura Red AM (10μM in 20% w/v pluronic acid) in un-supplemented F-12 medium. The dye containing solution was added to each culture dish as a 200μl meniscus and incubated at 37°C and 5% CO_2 for 90 minutes. Cells were then immersed in F-12 medium prior to imaging, for which they were washed and transferred to Krebs-Ringer-Hepes buffer. The Ca^{2+} dependent fluorescence of Fluo-3 / Fura Red was visualized using CLSM as described is section 2.2.8. Experiments were structured to analyze either the signal variability in the Ca^{2+} dependent Fluo-3 / Fura Red traces in the absence of any chemically induced response or to incorporate the addition of a known pharmacological modulator of intracellular Ca^{2+} (Chapter 4). For signal variability (SV) analysis data was acquired every 100ms for 30 second duration (300 frames/experiment) at 512 x 512 pixel resolution. For the analysis of intracellular Ca^{2+} handling, cells were imaged for 100 frames before the addition of ATP (100μM) and for a further 500 frames (1 minute in total). Cells in separate culture dishes were used per application of ATP to negate the effect of sequential ATP application in the same population of cells. Following an experimental series, 15-20 cells were selected

per area (typically 4-6 areas per dish) and data acquired from regions of interest (ROIs) of ~40μm^2 (>150 pixels). These were collected and analyzed using Leica software. Further analysis was carried out using Microsoft Excel, The Single Transient Analysis (STA) program (designed by Steven Barberini using MATLAB software), and GraphPad Prism. Chapter 4 describes the precise derivation of mathematical operations used to calculate signal variability in this thesis.

2.2.8.2 Preparation and Fluorescence analysis of fixed cells

Cells expressing eYFP-tagged constructs / cells loaded with fluo 3 were fixed with freshly prepared paraformaldehyde (4% (w/v) in PBS) to preserve their fluorescence in order to examine the relationship between voltage and intensity/ signal variability during CLSM. Cells were washed twice with PBS (pH 7.4) and fixed using paraformaldehyde (4% (v/v)). Fixed cells were rehydrated with PBS (pH 7.4) for 2 hours, and rinsed briefly with in dH_2O prior to being mounted in FluoSave^{TM} (Calbiochem). Fixed cells were dried at room temperature for 30 minutes and stored at 4°C. Fluorescence analysis of fixed cells was performed using confocal microscopy within 7 days.

2.2.9 Flow Cytometry and Fluorescence activated cell sorting (FACS)

Flow cytometry is a powerful technique that allows simultaneous multiparametric analysis of the physical and/or chemical characteristics of single particles, usually cells, as they flow in a fluid stream through an optical-to-electronic detection apparatus. The properties measured include a particle's relative size, relative

granularity or inner complexity (i.e. shape of the nucleus, the amount and type of the cytoplasmic granules or the membrane roughness), and relative fluorescence intensity. A beam of light (usually laser light of a single wavelength) is directed onto a hydro-dynamically-focused stream of fluid, and any suspended particle or cell from 0.2 - 150μm in size passing through the laser intercept scatters the light in some way. Any fluorescent molecules found within the cells or attached to the cells surface will be excited into emitting light at a longer wavelength than the light source. A number of detectors are aimed at the point where the laser intercepts the stream of fluid (see figure 2.8): one in line with the beam of light (Forward scatter or FSC) and several perpendicular to it (Side scatter or SSC) and one or more fluorescence detectors. FSC correlates with cell size and the extent of SSC depends on the cells granularity. The electronics system converts the detected light signals into electronic signals that can be processed by a computer. The data generated by flow cytometry can be plotted in a single dimension, to produce a histogram, in two-dimensional dot plots or even in three dimensions. Following lipid mediated transfection, CHO cells underwent selection for the eYFP-PLCζ and CONT-eYFP plasmids using G418 (500μg/ml). A sample of cells was removed from the culture at 5 hours, and then daily for a period of two weeks. Cells were collected by trypsinisation, adjusted to a density of 1×10^6 cells/ml in Flow buffer (section 2.1.6) and analysed for YFP expression on a BD FACSCalibur (San Diego, CA, USA), using 488nm Argon laser excitation and 530nm emission band pass filter.

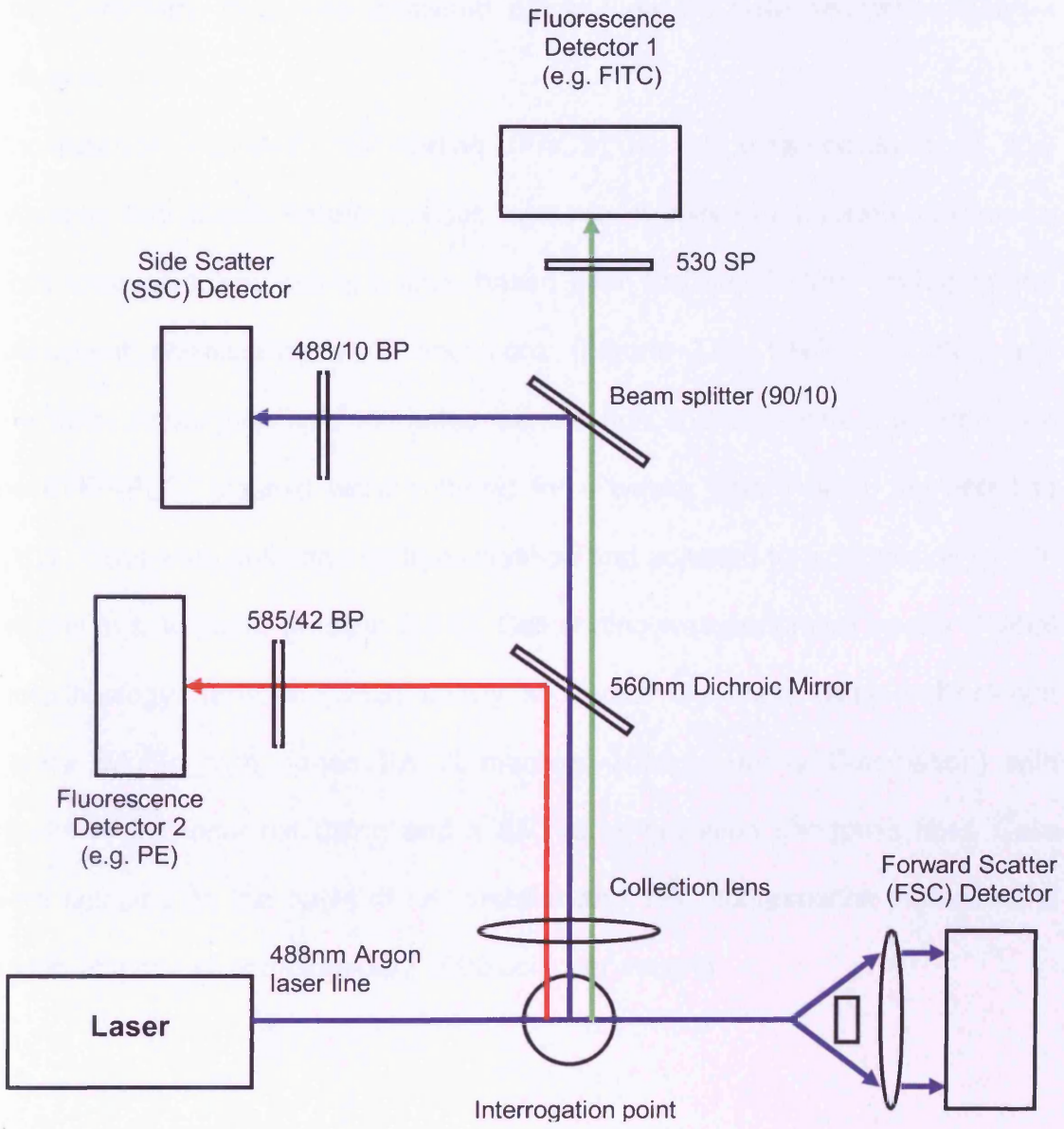

Figure 2.8 Flow Cytometry Optics

Simplified Layout of the optical system of a typical two colour flow cytometer (as viewed from above). Cells are depicted passing through the line of the 488nm argon laser. Fluorescence emitted by a cell at 90° to the excitation line is captured by three separate detectors after negotiating a series of barriers and filters. Band pass (BP) filters are desinged to restrict transmission of wavelengths either above (long pass or LP) or below (short pass or SP) their designated limits. The 585/42 BP allows the passage of wavelenghts 21nm either side of 585nm.

Flow Cytometry data was analysed using Flow Jo flow cytometry analysis software.

Fluorescence activated cell sorting (FACS) is a specialised form of flow cytometry that allows heterogeneous mixtures of cells to be sorted into two or more containers, one cell at a time, based upon the specific light scattering and fluorescent characteristics of each cell (Figure 2.9). CHO cells that had previously undergone lipid mediated transfection and subsequent selection for the eYFP-PLCζ plasmid were cultured for 4 weeks before being subjected to FACS. Cells were collected by trypsinisation and adjusted to a density of 1×10^6 cells/ml in flow buffer (section 2.1.6). Cell sorting was performed by the Central Biotechnology Services (CBS) facility at Cardiff University using a Beckman Coulter MoFlo high speed FACS machine (Dako-formerly Cytomation) with 488nm Argon laser excitation and a 530/40nm emission bandpass filter. Cells were selected on the basis of cell viability and YFP fluorescence intensity and sorted at a rate of approximately 7000 cells per second.

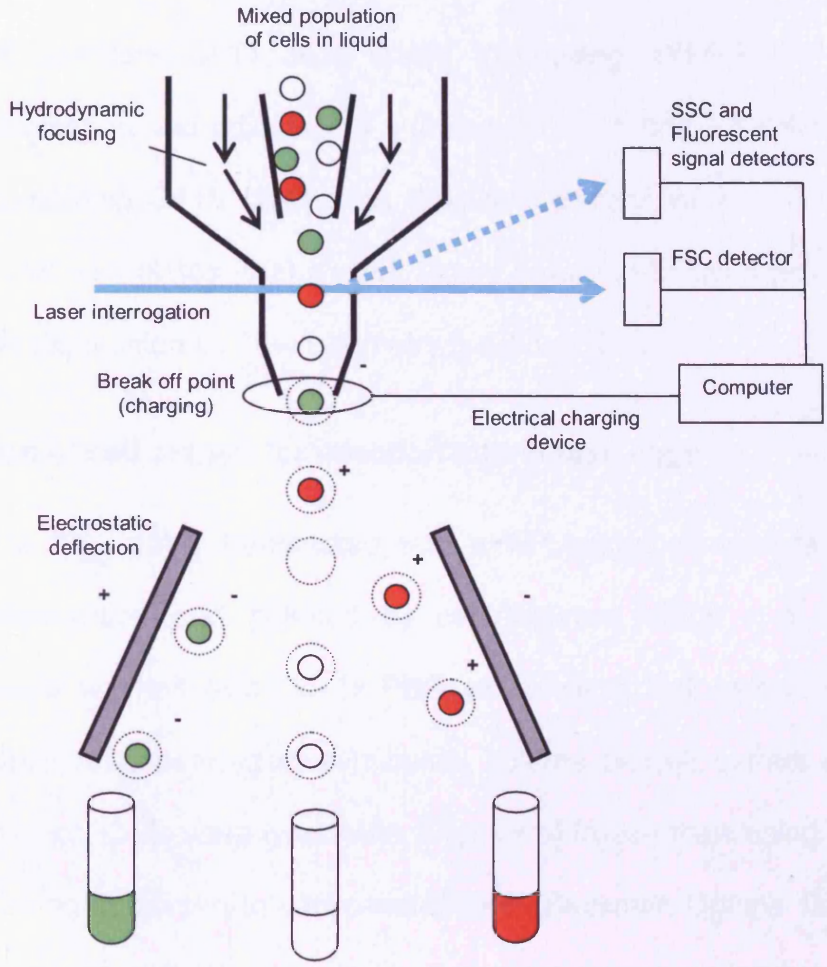

Figure 2.9 Fluorescence activated cell sorting (FACS)

Schematic diagram illustrating the basic principle of fluorescence activated cell sorting (FACS). FACS enables rapid separation of cells from a mixed population based upon preselected characteristics such as fluorescence emission, fluorescence intensity, cell size and cell viability. Following the hydrodynamic focussing of the sample, each cell is interogated with a beam of light. The computer determines how the cell will be sorted prior to it reaching the break off point. As the drop is created an electrical charge is applied to the stream and the newly formed drop will form with a charge. The charged droplets then fall through an electrostatic deflectin system that diverts droplets into containers based upon their charge. (SSC: side scatter, FSC: Forward scatter)

2.2.10 Clonal selection of cells expressing eYFP-PLCζ

Non-clonal G418 resistant CHO cells stably expressing eYFP-PLCζ were collected by trypsinisation and adjusted to a density of 15, 5 and 1.5 cells/ml of cF-12 medium containing G418 (500µg/ml). The suspensions were transferred into flat bottomed 96 well plates (200µl/well). Single colony wells were assessed for YFP transgene expression by flow cytometry (section 2.2.9).

2.2.11 Preparation of cell extract for injection into mouse eggs

CHO cells (~ 2 x 10^7) stably transfected with eYFP tagged constructs were harvested by trypinisation and pelleted by centrifugation (1200 x g, for 3 minutes). Cells were washed twice in 1x PBS and once in Cell extract buffer (section 2.1.6), then resuspended in a mimimal volume of Cell extract buffer (50% of pellet volume). Cells were lysed with 3 cycles of freeze-thaw using liquid nitrogen, before being subjected to ultracenrifugation (Beckman Optima TLX) at 100,000 xg for 1 hour at 4°C. The resulting supernatant was concentrated using a Microcon centrifugal filter device (10KD, Millipore) as per manufacturers instructions, snap frozen, and stored at -80°C.

2.2.12 Mouse Egg experiments

Mouse egg experiments were carried out in collaboration with Karl Swann and Yangsong Yu. Metaphase II eggs were collected from six week old female mice that had been stimulated to superovulate by injection of pregnant mare serum (PMS, Folligon) and human chorionic gonadotrophin (hCG, Folligon). Eggs were collected 14 hours post hCG administration and maintained in droplets of

HKSOM (see table 2.1) under mineral oil at 37°C. Prior to experiments, eggs were washed with M2 medium (Sigma)

For cell extract injections, eggs were incubated with 4μM Fura Red AM for 20 minutes. Injection needles were formed by pulling borosilicate glass capillaries (Harvard Apparatus Ltd, 1.5mm outer diameter and 0.86mm internal diameter) with an internal filament using a vertical pipette puller (Model P-30; Sutter Instruments). Injection needles were backfilled with ~1μl of cell extract (diluted 1 in 5 with KCl hepes buffer) using sterile micropipettes (Ependorf). Eggs were microinjected using an inverted microscope (TE2000, Nikon) equipped with hydraulic manipulators and a pressure pulse system. The volume of solution injected was estimated by the diameter of cytoplasmic displacement caused by the injection; which was ~1-5% of the eggs volume.

For single CHO cell injections, eggs were incubated with 4μM Fura PE3 AM for 30 minutes. CHO cells were harvested by trypsinisation (section 2.2.4) and resuspended in M2 medium. Injection needles were formed as described above ensuring an internal diameter slightly less than that of a single CHO cell. Single eggs were all injected with single cells using a Piezoinjector from Primetech (Japan).

Eggs were monitored for Ca^{2+} oscillatory activity in M2 medium using an epifluorescence microscope equipped with excitation and emission wheels and a cooled CCD camera (Photometrics Ltd). Ca^{2+} was measured as a fluorescence excitation ratio of 350/380nm. Emission was measured with a 535nm bandpass filter of 40nm band width.

Potassium Chloride	0.925g
Monopotassium Phosphate	0.238g
Sodium Pyruvate	0.11g
L-Glutamine	0.73g
Streptomycin sulphate	0.25g
Benzylpenicillin	0.315g
EDTA	0.019g
Magnesium sulphate	0.2465g
Sodium Lactate (syrup)	7.37ml
Sodium Bicarbonate	1.68g
Phenol red	0.05g
Hepes	23.8g

Working stock (1x)
on day of experim
grade water. The f
were added to the
to filter sterilisatio
glucose, 10µl of
chloride and 2
hydroxide.

CHAPTER 3
OPTIMISING EXPRESSION AND MONITORING Ca^{2+} IN CHO CELLS

CHAPTER 3 Optimising expression and monitoring Ca^{2+} in CHO cells

3.1 Introduction

3.1.1 Transfection methods

The process of introducing recombinant DNA into eukaryotic cells is defined as "transfection", and is considered a powerful tool for investigating the function of a gene of interest. Essentially, transfection is a method that neutralises the issue of introducing negatively charged molecules into cells with a negatively charged membrane. Numerous transfection techniques have been established over the past few decades that can be broadly classified as either chemical reagents or physical methods.

Calcium phosphate co-precipitation became a popular chemical transfection technique following the systematic examination of this method in the early 1970s (Graham *et al.*, 1973). The authors studied the effect of different cations, cationic and phosphate concentrations, and pH on the parameters of transfection. Calcium phosphate co-precipitation is widely used because the components are easily available and inexpensive, the protocol is easy to use and many different types of cultured cells can be transfected. A precipitate is produced by carefully mixing a buffered phosphate solution with a solution containing calcium chloride and DNA. The solution is dispersed onto the cultured cells and is taken up via endocytosis. Although early chemical transfection methods helped to establish transfection techniques, a number of alternative approaches now exist offering relatively higher efficiency, lower variability, and lower toxicity for a greater variety of cell types.

By 1980, artificial liposomes were being used to deliver DNA into cells (Fraley *et al.*, 1980). The development of synthetic cationic lipids by Felgner and colleagues was the next advancement in this technique commonly referred to as lipofection (Felgner *et al.*, 1987). The cationic head group of the lipid compound associates with the negatively charged phosphates of the DNA molecules. Sufficient liposome is used so that the liposome/nucleic acid complex has an overall net positive charge. This positive charge is attracted to the negative charge on the surface of the cell and the complex is taken up via endocytosis. Many different types of liposomes are commercially available for use in the transfection of mammalian cells including the frequently cited lipofectamine reagents (Invitrogen).

Alternative transfection techniques are available that do not rely on complexing the DNA for transefection. These physical methods include microinjection, electroporation and biolistic particle delivery. Direct microinjection of DNA into cultured cells is an effective technique to deliver DNA into individual cells, requiring specialised injection equipment, considerable labour, and technical expertise (Capecchi, 1980). This method is generally efficient; 50-100% of cells injected express the delivered DNA, although it is not suitable for studies requiring a large number of transfected cells. This technique has been used to transfer DNA into embryonic stem cells that are used to produce transgenic organisms (Bockamp *et al.*, 2002).

Electroporation is a popular physical method of transfection, often used for cell types that are particularly resilient to milder methods of gene transfer. This

method was first reported for gene transfer studies in 1982 (Wong *et al.*, 1982), and relies upon perturbation of the cell membrane by short pulses of high voltage which forms pores that allow the passage DNA into the cell (Shigekawa *et al.*, 1988). This technique requires the cells to be suspended in buffer, and even under optimal conditions approximately 50% of the cells die due to shock. Those that survive typically require 48 hours to recover and show efficient uptake of the DNA.

Another physical method of transfection is biolistic particle delivery, also referred to as particle bombardment or the "gene gun" approach (Yang *et al.*, 1990; Ye *et al.*, 1990). This method requires precipitation of the DNA onto gold particles, and relies upon high velocity delivery of these DNA/gold microcarriers to recipient cells. Initially used for DNA delivery into plants, this technique has since been used to deliver DNA into cultured cells as well as cells in vivo (Burkholder *et al.*, 1993; Klein *et al.*, 1992; Ogura *et al.*, 2005). As with other physical methods, this technique requires special equipment and is relatively costly.

Many novel methods have been developed for mammalian cell transfection, most of which claim improved efficiency, reduced toxicity or wider versatility. For example positively charged, highly branched molecules termed 'dendrimers' complex with negatively charged DNA and transfect cells in a manner similar to liposomes (Tang *et al.*, 1996). They are reported to have decreased toxicity over their liposome counterparts. Also a method termed 'magnetofection' has been shown to enhance delivery in a variety of cell types (Plank *et al.*, 2003), whereby DNA is complexed to magnetic particles, and a magnet is placed underneath the

tissue culture dish in order to bring DNA complexes into contact with a cell monolayer.

Our laborartory has examined the ability of ultrasonic standing waves (USW) to induce macromolecular uptake (Khanna *et al.*, 2006) and DNA transfection (unpublished observations) in cell suspensions by a process referred to as sonoporation (Discussed in Chapter 2, section 2.2.5.3). This chapter reports briefly on the suitability of this novel method for the transfection of adherent cells, and compares this technique with a selection of more established transfection methodologies.

3.1.2 Reporter genes

It is often desirable to measure the expression of a transgene following its transfection into a mammalian cell. The attachment or fusion of a reporter gene to the gene of interest is a method used frequently for this purpose. The two genes are under the same promoter and are transcribed into a single messenger RNA molecule, which is subsequently translated into protein. Many different reporter systems are in widespread use, and are typically chosen because the characteristics they confer on cells expressing them are easily identified and measured using established, convenient assays. Reporter genes can be useful in characterising gene expression in a number of ways, such as estimating transfection efficiency (percentage of cells transfected with a plasmid) or by acting as a surrogate for the subcellular localisation of another gene of interest.

3.1.2.1 Green fluorescent protein and its derivatives

Green fluorescent protein (GFP) has gained wide-spread use as a tool to visualise spatial and temporal patterns of gene expression in living tissue. The cloning of GFP from the jellyfish *Aequorea victoria* (Prasher *et al.*, 1992) and subsequent expression in nonjellyfish systems (Chalfie *et al.*, 1994; Inouye *et al.*, 1994) presented a protein that has since been used as an intrinsic intracellular reporter of gene expression, protein localisation and cell linage in vivo (Cubitt *et al.*, 1995; Gerdes *et al.*, 1996; Niswender *et al.*, 1995). Wild type (WT) GFP, when excited by blue light, emits a fluorescent and easily detectable green light (emission maximum at 508nm) with a spectral pattern similar to that of fluorescein. Its fluorescence is not dependant upon additional co-factors or substrates, making it useful in many cell types (Heim *et al.*, 1994; Inouye *et al.*, 1994). In addition to this, GFP fluorescence is stable, species independent, and can be monitored non-invasively in living cells using fluorescence microscopy or flow cytometry (Chalfie *et al.*, 1994; Inouye *et al.*, 1994). Following the cloning and expression of WT GFP, genetic manipulations were performed in attempts to alter its fluorescent properties. A variant of GFP (enhanced GFP or eGFP) was developed, which contains chromophore mutations ($S^{65}T$ and $F^{64}L$), resulting in a protein 35 times brighter than WT GFP with increased photostability and an augmented excitation peak that was shifted to 488nm (Cormack *et al.*, 1996; Zhang *et al.*, 1996). A broad range of fluorescent protein genetic variants have been developed that feature fluorescence emission spectral profiles spanning almost the entire visible light spectrum. The enhanced yellow fluorescent protein

(eYFP) variant used in this thesis is structurally equivalent to GFP with five additional mutations (S65G, V68L, Q69K, S72A, and T203Y) that increase the emission wavelength to 527nm and the brightness (Grynkiewicz *et al.*, 1985; Tsien, 1998). eYFP has been used previously as a reporter gene to study the expression of PLCζ in somatic cells (Coward *et al.*, 2006).

3.1.2.2 Bioluminescence

Bioluminescence is a natural process in which living organisms convert chemical energy into visible light. Many different organisms, ranging from bacteria and fungi to beetles and fish are endowed with the ability to emit light (Campbell, 1988; Wilson *et al.*, 1998). The majority of bioluminescent insects are beetles belonging to the families of Elateridae (e.g. click beetles), Phengodidae (the railroad worm) and Lampyridae (the fireflies) (Campbell, 1988; Wilson *et al.*, 1998).

Fireflies exhibit there characteristic flashing light from an abdominal organ (lantern) as a signal between potential mates. Each species of firefly has a unique pattern of flashes to provide distinction from other species in the geographical area. Fireflies emit light ranging in colour from green to yellow (550-580nm) (Wood, 1995). The flashes of light are a result of an oxygen-dependent bioluminescent reaction that occurs between the luciferase enzyme and its substrate, luciferin.

The luciferase from the North American Firefly *Photinus pyralis* was the first to be cloned of all the beetle luciferases and has become the best characterised (de

Wet *et al.*, 1987; de Wet *et al.*, 1985). (From here onwards the generic term 'firefly luciferase' or 'luciferase' will be used to refer specifically to the luciferase of the firefly *P.pyralis*).

Firefly luciferase has long been used in biology as an indicator for monitoring ATP since the discovery that ATP is required for the bioluminescent reaction (McElroy, 1947). The cloning an sequencing of the firefly luciferase gene (*luc*) (de Wet *et al.*, 1987; de Wet *et al.*, 1985) and its successful expression in a variety of organisms has rapidly expanded the applicability of firefly luciferase as a reporter for gene expression and an indicator for molecular signals in vivo (Aflalo, 1991; Sala Newby *et al.*, 1999). Luciferase assays are very sensitive, rapid and utilise readily available substrates from commercial sources, making them a widely used analytical tool.

As indicated in figure 3.1, luciferase (Luc) catalyses the oxidative decarboxylation of luciferin (LH_2) in the presence of $MgATP^{2-}$. Firstly, the carboxylate group of luciferin is activated by acylation with ATP, in the presence of Mg^{2+}. The enzyme bound luciferyl adenylate (LH_2-AMP) is oxidised by molecular oxygen, with the intermediate formation of a cyclic peroxide (dioxetanone) and a molecule of AMP. The dioxetanone is decarboxylated releasing energy to generate CO_2 and an electronically excited state of oxyluciferin (*). Relaxation of oxyluciferin to the ground state is accompanied by the emission of light (λ_{max} = 562nm) (Deluca, 1976; Sala Newby *et al.*, 1999; Wilson *et al.*, 1998; Wood, 1995).

Figure 3.1 The firefly luciferase-luciferin bioluminescent reaction

Left: Picture of the North American firefly beetle reproduced from: *http://en.wikipedia.org/wiki/File:Photinus_pyralis_Firefly_3.jpg*
Firefly luciferase (Luc) catalyses the decarboxylation of luciferin (LH_2) in the presence of ATP, O_2 and Mg^{2+}, producing a yellow-green light as described in the reaction sequence outlined below. (See text for details)

(1) $Luc + LH_2 + MgATP^{2-} \rightarrow Luc{\bullet}LH_2\text{-}AMP + PP_i + Mg^{2+}$

(2) $Luc{\bullet}LH_2\text{-}AMP + O_2 \rightarrow Luc{\bullet}oxyluciferin^* + AMP + CO_2$

(3) $Luc{\bullet}oxyluciferin^* \rightarrow Luc{\bullet}oxyluciferin +$ LIGHT

3.1.3 Monitoring intracellular Ca^{2+} using fluorescent indicators

For over two decades researchers have been using fluorescent Ca^{2+} indicators to study the regulation of intracellular Ca^{2+}. A wide variety of Ca^{2+} indicators are currently available, with excitation and emission spectra ranging from UV to visible colours. The most commonly used indicators are chemical fluorescent probes whose optical properties change when they bind Ca^{2+}. Fluorescent Ca^{2+} indicators were originally derived from BAPTA (a membrane permeable Ca^{2+} chelating agent), and most of the classical members of this group were created by Tsien and colleagues in the 1980s (Grynkiewicz *et al.*, 1985; Minta *et al.*,

1989; Tsien, 1980; Tsien, 1981; Tsien *et al.*, 1982). They can be broadly divided into single and dual (ratiometric) wavelength indicators on the basis of their spectral changes in response to Ca^{2+} elevation. Single wavelength Ca^{2+} sensitive indicators such as Fluo-3 change their emission intensity upon binding Ca^{2+}. However, the intensity of the emission is directly proportional to both the ambient Ca^{2+} and the indicator concentration, so careful calibration is required.

Ratiometric indicators, such as Fura-2 offer the advantage of eliminating artefacts that may arise due to indicator concentration. They are used to measure the ratio of fluorescent signals at two distinct wavelengths, which enables the precise quantification of changes in Ca^{2+} concentration. However, the majority of ratiometric indicators require UV excitation, which can damage cells and result in enhanced autofluorescence. In addition, the exclusive requirement for UV excitation may be limited by hardware and experimental considerations.

The majority of fluorescent indicators are cell impermeant. It is therefore necessary to adopt one of the many invasive or biochemical techniques that are available to introduce the indicator into the cytoplasm of the cell. Many of the fluorescent Ca^{2+} indicators are available as acetoxymethyl (AM) ester derivatives (Tsien, 1981; Tsien *et al.*, 1982). The AM form of the indicators can passively diffuse across cell membranes, and undergo hydrolysis by endogenous esterases once they reach the cell cytoplasm. This results in cleavage of the AM group which restores the cell-impermeant properties of the indicator, thus preventing leakage from the cell. Due to the low aqueous solubility of the AM

forms, some dispersing agents such as Pluronic F-127 are often used to facilitate cell loading (Takahashi *et al.*, 1999). Not all fluorescent Ca^{2+} indicators are available as the cell-permeable ester form.

Several of the indicators experience the issue of compartmentalisation. This is overcome by linking the indicator to a dextran of >10,000 molecular weight. These indicator-dextran conjugates cannot cross the plasma membrane and therefore require some invasive techniques for introducing them into the cell (e.g. microinjection or scrape loading). Once inside the cell, the indicator is retained within the cytosol providing more precise estimations of the cytosolic ion concentration over extended periods of observation (Takahashi *et al.*, 1999).

3.1.4 Previous studies involving the expression of PLCζ in somatic cells

In April 2006, Coward *et al.* published a paper describing the in vivo gene transfer and expression of a recombinant form of PLCζ in mouse sperm. As part of that study, the transient expression of PLCζ tagged with eYFP was assessed in COS cells (derived from the kidney cell line of the African green monkey) and in Human Embryonic Kidney (HEK) 293 cells. Images taken of COS cells displaying expression of PLCζ-eYFP show the existence of two main patterns of fluorescence: either a grainy cytoplasmic distribution or a nuclear distribution. Myc or Venus tagged PLCζ has also been shown to localise to the pronucleus (PN) of mouse zygotes and early embryos (Halet *et al.*, 2002; Sone *et al.*, 2005). Ca^{2+} oscillations stop at the time of PN formation (Jones *et al.*, 1995), but continue without stopping with the prevention of PN formation by injection of a lectin, WGA (Marangos *et al.*, 2003). The translocation of PLCζ into the PN is

therefore considered to play an important role in the cessation of Ca^{2+} oscillations at the interphase of a cell cycle (Halet *et al.*, 2004; Kono *et al.*, 1995; Marangos *et al.*, 2003). Coward *et al.*,(2006) offer no explanation as to why PLCζ-eYFP displays these two distinct patterns of localisation in COS cells, however suggest that this may be linked to cell cycle events. HEK 293 cells were transfected with the same PLCζ-eYFP in order to confirm that this construct was generating a protein of the correct molecular weight. Immunoblotting revealed a protein band with an apparent molecular weight of ~100kDa, consistent with the addition of the eYFP protein (27kDa) to the mouse PLCζ protein (74kDa).

In September 2006, Kuroda *et al.* reported on the role of the X/Y linker region and N-terminal EF-hand domain in nuclear translocation and Ca^{2+} oscillation-inducing activity of PLCζ. This was the first study to demonstrate Ca^{2+} oscillations in somatic cells following the expression of PLCζ. The results show that 24 hours after transfection using FuGENE6 (Roche Diagnostics), repetitive Ca^{2+} spikes at intervals of ~3 minutes were observed in 12/17 COS cells expressing venus tagged PLCζ. No Ca^{2+} oscillations were observed in any of the 18 cells expressing the inactive D210R mutant or in non-transfected COS cells. This study also reports the nuclear accumulation of PLCζ in COS cells and its D210R mutant. In contrast to the observations of Coward *et al.*,(2006), the confocal images taken of cells 48 and 72 hours after transfection suggest an increase in active import into the nucleolus over time, with no report of cells displaying any other patterns of distribution. It is suggested that the less marked nucleolar

accumulation observed in cells expressing the D210R mutant could be due to its inability to induce Ca^{2+} oscillations.

In 2007, Yoshida *et al.* successfully induced broad ectopic PLCζ expression in transgenic mice. Reverse transcription polymerase chain reaction (RT-PCR) and immunoblot analysis confirmed recombinant PLCζ protein expression in a range of tissues, including heart, skeletal muscle, lung, liver, spleen, kidneys, testes and ovaries. Their experiments revealed that endogenous PLCζ expression initially had no effect, and the mice appeared healthy. Their oocytes matured normally and established MII, but subsequently exhibited autonomous Ca^{2+} oscillations, second polar body extrusion, pronucleus formation and parthenogenetic development. Transgenic males remained largely asymptomatic; however females developed abdominal swellings caused by benign ovarian teratomas. Yoshida *et al.*,(2007) conclude that the activity of PLCζ is restricted to oocytes when low level expression is forced ectopically in multiple tissues, however the level of PLCζ in somatic tissues was not established. They suggest that the cellular machinery required to transduce PLCζ signalling is restricted to the tissues in which PLCζ is normally active. They propose that this may involve tissue specific accessory factors such as adaptors that bind PLCζ.

In 2008, Ito *et al.* published a paper which reported the difference in Ca^{2+} oscillation inducing activity and nuclear translocation ability of PLCζ between mouse, rat, human and medaka fish. PLCζ from all species was capable of inducing Ca^{2+} oscillations in mouse eggs with variable degrees of activity.

Species differences were observed in nuclear translocation experiments involving mouse and rat eggs. Unlike mouse; rat, human and medaka PLCζ did not accumulate in the pronucleus (PN) of mouse eggs. Also, rat PLCζ could not enter rat PN, whereas mouse could. Experiments involving the expression of PLCζ from these four animal species in COS cells also show apparent differences in their nuclear translocation ability. These differences however only partially reflect the observations reported in eggs. Mouse PLCζ was strongly accumulated in the nucleoli of COS cells at 48 hours after transfection as had been reported previously (Kuroda *et al.*, 2006). In contrast, rat PLCζ displayed a cytoplasmic distribution with no obvious signs of nuclear translocation. Despite their absence from the mouse PN, nuclear translocation was observed for both human and medaka PLCζ in COS cells. Ito *et al.*,(2008) suggest that the nuclear translocation of human PLCζ in COS cells may be due to the fact that human and monkey PLCζ share identical nuclear localisation sequences (NLS). They also propose that the nuclear translocation observed with medaka PLCζ could be a result of diffusion due to its relatively smaller size.

These data all suggest that a systematic investigation of PLCζ expression in somatic cells is warranted.

3.1.5 Objectives

The most suitable transfection technique and conditions for a particular cell type must be systematically and empirically determined because inherent properties of the cell influence the success of any specific transfection method. The preliminary aim of this chapter was to determine the most appropriate transfection techniques for examining the effects of transient expression of PLCζ in CHO cells, and for the eventual production of a stable cell line (Chapter 5). The advantages and disadvantages of a variety of commonly used transfection methods were compared together with a brief assessment of the applicability of the novel technique of sonoporation that has been used experimentally in our laboratory.

This chapter reports on the pattern of cellular localisation observed with eYFP-PLCζ, and examines the effect of transient PLCζ-LUC expression on Ca^{2+} homeostasis.

3.2 Results

3.2.1 Restriction digests of the DNA constructs

The constructs shown in this thesis were prepared by Michail Nomikos, Christopher Saunders, or in collaboration with Andreas Rossbach. Diagrammatic structural details of the DNA constructs are shown in Chapter 2 (section 2.2.1). Restriction digests were used to confirm successful ligation, and to ensure that the plasmids had not undergone any deletions or spontaneous recombination with the bacterial DNA during propagation. Digests of the DNA constructs with restriction enzymes yields several fragments of different molecular weights which can be identified after agarose gel electrophoresis and act as a 'fingerprint' for the complete recombinant plasmid. Figure 3.2.1 shows the predicted DNA cleavage fragments for each construct.

For the luciferase tagged constructs, EcoRI cuts once in the multiple cloning site of the pCR3 vector and once at the 587 position of luciferase sequence, resulting in two bands for each construct. The predicted size of the bands after digestion for the luciferase tagged constructs are 6156 and 587bp for pCR3-LUC, and 6156 and 2542bp for PLCζ-LUC (Figure 3.2.1).

For the eYFP construct, NcoI cuts three times in the pcDNA3.1 vector backbone at positions 610, 2751 and 3486, and once at position 860 of the eYFP insert, resulting in 4 bands. The predicted sizes of the bands after digestion are 3347bp, 1891bp, 735bp and 250bp (Figure 3.2.1).

For the eYFP-PLCζ and eYFP-^{D210R}PLCζ constructs, NcoI cuts three times in the pcDNA3.1 vector backbone at positions 610, 4727 and 5462, and three times at

A)

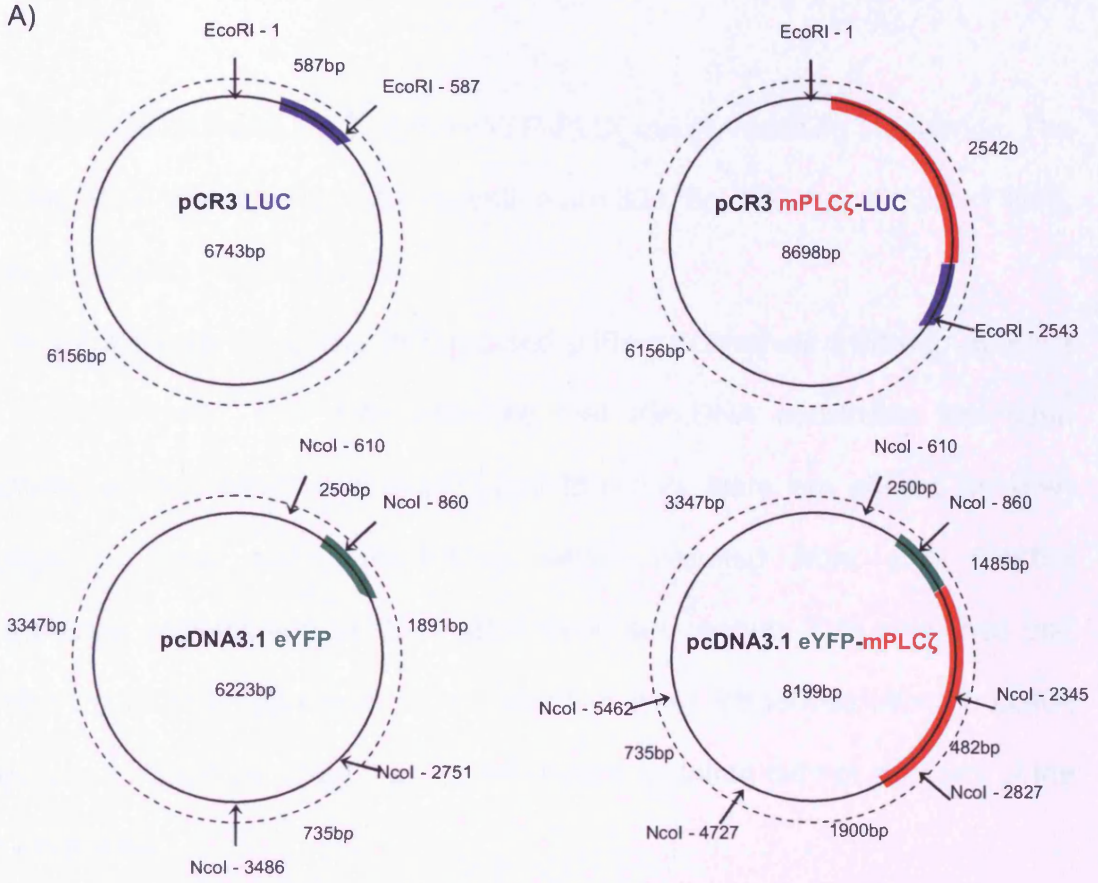

B)

DNA Construct	Restriction enzyme	Estimated Fragments (base pair)					
LUC	EcoRI	6156bp	587bp				
PLCζ-LUC	EcoRI	6156bp	2542bp				
eYFP	NcoI	3347bp	1891bp	735bp	250bp		
eYFP-PLCζ	NcoI	3347bp	1900bp	1485bp	735bp	482bp	250bp
eYFP-D210R-PLCζ	NcoI	3347bp	1900bp	1485bp	735bp	482bp	250bp

Figure 3.2.1 Predicted restriction fragments of the DNA constructs
A) Construct maps illustrating the restriction digest sites of the specified enzymes (represented by the black arrows) and the subsequent restriction fragment sizes (base pairs). The luciferase (LUC) reporter is indicated in blue, the enhanced yellow fluorescent protein (eYFP) reporter is indicated in green and mouse PLC zeta (mPLCζ) is indicated in red.
B) Summary of the expected sizes of the cleavage fragments for each of the DNA constructs.

positions 860, 2345 and 2827 of the eYFP-PLCζ insert, resulting in 6 bands. The predicted sizes of the bands after digestion are 3347bp, 1900bp, 1485bp, 735bp, 482bp and 250bp (Figure 3.2.1).

Figure 3.2.2 shows the characteristic band patterns observed following agarose gel electrophoresis. This data indicated that the DNA constructs had been generated in the correct orientation, and that they were not altered by DNA propagation. Base pair substitutions which resulted from site directed mutagenesis were verified by automated cycle sequencing. This confirmed that no other mutations apart from those intended were introduced into the cDNA sequence. It should be noted that the introduced mutation did not alter any of the restriction sites.

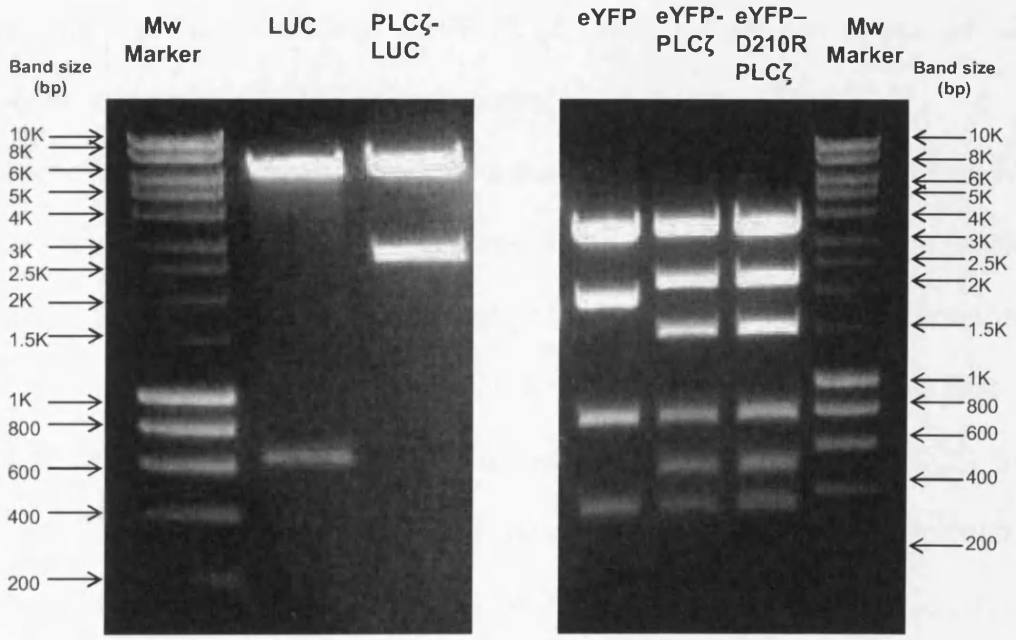

Figure 3.2.2 Restriction digest patterns of the DNA constructs
Figure 3.2.2 shows a 1% agarose gel demonstrating the characteristic restriction patterns obtained following enzymatic digestion of DNA maxi preps corresponding to positive clones of the constructs indicated above. Luciferase (LUC) and enhanced yellow fluorescent protein (eYFP) tagged constructs were digested using the EcoRI and NcoI restriction enzymes respectively. Molecular weight marker (Mw Marker = Hyperladder I).

3.2.2 Expression of the DNA constructs in mouse eggs

cRNA corresponding to luciferase tagged constructs were prepared (by Michail Nomikos) and microinjected (by Karen Campbell) in mouse eggs (Nomikos *et al.*, 2005). The left panel of figure 3.3A shows that the eggs injected with cRNA encoding PLCζ-LUC construct caused a series of Ca^{2+} oscillations in eggs that lasted several hours. At the end of the fluorescence recording interval, luminescence was measured from the same eggs (in the absence of fluorescence excitation) to confirm luciferase expression (Figure 3.3A right image).

cRNA corresponding to eYFP tagged constructs were prepared and microinjected (by Yuansong Yu) in mouse eggs. Figure 3.3B shows that the eggs injected with cRNA encoding eYFP-PLCζ also caused a series of Ca^{2+} oscillations in eggs that lasted several hours.

The X and Y domains of PLCζ contain the active residues 178His (Histidine), 210Asp (Aspratate) and 223His (Histidine) that have been shown to be involved in catalysis (Ellis *et al.*, 1993; Ellis *et al.*, 1998). These residues are conserved across all PLC families (Katan, 1998). DNA constructs containing the mutation of Aspartate at residue 210 in PLCζ to an arginine residue (D210R-PLCζ) have previously been injected into eggs and have failed to produce Ca^{2+} oscillations (Saunders *et al.*, 2002). This suggests that 210Asp is essential for PLCζ enzyme activity.

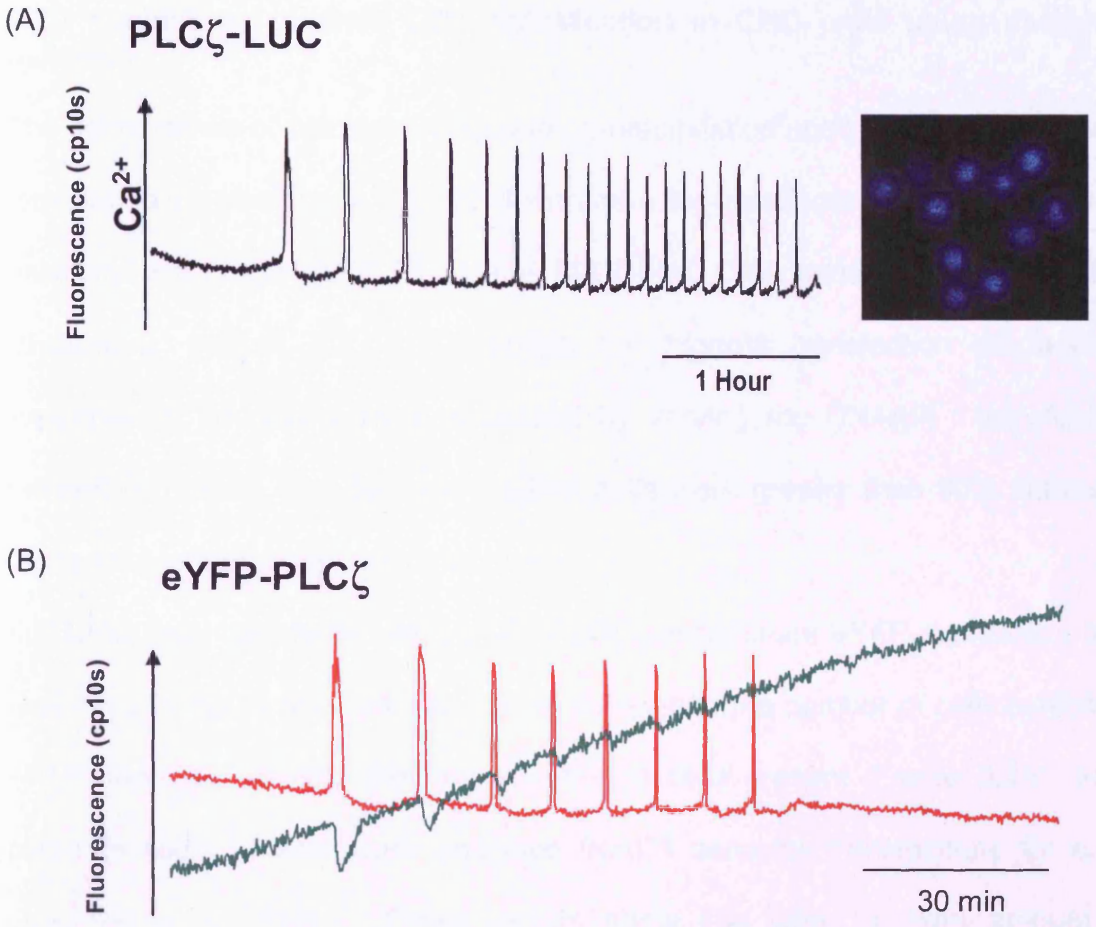

Figure 3.3 Eggs injected with PLCζ-LUC and eYFP-PLCζ.

(A) Eggs were injected with OGBD and cRNA encoding PLCζ-LUC. Left panel shows a representative fluorescence trace from a single egg showing the changes in intracellular Ca^{2+} levels that were measured continuously for 4 hours. The right panel shows an integrated image over 30 minutes of the luciferase luminescence signal from the same eggs from which Ca^{2+} measurments were taken. (Images courtesy of Karen Campbell) (Nomikos *et al.*, 2005).
(B) Eggs were injected with Fura 2 dextran and cRNA encoding eYFP-PLCζ. The red line represents the changes in intracellular Ca^{2+} levels from a single egg that was measured continuously for 2 hours. The green line represents the eYFP expression levels from the same egg. (Image courtesy of Yuansong Yu).

3.2.3 Optimising plasmid DNA transfection in CHO cells using chemical methods

The performance of calcium phosphate co-precipitation and the cationic liposome formulation Lipofectamine^{TM} 2000 (Invitrogen) for transfection of CHO cells was assessed using the eYFP-PLCζ and PLCζ-LUC DNA constructs (described in Chapter 2, section 2.2.5). To obtain the highest transfection efficiencies, experimental conditions were optimized by varying the DNA(μl) : transfection reagent (μl) ratios, and by ensuring that cells were greater than 90% confluent (as recommended by the manufacturer).

For CHO cells transfected with eYFP-PLCζ, recombinant eYFP expression was assessed 24 hours after transfection by comparing the number of cells exhibiting eYFP fluorescence with the total number of cells present (Figure 3.4A). Four separate fields of view were analysed from 3 separate transfections for each experimental condition. These results show that when a fixed amount of transfection reagent is used, it is possible to increase the expression levels of recombinant eYFP in CHO cells by increasing the DNA concentration from 2μg to 6μg (for Lipofectamine 2000) and 8μg (for calcium phosphate). An increase in the DNA concentration from 6μg to 8μg with Lipofectamine 2000 failed to enhance the levels of eYFP expression further. When comparing the eYFP expression levels obtained with both chemical transfection reagents, Lipofectamine 2000 resulted in superior transfection efficiencies for each of the DNA concentrations assessed. The expression levels of eYFP were increased significantly ($p<0.05$) by using Lipofectamine 2000, both for 4μg and 6μg of DNA.

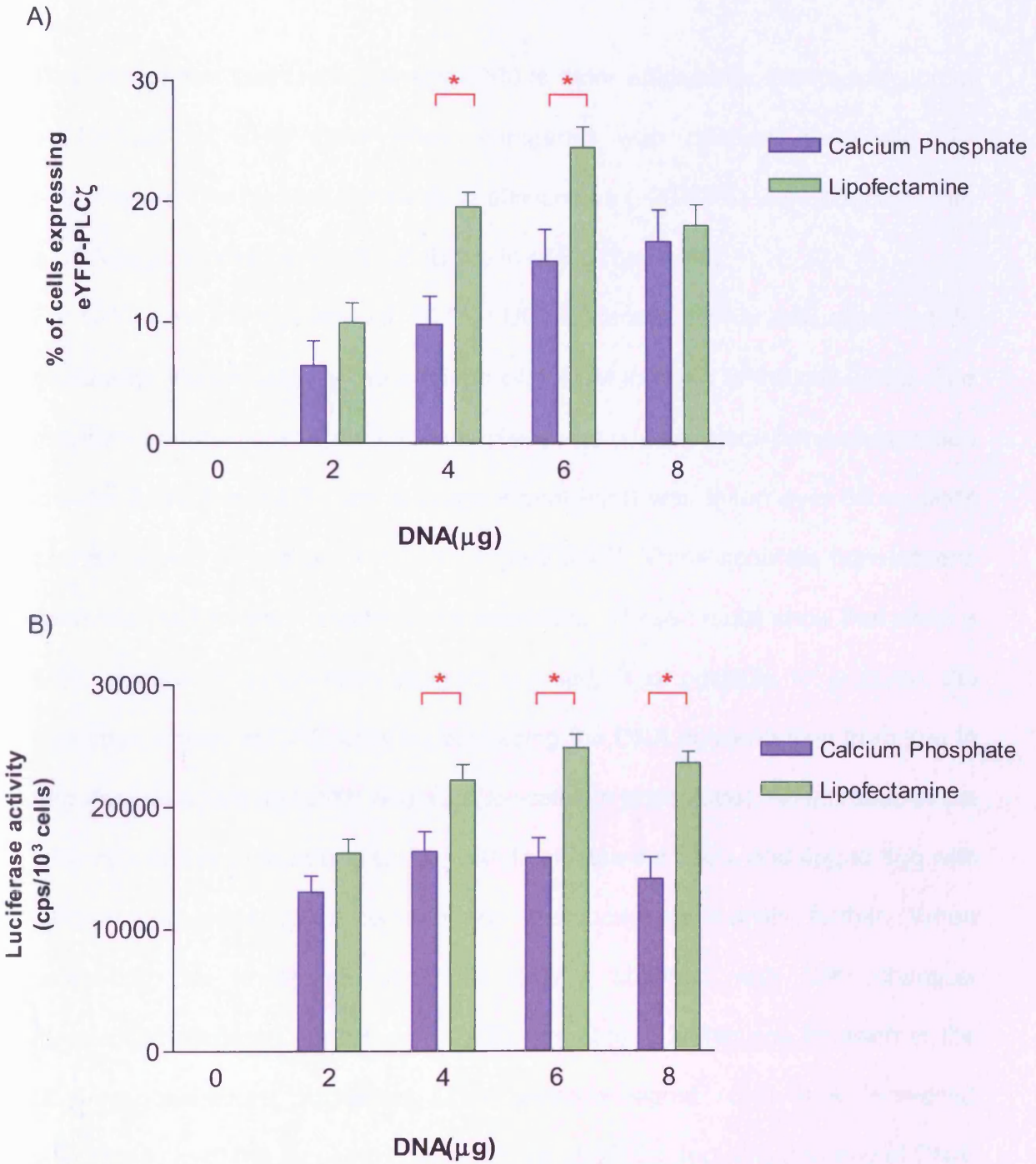

Figure 3.4 Calcium phosphate and Lipofectamine 2000 transfections of CHO cells
CHO cells were transfected with either the eYFP-PLCζ (A) or PLCζ-LUC (B) DNA construct using the standard calcium phosphate co-precipitation/ Lipofectamine 2000 protocol (as described in Chapter 2, section 2.2.5). For cells transfected with eYFP-PLCζ (A), the endogenous fluorescence of eYFP was used to determine the efficiency of plasmid transfection by comparison with the total number of cells present 24 hours after transfection. For cells transfected with PLCζ-LUC (B), cells were harvested 24 hours after transfection and assayed for luciferase activity (as described in Chapter 2, section 2.2.7). Data are presented as mean ± S.E.M. (n=3). cps denotes luminescent counts per second. * = $p<0.05$.

This data shows that Lipofectamine 2000 is more efficient for the transfection of eYFP-PLCζ in CHO cells when compared with calcium phosphate co-precipitation. The highest transfection efficiencies (~20-25%) were obtained with a DNA (μg) : Lipofectamine 2000 (μl) ratio of 3:5 (6μg:10μl).

For CHO cells transfected with PLCζ-LUC, luciferase activity was assessed 24 hours after transfection by the addition of 100μM luciferin to the cell lysate. The resultant bioluminescent reaction took place in a custom made luminometer (see chapter 2, section 2.2.7), the average signal (cps) was taken over 60 seconds and expressed as cps per 10^3 cells (Figure 3.4B). Three separate transfections were analysed for each experimental condition. These results show that when a fixed amount of transfection reagent is used, it is possible to increase the luciferase activity in CHO cells by increasing the DNA concentration from 2μg to 6μg (for lipofectamine 2000) and 4μg (for calcium phosphate). An increase in the DNA concentration from 6μg to 8μg with lipofectamine 2000, and 4μg to 8μg with calcium phosphate failed to enhance the luciferase activity further. When comparing the levels of luciferase activity obtained with both chemical transfection reagents, lipofectamine 2000 resulted in higher cps for each of the DNA concentrations assessed. The average signal (cps) was increased significantly ($p<0.05$) by using Lipofectamine 2000, for 4μg, 6μg and 8μg of DNA. This data shows that Lipofectamine 2000 is more efficient for the transfection of PLCζ-LUC in CHO cells when compared with calcium phosphate co-precipitation. The highest transfection efficiency, demonstrated by a luciferase activity of

~25,000 cps/10^3 cells was obtained with a DNA (μg) : Lipofectamine 2000 (μl) ratio of 3:5 (6μg:10μl).

Despite the optimisation of DNA transfection with both calcium phosphate and Lipofectamine 2000, initial imaging experiments revealed that cells displaying reporter gene expression were unevenly distributed throughout the cell culture dish and often failed to lie within close proximity to one another. This had a noticeable effect on the cells numbers obtainable for transient gene expression analysis in single fields of view. Figure 3.5 is representative of the typical cell numbers expressing PLCζ-LUC 24 hours following transfection with lipofectamine 2000. On average, ~20 cells per field of view were observed using a x10 magnification objective (Figure 3.5A). This combined with the integration time required to identify the cells displaying luciferase expression made it increasingly difficult to locate more than 1 or 2 cells per field of view when using an objective of higher magnification power (x40 oil immersion) (Figure 3.5B). Although well suited to experiments involving the generation of stable cell lines, due to the total number of cells transfected in a single culture dish (Chapter 5), these chemical transfection techniques do not appear to be suitable for the analysis of transient gene expression in this instance, especially if experiments require the use of higher magnification objectives.

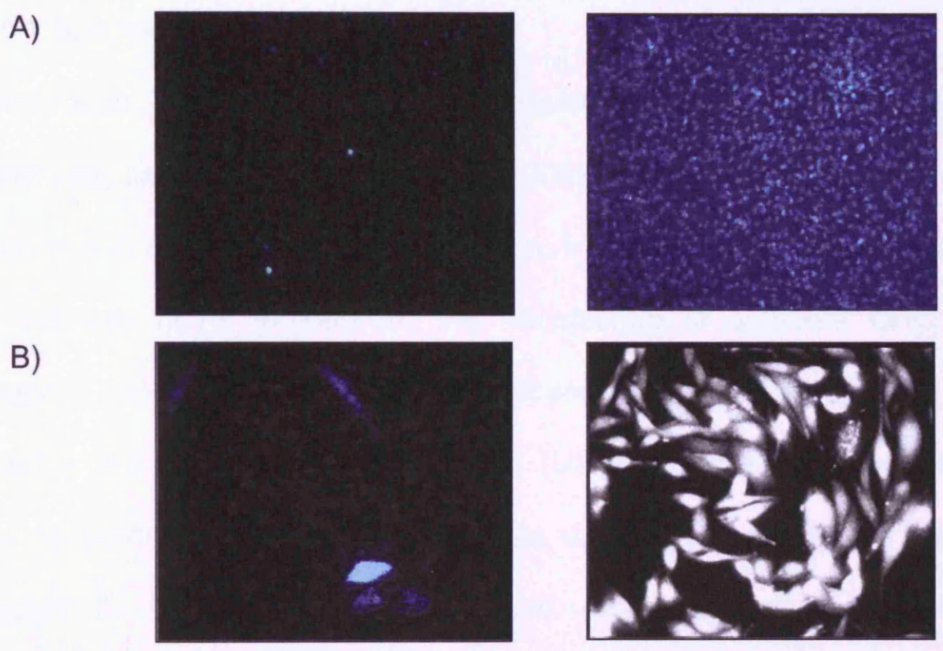

Figure 3.5 Expression of PLCζ-LUC in CHO cells following Lipofectamine 2000 mediated transfection

CHO cells were imaged for PLCζ-LUC expression 24 hours following lipofectamine 2000 mediated transfection, in a buffer containing 100μM luciferin using the Photek imaging system (as described in Chapter 2, section 2.2.6). Figure 3.4A is representative of the typical number of cells showing luciferase expression (Left panel) when imaged using a x10 magnification objective. Also shown in the panel on the right is the Hoechst fluorescence image of the same cells, demonstrating the total number of cells in the field of view. Figure 3.4B is representative of the optimal number of cells showing luciferase expression (Left panel) when imaged using a x40 oil immersion objective. The panel on the right is the Fluo 3 fluorescence image of the same cells, demonstrating the total number of cells in the field of view.

3.2.4 Optimising plasmid DNA transfection in CHO cells using physical methods

3.2.4.1 Sonoporation

Sonoporation has been used successfully in our laboratory to induce macromolecular uptake (Khanna *et al.*, 2006) and DNA transfection (unpublished observations) of CHO cells in suspension. In order to establish the suitability of this relatively novel method for the transfection of adherent CHO cells, an analogous experimental design was employed.

Firstly, a new ultrasonic standing wave (USW) minichamber was designed in order to accommodate glass cover slips upon which CHO cells were grown (Chapter 2, figure 2.4). The optimum parameters were established by assessment of the levels of FITC-dextran uptake together with the levels of cell viability (determined by propidium iodide staining). Optimisation of this technique involved varying the voltage intensity (40-80V), the duration of the ultrasound pulse (2sec-1min), cell density (50-100% confluency) and contrast agent concentration (2-10%).

Initial permeabilisation experiments seemed promising, with isolated areas of the glass coverslip displaying reasonable levels of FITC-dextran uptake with relatively little effect on cell viability as illustrated in Figure 3.6. Despite the non-uniform nature of the macromolecular uptake across the cover slip, positively labelled cells appeared in distinct regions and displayed increased proximity when compared to that of chemical transfection methodologies. It should be noted however that the levels of FITC-dextran uptake shown in Figure 3.6 were

not easily reproducible, and it is therefore unlikely that consistent transfection results could be achieved using this technique.

CHO cells were then exposed under these optimised experimental conditions (70% confluency, 40V, 2sec pulse length, 5% contrast agent) to a range of eYFP DNA concentrations (100ng-10µg). None of the DNA concentration tested resulted in transient eYFP expression in CHO cells when imaged over a 72 hour period following ultrasound exposure. This data suggests that further optimisation beyond the scope of this thesis is required to successfully transfect adherent CHO cells using the method of sonoporation.

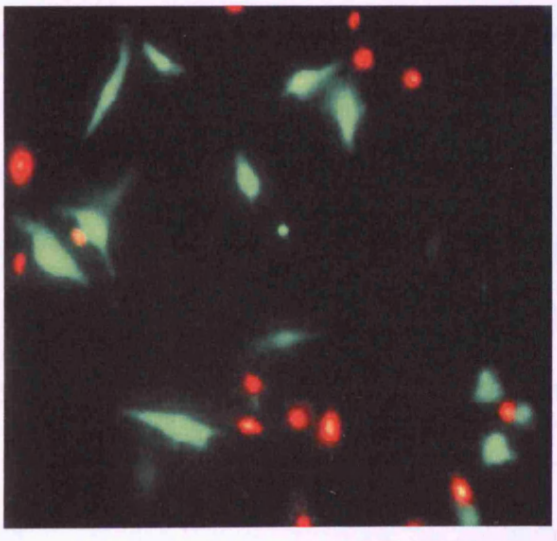

Figure 3.6 Sonoporation induced macromolecular uptake by adherent CHO cells

This figure shows a fluorescence image of adherent CHO cells demonstrating the optimum levels of FITC-Dextran uptake (Green) obtainable following ultrasound exposure (1.72MHz, 40V) for 2 seconds. Imaged using a x40 oil immersion objective. (The average cell count in a single area was ~50 cells). Cell viability was assessed using propidium iodide (shown in red). These distinct areas of FITC-dextran loaded cells were not seen uniformely throughout the glass coverslip, and were not easily reproducible.

3.2.4.2 Microinjection

Although less suitable for studies requiring large numbers of transfected cells, single cell microinjection permits the precise control of the amount, timing and location of delivery (Zhang *et al.*, 2008). This robust physical delivery method achieves high transduction efficiency in the majority of cell types, including cultured primary cells and oocytes.

The injection parameters that can be optimised when using the FemtoJet microinjector system include the injection pressure (Pi), injection time (Ti) and compensation pressure (Pc). The Pi is the pressure which is needed to drive the fluid from the capillary into the cells and together with the Ti determines the volume of the sample injected. It is crucial to use an optimal Pi; using a low Pi may result in inefficient injection while using higher Pi values risks damaging the internal structure of the cell. The Pc maintains a low positive pressure inside the capillary to prevent back filling of the needle, and is dependent upon the viscosity of the sample (Bartoli *et al.*, 1997).

Microinjection into adherent CHO cells was carried out under phase contrast microscopy, initially using ranges of Pi (50-100 hPa), Pc (20-70 hPa) and Ti (0.1-0.5 secs). Determination of the most suitable microinjection conditions was carried out in two stages. Firstly, FITC-dextran was used as a marker of successful injection. This was followed by the assessment of cell viability using propidium iodide. Cells were injected under phase microscopy using a range of times and pressures to find the optimal Pi, Pc and Ti parameters that did not cause cell damage such as prolonged deformation or cell rupture. Having

identified the optimal parameters, cDNA encoding eYFP was injected into the nuclei of CHO cells to verify that, under the microinjection conditions determined above, the cells remained viable and expression-competent.

Following extensive evaluation of specific microinjection protocols, optimal conditions for transfection efficiency and cell viability were determined at injection pressure (Pi) of 90 hPa, compensation pressure (Pc) of 80 hPa and an injection time (Ti) of 0.1 seconds. These conditions typically resulted in a transfection efficiency of >75% as depicted in Figure 3.7. Transfection efficiencies were determined by comparing the number of cells showing eYFP expression (Figure 3.7A) with the total number of cells successfully injected (indicated by Alexa 594-dextran fluorescence, Figure 3.7B). It can be seen that the intensity of Alexa 594 signal is not homogenous in all microinjected cells. The differences in signal could be an artefact of the heterogeneity of cell size and shape, but it is also possible that it is an indicator of the amount of sample injected into each of the cells. The levels of eYFP expression are also heterogeneous in all microinjected cells; however this does not appear to correlate with the intensity of the Alexa 594 signal, which suggests that expression levels may be determined by factors other than the amount of cDNA delivered into the cell. Figure 3.7C shows that cells that have undergone microinjection have a slightly ruffled appearance 3 hours after cDNA delivery. Despite this, the cells remain viable and are able to express recombinant eYFP for at least 48 hours.

Due to the precise control over the location of delivery using this technique, the number of cells available for fluorescence analysis in a single filed of view at

higher magnification is greatly improved when compared to the other transfection methodologies assessed during this study. Figure 3.7 is representative of the typical number of cells expressing recombinant eYFP 3 hours following microinjection when viewed using a x63 oil immersion objective.

This data suggests that microinjection is a suitable transfection technique for the analysis of transient gene expression, enabling the imaging of very large numbers of cells (15-25 cells per experiment, n = 4-6).

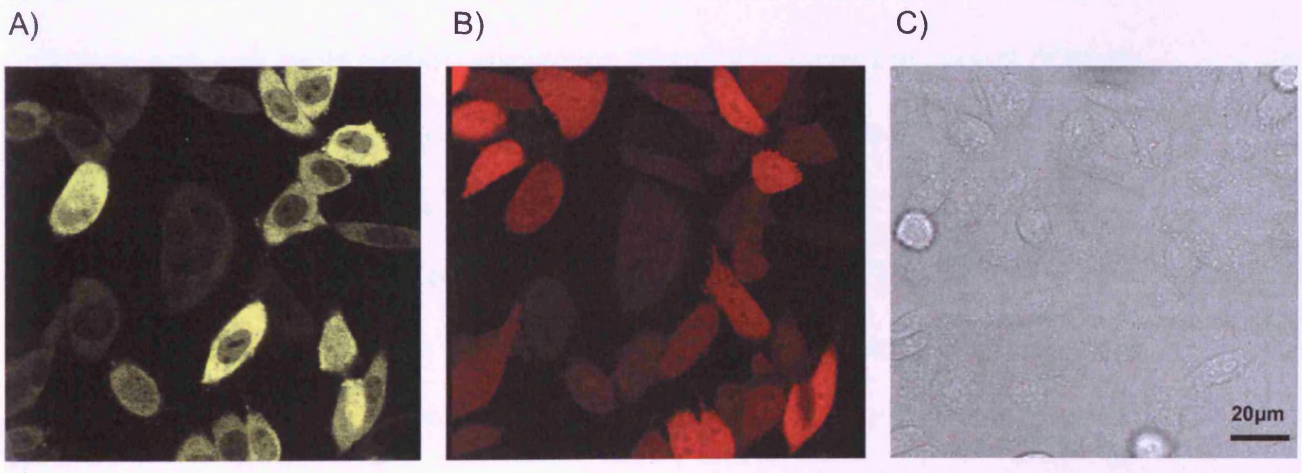

Figure 3.7 Microinjection of cDNA encoding eYFP into CHO cells

CHO cells imaged for eYFP expression (A) and Alexa 594-dextran fluorescence (B) using confocal microscopy (x63 magnification). (C) is a phase contrast image of the same field of view. Images were taken 3 hours after DNA microinjection.

3.2.5 Cellular localisation of eYFP-PLCζ

Previous studies have reported differing results in terms of the cellular localisation observed when expressing PLCζ in somatic cells. Coward *et al.*, (2006) report two main patterns of distribution; either grainy cytoplasmic distribution or nuclear distribution, and suggest that this could be linked to cell cycle events. Others describe an active import into the nucleus of somatic cells, which is considered to be a time (Kuroda *et al.*, 2006) or species (Ito *et al.*, 2008) dependent phenomenon. The lipid mediated transfection techniques employed in all of these studies have the disadvantage of being unable to permit the precise control of timing and amounts of exogenous material introduced into the cell. An optimised and well controlled microinjection strategy enables the control of these parameters, allowing a more defined time course analysis of the cellular translocation of recombinant expression.

DNA constructs encoding eYFP, eYFP-PLCζ and eYFP-^{D210R}PLCζ were successfully microinjected into CHO cells, using the parameters described above (3.2.4.2). The use of Alexa-594 conjugated dye enabled the easy visual detection of microinjected cells without interference of the eYFP fluorescent signal. Injected cells were visualised using confocal microscopy 3, 5, 24 and 48 hours following the delivery of the DNA.

Figure 3.8 shows that high levels of recombinant eYFP expression were detected as early as three hours after DNA delivery and persisted for at least 2 days, for all of the DNA constructs examined. The expression of eYFP alone (Figure 3.8, top panel) showed that the fluorescent signal in the cells nucleus was

comparable to that in the cytoplasm of 100% of the cells analysed. This pattern of localisation remained unchanged throughout all of the time points examined. This suggests that eYFP passively diffuses into the nucleus of somatic cells. eYFP was not accumulated in the nucleoli of CHO cells, as indicated by black spots in the nucleus.

eYFP-PLCζ dislayed two distinct patterns of localisation over the duration of the time course experiment (Figure 3.8, bottom panel). At 3 and 5 hours following DNA delivery, 100% of cells showed a clear cytoplasmic distribution, with no sign of obvious nuclear translocation. In contrast to this, at 24 hours the majority of cells (~78%) show noticeable nuclear translocation. Particularly, the fluorescence in the nucleoli was strikingly enhanced. At 48 hours, the majority of cells (~82%) also showed obvious nuclear translocation, however at this later time point the eYFP signal in the nucleoplasm was comparible to that of the nucleoli. The cells that did not show obvious nuclear translocation at 24 and 48 hours maintained a clear cytoplasmic distribution identical to that observed at 3 and 5 hours. This data suggests that the nuclear import of PLCζ is relatively slow, while PLCζ that entered the nucleoplasm is concentrated to nucleoli.

For eYFP-^{D210R}PLCζ (Figure 3.8, centre panel) the pattern of cellular localisation 3 and 5 hours following DNA delivery was comparable to that of eYFP-PLCζ, with 100% of the cells showing a clear cytoplasmic distribution. Unlike eYFP-PLCζ, eYFP-^{D210R}PLCζ did not show any obvious signs of nuclear accumulation at later time points (24/48 hours), and the majority of cells (>90%) maintained the same

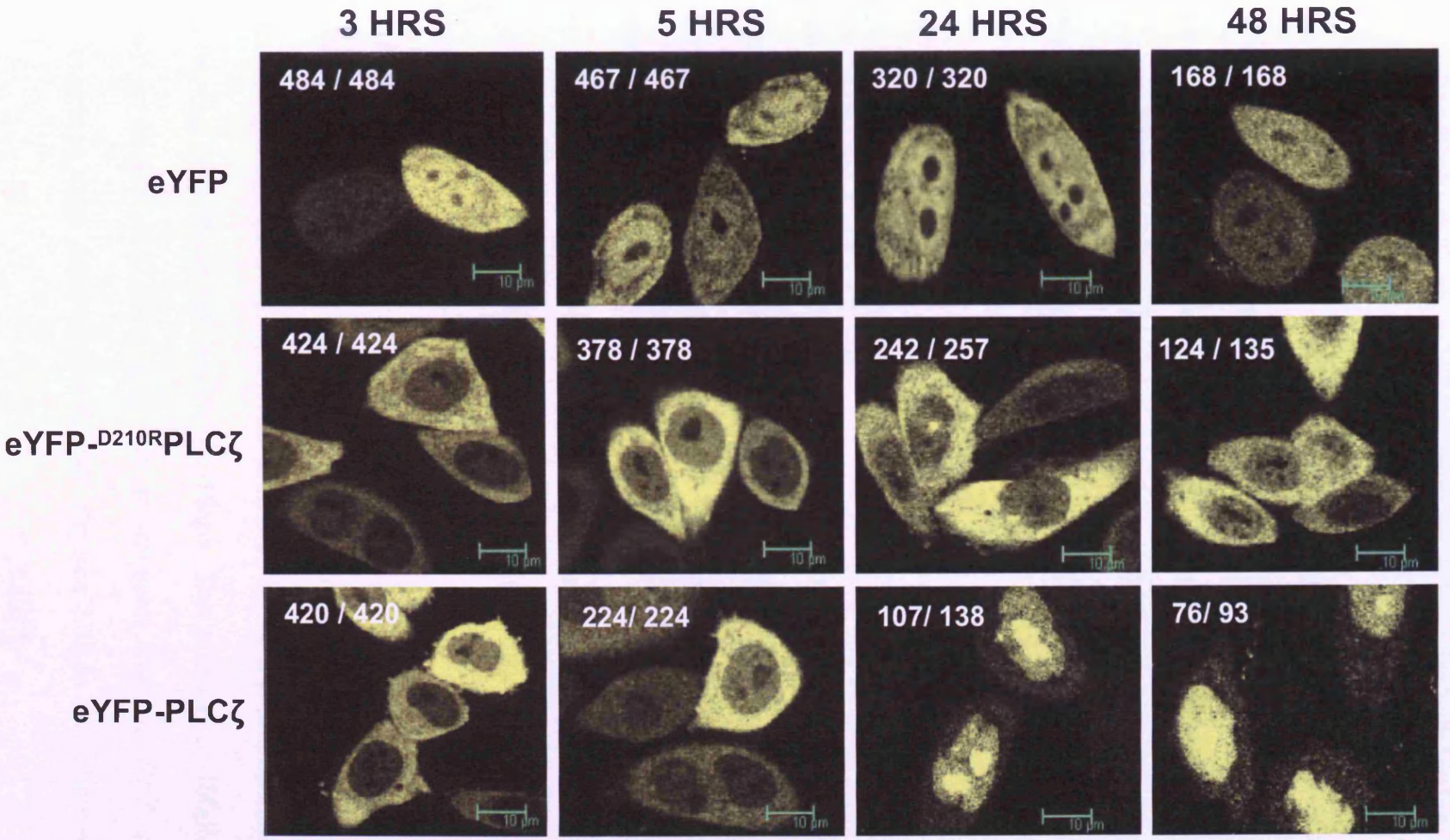

Figure 3.8 Cellular localisation of PLCζ and its inactive D210R mutant in CHO cells.

Confocal images acquired at the indicated time after microinjection of respective cDNA. Each image is representative of the pattern of localisation observed in the majority of cells at each time point. The number of cells displaying the indicated pattern of localisation is shown in white alongside the total number of cells analysed in each instance. Scale bar represents 10µm.

cytoplasmic localisation. The remaining cells displayed a less obvious cytoplasmic accumulation, whereby the fluorescent signal in the cytoplasm was comparable to that of the nucleus; however they showed no distinct pattern of nuclear translocation. This data suggests that the nuclear accumulation of PLCζ may be linked to its activity in somatic cells, as the inactive D210R mutant fails to show any signs of nuclear translocation.

3.2.6 Ca^{2+} in CHO cells expressing PLCζ-LUC

Calcium oscillations induced by PLCζ expression have previously been reported in somatic cells (Kuroda *et al.*, 2006). Here, CHO cells were injected with cDNA encoding LUC or PLCζ-LUC together with the fluorescent indicator Oregon Green Bapta Dextran (OGBD) to measure Ca^{2+}. The image in Figure 3.9 shows a group of cells that were both luminescent (representing recombinant expression) and fluorescent (used as a marker of successful microinjection in addition to measurement of intracellular Ca^{2+}).

Intracellular Ca^{2+} was measured in cells 3, 5 and 24 hours following microinjection. The average luminescence recorded in single CHO cells expressing PLCζ-LUC ranged from 1-10cps, whilst the luminescence in cells expressing LUC alone ranged from 1-15cps. The addition of 100μM ATP was used to assess the cells response to receptor induced Ca^{2+} mobilisation (Examined in more detail in Chapter 4). Figures 3.10 to 3.12 show examples of

the Ca^{2+} changes observed in some, but not all cells at 3, 5 and 24 hours respectively. Table 3.1 summarises the results of these experiments, indicating

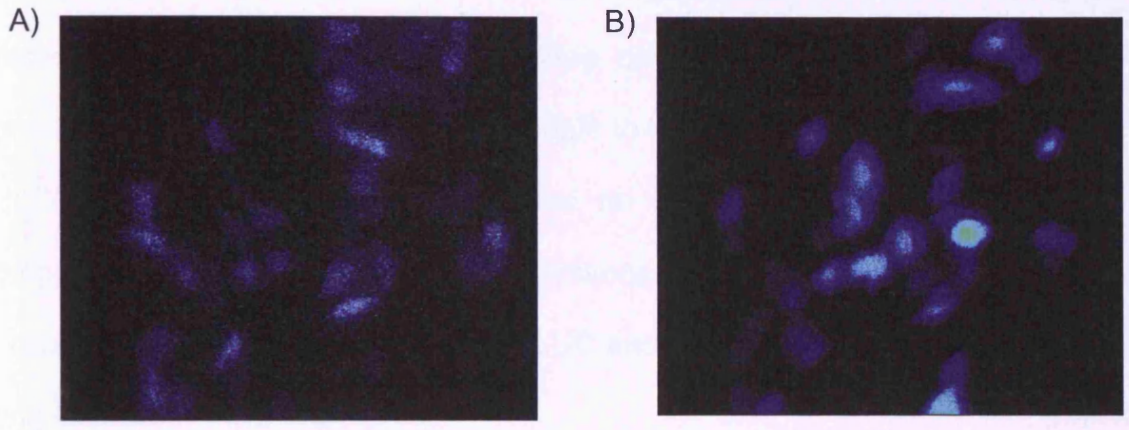

Figure 3.9 Luminescence and Fluorescence in the same cells

The luminescence (A) and fluorescence (B) images are shown of a group of CHO cells that had been injected with cDNA encoding PLCζ-LUC and OGBD.

the proportion of cells displaying Ca^{2+} oscillations, the frequency of the oscillations and the proportion of cells presenting a response to the addition of ATP.

Ca^{2+} oscillations were recorded in <40% of cells expressing PLCζ-LUC at 3, 5 and 24 hours following microinjection of cDNA. The centre panels of figures 3.10 to 3.12 show representative traces of typical pattern of oscillations observed. Statistical analysis revealed no significant change in the frequency of the oscillations between the individual time-points analysed (Table 3.1).

Tables 3.1 shows that a comparable proportion of cells (~30-35%) either expressing LUC alone or injected with OGBD also show Ca^{2+} oscillations at 3, 5 and 24 hours. Figures 3.10 to 3.12 show representative traces of the typical pattern of oscillations observed in these cells. The frequencies of the Ca^{2+} oscillations recorded were also comparable to those observed in cells expressing PLCζ-LUC. Statistical analysis revealed no significant changes in either the proportion of cells displaying Ca^{2+} oscillations or the frequencies at which they occur between cells expressing PLCζ-LUC and either of the control groups (LUC and OGBD).

Table 3.1 shows that almost all cells (>99%) show a response to the addition of ATP (100μM). Examples of the typical Ca^{2+} changes observed as a result of this purinergic receptor stimulation are shown in figures 3.10 to 3.12. Statistical analysis revealed that the expression of PLCζ-LUC did not alter the proportion of cells showing a response to ATP induced Ca^{2+} mobilisation.

This data suggests that the Ca^{2+} oscillations observed in CHO cells are not induced specifically by the expression of PLCζ-LUC, and a more likely to be as a result of spontaneous Ca^{2+} activity within the somatic cell line. The expression of PLCζ-LUC does not appear to affect receptor induced Ca^{2+} mobilising, suggesting that the cells Ca^{2+} signalling network remains unchanged. It is possible however that the expression of PLCζ induces subtle changes in the Ca^{2+} homeostasis of somatic cells that are not apparent without more detailed analysis (See Chapter 4).

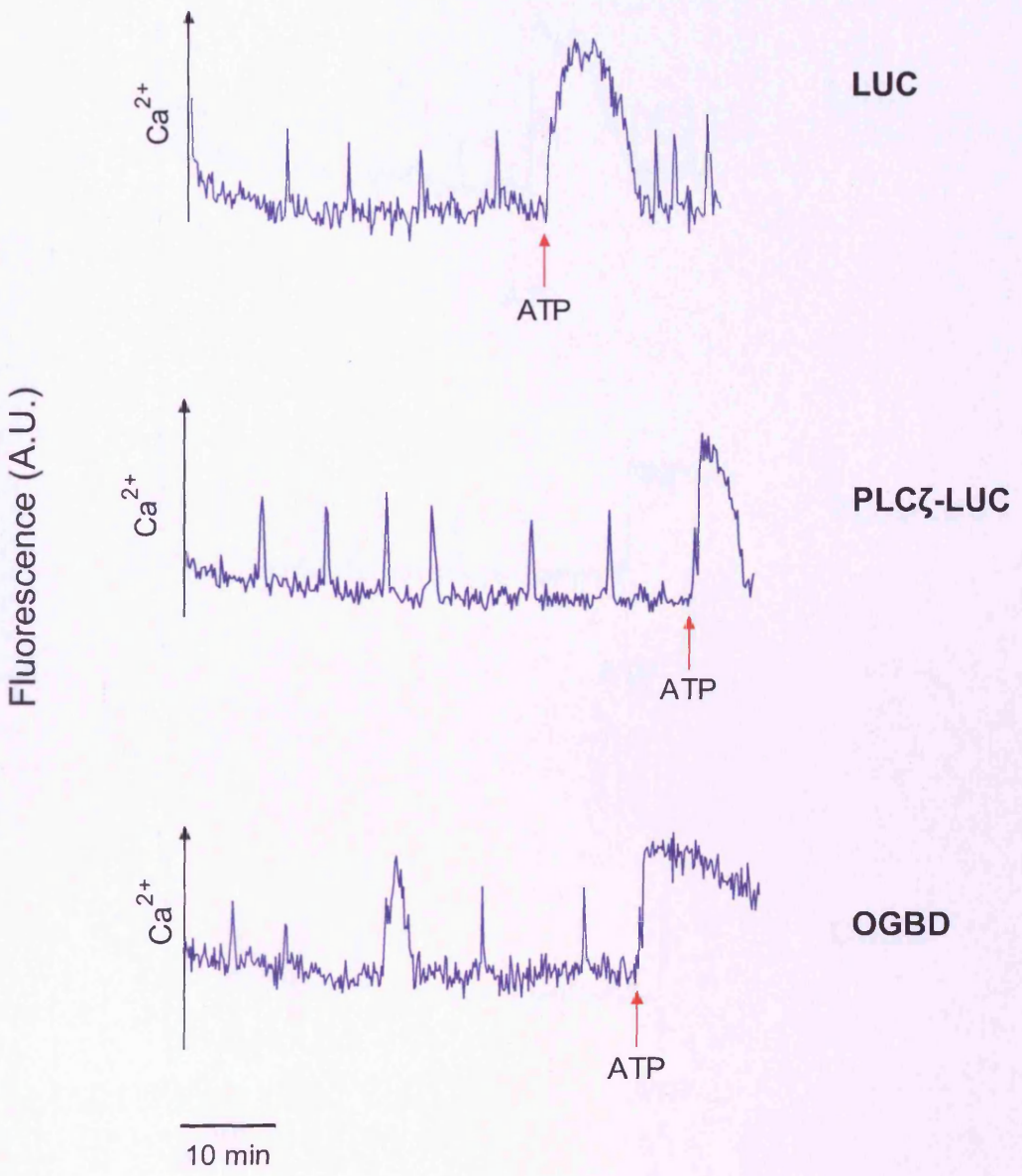

Figure 3.10 Ca^{2+} changes observed in CHO cells 3 hours following microinjection

CHO cells were microinjected with the fluorescent Ca^{2+} indicator OGBD (0.5mM) together with cDNA encoding LUC (top panel) or PLCζ-LUC (centre panel). Cells were also injected with OGBD alone (bottom panel). The traces are representative of typical Ca^{2+} changes observed in some, but not all cells within each experimental group. Cells were imaged for OGBD fluorescence for at least 30 minutes prior to the addition of ATP (100μM, red arrow).

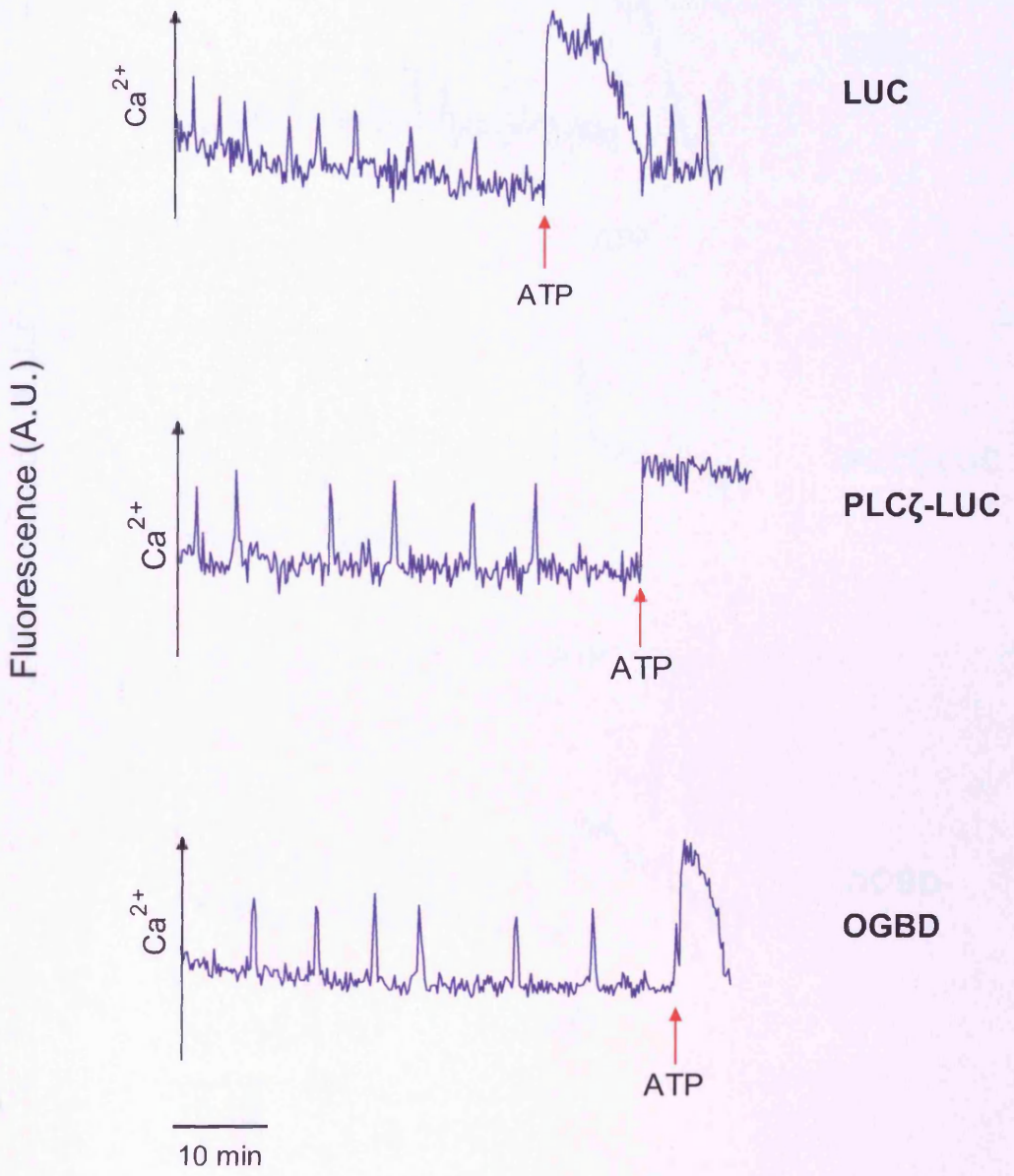

Figure 3.11 Ca^{2+} changes observed in CHO cells 5 hours following microinjection

CHO cells were microinjected with the fluorescent Ca^{2+} indicator OGBD (0.5mM) together with cDNA encoding LUC (top panel) or PLCζ-LUC (centre panel). Cells were also injected with OGBD alone (bottom panel). The traces are representative of typical Ca^{2+} changes observed in some, but not all cells within each experimental group. Cells were imaged for OGBD fluorescence for at least 30 minutes prior to the addition of ATP (100μM, red arrow).

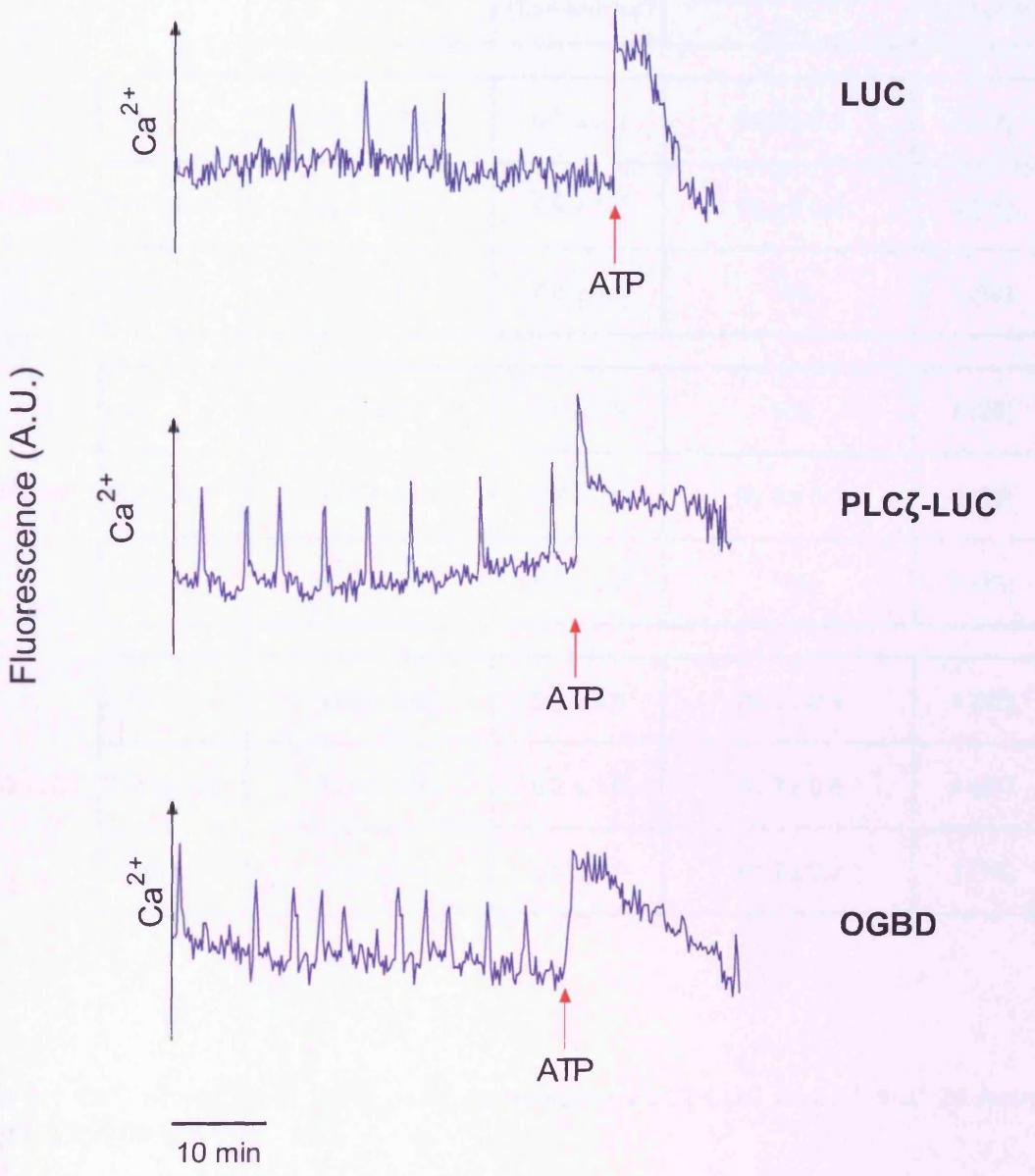

Figure 3.12 Ca^{2+} changes observed in CHO cells 24 hours following microinjection

CHO cells were microinjected with the fluorescent Ca^{2+} indicator OGBD (0.5mM) together with cDNA encoding LUC (top panel) or PLCζ-LUC (centre panel). Cells were also injected with OGBD alone (bottom panel). The traces are representative of typical Ca^{2+} changes observed in some, but not all cells within each experimental group. Cells were imaged for OGBD fluorescence for at least 30 minutes prior to the addition of ATP (100μM, red arrow).

		Proportion of cells showing oscillations (%)	Frequency (Spikes/hour)	Proportion of cells responding to ATP (%)	n number (total cells)
3 HOURS	LUC	35.1 ± 3.6	6.9 ± 0.9	99.8 ± 0.3	4 (47)
	PLCζ-LUC	36.0 ± 3.0	7.9 ± 1.0	99.3 ± 0.5	4 (45)
	OGBD	31.9 ± 3.7	7.0 ± 0.7	100	3 (18)
5 HOURS	LUC	25.1 ± 8.6	6.0 ± 0.9	100	4 (29)
	PLCζ-LUC	31.0 ± 3.2	5.7 ± 0.6	99.8 ± 0.3	4 (50)
	OGBD	31.1 ± 5.9	6.0 ± 0.9	100	3 (13)
24 HOURS	LUC	31.0 ± 4.8	5.9 ± 0.8	99.0 ± 0.4	4 (22)
	PLCζ-LUC	33.4 ± 3.9	6.2 ± 1.0	99.0 ± 0.6	4 (21)
	OGBD	29.0 ± 2.4	6.5 ± 0.8	99.3 ± 0.3	3 (14)

Table 3.1 Ca^{2+} changes in CHO cells expressing PLCζ-LUC at 3, 5 and 24 hours following microinjection.

CHO cells were injected with OGBD and cDNA encoding LUC or PLCζ-LUC. Cells were also injected with OGBD alone. Cells were imaged for OGBD fluorescence at 3, 5 and 24 hours following microinjection. Data is given as mean ± S.E.M. n= the number of experimental runs. The total number of cells analysed is shown in parentheses.

3.2.7 Resting intracellular Ca^{2+} levels in cells expressing PLCζ-LUC

Basal Ca^{2+} levels in cells expressing PLCζ-LUC were calculated from OGBD fluorescence data using the following equation:

$$[Ca^{2+}] = K_d\ (F - F_{min})/(F_{max} - F)$$

(Grynkiewicz *et al.*, 1985)

Where K_d, the dissociation constant for the rate of Ca^{2+} dissociation from OGBD in the cell cytoplasm was taken from the published value of 430nM (Thomas *et al.*, 2000). F_{max} and F_{min} represent maximum and minimum fluorescence signals respectively, and F represents fluorescent signal at any time. F_{max} was the peak fluorescence after the addition of ionomycin (5μM) (Figure 3.13). Ionomycin is a pore forming ionophore which mobilises intracellular Ca^{2+}, enabling the calibration of the Ca^{2+} dependent fluorescence of OGBD. F_{min} was approximated to be zero since the fluorescence of OGBD is extremely low in the absence of Ca^{2+} (Molecular probes). Figure 3.14 shows that the expression of PLCζ-LUC in CHO cells does not affect the resting intracellular Ca^{2+} levels when compared with cells expressing LUC or cells injected with OGBD. This data suggests that the expression of PLCζ in somatic cells has no obvious effect on resting intracellular Ca^{2+} or spontaneous Ca^{2+} oscillations.

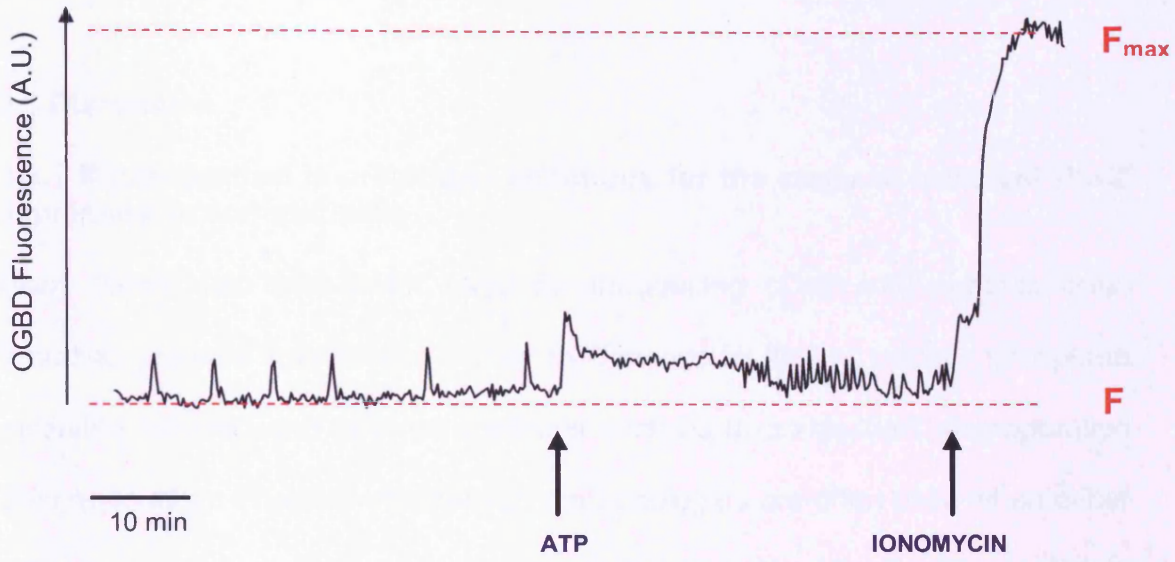

Figure 3.13. Determination of maximal (F_{max}) Ca^{2+} dependent intracellular OGBD fluorescence.
F_{max} was determined at the end of each experiment by the addition of the ionophore ionomycin (5μM). This value in conjuction with the initial fluorescence (F), were used to calculate the resting intracellular Ca^{2+} concentration.

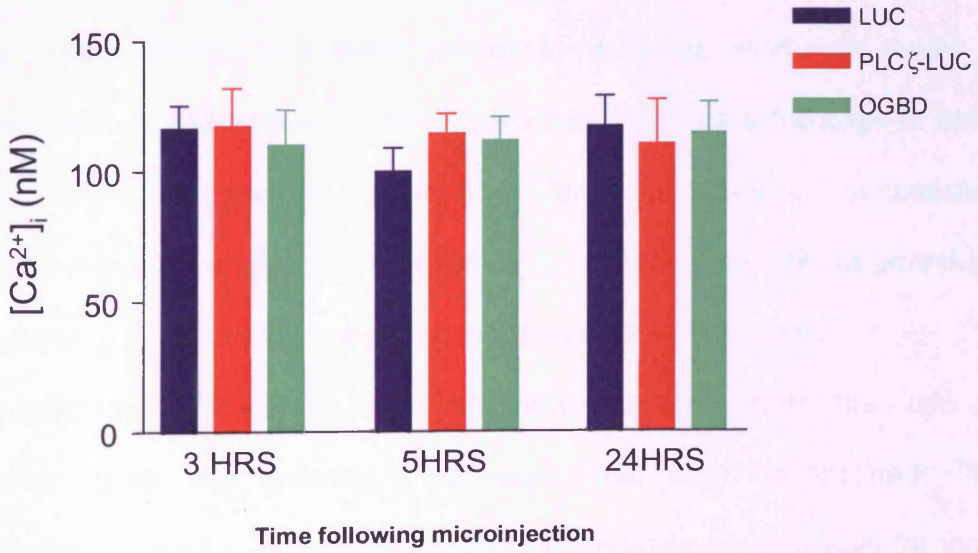

Figure 3.14 Resting intracellular Ca^{2+} levels in CHO cells expressing PLCζ-LUC
Resting intracellular Ca^{2+} levels were calculated by the method detailed in section 3.2.7. Intracellular Ca^{2+} levels of cells expressing PLCζ-LUC (red) were compared with that of cells expressing LUC alone (blue) and cells injected with OGBD only (green). Data are given as mean ± S.E.M (n=>3, 5-10 cells per experiment).

3.3 Discussion

3.3.1 Microinjection is a suitable technique for the study of transient PLCζ expression in somatic cells

Many techniques have been used for introducing cDNA into somatic cells, including chemical transfection (either by commercial lipid or calcium phosphate mediated transfer) and physical methods such as microinjection, elecroporation or sonoporation. Physical transfection methodologies are often used when either lipid or chemical mediated transfection is not possible (e.g. for expression in primary cells) and are not always considered to be the optimal choice for use in cell lines for various reasons, depending on the nature of the study. For example, microinjection cannot practically be used for expression in large populations of cells such as when attempting to establish a stably transfected cell line.

Calcium phosphate and lipid mediated transfer using Lipofectamine 2000 were optimised in this study, and were shown to generate moderate levels of recombinant protein expression. These techniques offer the advantage of being rapid and simple to perform, generating large numbers of successfully transfected cells with minimal effort. However, such techniques fail to permit the precise control of the amount, timing and location of cDNA delivery.

High transfection efficiencies were routinely obtained with the use of microinjection once the optimised conditions had been established. This technique offers control over the timing of cDNA delivery which allows for more accurate time course analysis in transient expression studies. Also, the proximity of cells displaying recombinant protein expression was greatly improved which enabled the analysis of larger cell numbers.

3.3.2 Cellular localisation of PLCζ in somatic cells appears to be dependent upon time after transfection

Macromolecular transport between the nucleus and cytoplasm of eukaryotic cells occurs via large multi-protein structures termed nuclear pore complexes (NPCs) that are embedded in the nuclear envelope (Suntharalingam *et al.*, 2003; Tran *et al.*, 2006). Passive diffusion of molecules ≤ 40kDa through NPCs does occur, however most macromolecules require specific transport signal sequences to enter and exit the nucleus via the NPC (Lange *et al.*, 2007). Many proteins contain predicted nuclear localisation signal (NLS) and nuclear export signal (NES) sequences which are required for entering and exiting the nucleus. These targeting signals consist of a weak consensus of three to four hydrophobic residues which are often identified by computer searches (Pemberton *et al.*, 2005).

The site or region of the PLCζ molecule responsible for its nuclear translocation ability has been shown to include residues 374-381 in the X/Y linker region, in which the basic amino acids Arg^{376}, Lys^{377}, Arg^{378}, Lys^{379} and Lys^{381} are considered essential (Kuroda *et al.*, 2006). Nuclear accumulation of PLCζ in somatic cells was reported to be a slow process, demonstrated by increasing levels of PLCζ-Venus in the nucleoplasm of COS cells between 48 and 72 hours following lipid mediated transfection (Kuroda *et al.*, 2006). The results in this chapter demonstrate a more marked increase in nuclear localisation with time after transfection, with CHO cells showing no obvious nuclear accumulation until 24 hours after cDNA delivery by microinjection. This data also suggests that the

transport of PLCζ into the nucleus of somatic cells is a gradual process dependent upon time after transfection.

It must be noted however that not all cells display an obvious pattern of nuclear accumulation at 24 and 48 hours following microinjection. Approximately 20% of cells have a distinct cytoplasmic distribution identical to the pattern observed at earlier time points. (Coward *et al.*, 2006) also reported this cytoplasmic pattern of distribution in somatic cells 48 hours following transfection of PLCζ, and suggest that it may be linked to cell cycle events. This is an interesting theory that supports the proposal that the nuclear localisation of PLCζ observed in mouse zygotes and early embryos (Halet *et al.*, 2004; Sone *et al.*, 2005; Yoda *et al.*, 2004) may explain the cell cycle dependent regulation of Ca^{2+} oscillations after fertilisation (Halet *et al.*, 2004; Sone *et al.*, 2005).

PLCδ1 has a nuclear import signal at a lysine-rich sequence in the C terminus of the X domain (Okada *et al.*, 2002); however it is not accumulated to the PN (Yoda *et al.*, 2004) or the nucleus (Yamaga *et al.*, 1999). Nuclear import and export is balanced due to the existence of an export signal at a leucine rich sequence in EF1 (Kuroda *et al.*, 2006; Yamaga *et al.*, 1999). Kuroda *et al.*, (2006) propose that I31-C43 in EF1 of PLCζ may correspond to the export signal sequence of PLCδ1, however this has not been experimentally verified. Should PLCζ contain a nuclear export signal, then differences in the rate of nuclear import and export may account for the two distinct patterns of cellular localisation observed.

3.3.3 PLCζ expression has no obvious effect on intracellular Ca^{2+} homeostasis in somatic cells

PLCζ expression has been reported to induce Ca^{2+} oscillations in ~70% of COS cells 24 hours following transfection, whilst the expression of D210R was without effect (Kuroda *et al.*, 2006). This observation was made from a relatively small experimental group, with less than 20 cells in each category. In contrast to this, the results of this chapter suggest that the expression of PLCζ has no effect on the cellular Ca^{2+} homeostasis of somatic cells. The oscillations recorded in cells expressing PLCζ were found to be present in a comparable proportion of cells in both control groups (i.e. cells expressing LUC alone, and cells injected with OGBD). Statistical analysis revealed no differences in the frequency of the oscillations observed, either between experimental groups or between each of the time points examined. CHO cells expressing PLCζ also retained a response to receptor induced Ca^{2+} mobilisation, and resting Ca^{2+} levels were unaffected. It is possible that the oscillations observed are induced by the method of microinjection, or they could be due to spontaneous Ca^{2+} activity within this cell type. Calcium signalling is believed to play a crucial role in driving cells through different stages of the cell-division cycle (Kao *et al.*, 1990; Poenie *et al.*, 1985). For example, a surge in Ca^{2+} controls the nuclear envelope breakdown and exit from mitosis in eggs (Steinhardt *et al.*, 1988). Changes in intracellular Ca^{2+} have also been shown to characterise the metaphase-anaphase transition (Poenie *et al.*, 1986; Ratan *et al.*, 1986) and G1/S phase transition (Russa *et al.*, 2009) in some somatic cells, however the significance of these Ca^{2+} changes in the cell

cycle remains to be determined. There is no evidence to suggest that the oscillations observed in this study are a direct result of PLCζ expression. These results show that PLCζ appears to have no obvious effect on intracellular Ca^{2+} homeostasis in somatic cells, irrespective of its cellular localisation, which suggests that its activity is specific to oocytes.

CHAPTER 4
INVESTIGATING THE EFFECTS OF PLCζ EXPRESSION ON RECEPTOR INDUCED Ca^{2+} MOBILISATION AND HOMEOSTASIS

CHAPTER 4 INVESTIGATING THE EFFECTS OF PLCζ EXPRESSION ON RECEPTOR INDUCED Ca^{2+} MOBILISATION AND HOMEOSTASIS

4.1 Introduction

4.1.1 Analysis of agonist induced Ca^{2+} transients

This study investigates the intracellular Ca^{2+} ($[Ca^{2+}]_i$) changes induced by adenosine triphosphate (ATP) in CHO cells expressing PLCζ. $[Ca^{2+}]_i$ was measured with the fluorescent Ca^{2+} indicator Fluo 3 in single cells (Chapter 2, section 2.2.8.1). The proposal is that a change in agonist-induced Ca^{2+} release will be evident if there is any major alteration of the $InsP_3$ signalling pathway.

In addition to its important role in cellular metabolism, ATP has also been shown to act as an extracellular signalling molecule (Burnstock, 1990; Dubyak *et al.*, 1993). ATP acts on many receptors including P_2-purinergic receptors which have been classified into two main subtypes on the basis of their agonist and antagonist selectivity, and their molecular structure (for reviews see (Fredholm *et al.*, 2000; Khakh, 2001; von Kugelgen *et al.*, 2000). P_{2X} receptors are ligand-gated ion channels which conduct Na^+ and Ca^{2+} from the extracellular medium. To date, seven separate genes coding for P_{2X} subunits have been identified and named as P_{2X1} through to P_{2X7} (Gever *et al.*, 2006; North, 2002). P_{2X} receptor subunits are comprised of two transmembrane spanning domains connected by a large extracellular loop, with intracellular carboxyl and amino termini. ATP binds to the extracellular loop of the P_{2X} receptor, resulting in a conformational change in the structure of the ion channel that causes the opening of the ion-permeable pore allowing cations to enter the cell. In contrast, P_{2Y} receptors are

G-protein coupled receptors (GPCRs), with a structure comprising seven transmembrane helices. To date, eight mammalian P_{2Y}-receptors have been identified that have been subdivided into the five $G_{(q)}$-coupled subtypes (P_{2Y1}, P_{2Y2}, P_{2Y4}, P_{2Y6}, P_{2Y11}), and three $G_{(i)}$-coupled subtypes (P_{2Y12}, P_{2Y13}, P_{2Y14}) linking them with phosphoinositide and adenylate cyclase metabolism respectively (von Kugelgen, 2006). The $G_{(q)}$ protein is a heterotrimeric G protein subunit that activates phospholipase C (PLC). PLC hydrolyses PIP_2 resulting in the formation of two second messengers, DAG and $InsP_3$ (Berridge, 1993; Putney *et al.*, 1993). DAG activates protein kinase C (PKC), and $InsP_3$ binds to $InsP_3R$ on the ER which leads to Ca^{2+} release (Ferris *et al.*, 1989; Maeda *et al.*, 1991). With prolonged P_{2Y} receptor activation, there is an associated Ca^{2+} influx in response to Ca^{2+} store depletion which is referred to as capacitative Ca^{2+} entry (CCE).

It has been shown that CHO cells endogenously express P_{2Y1}, P_{2Y2} and P_{2X7} receptors (Iredale *et al.*, 1993; Marcet *et al.*, 2003; Marcet *et al.*, 2004; Michel *et al.*, 1998). In populations of CHO cells, the addition of ATP results in a rapid increase in intracellular Ca^{2+} followed by a slowly declining secondary (plateau-like) phase. Omission of Ca^{2+}, and inclusion of a non-specific calcium channel antagonist, such as Ni^{2+} in the extracellular medium, has been shown to prevent this secondary phase, suggesting that Ca^{2+} influx forms part of the overall response (Burnstock, 1990).

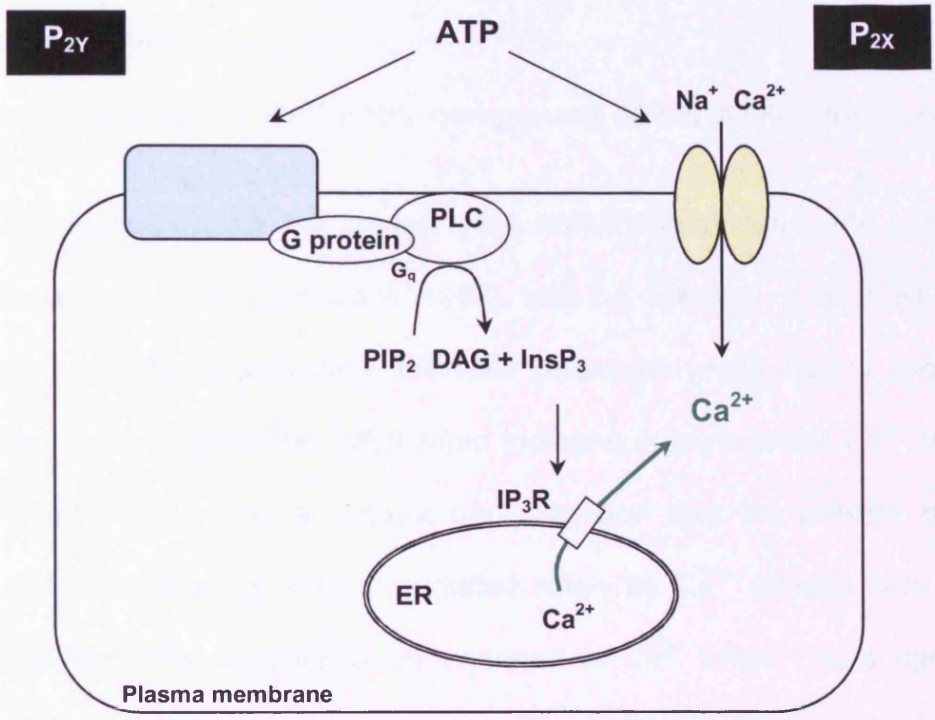

Figure 4.1 Signalling pathways of P_2-purinergic receptors activated by ATP

Adenosine triphosphate (ATP) acts on two types of P_2-purinergic receptors, one of which (P_{2X}) is a ligand gated ion channel, and the other (P_{2Y}) is a G-protein coupled receptor linked to the phosphoinositide signalling pathway via the G_q alpha subunit. G_q activates phospholipase C (PLC) which hydrolyses phosphatidylinositol 4,5-bisphosphate (PIP_2) to form second messengers diacyl glycerol (DAG) and inositol-1,4,5-triphosphate ($InsP_3$). $InsP_3$ activates $InsP_3$ receptors ($InsP_3R$) on the endoplasmic reticulum (ER) which opens calcium (Ca^{2+}) channels allowing mobilisation of Ca^{2+} into the cytosol.

4.1.2 Objective

In light of the involvement of $InsP_3Rs$ in the Ca^{2+} cycling observed at fertilisation, this chapter investigated whether the expression of PLCζ in CHO cells alters agonist-induced $InsP_3R$-dependent Ca^{2+} handling. This chapter also investigated whether PLCζ expression induces subtle changes in basal cellular Ca^{2+} handling in this cell type. The methods implemented in this analysis are described in detail in section 4.2.

4.2 Method Development

4.2.1 Investigating the Ca^{2+} entry component of the ATP-induced transient in CHO cells.

The CHO cell line used in the present study was found to respond to ATP as had been shown previously (Burnstock, 1990), with the omission of extracellular Ca^{2+} resulting in a characteristically different response which clearly lacked the secondary phase, whilst the initial rapid increase in intracellular Ca^{2+} remained intact (Figure 4.2). This is a clear demonstration that the primary response following the addition of ATP is mediated solely by Ca^{2+} release from the ER, whilst the persistent elevation is underpinned by Ca^{2+} influx. This suggests that the Ca^{2+} response investigated in this thesis involves the combined action of P_{2Y} purinergic receptors and capacitative calcium entry.

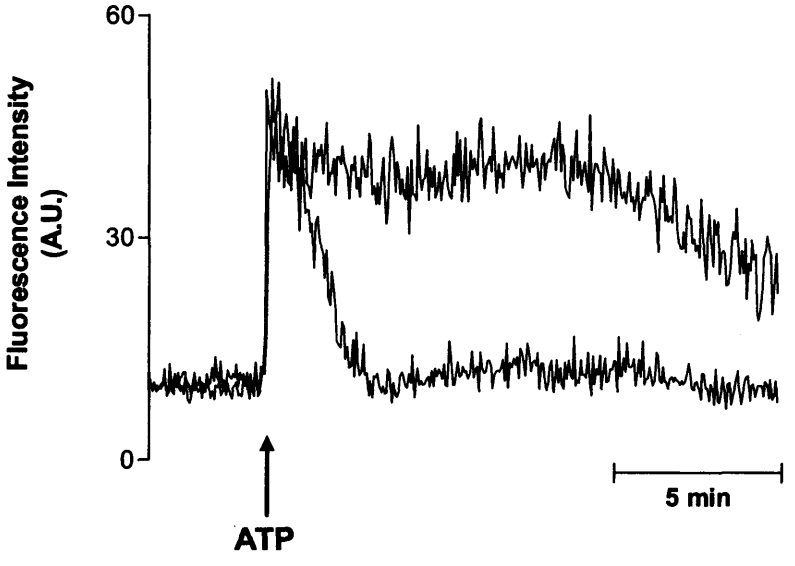

Figure 4.2 The ATP-induced transient in CHO cells
The effect of extracellular Ca^{2+} on the intracellular Ca^{2+} response elicted by ATP (100μM). CHO cells were loaded with the Ca^{2+} indicator Fluo 3 prior to imaging. Under control conditions (1.3mM extracellular Ca^{2+}, represented by the blue line) the initial rapid increase in intracellular Ca^{2+} was followed by a slowly declining secondary plateau phase. However the omission of calcium from the extracellular medium (represented by the red line) resulted in a characteristically different response which clearly lacked the secondary plateau. Each of the traces shown is representative of 99% of the responses (n = 4, 18-20 cells per experiment).

4.2.2 Analysis methods implemented in the assessment of Ca^{2+} handling

The following characteristics of the Ca^{2+} responses in CHO cells were quantified in order to assess whether the expression of PLCζ alters cellular $InsP_3R$-dependent Ca^{2+} handling. These parameters are illustrated and defined in figure 4.3.

I. The amplitude of the Ca^{2+} release: This represents the magnitude of the change in Fluo 3 fluorescence following ATP addition, and was expressed as $F-F_0/F_0$, where F is the maximum fluorescence observed and F_0 is the resting Fluo 3 fluorescence determined in resting cells.

II. Rate of Ca^{2+} release: This is represented by a change in Fluo 3 fluorescence as a function of time (dF/dt), and was expressed as the relative increase in fluorescence over time, from basal to peak fluorescence.

III. The proportion of cells that did not exhibit ATP-induced Ca^{2+} release was analysed. These cells are referred to as being non-responsive.

IV. Basal cellular Ca^{2+} handling was examined using a form of noise analysis termed signal variability (SV) (Section 4.2.3).

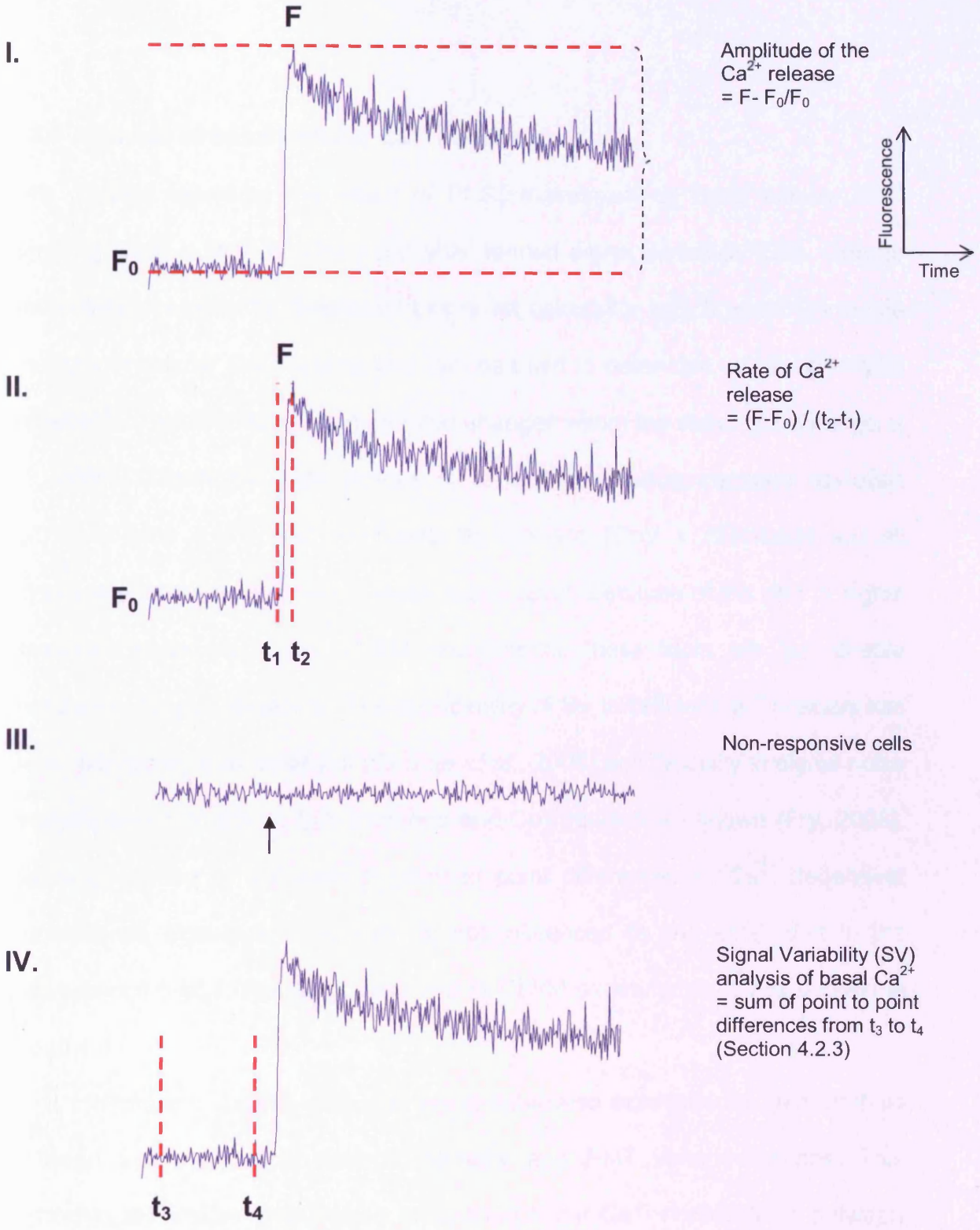

Figure 4.3 Schematic representations of the ATP-induced Ca^{2+} transient analysis parameters

I., II. and IV represent typical Ca^{2+} transients induced by the addition of ATP (100μM) in CHO cells loaded with fluo 3. The equations for the parameters measured are detailed alongside each figure. F = maximum fluorescence; F_0 = basal fluorescence; t_1= time of agonist addition; t_2 = time at which maximum fluorescence occurs. t_3 to t_4 = 30 second time period used to calculate basal Ca^{2+} signal variability (SV). III. represents a typical trace of a cell that did not exhibit agonist-induced Ca^{2+} release. The black arrow corresponds to the time of the agonist addition.

4.2.3 Analysis of basal cellular Ca^{2+} handling

This chapter examines the effect of PLCζ expression on basal cellular Ca^{2+} handling using a form of 'noise analysis' termed signal variability (SV). George and colleagues recently developed this novel calculation which quantifies subtle changes in cellular Ca^{2+} cycling that can be used to determine cell-to-cell signal variability, in addition to agonist-induced changes within the same cell (George *et al.*, 2006). Commonly used indices of variability including standard deviation (SD), variance (SD^2) and coefficient of variance (CoV = SD/mean) are all intrinsically linked to a constant mean signal level. Because of the drift in signal frequently observed in our CLSM experiments, these tools are not reliable measures of signal variability. The applicability of SV to cellular Ca^{2+} analysis has been extensively characterised (George *et al.*, 2006) and its utility in signal noise analysis over and above SD, Variance and CoV have been shown (Fry, 2008). SV is calculated by the sum of point to point differences in Ca^{2+} dependent fluorescence signals and as such is not influenced by the small drift in the fluorescence signal frequently observed in CLSM experiments. SV is defined in figure 4.4.

As a pre requisite for this analysis, this chapter also examines the relationships between SV, mean fluorescence intensity and PMT voltage settings. This highlights the issues faced when comparing basal Ca^{2+} homeostasis between different cells exhibiting a broad range of fluorescence intensities.

For a set of k intensity values; $x_1, x_2, x_3 \ldots\ldots\ldots x_k$

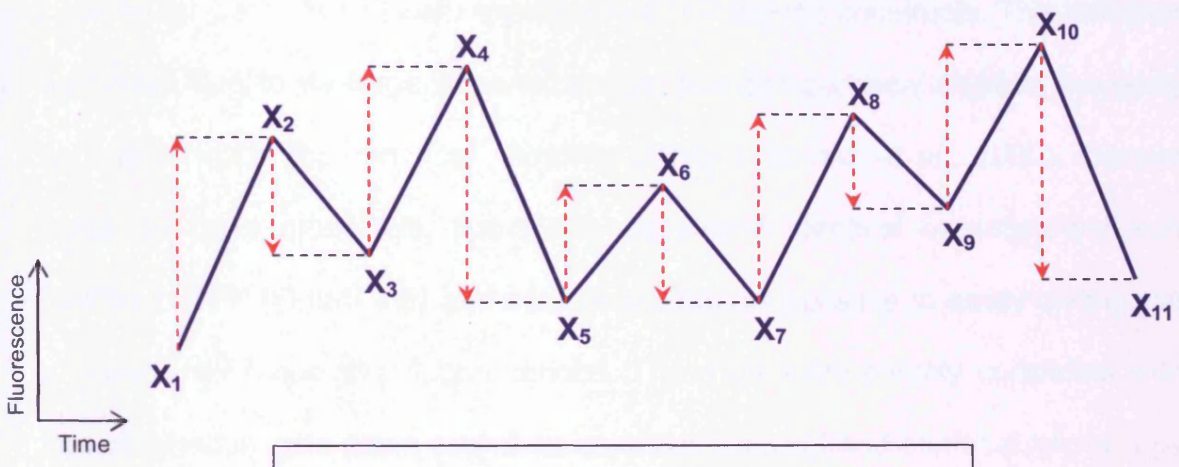

$$SV = \sum_{n=1}^{n=k-1} \left| (x_{n+1} - x_n) \right|$$

Figure 4.4 Definition of Signal Variability (SV)

Signal Variability is the sum of the moduli of the differences between successive intensity values.

4.2.4 The use of fluo-3 to measure changes in intracellular Ca^{2+}

The Ca^{2+} indicator fluo-3 was initially chosen to determine changes in intracellular Ca^{2+} in CHO cells expressing eYFP tagged constructs. This indicator was used due to its large dynamic range, low compartmentalisation tendency and appropriate apparent Ca^{2+} binding affinity (Thomas *et al.*, 2000). Despite these desirable properties, fluo-3 has an almost identical excitation/emission profile to eYFP (Figure 4.5) and as a result it is not possible to easily distinguish between their respective fluorescences. These data are entirely consistent with that obtained in cells using a lambda scanning protocol and confocal microscopy (data not shown).

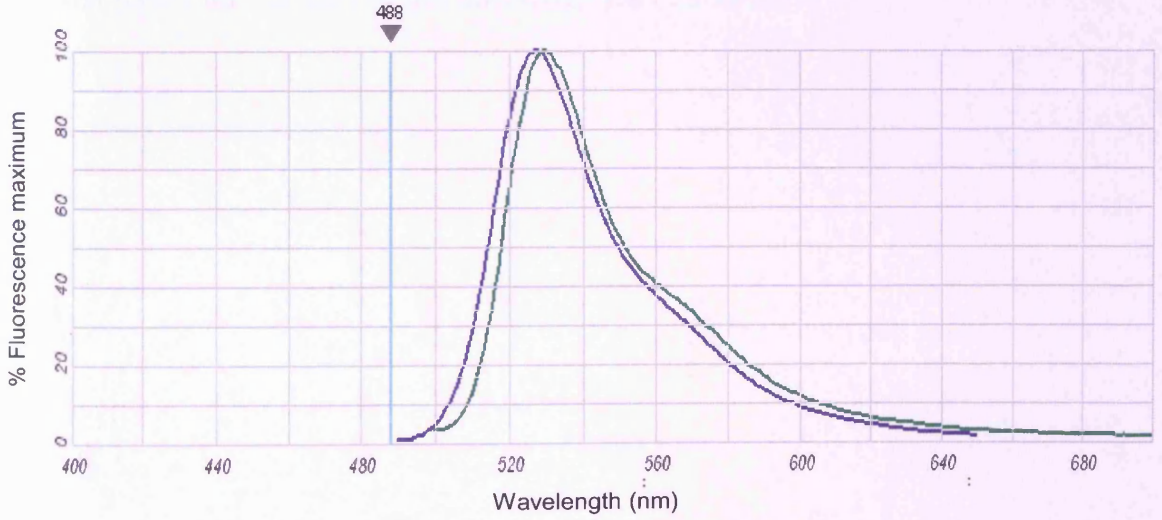

Figure 4.5 Fluorescence emission spectra of enhanced yellow fluorescent protein (eYFP) and fluo-3.
The green line represents the emission spectra for eYFP and the dark blue line represents the emission spectra for fluo 3. The vertical light blue line indicates the position of the 488nm laser line. Spectra generated using Molecular Probe's Fluorescence Spectra Viewer (Invitrogen). http://probes.invitrogen.com/servlets/spectraviewer

This posed two potential problems: 1) Cells expressing the eYFP tagged constructs may not be easily identified by their fluorescence when loaded with fluo-3, and 2) Changes in the intensity of fluorescence emitted in the 510-540nm region may not be solely due to Ca^{2+} dependent changes in fluo-3 if the eYFP fluorescence was altered by the addition of the agonist or Ca^{2+} itself. However, cells expressing eYFP tagged constructs were easily identified due to the fluorescence intensity of eYFP being significantly higher than that of fluo-3 (Figure 4.6A). Additionally, the fluorescence intensity of eYFP remains unaltered following ATP induced Ca^{2+} mobilisation from the intracellular stores (Figure 4.6B). This suggests that the fluorescence changes observed upon agonist addition to fluo-3 loaded cells expressing eYFP tagged constructs are due exclusively to changes in the fluorescence of fluo-3.

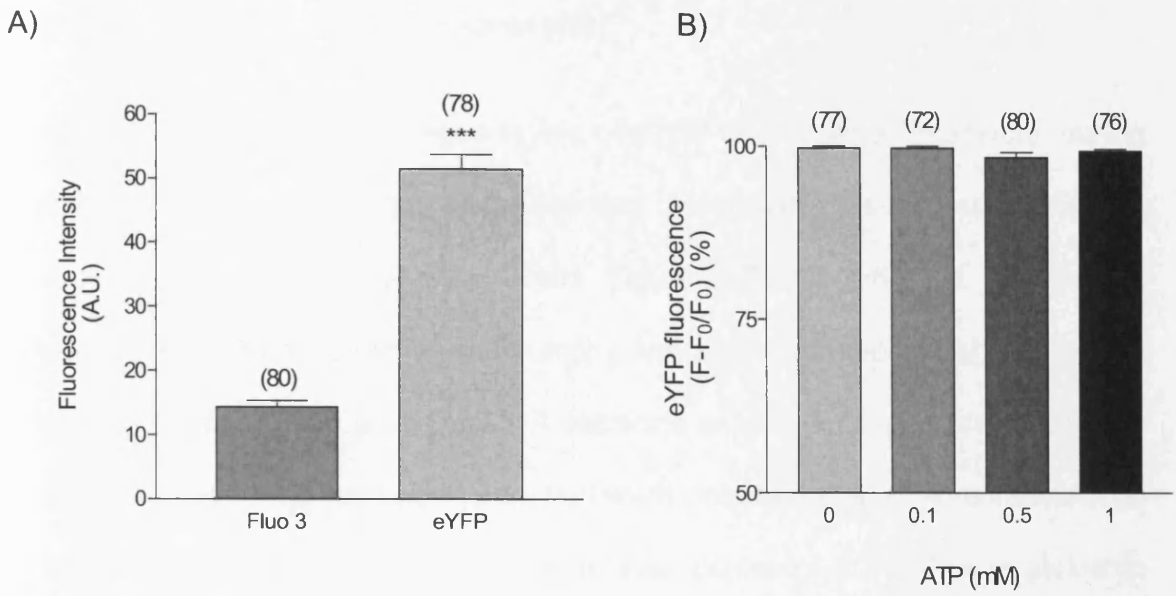

Figure 4.6 eYFP Fluorescence is independent of ATP-induced Ca^{2+} release

A) Typical eYFP fluorescence intensity 3 hours following microinjection of DNA constructs is significantly higher than the fluorescence intensity exhibited by cells loaded with the Ca^{2+} indicator fluo-3. Data were acquired from regions of interest (ROI) representing single resting (non-stimulated) cells, of approximately 40μm^2. Data are shown as mean ± S.E.M (n=4, the number of cells analysed is shown in the parentheses). ***=$p<0.001$. B) The amplitude of the change in eYFP fluorescence (F/F_0) is given as the maximum fluorescence determined following ATP addition (F) expressed as a percentage of the eYFP fluorescence measured in resting cells (F_0, 100%). Data represent mean values ± S.E.M (n=4, the number of cells analysed is shown in the parentheses).

4.2.5 Heterogeneity of eYFP expression

CHO cells display heterogeneous levels of eYFP fluorescence intensities during transient expression following microinjection, presumably as a result of varying levels of DNA delivery between cells (figure 4.7). In order to assess the association between fluorescence intensity and signal variability (SV), regions of interest (~40μm^2 , >150 pixels) from 4 separate experiments were selected. The average fluorescence intensities per pixel were obtained at a photomultiplier tube (PMT) voltage setting of 1000V using a laser power of 20%. The relationship between fluorescence intensity and SV for each region of interest ROI is outlined in the scatter plot in figure 4.7(c). The fluorescence signal becomes increasingly saturated at fluorescence intensities above 120 (mean pixel value) due to an 8-bit image resolution that results in 2^8 (or 256) levels of intensity for each pixel. The signal from a defined ROI which typically comprises >150 pixels is intrinsically linked to sub-saturation pixels. As pixels within the ROI progressively saturate, the SV will appear to decrease. Therefore, two options presented themselves: either to set a threshold of fluorescence intensity above which data would be eliminated, or to adjust the PMT voltage setting thus enabling cells exhibiting higher levels of expression to be included in the analysis. Eliminating the data would have sacrificed a large number of data points and would also have prevented the examination of cells displaying higher levels of PLCζ expression, hence this option was ruled out.

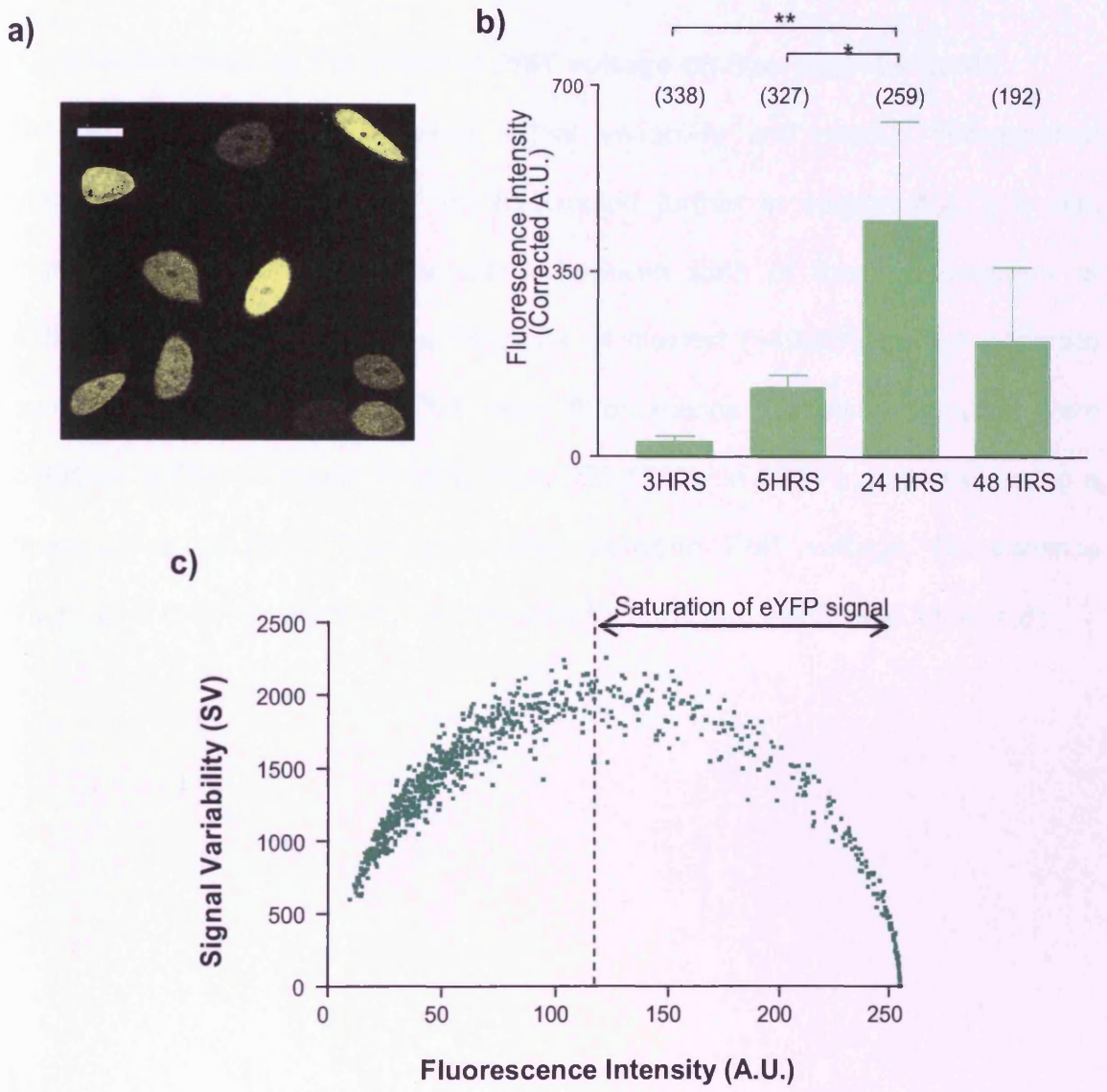

Figure 4.7 Heterogeneity of eYFP expression following microinjection

a) eYFP expression in CHO cells 24 hours after DNA microinjection. Bar represents 20µm.
b) Bar chart representing actual eYFP fluorescence intensities across the transient phase of expression. Images were acquired at PMT voltage settings ranging 750V-1000V, and single cell fluorescence intensities were corrected post acquisition using the Boltzman equation in figure 4.8. Data is presented as mean ± SEM (n=4, number of cells analysed is shown in parentheses). *=$p<0.05$, **=$p<0.01$
c) Scatter Plot of data obtained from CHO cells expressing eYFP at 24 hours post DNA microinjection. All images were acquired at a PMT setting of 1000V. Each dot represents the signal variability (SV) and fluorescence intensity (arbitary units) of a single region of interest (ROI) (n=4)

4.2.6 Understanding the effect of PMT voltage on fluorescent signals

Due to the correlation between signal variability and relative fluorescence intensity shown in figure 4.7 (c) (discussed further in section 4.2.7), It was important to assess the association between both of these parameters at different PMT voltage settings. Regions of interest (~40μm^2) from 4 separate experiments were selected. The mean fluorescence intensities per pixel were obtained at PMT voltages ranging from 500-1250V in 100V increments, using a laser power of 20%. The relationship between PMT voltage, fluorescence intensity and SV for each ROI was plotted for fluo3 and eYFP (see figure 4.8).

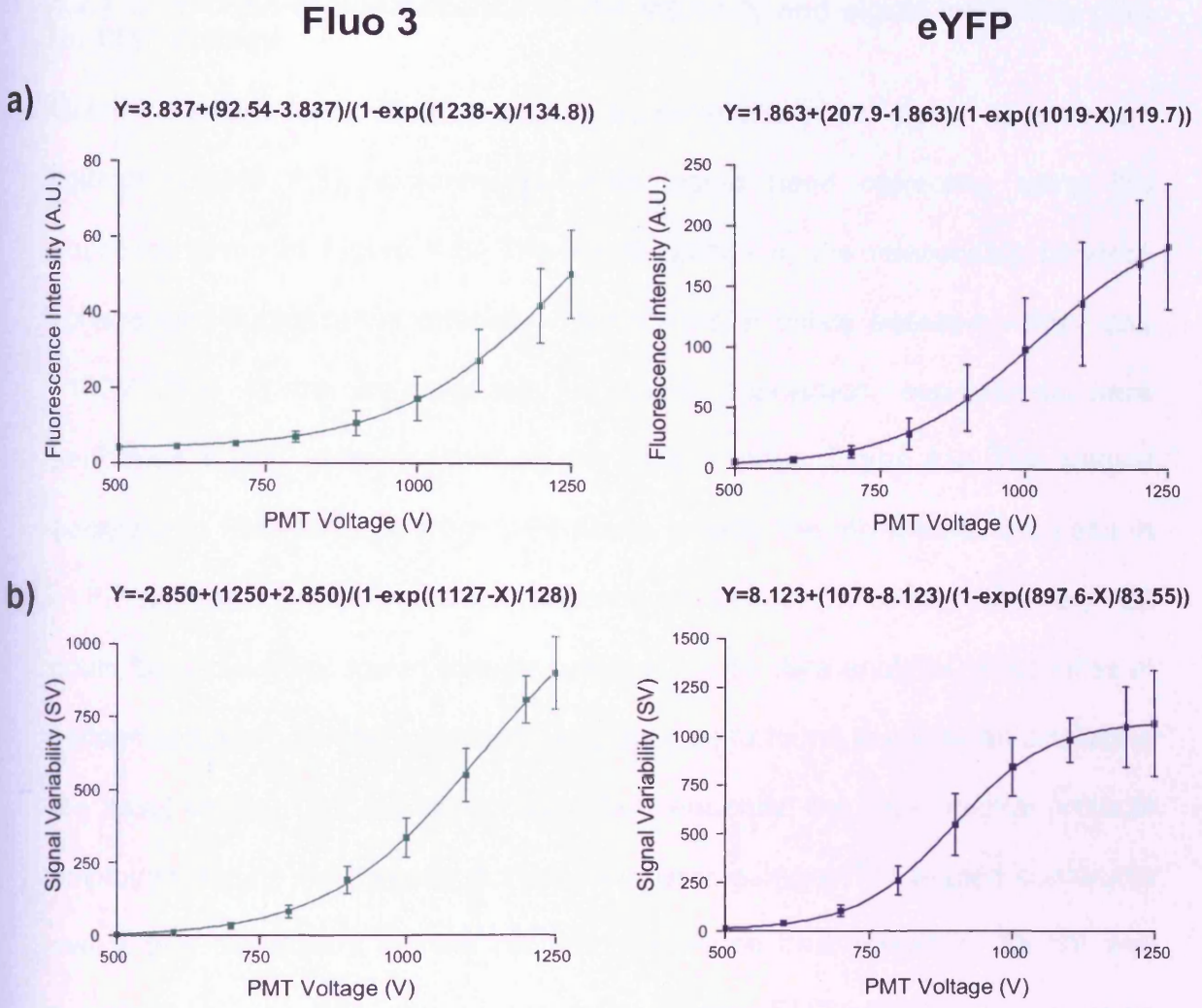

Figure 4.8 The dependency of fluorescence intensity and signal variability (SV) on PMT voltage settings.

PMT voltage plotted against (a) relative fluorescence intensity and (b) signal variability (SV) for fluo-3 and eYFP. (n = 4 for all traces, >74 ROI in each instance). The data was fitted to a Boltzman equation yielding the non-linear regression shown above each trace. The Boltzman sigmoidal equation is defined as Y=bottom+(top-bottom)/(1+exp((V50-X)/slope)).

4.2.7 Correction of fluorescence signal intensity and signal variability (SV) for PMT Voltage

Given the dependency of fluorescence signal intensity and signal variability on voltage (Figure 4.8), experimental data would need correcting using the equations given in Figure 4.8. The linear portion of the relationship between voltage and fluorescence intensity / SV for eYFP exists between ~800V and 1100V. Due to the heterogeneity of eYFP expression, experiments were performed at PMT settings spanning this voltage range (Figure 4.9). The gradual decrease in PMT settings from 3-24 hours reflects the incremental increase in eYFP expression, such that a fluorescence signal intensity of approximately 120 could be achieved at lower voltage settings. Upon data analysis, differences in voltage settings between experimental groups were found to create an artefact in the basal cellular Ca^{2+} handling data. Consequently, the experimental protocol employed during the investigation of cells expressing eYFP tagged constructs meant that fluorescent signals required correction post-aquisition. All SV and fluorescence intensities values were corrected to a PMT setting of 1000V using the equations outlined in figure 4.8.

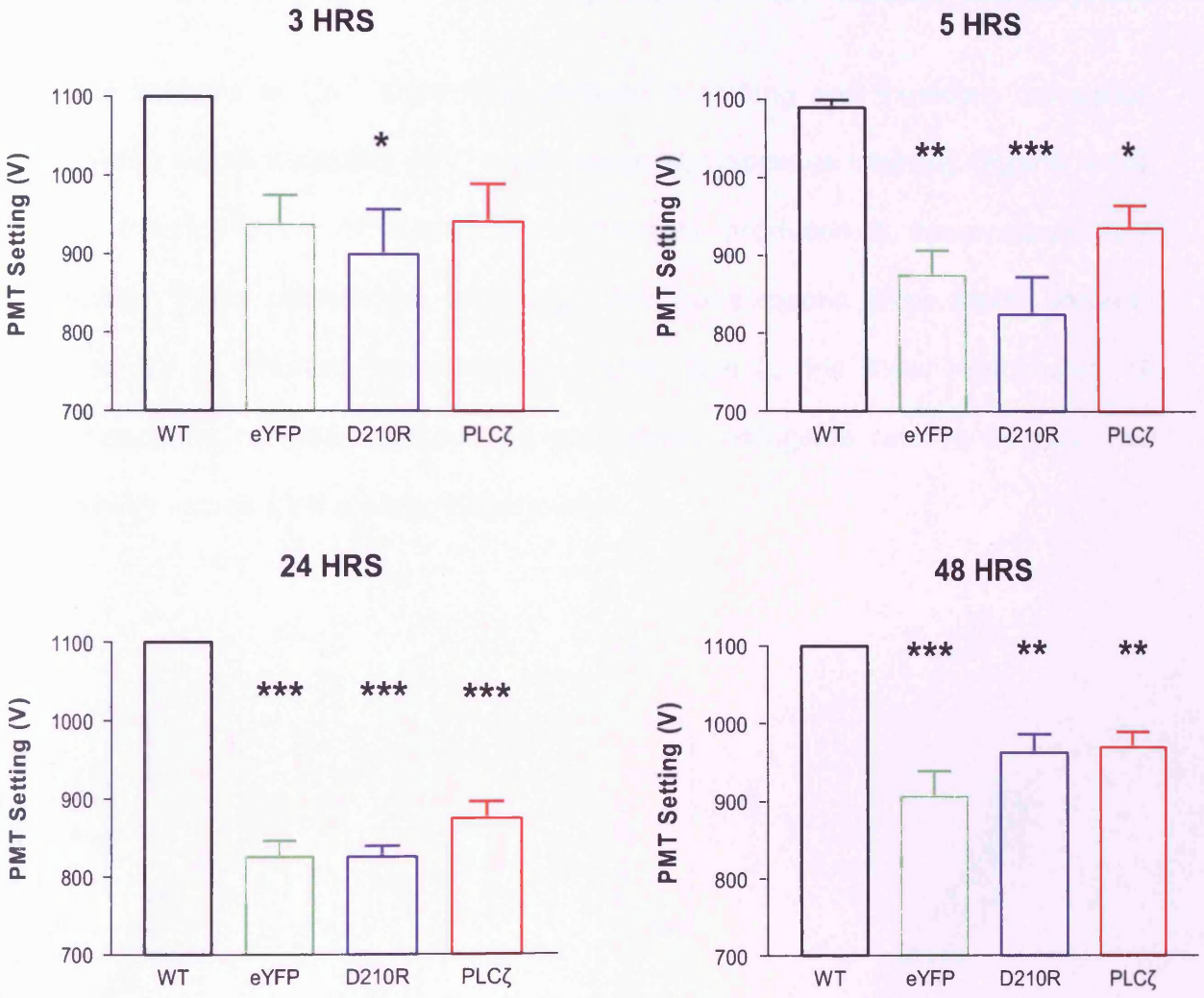

Figure 4.9 Photomultiplier Tube (PMT) voltage settings used for Ca^{2+} imaging experiments on cells expressing eYFP-tagged constructs
CHO cells expressing eYFP tagged constructs and loaded with the Ca^{2+} indicator fluo 3 were imaged at PMT voltage settings spanning the 800V-1100V range. Wild type (WT) CHO cells loaded with fluo 3 were imaged at ~1100V in all instances. Data is expressed as mean ± SEM (n=4, >360 cells in each experimental group. *=p<0.05, **=p<0.01, ***=p<0.001 when compared to WT CHO cells)

4.2.8 Understanding the relationship between fluorescence intensity and SV

Initial analysis of Ca^{2+} signalling revealed a striking and expected correlation between signal variability (SV) and relative fluorescence intensity (Figure 4.10). Log transformation of fluorescence intensity produced a linear association between these parameters, enabling direct comparisons to be made between mean SV of different experimental groups. Due to this linear relationship, all comparisons of mean SV will be considered alongside relative fluorescence intensity values for the same experiments.

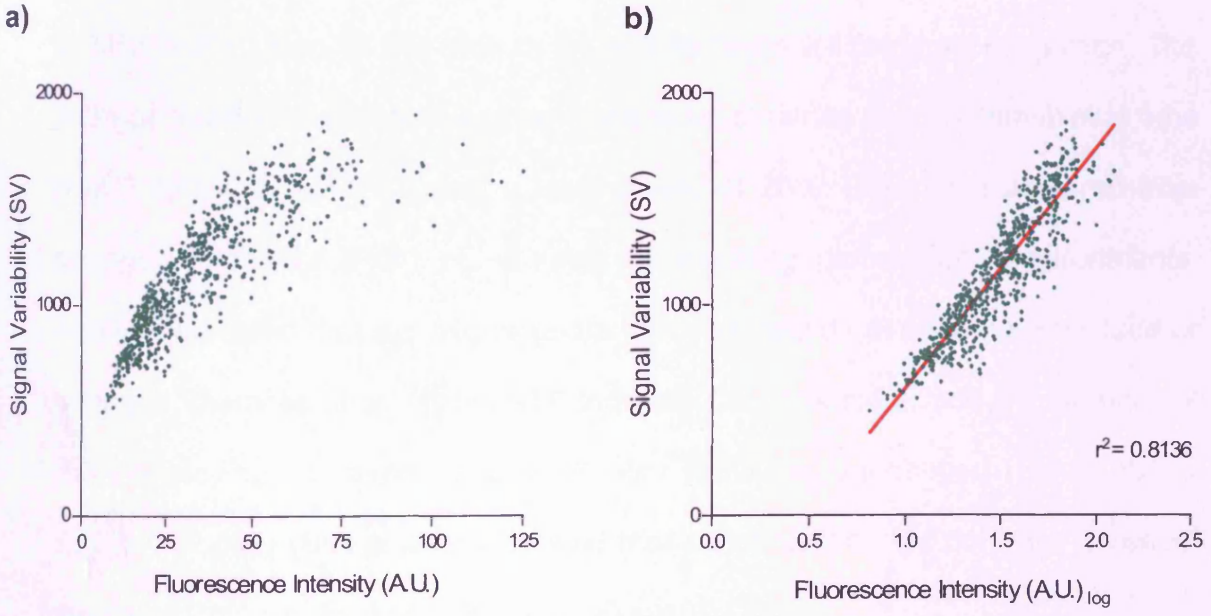

Figure 4.10 Correlation between signal variability (SV) and mean fluorescence intensity
Scatter plot of data obtained from fluo-3 loaded CHO cells expressing eYFP showing the relationship between signal variability (SV) and mean fluorescence intensity (n=8, >600 cells). The rise in the intensity of the fluorescent signal is associated with an increase in SV (a). Log transformation of fluorescence intensity reveals a linear association with an r^2 value of = 0.8136 and a p value of <0.001. Note that the data displayed here bears the typical profile of fluorescence intensities below 120 units as described in figure 4.7c.

4.3 Results

4.3.1 Microinjection of CHO cells does not alter cellular Ca^{2+} handling

Although the data presented in Chapter 3 suggests that under optimised conditions, microinjection was well tolerated by CHO cells, the microinjection procedure itself may modulate some aspects of cellular phenotype and signalling. Consequently, control experiments were performed to assess whether any changes in Ca^{2+} handling were attributable to microinjection. CHO cells microinjected with the buffer used for all microinjection experiments (KCl Hepes containing 2.5mg/ml Alexa 594) were compared with wild type CHO cells. Cells were loaded with fluo-3 AM and imaged for Ca^{2+} dependent fluo-3 fluorescence in KRH buffer using CLSM at 3, 5, 24 and 48 hours following microinjection. The average fluorescence intensities per pixel were obtained at a photomultiplier tube (PMT) setting of 1000V, using a laser power of 20%. Data were acquired from regions of interest (ROI) of ~40μm^2 representing global Ca^{2+} environments. Analysis revealed that the microinjection procedure did not alter the amplitude or temporal characteristics of the ATP-induced Ca^{2+} transient, and the number of cells displaying no response to ATP also remained unchanged (Figure 4.11). Signal variability (SV) analysis showed that microinjection did not have an effect the basal Ca^{2+} handling of CHO cells (Figure 4.12).

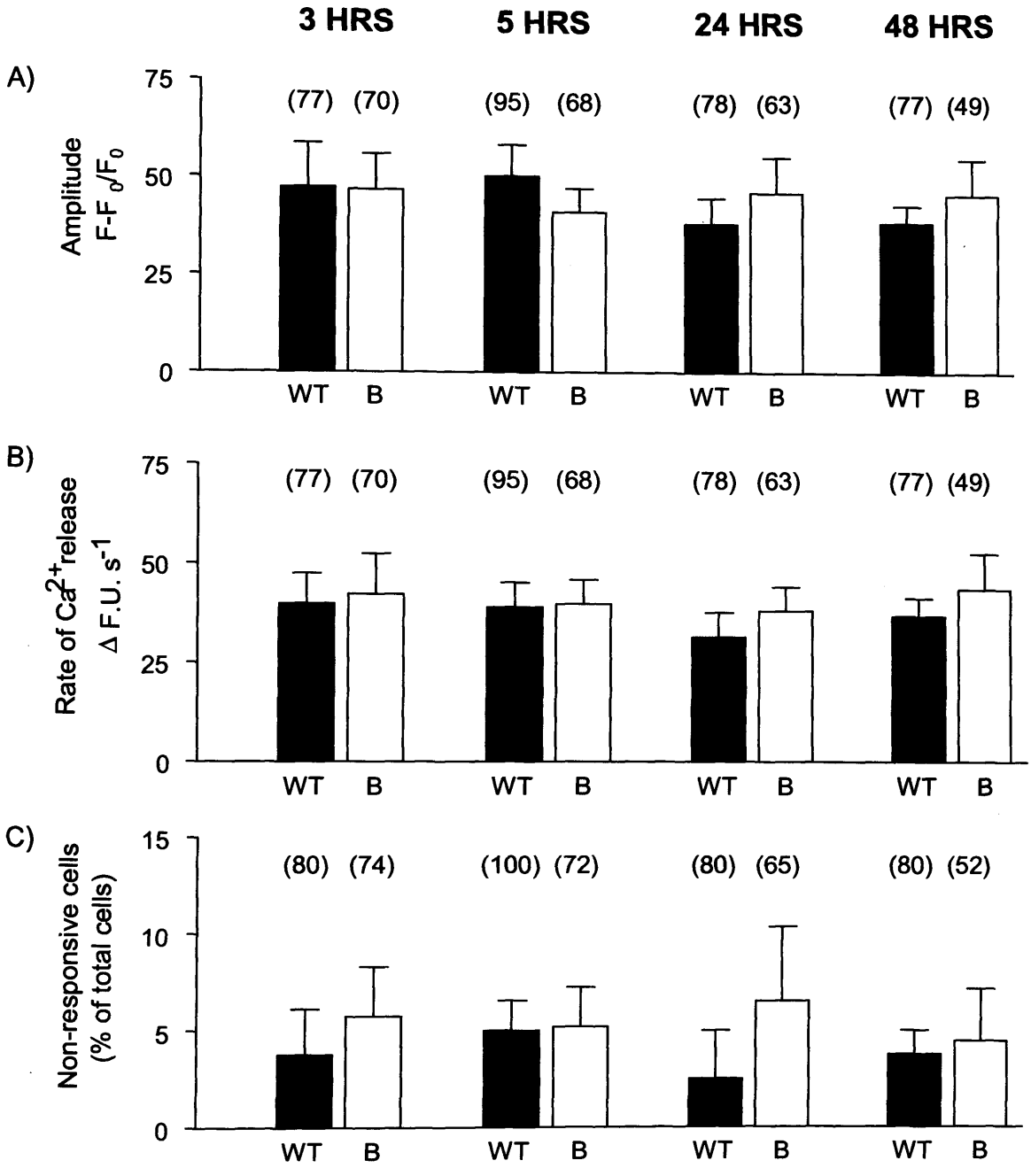

Figure 4.11 Analysis of the effects of microinjection on the ATP-induced Ca^{2+} transient in CHO cells over a 48 hour time period.

The following parameters of the ATP-induced Ca^{2+} transients in wild type (WT) CHO cells (black) or CHO cells microinjected with KCL Hepes Buffer (B) (white) were analysed at 3, 5, 24 and 48 hours: A) Amplitude of the Ca^{2+} release ($F-F_0/F_0$), B) Rate of the Ca^{2+} release, plotted as a change in the Ca^{2+} dependent Fluo 3 fluorescence per second and C) The number of cells exhibiting no response. Data are given as mean ± SEM. (n=4, number of cells analysed is shown in parentheses).

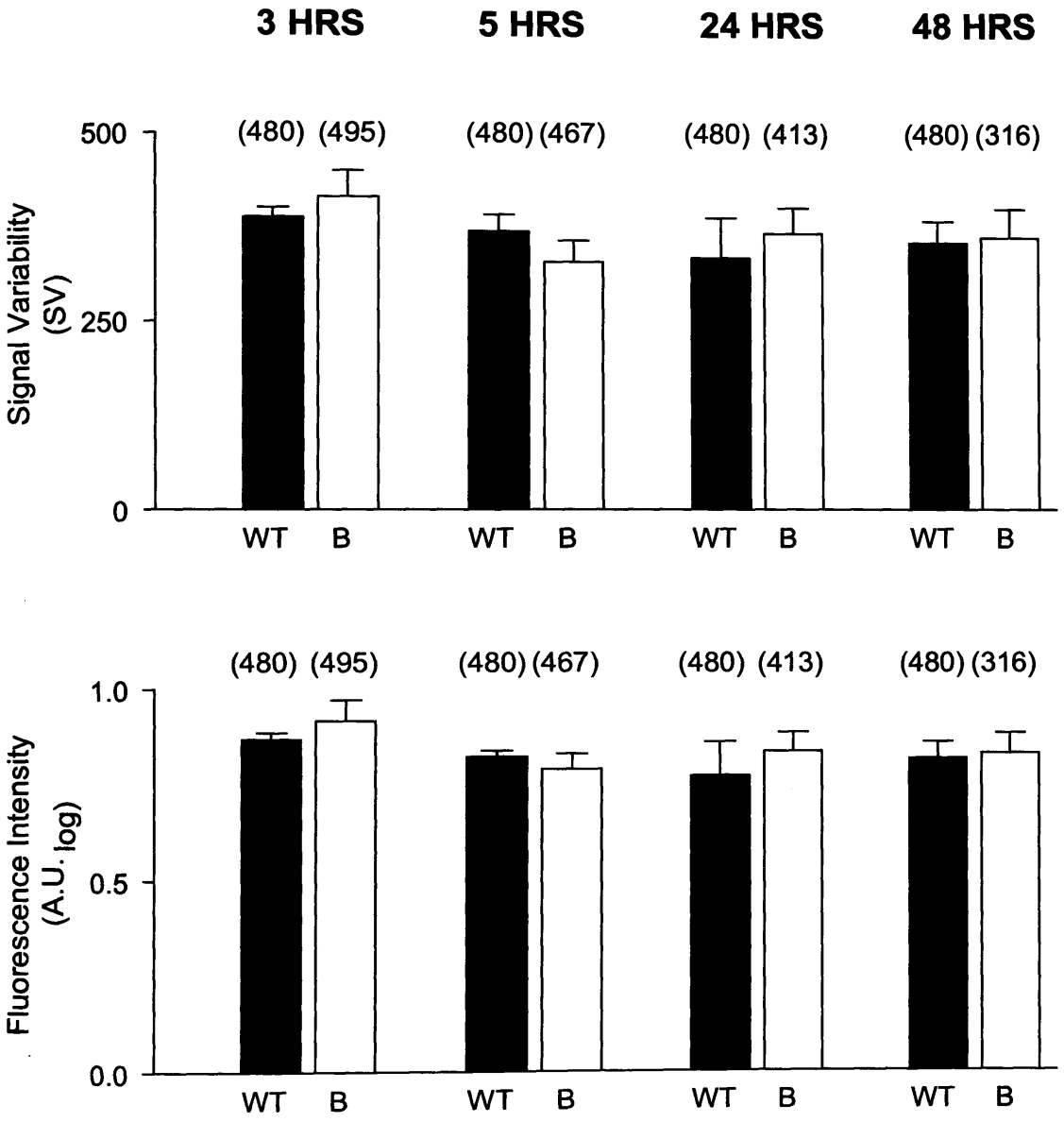

Figure 4.12 Microinjection does not have an effect on basal cellular Ca^{2+} handling
Signal variability (SV), where SV is the sum of point to point differences in Ca^{2+} signals over a 30 second time period remains unchanged in CHO cells microinjected with KCl Hepes Buffer (B, white) when compared with wild type (WT) CHO cells (black) at 3, 5, 24 and 48 hours following microinjection. Changes in SV are considered alongside mean fluorescence intensities for each experimental group due to the linear relationship between these parameters. Data are given as mean ± SEM. (n=4, number of cells analysed is shown in parentheses).

4.3.2 The expression of eYFP-PLCζ does not alter the spatio-temporal characteristics of the ATP-induced Ca^{2+} transient.

The data presented in chapter 3 suggests that CHO cells are capable of expressing high levels of PLCζ without any obvious effect upon Ca^{2+} handling. This raises the question as to how cell types other than the oocyte are capable of retaining PLCζ in a seemingly inactive state. Detailed analysis of intracellular Ca^{2+} handling could reveal subtle changes in the Ca^{2+} signalling machinery that may lead to a possible explanation of how cells are capable of expressing this protein whilst maintaining an apparently normal phenotype.

The ATP-induced Ca^{2+} transients of CHO cells expressing eYFP-PLCζ were analysed using the parameters outlined in figure 4.3. They were compared with the agonist responses of CHO cells expressing eYFP alone, the inactive mutant eYFP-^{D210R}PLCζ and wild type (WT) CHO cells. Transfected cells were microinjected with high-purity plasmid DNA as described in Chapter 2 section 2.2.5.4, and visualised for fluo-3 dependent changes in intracellular Ca^{2+} at 3, 5, 24 and 48 hours after injection using CLSM. The average fluorescence intensities per pixel were obtained at photomultiplier tube (PMT) settings ranging from 800V to 1100V, using a laser power of 20%. Data were acquired from regions of interest (ROI) of ~40μm^2 representing global Ca^{2+} environments. Analysis revealed that PLCζ expression at 3, 5, 24 and 48 hours did not alter the amplitude or temporal characteristics of the ATP-induced Ca^{2+} transient, and the number of cells responding to ATP stimulation also remained unchanged (Figures 4.13 and 4.14).

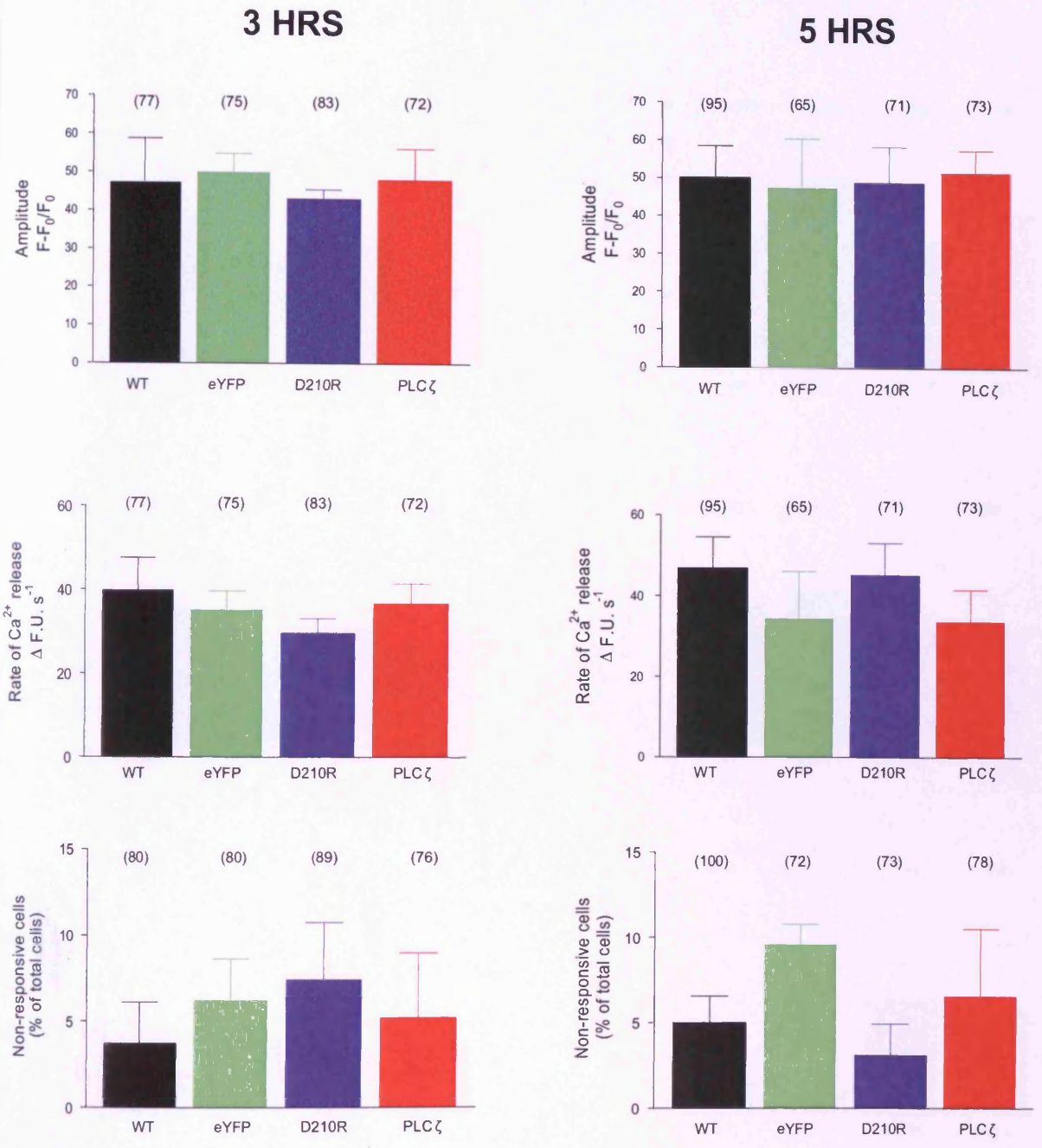

Figure 4.13 The expression of PLCζ has no effect on the ATP-induced Ca^{2+} transient in CHO cells at 3 and 5 hours post microinjection.
The following parameters of the ATP-induced Ca^{2+} transients in wild type (WT) CHO cells (black), and cells expressing eYFP (green), eYFP-^{D210R}PLCζ (blue) or eYFP-PLCζ (red) were analysed at 3 and 5 hours following transfection: A) Amplitude of the Ca^{2+} release ($F- F_0/F_0$), B) Rate of the Ca^{2+} release, plotted as a change in the Ca^{2+} dependent Fluo 3 fluorescence per second and C) The number of cells exhibiting no response. Data are given as mean ± SEM. (n=4, number of cells analysed is shown in parentheses).

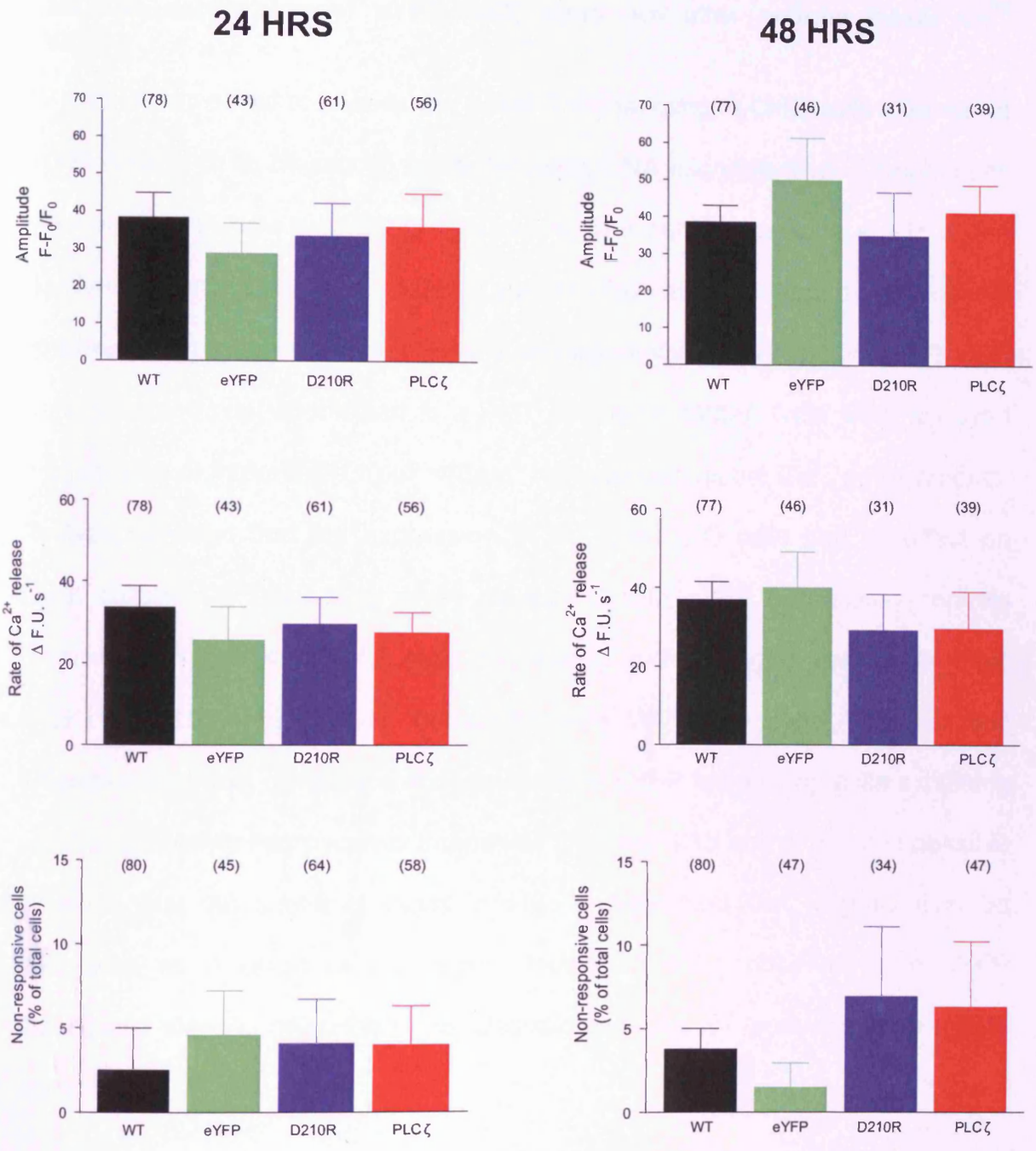

Figure 4.14 The expression of PLCζ has no effect on the ATP-induced Ca^{2+} transient in CHO cells over at 24 and 48 hours post microinjection.
The following parameters of the ATP-induced Ca^{2+} transients in wild type (WT) CHO cells (black), and cells expressing eYFP (green), eYFP-^{D210R}PLCζ (blue) or eYFP-PLCζ (red) were analysed at 24 and 48 hours following transfection: A) Amplitude of the Ca^{2+} release (F- F_0/F_0), B) Rate of the Ca^{2+} release, plotted as a change in the Ca^{2+} dependent Fluo 3 fluorescence per second and C) The number of cells exhibiting no response. Data are given as mean ± SEM. (n=4, number of cells analysed is shown in parentheses).

4.3.3 The expression of eYFP-PLCζ does not alter cellular basal Ca^{2+} handling

SV was implemented to assess the basal Ca^{2+} handling in CHO cells expressing eYFP-PLCζ at 3, 5, 24 and 48 hours following DNA microinjection. Comparisons were made with wild type (WT) CHO cells, and cells expressing eYFP or the inactive mutant eYFP-^{D210R}PLCζ. Due to the aforementioned relationship between voltage, fluorescence intensity and signal variability (section 4.2.7), data were corrected post-acquisition to a PMT setting of 1000V. Data were acquired from regions of interest (ROI) of ~40μm^2 representing global Ca^{2+} environments. Analysis revealed that the expression of PLCζ in CHO cells had no effect on basal cellular Ca^{2+} handling when compared with eYFP expressing controls (Figures 4.15 and 4.16). All cells expressing eYFP tagged constructs have significantly higher SV when compared with WT CHO cells; however this difference is almost certainly a consequence of eYFP expressing cells exhibiting significantly higher fluorescence intensities (Figures 4.15 and 4.16). It is possible however; that the subtle changes in Fluo-3 dependent Ca^{2+} signals may be concealed as a result of the higher levels of noise observed with eYFP fluorescent signals or indeed the unavoidable use of post-acquisition data correction.

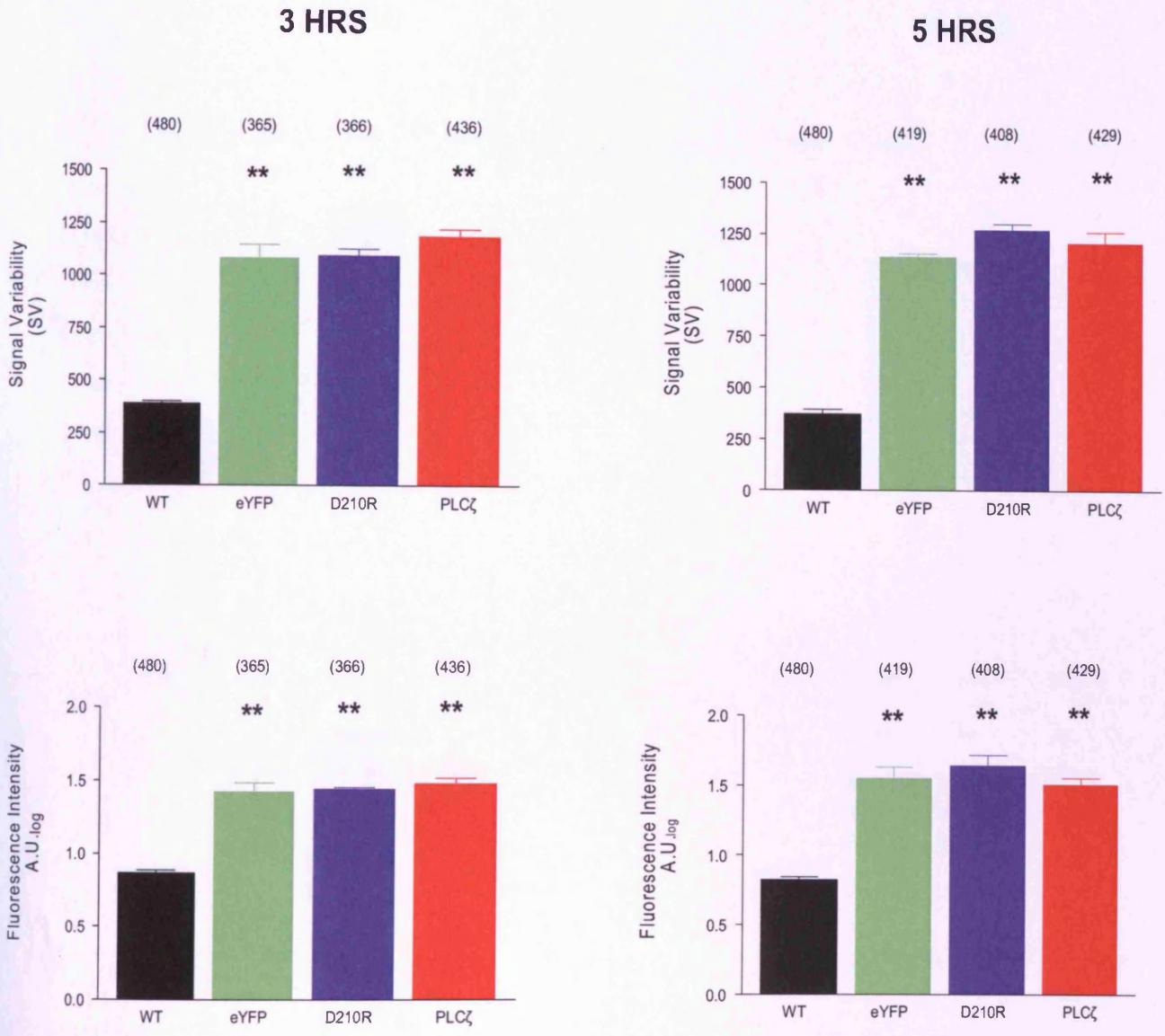

Figure 4.15 PLCζ expression has no effect on basal cellular Ca^{2+} handling at 3 and 5 hours post microinjection

Signal variability (SV), where SV is the sum of point to point differences in Ca^{2+} signals over a 30 second time period remains unchanged in CHO cells expressing eYFP-PLCζ (red) when compared with eYFP expressing control cells (eYFP; green and eYFP-^{D210R}PLCζ; blue) at 3 and 5 hours following transfection. Changes in SV are considered alongside mean fluorescence intensities for each experimental group due to the linear relationship between these parameters. Data are given as mean ± SEM. ** represents $p<0.01$ when compared with wild type (WT) CHO cells (n=4, number of cells analysed is shown in parentheses).

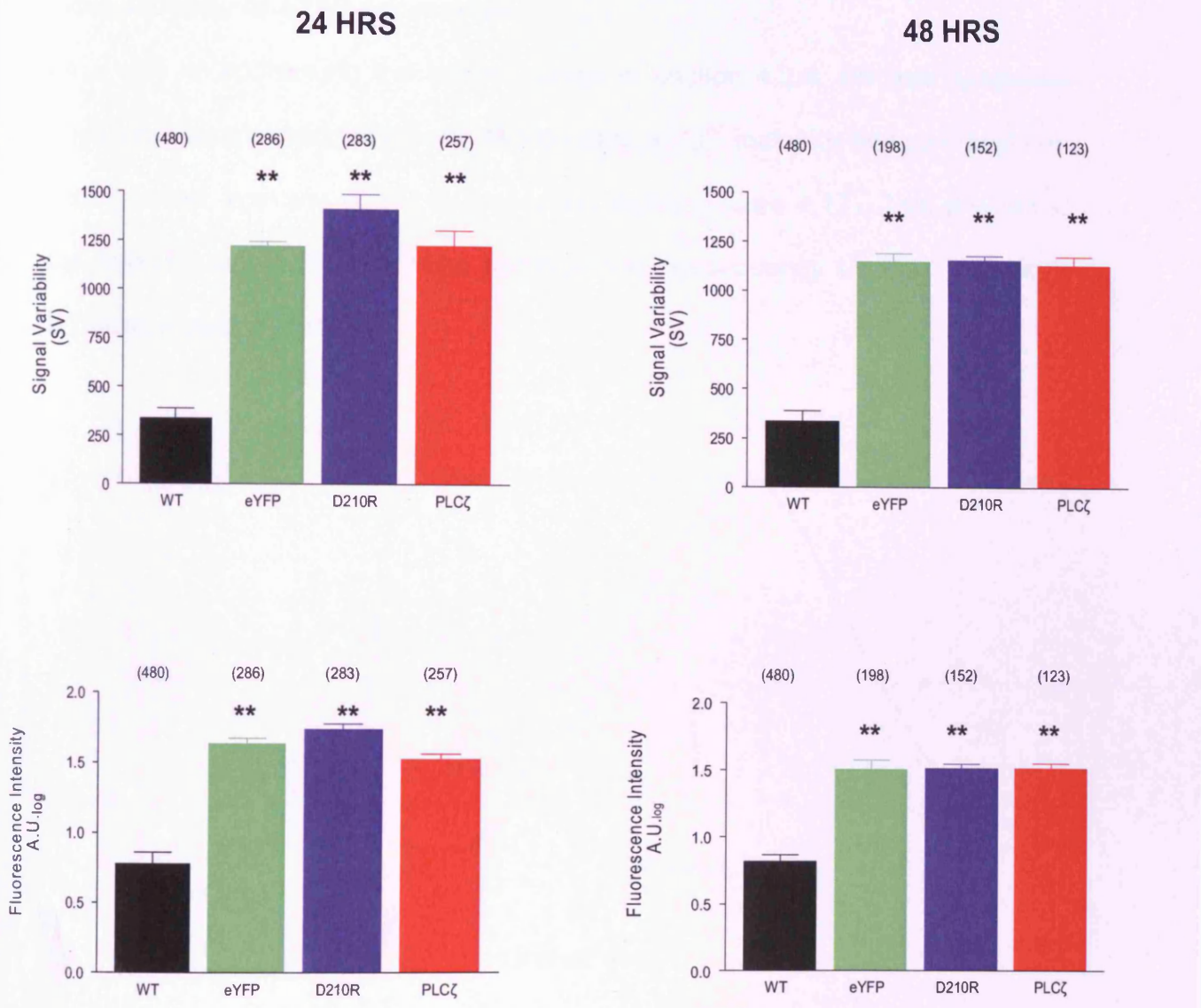

Figure 4.16 PLCζ expression has no effect on basal cellular Ca^{2+} handling at 24 and 48 hours post microinjection

Signal variability (SV), where SV is the sum of point to point differences in Ca^{2+} signals over a 30 second time period remains unchanged in CHO cells expressing eYFP-PLCζ (red) when compared with eYFP expressing control cells (eYFP; green and eYFP-^{D210R}PLCζ; blue) at 24 and 48 hours following transfection. Changes in SV are considered alongside mean fluorescence intensities for each experimental group due to the linear relationship between these parameters. Data are given as mean ± SEM. ** represents $p<0.01$ when compared with wild type (WT) CHO cells (n=4, number of cells analysed is shown in parentheses).

4.3.4 The use of Fura Red enables the analysis of SV to be made independently of eYFP expression.

As a way of addressing the issues raised in section 4.2.4, SV was assessed under the same experimental conditions using a Ca^{2+} indicator that can easily be distinguished from the eYFP fluorescence signal (Figure 4.17). This prevented the need to adjust PMT voltage settings and consequently avoided any post-acquisition data correction.

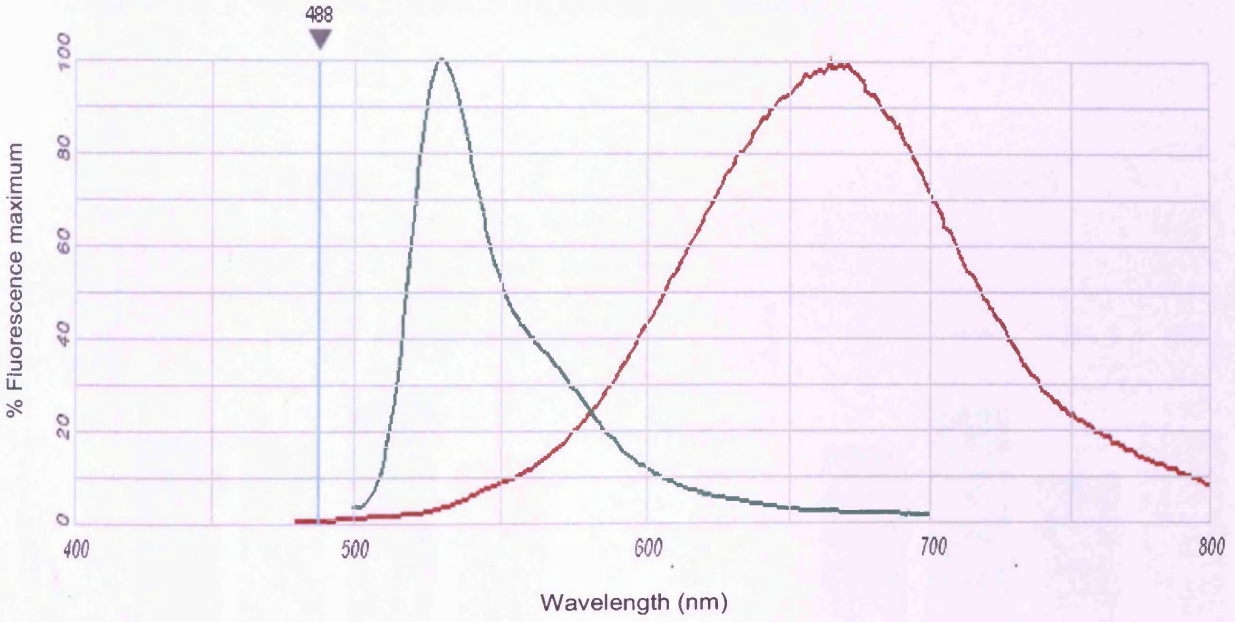

Figure 4.17 Fluorescence emission spectra of enhanced yellow fluorescent protein (eYFP) and Fura Red.
The green line represents the emission spectra for eYFP and the red line represents the emission spectra for Fura Red. The vertical light blue line indicates the position of the 488nm laser line. Spectra generated using Molecular Probe's Fluorescence Spectra Viewer (Invitrogen). http://probes.invitrogen.com/servlets/spectraviewer

Transfected cells were microinjected with high-purity plasmid DNA as described in section 2.2.5.4, and visualised for Fura Red dependent changes in intracellular Ca^{2+} at 5 and 24 hours after injection using CLSM. The average fluorescence

intensities per pixel were obtained at photomultiplier tube (PMT) settings of 1000V, using a laser power of 20%. Data were acquired from regions of interest (ROI) of ~40μm^2 representing global Ca^{2+} environments. Analysis revealed that the expression of PLCζ in CHO cells had no effect on basal cellular Ca^{2+} handling when compared with eYFP expressing controls and wild type (WT) CHO cells (Figure 4.18), confirming the assertion in section 4.3.4 that any significant changes in SV were a consequence of differences in eYFP fluorescence intensities between experimental groups.

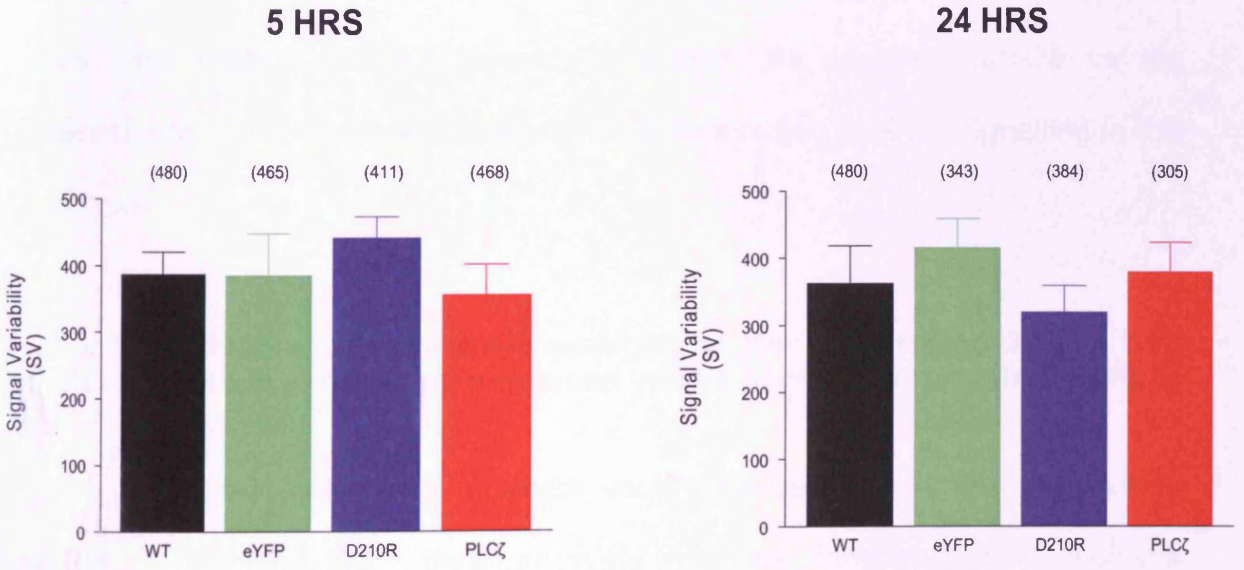

Figure 4.18 The use of Fura Red to assess SV confirms that PLCζ expression has no effect on basal cellular Ca^{2+} handling at 5 and 24 hours post microinjection
Signal variability (SV), where SV is the sum of point to point differences in Ca^{2+} signals over a 30 second time period remains unchanged in CHO cells expressing eYFP-PLCζ (red) when compared with eYFP expressing control cells (eYFP; green and eYFP-^{D210R}PLCζ; blue) and wild type (WT) CHO cells (black) at 5 and 24 hours following transfection. Data are given as mean ± SEM. (n=4, number of cells analysed is shown in parentheses).

4.4 Discussion

4.4.1 Microinjection does not affect Ca^{2+} signalling in CHO cells over a 48 hour time period.

This chapter demonstrates that microinjection does not have an effect on the agonist-induced $InsP_3R$-dependent Ca^{2+} transient, or on cellular basal Ca^{2+} handling in CHO cells 3-48 hours after DNA delivery. Microinjection did not alter the amplitude or rate of Ca^{2+} release of the transient generated by the addition of extracellular ATP. The proportion of cells failing to respond to agonist stimulation also remained unchanged. Analysis of signal variability (SV) revealed that microinjection also has no effect on Ca^{2+} cycling in resting (non-stimulated) CHO cells. This method of DNA delivery was therefore deemed suitable for the assessment of the affects of transient PLCζ expression on Ca^{2+} signalling in this cell type.

4.4.2 The advantages and disadvantages of the use of Fluo 3 as a Ca^{2+} indicator in cells expressing enhanced yellow fluorescent protein (eYFP).

The use of a ratiometric Ca^{2+} indicator would have been favourable, due to their ability of providing Ca^{2+} measurements that are independent of indicator concentration, thereby avoiding issues with uneven indicator distribution. However, such indicators require UV excitation which was not achievable with the lasers available on the confocal microscope used in this study. This limited us to the use of single wavelength indicators, preferably those exhibiting a large dynamic range (i.e. the change in intensity upon Ca^{2+} binding is large, giving a

higher signal-to-noise ratio thus allowing the measurement of small changes in Ca^{2+}) and minimal compartmentalisation. Despite Fluo-3 having an almost identical emission profile to eYFP, preventing distinction between their respective fluorescences, it was shown that the eYFP fluorescence was independent of ATP or the mobilized Ca^{2+}. This indicates that the determination of agonist-induced Ca^{2+} release in this study, calculated by the measurement of relative changes in intracellular fluorescence was entirely attributable to Ca^{2+} dependent changes in fluo 3 fluorescent signals. However, eYFP was expressed at levels which resulted in significantly higher fluorescence intensities when compared with fluo 3. This meant that we could not discount the possibility that any subtle changes in cellular basal Ca^{2+} handling were being concealed by the noise of the eYFP signal. Fura Red is a visible wavelength excitation fluorescence indicator that offers both single wavelength and ratiometric Ca^{2+} measurement by excitation at 420nm and 480nm. When used as a single wavelength indicator with excitation at 488nm, Fura red exhibits a decrease in emission upon Ca^{2+} binding. When measuring a large Ca^{2+} transient the signal falls to background levels. This property renders Fura Red less suitable as an indicator for measuring the spatio-temporal characteristics of the ATP-induced Ca^{2+} transients in CHO cells. Fura Red does however offer certain advantages in the analysis of SV of basal cellular Ca^{2+} handling in cells expressing eYFP, namely due to its red emission profile which eliminates interference from the yellow part of the visible spectrum.

This chapter also reports on the issues faced when using a novel method of 'noise' analysis to determine Ca^{2+} signal variability in cells exhibiting a broad

range of fluorescent intensities, with emphasis on the need to employ an experimental set up that utilises a Ca^{2+} indicator with a fluorescence emission that can be easily distinguished from the emission of the reporter protein.

4.4.3 PLCζ expression does not alter intracellular Ca^{2+} handling in CHO cells.

Acknowledging the limitations of the present experimental system, the data presented in this chapter is consistent with the concept that PLCζ does not alter agonist-induced Ca^{2+} responses or basal intracellular Ca^{2+} signals in CHO cells between 3 and 48 hours following DNA microinjection. This finding is confirmed by the use of the enzymatically inactive D210R mutant, which is entirely comparable to the data derived from full length PLCζ. The amplitude and rate of Ca^{2+} release of the agonist-induced transient remained unchanged when compared with that of wild type (WT) CHO cells, and cells expressing eYFP or the inactive mutant D210R-PLCζ. The proportion of cells failing to respond to agonist stimulation was also unaffected. Analysis of signal variability (SV) revealed that PLCζ expression has no effect on Ca^{2+} cycling in resting (non-stimulated) CHO cells. These findings suggest that PLCζ expression fails to perturb the $InsP_3R$-dependent signalling pathway in CHO cells at the time points assessed. The possibility that PLCζ expression stimulates $InsP_3R$-induced Ca^{2+} release in CHO cells at time points other than those examined can not be discounted. Additional experiments involving the microinjection of RNA encoding PLCζ, or indeed PLCζ protein could enable the monitoring of intracellular Ca^{2+} at earlier time points. This could reveal if PLCζ has an initial effect on Ca^{2+}

signalling upon its introduction to the intracellular environment of CHO cells that is subsequently "switched off" resembling the cessation of Ca^{2+} oscillations at fertilisation. However, time limitations precluded these interesting further investigations.

CHAPTER 5
STABLE EXPRESSION OF PLCζ IN CHO CELLS

CHAPTER 5 STABLE EXPRESSION OF PLCζ IN CHO CELLS

5.1 Introduction

5.1.1 Mammalian expression systems

The production of protein in mammalian cells is an important tool in which recombinant protein function and effects of protein expression on dynamic cell signalling pathways can be studied. Cultivated mammalian cells possess the appropriate machinery for protein folding and post-translational modification that enable the production of fully active proteins with correct conformation. Chinese Hamster Ovary (CHO) cells are widely used for transfection, expression and large scale recombinant protein production. Since CHO cells provide precise and stable glycosylation, they have the ability to produce a post-translationally modified product that is a more accurate *in vitro* rendition of the natural protein (Sheeley *et al.*, 1997; Werner *et al.*, 1998). Transfected genetic material can be expressed in target cells either temporarily or permanently depending on the methods utilized and the experimental questions being investigated.

Transient transfections are used most commonly to analyze the short term (~48 hours) consequences of protein expression. Genetic material is introduced and gene products are expressed in the target cells however the nucleic acids do not integrate into the host cell genome. Within a few days most of the foreign DNA is degraded by nucleases or diluted by cell division, and after a few weeks its presence can no longer be detected. Stably transfected cells produce recombinant proteins on a continuous basis (months to years), and therefore

require the transfected DNA to replicate in synchrony with the cell. This occurs as a result of spontaneous and random integration of the transfected DNA into the cells genome by recombination (Chisholm, 1995). As integration is a rare phenomenon (1 in 10^4 for mammalian cells), cells exhibiting stable expression must be selected and amplified by using selectable markers, for example by transfecting a gene of non-mammalian origin that establishes drug resistance in cell culture. Frequently, the DNA of interest is transfected with the selectable marker on the same plasmid, with a separate transcription unit.

One of the most commonly used selectable markers in mammalian culture is the bacterial aminoglycoside phosphotransferase gene (*neo*). Expression of this gene confers resistance to the antibiotic G418 sulphate (Geneticin®, Invitrogen) by directing the synthesis of the aminoglycoside phosphotransferase enzyme (APH), which renders the antibiotic inactive through phosphorylation. G418 is similar in structure to neomycin, kanamycin and gentamycin which kill non-resistant eukaryotic cells by blocking protein synthesis through interference with the function of the 80S ribosomal subunit. After transfection, cells are grown in a medium containing the selective anitibiotic. Selective pressure is applied over a period of 2-3 weeks or more, with frequent changes of medium to eliminate dead cells and debris, until stable transfectants, which appear as distinct antibiotic-resistant clones, can be isolated and subcloned to multiwell plates for further propagation in selective medium.

Transient transfection of cells has the advantage of being a rapid process particularly useful for monitoring the efficiency of transfection procedures and for

verifying plasmid expression. Conversely, stably transfected cell lines circumvent the need for repeated transient transfection. Despite the time and effort involved in the generation and screening of stable cell clones expressing the protein of interest, once established, the stably transfected cell population provides a source of biological material that is readily available for further experimentation.

As discussed in chapter 3, transient expression of PLCζ tagged with venus (Kuroda *et al.*, 2006) and eYFP (Coward *et al.*, 2006) has been previously documented in COS-7 cells (a mammalian cell line derived from the kidney cells of the African green monkey). These investigations reported on the cellular localisation of the protein and its effects on Ca^{2+} homeostasis during the transient expression period. Despite the existence of these expression studies, a mammalian cellular system providing stable expression of PLCζ has yet to be reported.

5.1.2 Oocyte activation

The sperm factor theory describes a mechanism by which a soluble sperm factor is responsible for fertilisation induced Ca^{2+} oscillations (Swann, 1990; Swann *et al.*, 1994). The identification of the sperm factor has been investigated by isolation and purification of sperm extracts. Dale *et al.*,(1985) demonstrated that injection of a soluble fraction of sea urchin spermatozoa activates unfertilised sea urchin eggs and produced signs that a Ca^{2+} increase had taken place. This result was the first to suggest that fertilisation could occur successfully without any sperm-egg surface interaction. Since then, the method of injecting sperm extracts

has been employed to investigate the sperm factor theory across a range of species. In the species studied so far including pig (Machaty *et al.*, 2000), hamster (Swann, 1990), mouse (Swann, 1994), human (Homa *et al.*, 1994) and cow (Wu *et al.*, 1997), sperm extract injections activates oocytes with repetitive intracellular Ca^{2+} oscillations, similar to those that occur during fertilisation. In addition to this non-mammalian sperm extracts from xenopus, chicken and fish are also able to induce Ca^{2+} oscillations in mouse eggs (Coward *et al.*, 2003; Dong *et al.*, 2000). Parthenogenetic activation of mammalian oocytes is artificially induced by chemical agents including calcium ionophore (Steinhardt *et al.*, 1974b), ethanol (Cuthbertson, 1983), strontium (Fraser, 1987) and cyclohexamide (Bos-Mikich *et al.*, 1995). However, unlike sperm extracts the majority of the parthenogenetic treatments cause a monotonic increase in intracellular Ca^{2+}.

Another indisputable body of evidence in support of the soluble sperm factor theory came from intra-cytoplasmic sperm injection (ICSI), in which a single sperm is injected directly into an egg. This process, which bypasses the interaction of the sperm and egg, gives rise to intracellular Ca^{2+} oscillations (Nakano *et al.*, 1997) and results in successful egg activation and development (Kimura *et al.*, 1995b). It has been shown that round spermatids (precursor male gametes) possess the potential to achieve fertilisation and embryonic development when injected into eggs (Kimura *et al.*, 1995a; Kimura *et al.*, 1995c). However, the injection of round spermatids alone in mouse eggs is not capable of inducing an increase in intracellular Ca^{2+} and fails to result in egg

activation (Kimura *et al.*, 1995a; Kimura *et al.*, 1995c; Sato *et al.*, 1998). Methods for assisted egg activation for successful fertilisation by round spermatid injection include; the application of a high voltage pulse (Kimura *et al.*, 1995a; Kimura *et al.*, 1995c; Sasagawa *et al.*, 1996), and simultaneous injection with the $InsP_3R$ agonist adenophostin (Sato *et al.*, 1998) or sperm extracts (Sakurai *et al.*, 1999). The expression of recombinant PLCζ using a mammalian cell expression system could provide a means of generating an alternative egg activation agent.

5.1.3 Objective

Chapter 4 describes how the transient expression of PLCζ fails to modulate Ca^{2+} signalling in CHO cells, perhaps signifying that this protein is retained in an inactive form in this cell type. However, the possibility that this method of expression has resulted in the production of a form of PLCζ that is not fully functional cannot be overlooked. The overall aim of this chapter was to use CHO cells as a stable cellular expression system to produce PLCζ protein at high levels. The Ca^{2+} mobilizing activity of the PLCζ produced in this somatic cell line was subsequently examined in mouse oocytes.

5.2 Results

5.2.1 Establishing a mammalian system for the stable expression of PLCζ

5.2.1.1 G418-mediated selection of cells expressing eYFP tagged constructs

Because each eukaryotic cell line demonstrates a different sensitivity to the selective antibiotic G418 (with some exhibiting complete resistance to it), the optimum concentration required to kill non-transfected cells must be established for each new cell line or strain used for stable transfection. This is achieved by determining a killing curve for the cell line of interest. Prior to transfection, a dose-dependence curve was conducted on CHO cells to determine a suitable working concentration of G418 that would eliminate non-resistant cell populations (Figure 5.1). Since G418 only kills cells that are actively growing, CHO cells were seeded at a low density (1×10^5) in wells of a 6 well plate in order to prevent the cells becoming confluent over the duration of the experiment. The cells were exposed to increasing concentrations of G418 (0-1mg/ml, in 100µg/ml increments) for 8 days (n=3 per dose). Cells remaining after the 8 day incubation were harvested and counted by haemocytometry, shown in Figure 5.1. Increasing concentrations of G418 resulted in greater levels of cell death over the 8 day period. The dose at which G418 kills 50% of cells (Tox50) was ~100µg/ml. For this study, the concentration of G418 deemed sufficient to select for stable expression was 500µg/ml, as it was the lowest dose that eliminates the majority of cells following an 8 day incubation.

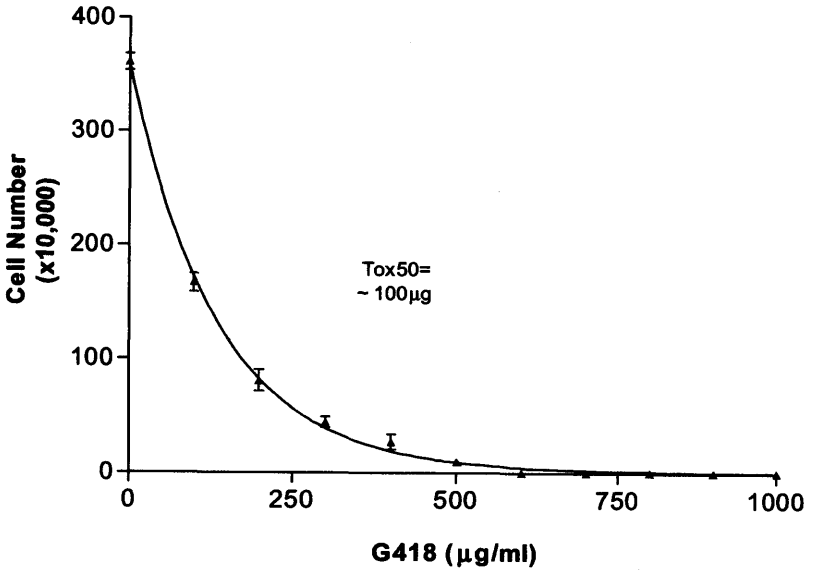

Figure 5.1 G418 dose-dependent elimination of non-resistant cell populations

CHO cell exposure to a range of G418 concentrations (0-1mg/ml) resulted in a dose dependent elimination of cells after 8 days. Tox50 (dose which resulted in the death of 50% of cells) is displayed on the graph. (data is presented as mean ± S.E.M. n=3 for each dose).

5.2.1.2 CHO cells express eYFP-PLCζ at low fluorescence intensities following antibiotic selection

The overall aim within this chapter was to devise a method to produce the PLCζ protein at levels high enough for assessment of its Ca^{2+} mobilising activity within oocytes. The presence of the *neo* gene on the eYFP tagged constructs enabled the selection of cells exhibiting stable expression following lipid mediated transfection using G418 (500µg/ml). Selective pressure was applied to cells that had undergone transfection either with the eYFP or eYFP-PLCζ construct for a period of two weeks, until distinct antibiotic-resistant clones were evident. eYFP facilitated the assessment of the generation of these stably transfected cells by flow cytometry. Figure 5.2 (a) is a typical two dimensional dot plot of forward scatter (FSC) vs side scatter (SSC), generated from data acquired by flow

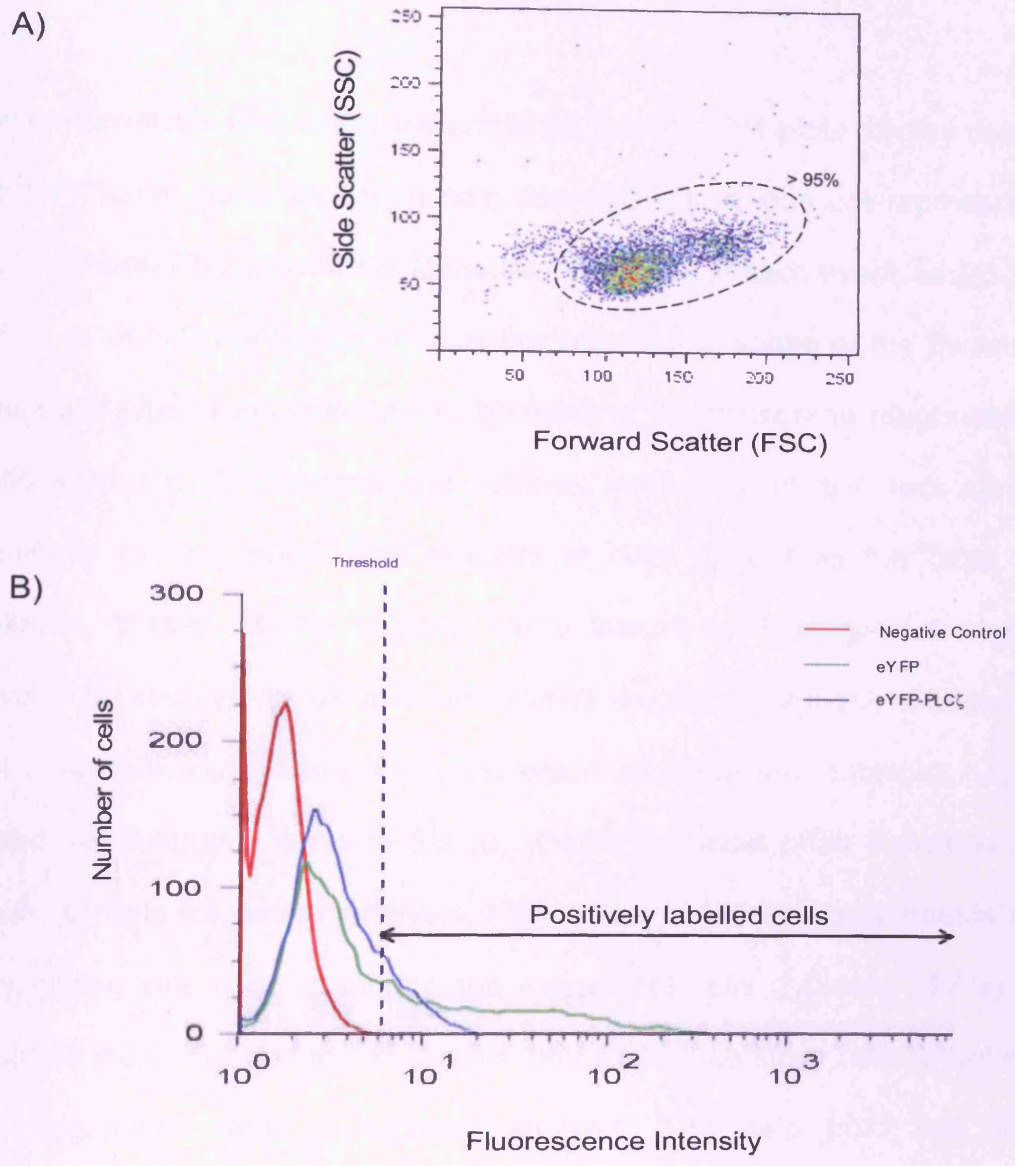

Figure 5.2 Flow cytometry data

Figure 5.2 (a) is a typical two dimentional dot plot of forward scatter (FSC) vs side scatter (SSC). The majority of the cells appear as a dense population of dots; each dot represents one acquired event. The isolated subset of cells used for further analysis is indicated by the gate drawn on the dot plot; thus excluding small cellular debris and large aggregates from subsequent analysis. The percentage of cells typically isolated within this gated region is indicated on the plot. 3 separate FSC vs SSC profiles measuring 5000 individual events/cells are acquired for each sample analysed by flow cytometry.

Figure 5.2 (b) shows typical overlayed histograms that were derived from two-dimentional dot plots as shown in figure 5.2 (a). This data is representative of the distribution of fluorescence intensities for the events acquired 2 days following transfection. The red line represents non-transfected CHO cells (negative control) and serves as a reference point against which all other experimental samples are compared. Cells expressing eYFP at fluorescence intensities that are higher than CHO cell auto-fluorescence are referred to as being positively labelled. The threshold for positively labelled cells is indicated by the horizontal blue line. The proportion of cells to the right of this threshold is used to calculate the percentage of positively labelled cells, as indicated by the gate drawn on the trace.

cytometric analysis of a single experimental sample. Dot plots display data from each particle/cell as a dot within both coordinate axis; one dot represents one acquired event. FSC provides a measure of the size of each event, whilst SSC is a measure of the granularity or inner complexity (i.e. shape of the nucleus, the amount and type of the cytoplasmic granules or the membrane roughness). The positions of the dots reflect the relative intensities of the two measured parameters for the event. The majority of cells appear as the most dense population of dots. Gates/ regions are a feature of flow cytometry analysis software that enables definition of boundaries around populations of interest. It is done by graphically drawing the gate/region after the raw data plot has been created, as illustrated in figure 5.2 (a). Gates are most often drawn to isolate subsets of cells for further analysis. For all flow cytometry experiments in this study, gating was used to isolate the majority of cells (typically >95%) which appear as the dense population of dots, and to exclude small cellular debris and large aggregates from subsequent analysis. The data from this isolated population was then used to construct a histogram depicting the number of cells and their relative fluorescence intensities as shown in figure 5.2 (b). Histograms are useful for flow cytometry data analysis as they allow the visualisation of the distribution of a single measured parameter (e.g. fluorescence) for the acquired events.

Overlayed histogram plots, as shown in figure 5.2 (b) are a valuable means of qualitatively comparing fluorescence intensities of different samples. Percentages of positive-expressing cells with fluorescence intensity values above

a set threshold (e.g. cell autofluorescence) can be determined by drawing a gate once the histogram has been generated. Negative control samples (i.e. non-transfected CHO cells) were acquired at the beginning of each flow cytometric analysis in order to establish a baseline reference point. The sensitivity of the fluorescent channel photomultiplier tube (PMT) was adjusted so that the negative control cells appear with intensities that are near zero but still on scale. This sample allows the assessment of the natural or auto-fluorescence of CHO cells, and establishes a reference point that can be used when describing the intensity of eYFP positive cells in subsequent experimental samples. Fluorescent intensities of experimental samples are relative to control samples, and cells expressing eYFP above the level of cell background auto-fluorescence are described as being positively labelled. Positively labelled cells are gated for as illustrated in figure 5.2 (b) and expressed as a percentage of total cells. Following lipid mediated transfection, a sample of cells was removed from culture at 5 hours, and then daily for a period of two weeks in order to assess levels of eYFP expression.

The data in Figure 5.3 shows that the typical transfection efficiencies for eYFP and eYFP-PLCζ transfectants were 3.9 ± 0.1% and 3.4 ± 0.3% respectively at 5 hours, with the percentage of positively labelled cells rising to 28.4 ± 0.5% and 16.6 ± 0.5% at day 2 corresponding to the peak of the transient transfection period. Following this, the levels of positively labelled cells fall to 10.6 ± 0.4% (eYFP) and 1.1 ± 0.2% (eYFP-PLCζ) which coincides with the period prior to complete antibiotic selection when non-transfected cells comprise part of the

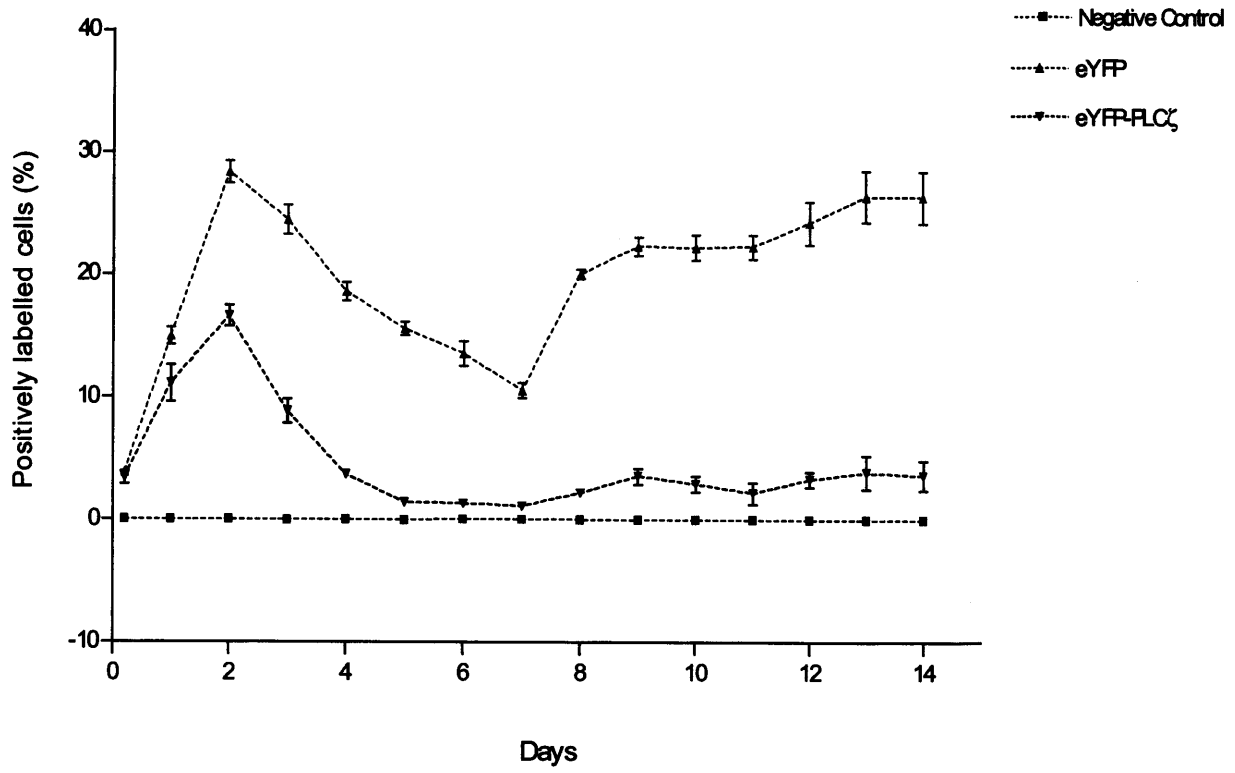

Figure 5.3 Analysing the generation of stable cell populations by flow cytometry
Figure 5.3 shows the proportion of positively labelled cells over a period of 2 weeks following the transfection of CHO cells with DNA encoding eYFP (represented by the green line) or eYFP-PLCζ (represented by the blue line). The red line represents non-transfected CHO cells (negative control) and serves as a reference point against which all other experimental samples are compared. Data is expressed as a percentage of the total number of cells (mean ± S.E.M). Results are representative of at least 6 separate transfections.

overall population. After 8 days of selective pressure, the point at which the majority of non-transfected cells are eliminated, the number of positively labelled cells increased gradually, before reaching a plateau of ~ 26% (eYFP) and ~ 4% (eYFP-PLCζ). After the 14th day, the proportion of positively labelled cells failed to increase significantly beyond this level (data not shown). The overlayed histogram in figure 5.2 (b) shows that both eYFP and eYFP-PLCζ stably transfected cell populations contain a large proportion of cells that are not positively labelled. It is possible that these cells fail to express the protein of

interest; however this does not explain their resistance to G418. A more probable explanation is that they express eYFP at levels that fall below the limit of positive detection, and as a result are not easily distinguishable from CHO cell autofluorescence. eYFP-PLCζ stables express significantly less positively labelled cells when compared with eYFP stables, thus making selection of a highly expressing clone by serial dilution more difficult.

5.2.1.3 Enrichment of the stable eYFP-PLCζ cell line

As a means of increasing the total number of positively labelled cells within the stably transfected eYFP-PLCζ population (i.e. cells with fluorescence intensities distinguishable from CHO cell auto-fluorescence), cell suspensions were subjected to fluorescence activated cell sorting (FACS). Positively sorted cells characterised by fluorescence intensities that are higher than CHO cell autofluorescence were selected and cultured in the presence of G418 to maintain selection of eYFP-PLCζ expressing cells. A sample of cells was removed from the culture 7 days post FACS and analysed by flow cytometry (Figure 5.4 b). FACS failed to eliminate all cells expressing below the positively labelled threshold. However, the proportion of positively labelled cells increased from 3.8 ± 0.6% to 22.4 ± 0.2%, thus increasing the probability of isolating a highly expressing clone by serial dilution. FACS sorted cells were subjected to serial dilution, and cells propagated from single clone colonies were screened by flow cytometry. Two of the thirty six single clone colonies exhibited a shift in fluorescence as depicted in figure 5.4 (c), with 67.2 ± 0.4% of cells displaying eYFP fluorescence intensities ~100 fold higher than CHO cell auto-fluorescence, whilst the remaining cells within the population continued to express at levels below the limit of positive detection.

Repeated propagation of these cells by serial dilution out-cloning, failed to increase the proportion of positively labelled cells resulting in a dual expressing population. However, an additional round of FACS selecting for the positively labelled cells, combined with further propagation by serial dilution out cloning

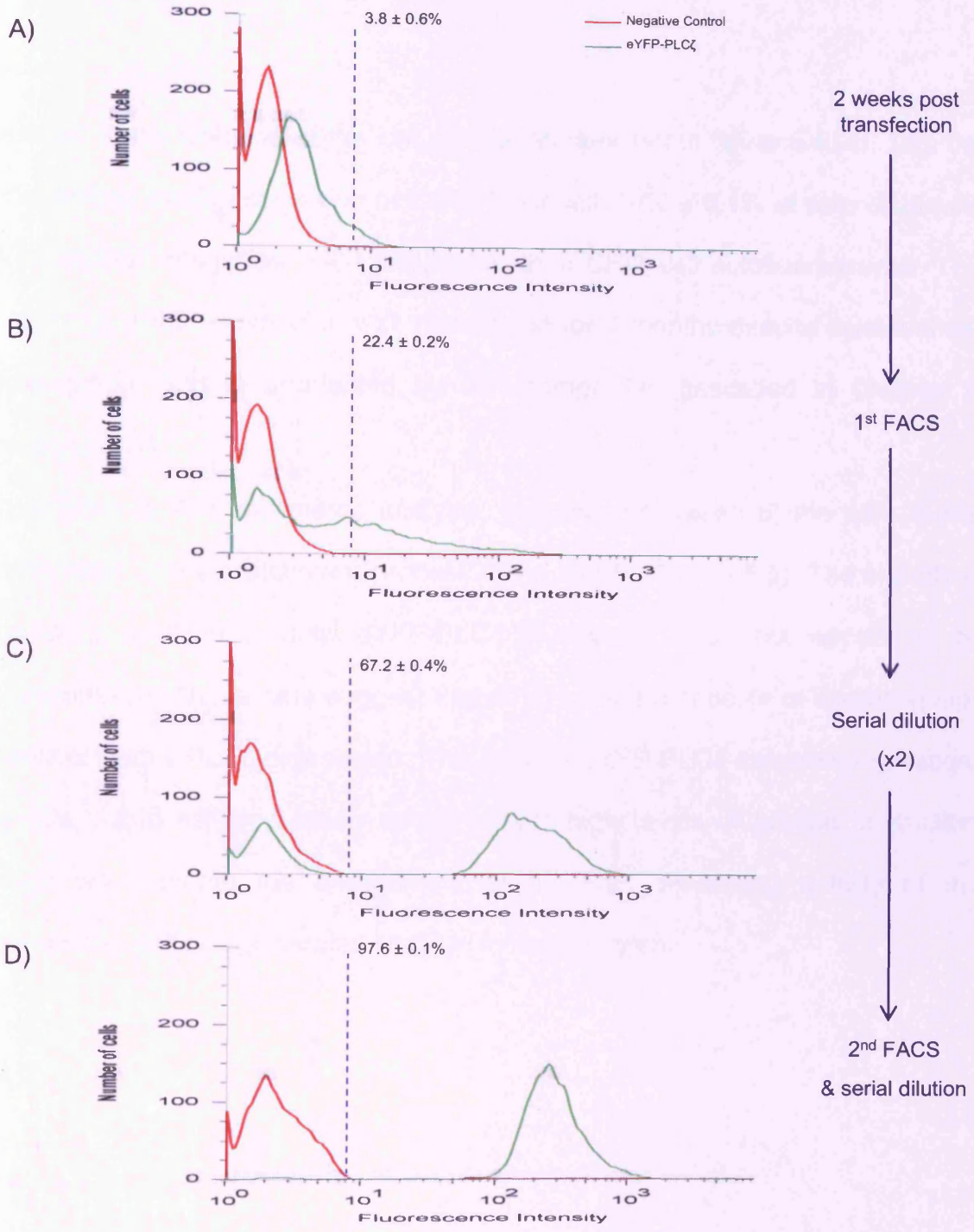

Figure 5.4 Enrichment of the stable eYFP-PLCζ cell line
This figure shows overlayed histograms representing the distribution of fluorescence intensities of non-transfected cells (negative control, red line), and cells exhibiting stable expression of eYFP-PLCζ (green line). The horizontal blue line represents the threshold for positive detection. Each histogram was generated by flow cytometric analysis, and corresponds to a different stage in the process of enrichment of eYFP expression; these stages are indicated to the right of the figure. Transfected cells that had been selected by G418 for a period of two weeks (A) were subjected to fluorescence activated cell sorting (FACS) (B). Single cell clones were then generated by serial dilutions (C), which were subsequently enriched further by an additional round of FACS and out-cloning (D).The proportion of positively labelled cells are indicated on each histogram (expressed as a percentage of total cells, mean ± SEM of three acquisitions measuring 5000 events).

resulted in the isolation of the cell population depicted in figure 5.4 (d). This cell line exhibits stable expression of eYFP-PLCζ with 97.6 ± 0.1% of cells displaying fluorescence intensities ~100 fold higher than CHO cell autofluorescence. This pattern of stable expression was maintained for 4 months despite continual cell propagation, and is unaffected by cryostorage (as described in Chapter 2, section 2.2.4).

In addition to flow cytometric analysis, images were taken of the cells during each stage of the enrichment process using CLSM (Figure 5.5). The viability of the cells exhibiting stable eYFP-PLCζ expression does not appear to be compromised. These data suggest that CHO cells are capable of tolerating high levels of stable PLCζ expression. The level of eYFP-PLCζ expression exhibited by this stable cell population should reflect high levels of protein production, which will facilitate the assessment of the Ca^{2+} mobilising activity of this mammalian cell line generated PLCζ in mouse oocytes.

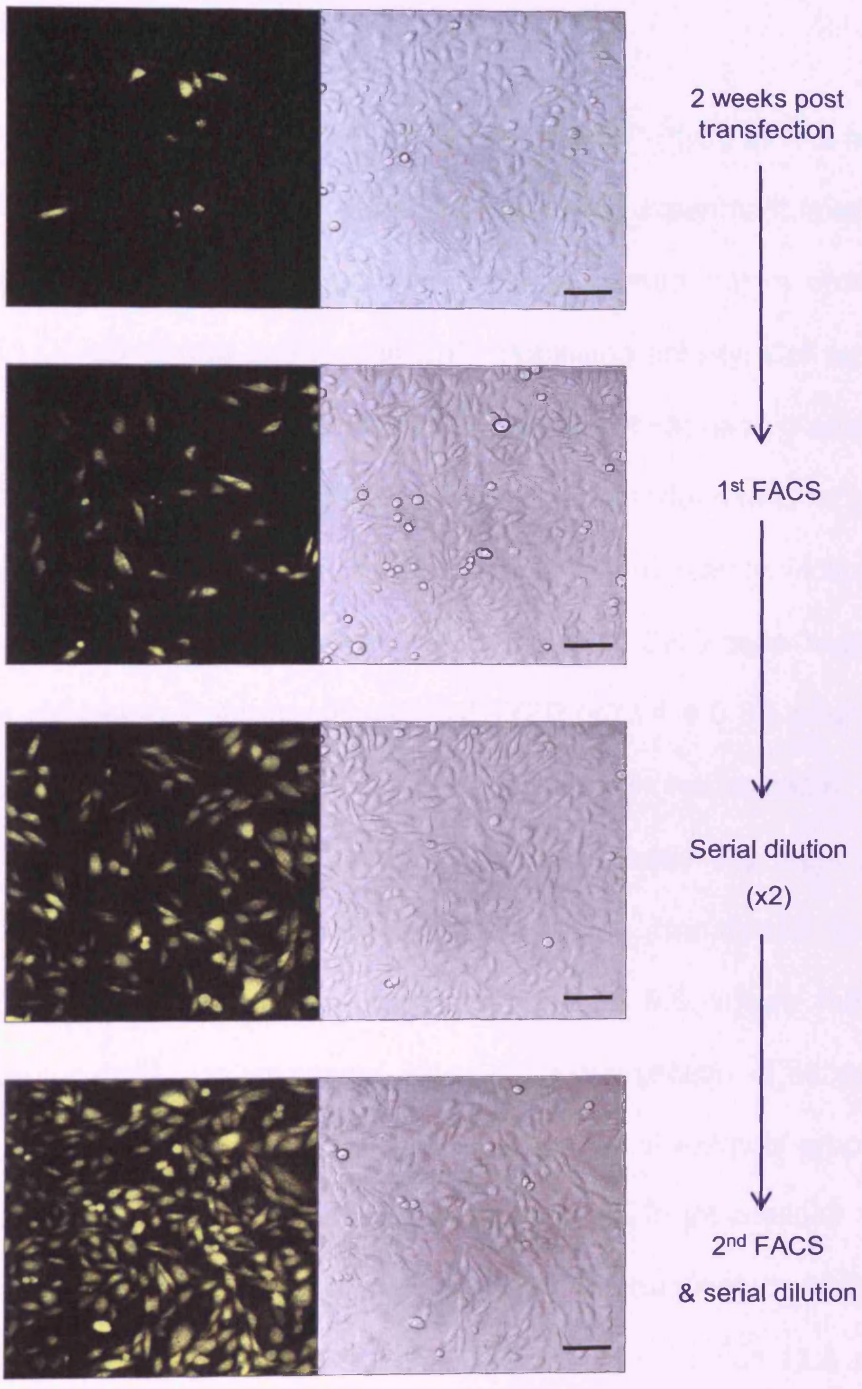

Figure 5.5 Images of the stable eYFP-PLCζ cell line
Figure 5.5 shows confocal images of the stable eYFP-PLCζ cell line at each stage of the enrichment process. See text for further details. Scale bar represents 50μm.

5.2.2 Microinjection of eYFP-PLCζ cell extracts

One possibility is that CHO cells tolerate high levels of eYFP-PLCζ as it is being expressed in a form that is not fully functional. The following experiment involving the injection of cell extracts into mouse oocytes was carried out in order to determine if the PLCζ generated possesses Ca^{2+} mobilising activity. Cell extract injections were peformed in collaboration with Karl Swann. Metaphase II-arrested mouse eggs were collected and loaded with Fura red as described in Chapter 2, section 2.2.13. Intracellular Ca^{2+} was monitored immediately following microinjection of cell extracts prepared from non-transfected CHO cells (negative control), and cells exhibiting stable expression of eYFP (~73.4 ± 0.6% positively labelled), or eYFP-PLCζ (97.6 ± 0.1% positively labelled) (cell extracts were prepared as described in Chapter 2, section 2.2.11). Typically 3-5 eggs were injected over a period of 10-20 seconds before being transferred to the fluorescence imaging system within 1-2 minutes. Figure 5.6 shows that no change in intracellular Ca^{2+} was observed following microinjection of either the negative control (n=4) or eYFP extract (n=6). Microinjection of extracts prepared from cells expressing eYFP-PLCζ induced a rapid increase in intracellular Ca^{2+} within 1-2 minutes followed by series of repetitive Ca^{2+} oscillations in 100% of oocytes (n=14). The frequency of the Ca^{2+} oscillations observed was 11.4 ± 1.4 spikes/hour, which persisted for the duration of the recording (typically 1-1.5 hours). These data suggests that the stable eYFP-PLCζ cell line is expressing some active PLCζ that is capable of inducing Ca^{2+} oscillations in oocytes that are comparable to those observed with sperm extract injections (Swann, 1994).

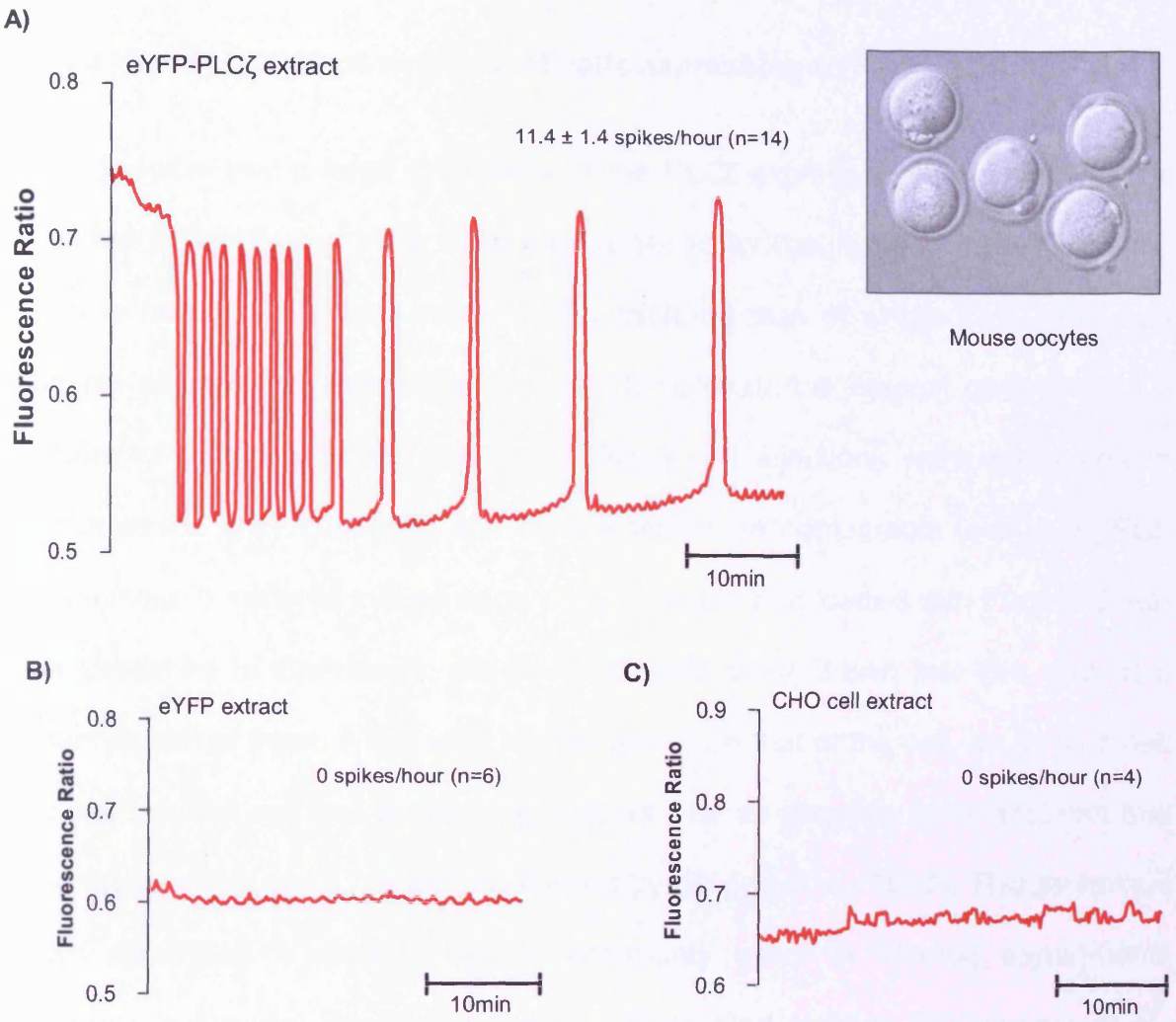

Figure 5.6 Microinjection of cell extracts into mouse oocytes

This figure shows the intracellular Ca^{2+} responses in mouse oocytes following the microinjection of extracts prepared from cells expressing eYFP-PLCζ (A), eYFP (B) or non-transfected CHO cells (C). Each trace is a recording from a single oocyte, and is representative of the typical observations made in each experimental group. The number of eggs within each group is indicated on every trace alongside the Ca^{2+} oscillation frequencies observed (expressed as mean ± SEM). The image to the right shows a bright field image of oocytes that have been injected with the eYFP-PLCζ extract.

5.2.3 Microinjection of single CHO cells expressing eYFP-PLCζ

It is possible that a large proportion of the PLCζ expressed by the eYFP-PLCζ cell line is inactive and this cannot be assesed by the injection of cell extracts. The following experiment involving the microinjection of single CHO cells into mouse oocytes was carried out in order to estimate the amount of active PLCζ contained within a single CHO cell. Single cell injections were performed in collaboration with Yuansong Yu using a technique comparable to that of ISCI. Metaphase II-arrested mouse eggs were collected and loaded with Fura PE3-AM as described in Chapter 2. Single CHO cells were drawn into the end of a micropipette of internal diameter slightly less than that of the cell, so as to break or weaken the cell wall while disturbing as little as possible the cytoplasm that surrounds the nucleus, a method devised by (Briggs *et al.*, 1952). This technique also resembles a method that is commonly used for cloning experiments whereby cell nuclei are transferred into enucleated oocytes (Wakayama *et al.*, 1999). Intracellular Ca^{2+} was monitored immediately following microinjection of either non-transfected CHO cells (negative control), or cells expressing eYFP-PLCζ (from the enriched stable cell population). Single cells were injected into single mouse eggs before being transferred to the fluorescence imaging system within 1-2 minutes. Figure 5.7 shows that no change in intracellular Ca^{2+} was observed following the microinjection of negative control cells (n=14). The injection of cells expressing eYFP-PLCζ induced a series of repetitive Ca^{2+} oscillations in 15/23 eggs which persisted for the duration of the recording (typically 1-6 hours). As observed with the cell extract injections (Figure 5.6) the

Ca^{2+} response was rapid, with the initial transient taking place within minutes of the cell injection. The frequency of the Ca^{2+} oscillations observed was 4.3 ± 0.8 spikes/hour. This data suggests that individual CHO cells are expressing active PLCζ at levels capable of inducing Ca^{2+} oscillations in mouse oocytes that are comparable to those observed following sperm extract injections (Swann, 1994).

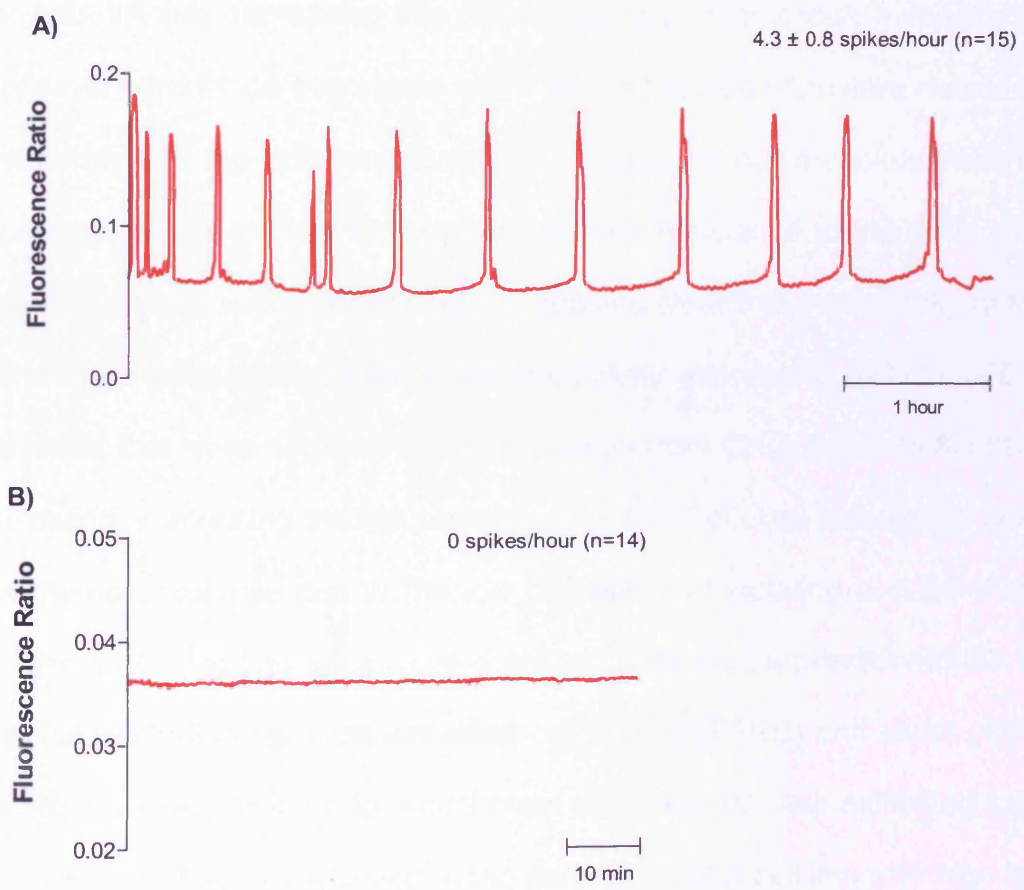

Figure 5.7 Microinjection of individual CHO cells into mouse oocytes

This figure shows the intracellular Ca^{2+} responses in mouse oocytes following the microinjection of single intact CHO cells either expressing eYFP-PLCζ (A), or non-transfected controls (B). Each trace is a recording from a single oocyte, and is representative of the typical observations made in each experimental group. The number of eggs within each group is indicated on every trace alongside the Ca^{2+} oscillation frequencies observed (expressed as mean ± SEM).

5.3 Discussion

5.3.1 Generation and enrichment of the stable eYFP-PLCζ cell line

To date, there have been no reports of a stable cell line expressing PLCζ. Expression of the recombinant PLCζ protein has proven difficult in bacterial expression systems, particularly with regards to expressing the more potent human form of the protein. Following antibiotic selection of CHO cells transfected with eYFP-PLCζ, it would have been easy to assume that these mammalian cells also had difficulty expressing this protein, as upon microscopic inspection, only a very small percentage expressed eYFP above the limit of positive detection. This could imply that the cells had somehow managed to downregulate/switch off the expression of this protein whilst retaining their resistance to antibiotic selection. Upon examination by flow cytometry, it became clear that the majority of the cells within this selected population were most likely expressing eYFP-PLCζ at very low levels that were not easily distinguishable from CHO cell auto-fluorescence. The option of enriching the cell population by serial dilution techniques alone was considered unsuitable due to the low probability of isolating a clone that would express above the limit of positive detection. This chapter demonstrates that the combination of fluorescence activated cell sorting (FACS) and serial dilution out cloning is a viable method for enrichment of stable cell lines exhibiting low levels of expression. This has resulted in the generation of a cell line with high levels of stable eYFP-PLCζ expression that is clearly distinguishable from cellular autofluorecence. The enrichment process has produced the first mammalian expression system to offer high levels of PLCζ protein production which could be valuable for subsequent experimental analysis of its mechanism of activation.

5.3.2 The PLCζ produced in CHO cells causes Ca^{2+} oscillations in mouse oocytes.

One of the main advantages of mammalian expression systems is that they possess the appropriate machinery for protein folding and post-translational modification that enable the production of fully active proteins with correct conformation. The results from previous chapters within this study revealed that the expression of eYFP-PLCζ had no effect on Ca^{2+} in CHO cells, and the possibility that this expression system had resulted in the production of a form of PLCζ that was not fully functional could not be disregarded. A suitable means of examining the activity of this protein was considered to be its delivery into mouse oocytes, a system in which the effects of PLCζ have been well characterised.

Injection of either cytosolic extracts or whole cells from the eYFP-PLCζ cell line produced Ca^{2+} oscillations in mouse eggs, confirming that the PLCζ generated by this mammalian expression system is fully functional. Interestingly, despite individual cells expressing enough PLCζ to trigger Ca^{2+} oscillations in an oocyte, the Ca^{2+} homeostasis in the somatic cell line remained unperturbed. These results imply that the enzymatic activity of PLCζ may be reversibly inhibited in somatic cells, or else specifically stimulated by factors in the egg cytoplasm.

CHAPTER 6
GENERAL DISCUSSION

CHAPTER 6 GENERAL DISCUSSION

6.1 PLCζ and the implications of the current results

In the quest to explain the generation of Ca^{2+} oscillations at fertilisation, the content hypothesis was proposed as an alternative to receptor mediated activation of the $InsP_3$ pathway (Swann, 1990; Swann *et al.*, 1994). This theory describes a mechanism by which a soluble sperm factor is released into the egg, capable of activating the $InsP_3$ signalling pathway and the subsequent Ca^{2+} release from the ER. Microinjection of sperm extracts, or whole sperm in eggs produced a series of Ca^{2+} oscillations in a range of different species much like those seen at fertilisation (Kyozuka *et al.*, 1998; Palermo *et al.*, 1992; Stricker, 1997; Swann, 1990; Swann *et al.*, 1994; Tang *et al.*, 2000; Wu *et al.*, 1997).

It was proposed that a sperm specific PLC activity could explain the ability of a soluble, mammalian sperm extract to cause Ca^{2+} oscillations (Jones *et al.*, 2000; Jones *et al.*, 1998; Parrington *et al.*, 2002). However, microinjection of recombinant proteins corresponding to most of the known PLC isoforms expressed in sperm, including PLCβ1, γ1, γ2 and δ1 failed to mimic the Ca^{2+} oscillations observed at fertilisation (Jones *et al.*, 2000; Parrington *et al.*, 2002; Runft *et al.*, 2002), or only managed to initiate Ca^{2+} oscillations at non-physiological concentrations (Mehlmann *et al.*, 2001). Analysis of a mouse testis expressed sequence tag (EST) database led to the production of a full length cDNA encoding a novel sperm specific PLC sequence, termed PLCζ (Saunders *et al.*, 2002). Microinjection of cRNA encoding mouse (Saunders *et al.*, 2002), human and simian (Cox *et al.*, 2002) PLCζ into mouse eggs produced fertilisation

like Ca^{2+} responses. Furthermore, these oscillations were abolished when PLCζ was immunodepleted from native sperm extracts (Saunders *et al.*, 2002; Swann *et al.*, 2004). The presence of PLCζ has also been demonstrated in boar and hamster sperm (Saunders *et al.*, 2002). Microinjecting recombinant PLCζ that was synthesised using a baculovirus expression system was able to trigger Ca^{2+} oscillations in mouse eggs (Kouchi *et al.*, 2004). Significantly, the amount of PLCζ required to initiate Ca^{2+} transients in eggs correlates with the approximate concentration of PLCζ in a single sperm (20-50fg) (Saunders *et al.*, 2002). PLCζ is becoming increasingly accepted as the physiological activator of embryo development in mammals and perhaps other vertebrates. The mechanism of action of PLCζ is still unclear; it is not known how it is regulated or if its effects are specific to eggs, and it may be autonomously active when introduced into the egg by the sperm during fertilisation.

Relatively little work has focused on examining the activity of PLCζ in somatic cells. Previous studies have reported on the cellular localisation of PLCζ (Coward *et al.*, 2006; Ito *et al.*, 2008; Kuroda *et al.*, 2006) and its ability to induce Ca^{2+} oscillations (Kuroda *et al.*, 2006) in mammalian cell lines. The findings of this thesis also confirm the nuclear translocation ability of PLCζ in somatic cells, however the results suggest that this phenomenon is linked to time after transfection as apposed to the Ca^{2+} mobilising activity of PLCζ that has been suggested previously (Kuroda *et al.*, 2006).

CHO cells were transfected with luciferase or eYFP tagged PLCζ. The frequency of the spontaneous Ca^{2+} oscillations observed in these cells was unaffected by

PLCζ expression. Similarly, there was no evident change in resting Ca^{2+} levels, nor any subtle change in the variability in resting Ca^{2+}. There were no differences in the response to extracellular ATP when compared with control eYFP transfected cells, or to cells transfected with eYFP tagged to a catalytically inactive PLCζ. Overall, there is no evidence to suggest that PLCζ perturbs Ca^{2+} homeostasis in somatic cell lines.

Despite the lack of effect on Ca^{2+} in CHO cells, either injection of cytosolic extracts, or whole cells from a stably transfected eYFP-PLCζ cell line were able to induce Ca^{2+} oscillations in mouse eggs. This effect was not seen with untransfected CHO cells. These data suggest that PLCζ is inactivated when expressed in a cell line and yet active when subsequently introduced into an egg. Broad ectopic expression of PLCζ has been shown to have minimal effects in transgenic mice (Yoshida *et al.*, 2007). The authors conclude that the activity of PLCζ may be restricted to oocytes, and suggest that this is the only tissue that possesses the cellular machinery required to transduce PLCζ signalling. It is important to mention that the low level of ectopic expression observed in the transgenic mice was not quantified. The results of this thesis imply that somatic cells are capable of tolerating much higher levels of PLCζ, which was shown to be active upon its introduction into mouse eggs.

6.2 Estimation of protein expression levels

An effective way to measure how much protein is being expressed in living cells is to use cDNA constructs tagged with firefly luciferase. Unlike fluorescence

based methods, luminescence does not suffer from interference from auto-fluorescence, and as a result provides a highly sensitive technique for the quatification of protein levels. When considering that mouse PLCζ is active in mouse eggs at concentrations as low as 1-10nM (Kouchi *et al.*, 2004), this issue of sensitivity is particularly significant. One advantage of fluorescent probes is that high resolution confocal imaging can be employed, which is better suited to studies concerning the cellular localisation of the expressed protein. Photon imaging cameras, like the one used in this thesis, enable the identification of which individual cells are expressing luciferase allowing the quantitative analysis of how much luciferase-tagged protein is being expressed.

Previous work in our laboratory lead to the construction of a calibration curve which has enabled users of our photon imaging system to ascertain the amount of PLCζ-LUC protein that was being expressed in eggs following cRNA injections (Campbell, 2007; Nomikos *et al.*, 2005; Swann *et al.*, 2007). To do this, mouse eggs had been injected with known amounts of firefly luciferase cRNA or protein. After luminescence imaging, eggs from each group were lysed with 1% Triton x100 in a PBS buffer containing 1mM $MgCl_2$, 1mM ATP and 100μM luciferin. The lysis took place in a custom built luminometer (see Chapter 2, section 2.2.7) and the average signal (cps) was taken over 60 seconds. The luminometer was calibrated with purified native luciferase protein. A relationship was then obtained (Figure 6.1) that can be used to calculate unknown protein content in eggs that have been injected with a luciferase tagged construct.

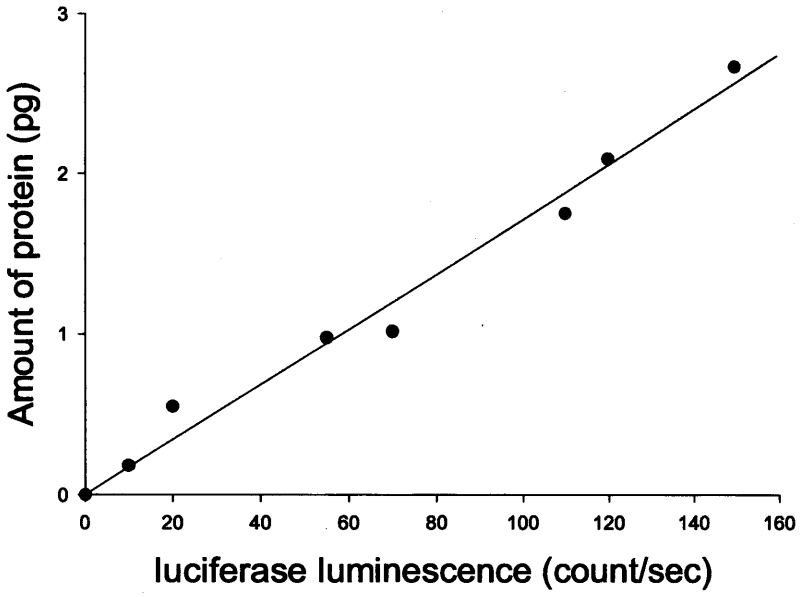

Figure 6.1 Calibration for quantification of protein expression
Calibration curve constructed to calculate the amount of PLCζ-LUC protein being expressed. (provided by Karl Swann).

In the experiments presented in this thesis, the average luminescence signal recorded in single CHO cells expressing PLCζ-LUC ranged from 1-10cps. The experimental setup used for recording the expression in cells was estimated to be approximately one and a half times more sensitive than the set up used for the calibration in eggs. With this in mind, 10cps from a single cell equates to ~6cps had the same set up have been employed. Using the calibration in figure 6.1, the amount of PLCζ protein expressed in a single CHO cell with an average signal of 10cps was estimated to be approximately 130fg. Individual cells are expressing within and above the range of PLCζ required to initiate Ca^{2+} oscillations in eggs (20-50fg) (Saunders *et al.*, 2002), and are therefore considered to be expressing at levels comparable with that of sperm. When comparing the relative volume of an average CHO cell (~2pl) to that of an egg

(~200pl), these cells are clearly capable of tolerating ~200-300 fold more PLCζ than the amount required to induce Ca^{2+} release in an egg.

The calibration of eYFP is not as straightforward due to variation in experimental factors such as excitation light, focal depth and camera sensitivity; all of which would require standardisation with recombinant eYFP. However, with this in mind, it is possible to estimate levels of protein expression based on the following assumptions. The detection limit of wild type GFP in a typical mammalian cell has been determined to be ~1μM over cellular autofluorescence (Niswender *et al.*, 1995). Mutant GFPs with improved extinction coefficients decrease this limit and allow the detection of lower levels of fluorescence (Cormack *et al.*, 1996; Heim *et al.*, 1995). It is reasonable to assume that the cells of the stable eYFP-PLCζ population which were typically ~10-100 fold brighter than cellular autofluorescence contain at least 10μM eYFP-PLCζ. Consequently, an estimate of the amount of eYFP-PLCζ (100,000 Mw) per typical CHO cell of 1-2pL volume equates to approximately 1-2pg. This approximate calculation suggests that the stably transfected CHO cells generated as part of this thesis have a cytoplasmic concentration of PLCζ ~1000 fold higher than the amount required to induce Ca^{2+} oscillations in an egg, which is consistent with the PLCζ-LUC results. It is possible that a proportion of the 1-2pg of protein is inactivated; however the single cell injection experiments (Chapter 5) confirm that individual CHO cells contain at least the required amount of active PLCζ to induce Ca^{2+} release in an egg.

6.2.1 Cell extract injections

The generation of cell extract enables the isolation of protein from a large number of cells. The cytosolic fraction of cells expressing eYFP-PLCζ was prepared into a 20µl extract as described in Chapter 2, section 2.2.11. The number of cells used in all extract preparations was calculated using haemocytometry (typically ~2 x 10^7 cells). Extracts were diluted (1 in 5) in order to facilitate injection, and taken together with the estimated injection volume of ~1-5pl, a calculation was performed in order to determine the number of cells that correspond to the amount of extract injected. This revealed that amount of cell extract delivered into eggs was equivalent to injecting ~1-5 CHO cells. This data also suggests that individual cells expressing eYFP-PLCζ are expressing PLCζ at levels capable of inducing Ca^{2+} oscillations in eggs; an estimation which is supported by experiments involving single cell injections.

6.3 The conundrum of PLCζ expression in cells

The data presented in this thesis demonstrates that somatic cells can tolerate levels of PLCζ 100 -1000 fold higher than the amount required to induce Ca^{2+} release in an egg, without exhibiting any apparent perturbations in Ca^{2+} homeostasis. This suggests that PLCζ is completely inactivated when expressed in a somatic cell line. However, injections of cytosolic extracts, or whole cells from the eYFP-PLCζ transfected cell line confirmed that the PLCζ expressed within these cells is capable of inducing Ca^{2+} release upon its introduction into mouse eggs. The results imply that the enzymatic activity of PLCζ may be

reversibly inhibited in somatic cells, or else specifically stimulated by factors in the egg cytoplasm. These hypotheses are considered in the following sections.

6.4 Inhibition of PLCζ activity in somatic cells

If the activity of PLCζ is inhibited in somatic cells, it is worth considering the following possible mechanisms.

6.4.1 Nuclear Translocation

It is possible that nuclear sequestration may be involved in the inhibition of PLCζ activity. The expression of PLCζ-Venus in mouse eggs increases for up to 3 hours following cRNA injection until a steady level is attained at 4-5 hours (Yoda *et al.*, 2004). Expressed PLCζ is distributed homogenously throughout the egg cytoplasm without membrane association or any localisation. Interestingly, PLCζ translocates into the pronucleus (PN) formed at 5-6 hours (Yoda *et al.*, 2004), which is consistent with an earlier observation that the PN formed after fertilisation has Ca^{2+} releasing activity when introduced into an unfertilized egg (Kono *et al.*, 1995). Previous work has shown that Ca^{2+} oscillations after fertilisation (Deguchi *et al.*, 2000; Jones, 1998) or after injection of RNA encoding PLCζ (Larman *et al.*, 2004) cease around the time of PN formation, suggesting that nuclear translocation of PLCζ may be responsible for the termination of oscillations. Ca^{2+} oscillations continue over 10 hours when PN formation is prevented by injection of a lectin, WGA (Marangos *et al.*, 2003), or when a point mutation is added to a putative nuclear translocation signal (NLS) region of PLCζ (Larman *et al.*, 2004). During early development, Ca^{2+} oscillations reappear at

the stage of nuclear envelope breakdown just before the first cell division (15-16 hours after fertilisation) and cease after the first cleavage (Larman *et al.*, 2004). Subsequently, PLCζ translocates again to the nuclei of the 2 cell embryo after the first cleavage (Larman *et al.*, 2004; Sone *et al.*, 2005). These results have lead to the view that the movement of PLCζ between the cytoplasm and the nucleus may turn on and off a series of $InsP_3$-dependant Ca^{2+} rises in a cell cycle dependent manner.

However, this is unlikely to explain the lack of PLCζ activity observed in the current study since no changes in Ca^{2+} were observed before nuclear translocation had taken place (3 and 5 hours following DNA delivery). Nuclear sequestration of PLCζ may also be limited by capacity, and it is unlikely that all of the PLCζ is localised to the nucleus at high expression levels, such as in the stably transfected eYFP-PLCζ cell line. This suggests that there may be other mechanisms for inhibiting the activity of PLCζ in somatic cells.

6.4.2 Downregulation of $InsP_3R$

In eggs, $InsP_3R$ downregulation and Ca^{2+} store depletion have been proposed as possible alternative mechanisms for the termination of Ca^{2+} oscillations following fertilisation (Jellerette *et al.*, 2000). Cells also have the ability to adapt to long term exposure to an agonist by down regulation of receptors. Chronic stimulation of receptors linked to $InsP_3$ formation has been shown to cause a reduction in the number of $InsP_3R$ and a decrease in sensitivity of the intracellular Ca^{2+} stores to $InsP_3$ (Wojcikiewicz *et al.*, 1991; Wojcikiewicz *et al.*, 1992). Downregulation of $InsP_3R$ has been shown to inhibit Ca^{2+} release in mouse eggs (Brind *et al.*, 2000;

Jellerette *et al.*, 2000), and has been proposed to partly explain the cessation of Ca^{2+} oscillations 3-4 hours after fertilisation. It is reasonable to assume therefore that $InsP_3R$ downregulation could account for the lack of effect of PLCζ on Ca^{2+} in somatic cells.

Results in mouse oocytes have shown that different levels of PLCζ protein expression alter the pattern of Ca^{2+} oscillations observed (Yu *et al.*, 2008b). Increased expression of PLCζ correlates with a quicker onset and higher frequency of Ca^{2+} oscillations. Interestingly, higher levels of PLCζ expression also cause a gradual decrease in spike amplitude and a more rapid termination of Ca^{2+} transients. The experimental protocol employed during this study made it impractical to monitor the intracellular Ca^{2+} of cells expressing PLCζ sooner than 3 hours following cDNA delivery. It is therefore possible that PLCζ does perturb the intracellular Ca^{2+} in somatic cells at earlier time points, which would suggest that somatic cells, like eggs, possess an innate ability to limit the duration of Ca^{2+} signals initiated by PLCζ. This could involve downregulation of $InsP_3Rs$.

Sperm extracts have been shown to trigger Ca^{2+} oscillations in rat hepatocytes (Berrie *et al.*, 1996). Two distinct types of oscillations were recorded, either an early transient that displayed further secondary oscillations during the falling phase, or late transients that were more variable in peak height. Hepatocytes displayed between one and 19 early transients, and up to eight of the later transients (n= 10 cells). Ca^{2+} oscillations were initiated within minutes following extract injection, and were shown to continue for approximately 1.5 hours. This data shows that PLCζ is capable of inducing Ca^{2+} oscillations in hepatocytes

which appear to be limited in their duration. In order to assess if PLCζ is capable of inducing a similar Ca^{2+} response in CHO cells, future experiments could involve the injection of RNA encoding PLCζ with a prolonged Ca^{2+} imaging period, much like the experiments performed using mouse oocytes. It would also be interesting to observe the effects of injecting extracts prepared from the stably transfected eYFP-PLCζ cell line into CHO cells.

High levels of PLCζ promote sustained DAG production in mouse eggs which can lead to PKC-mediated Ca^{2+} influx and subsequent overloading of Ca^{2+} stores (Yu *et al.*, 2008a). The series of secondary Ca^{2+} oscillations induced by PKC overstimulation have been proposed to have a major negative effect on eggs; such as failure to develop to blastocyst stages despite having formed pronuclei (Berrie *et al.*, 1996; Yu *et al.*, 2008a). Downregulation of $InsP_3R$ could account for the lack of PLCζ activity in CHO cells; however it is possible that cells would experience adverse effects of sustained DAG production and subsequent PKC activation, such as changes in Ca^{2+} homeostasis and cell proliferation. The results of this thesis do not indicate any marked irregularities in CHO cells expressing PLCζ that would indicate persistent DAG production, however such an effect cannot be ruled out. It would be interesting to assess the levels of DAG in cells expressing PLCζ. This could be achieved by performing a protein phosphorylation assay using a PKC substrate, such as MARCKS (Myristoylated Alanine Rich C Kinase Substrate) protein (Arbuzova *et al.*, 1998). Also, DAG production in the plasma membrane could be assessed using a fluorescently tagged CI domain of PKC (Yu *et al.*, 2008a).

In addition to this, CHO cells expressing PLCζ have a comparible Ca^{2+} response to extracellular ATP when compared with control eYFP transfected cells and with cells transfected with eYFP tagged to a catalytically inactive PLCζ. It is reasonable to assume that the agonist response would be modified in some way had the $InsP_3Rs$ become downregulated. So it seems again unlikely that $InsP_3R$ downregulation alone explains the lack of PLCζ activity in somatic cells. A more precise method of assessing possible $InsP_3R$ downregulation as a result of PLCζ expression would be to perform an immunoblot for $InsP_3Rs$, which could be carried out using the stably transfected eYFP-PLCζ cell line.

6.4.3 Regulation of PLCζ by phosphorylation

One possibility is that PLCζ is regulated by phosphorylation. Reversible phosphorylation is a highly effective means of switching the activity of target proteins. Phosphorylation and dephosphorylation, catalysed by protein kinases and protein phosphatases, can modify the function of a protein in many ways; such as facilitating or inhibiting movement between subcellular compartments, by increasing or decreasing its biological activity, or by initiating or disrupting protein-protein interactions (Cohen, 2002). There are a number of bioinformatic resources available which allow users to search for motifs within DNA sequences of proteins that are likely to be phosphorylated by specific protein kinases. Entering the DNA sequence of PLCζ into a commonly used world-wide-web interfaced bioinformatics computer program (Obenauer *et al.*, 2003) identified potential phosphorylation sites for PKC, CamKII and various other kinases.

Phosphorylation could therefore provide an alternative mechanism for regulating the activity of PLCζ in somatic cells. Alternatively, it may be that the regulation of PLCζ requires a specific protein kinase that is only present within the egg. There are no previous studies discussing the phosphorylation of PLCζ, and there is no clear evidence either for or against it as a potential means of regulation.

6.5 Mechanism of action of PLCζ

Another means of regulating the activity of PLCζ could involve the way in which it targets PIP_2. The four well characterised isoforms of PLC (β, γ, δ, ε) interact with plasma membranes by different mechanisms (Rebecchi *et al.*, 2000; Rhee, 2001). The pleckstrin homology (PH) domain functions to target PLCδ1 with high affinity and specificity to the lipid PIP_2 (Ferguson *et al.*, 1995; Garcia *et al.*, 1995; Lemmon, 2003; Lemmon *et al.*, 2000; Lemmon *et al.*, 1995), whilst PLCs β, γ, and ε bind to specific plasma membrane proteins (Kelley *et al.*, 2006; Kelley *et al.*, 2004; Suh *et al.*, 2008; Wang *et al.*, 1999). Membrane interactions are important to PLCs as they enhance the catalytic activity of the enzyme by exposing them to higher local concentrations of their PIP_2 substrate (Rebecchi *et al.*, 2000; Rhee, 2001). It remains to be determined whether PLCζ is targeted to membranes via protein-protein interactions like the β, γ, and ε isoforms, or via protein-lipid interactions like the δ1 isoform. It is also unclear which type of membrane PLCζ targets. It is possible that it interacts with either a distinct vesicular PIP_2-containing membrane, or a PIP_2-containing microdomain within the plasma membrane (Rice *et al.*, 2000; Swann *et al.*, 2001).

Previous work has shown that the binding of PLCζ to PIP_2 may involve the X-Y linker or the C2 domain (Nomikos *et al.*, 2007). These domains were expressed as GST fusion proteins and their binding to phosphoinositides spotted on PIP strip membranes was examined. The results were compared to the binding capacity of the equivalent domains of PLCδ1. Both PLCδ1 and PLCζ were shown to bind PIP_2, but only the X-Y and C2 domains from PLCζ were shown to bind PIP, and to a lesser extent to PIP_2 (Nomikos *et al.*, 2007). This data suggests that the X-Y linker region and C2 domain play an important role in targeting PLCζ to its substrate.

In addition to this, the unique properties of the different PLCζ domains have been investigated by generating a series of PLC chimeras involving the substitution of the domains of PLCδ1 (PH, C2, EF hands and X-Y linker) into PLCζ (Gonzalez Garcia, 2008). These chimeras were tagged with luciferase and their Ca^{2+} oscillation inducing activity was monitored in mouse eggs. The addition of the PH domain of PLCδ1 to PLCζ did not alter its activity in eggs. Replacing either the X-Y linker or EF hand domain of PLCζ with those from PLCδ1 leads to a reduction in the ability of these chimeras to induce Ca^{2+} oscillations. Interestingly, replacing the C2 domain of PLCζ with that of PLCδ1 totally abolished its Ca^{2+} releasing activity in mouse eggs (Gonzalez Garcia, 2008). These results suggest that the C2 domain of PLCζ is essential for its activity in eggs. It is possible that the association of PLCζ with its specific plasma membrane target may be mediated by the interaction of X-Y linker or C2 domain with another membrane targeting protein, thereby compensating for its inherent lack of PH or SH domains.

6.6 Is there an Egg specific factor?

The work in this thesis suggests a conundrum for understanding how somatic cells tolerate high levels of PLCζ. The conundrum that exists in nature is that sperm cells also show no evidence of abnormal PI signalling despite containing ~1000 times more PLCζ than the amount required to trigger Ca^{2+} release and PI turnover in an egg. This is comparable to the situation observed in somatic cells during this study, whereby CHO cells are also capable of tolerating relatively high levels of PLCζ expression. When PLCζ is introduced into an egg by sperm it appears to be fully active, and induces a Ca^{2+} response within minutes. This was also the case with injections of either cell extract or single cells from the stably transfected eYFP-PLCζ cell line. The question remains as to how PLCζ is seemingly inactive when expressed in sperm and somatic cells and yet active when subsequently introduced into an egg. The data presented in this thesis does not rule out a specific inhibition of PLCζ in somatic cells; however, the stimulation of PLCζ by egg specific factor not only explains these observations, but also offers an interesting explanation for the conundrum that exists in nature. As mentioned previously, it is possible that PLCζ associates with its specific membrane target by interacting with another membrane targeting protein, much like the PLC β, γ, and ε isoforms. Based on the experimental findings of this thesis, one can propose a hypothetical mechanism for PLCζ action that involves an interaction with an egg specific factor (Figure 6.2). If the interaction involved the C2 domain, this would be analogous to the mechanism of action of PLCβ (Suh *et al.*, 2008). It is likely that this factor is associated with a membrane due to

the cellular location of PIP_2, however it remains to be determined if this involves the plasma membrane or the membrane of an intracellular organelle. Once PLCζ is associated with this egg specific factor, it could then bind and hydrolyse its substrate leading to the generation of $InsP_3$ and subsequent Ca^{2+} release from intracellular stores. Identification of this egg specific factor interaction could involve the use of a pull down assay, whereby PLCζ is expressed as a fusion protein (e.g. myc tagged) in eggs and then immobilised using an affinity ligand specific to the fusion tag. The entire complex could then be eluted from the affinity support and evaluated by SDS-PAGE. Having identified the egg specific factor, it would be interesting to then introduce this protein into somatic cells expressing PLCζ in order to examine the effects on Ca^{2+} signalling.

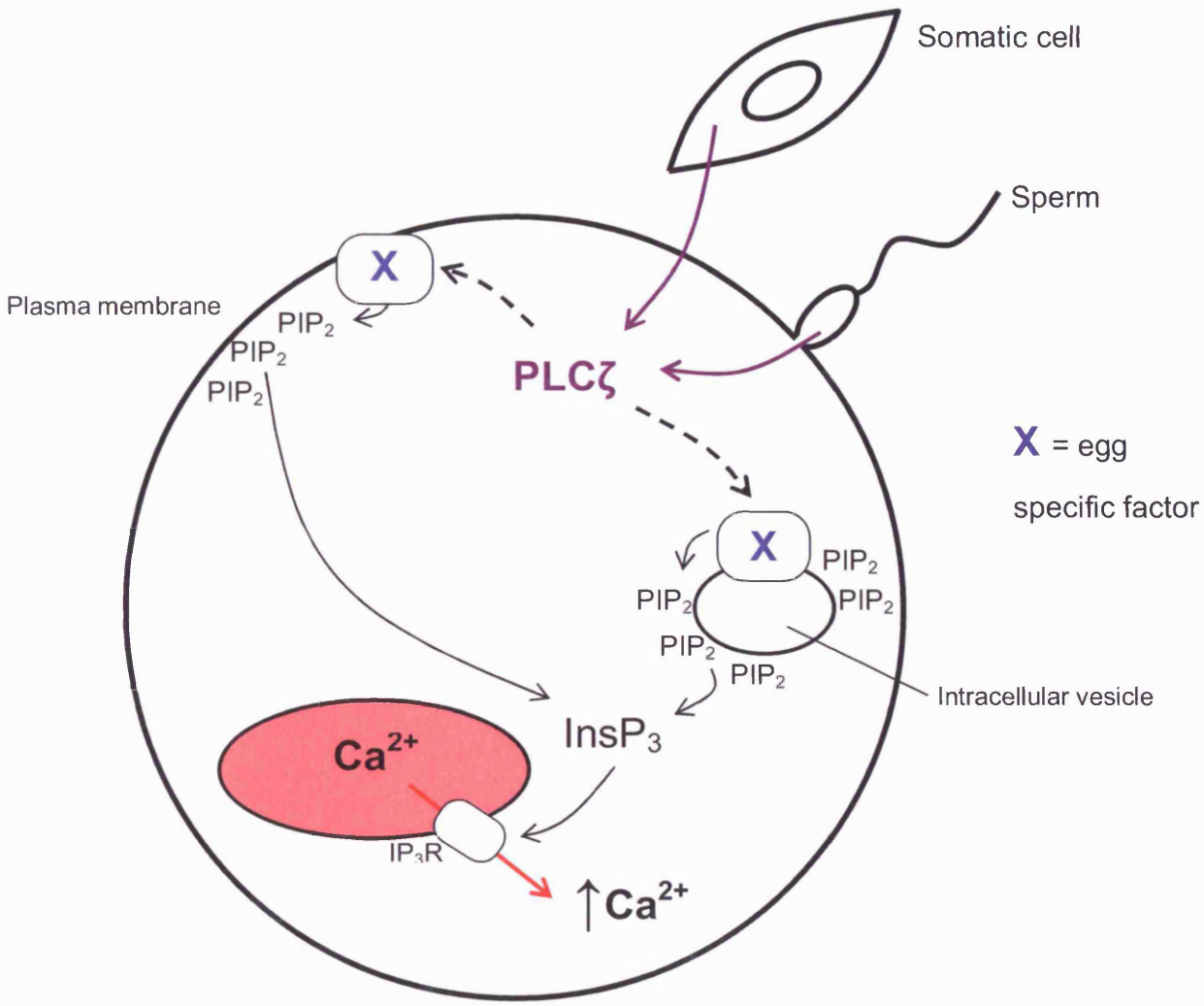

Figure 6.2 Hypothetical mechanism of PLCζ action based on the findings of this thesis.
(See text for explanation and references)

BIBLIOGRAPHY

BIBLIOGRAPHY

AARHUS, R., GRAEFF, R.M., DICKEY, D.M., WALSETH, T.F. & LEE, H.C. (1995). ADP-ribosyl cyclase and CD38 catalyze the synthesis of a calcium-mobilizing metabolite from NADP. *J Biol Chem*, **270,** 30327-33.

AFLALO, C. (1991). Biologically localized firefly luciferase: a tool to study cellular processes. *Int Rev Cytol*, **130,** 269-323.

AITKEN, R.J. (1989). The role of free oxygen radicals and sperm function. *Int J Androl*, **12,** 95-7.

ALBERTS, B., BRAY, D., LEWIS, J., RAFF, M., ROBERTS, K. & WATSON, J.D. (1997). *Molecular Biology of the Cell.* New York, USA: Garland Publishing.

ARBUZOVA, A., MURRAY, D. & MCLAUGHLIN, S. (1998). MARCKS, membranes, and calmodulin: kinetics of their interaction. *Biochim Biophys Acta*, **1376,** 369-79.

AUSTIN, C.R. (1951). Observations on the penetration of the sperm in the mammalian egg. *Aust J Sci Res (B)*, **4,** 581-96.

AUSTIN, C.R. & BRADEN, A.W. (1952). Passage of the sperm and the penetration of the egg in mammals. *Nature*, **170,** 919-21.

BAK, J., BILLINGTON, R.A., TIMAR, G., DUTTON, A.C. & GENAZZANI, A.A. (2001). NAADP receptors are present and functional in the heart. *Curr Biol*, **11,** 987-90.

BAO, S., THRALL, B.D. & MILLER, D.L. (1997). Transfection of a reporter plasmid into cultured cells by sonoporation in vitro. *Ultrasound Med Biol*, **23,** 953-9.

BARTOLI, M. & CLAYCOMB, W.C. (1997). Transfer of macromolecules into living adult cardiomyocytes by microinjection. *Mol Cell Biochem*, **172,** 103-9.

BENKUSKY, N.A., FARRELL, E.F. & VALDIVIA, H.H. (2004). Ryanodine receptor channelopathies. *Biochem Biophys Res Commun*, **322,** 1280-5.

BERRIDGE, M.J. (1997). Elementary and global aspects of calcium signalling. *J Exp Biol*, **200,** 315-9.

BERRIDGE, M.J. (2007). Inositol trisphosphate and calcium oscillations. *Biochem Soc Symp*, 1-7.

BERRIDGE, M.J. (1993). Inositol trisphosphate and calcium signalling. *Nature*, **361,** 315-25.

BERRIDGE, M.J., BOOTMAN, M.D. & RODERICK, H.L. (2003). Calcium signalling: dynamics, homeostasis and remodelling. *Nat Rev Mol Cell Biol*, **4,** 517-29.

BERRIDGE, M.J., LIPP, P. & BOOTMAN, M.D. (2000). The versatility and universality of calcium signalling. *Nat Rev Mol Cell Biol*, **1,** 11-21.

BERRIE, C.P., CUTHBERTSON, K.S., PARRINGTON, J., LAI, F.A. & SWANN, K. (1996). A cytosolic sperm factor triggers calcium oscillations in rat hepatocytes. *Biochem J*, **313 (Pt 2),** 369-72.

BEZPROZVANNY, I., WATRAS, J. & EHRLICH, B.E. (1991). Bell-shaped calcium-response curves of Ins(1,4,5)P3- and calcium-gated channels from endoplasmic reticulum of cerebellum. *Nature*, **351,** 751-4.

BIRNBAUMER, L., ZHU, X., JIANG, M., BOULAY, G., PEYTON, M., VANNIER, B., BROWN, D., PLATANO, D., SADEGHI, H., STEFANI, E. & BIRNBAUMER, M. (1996). On the molecular basis and regulation of cellular capacitative calcium entry: roles for Trp proteins. *Proc Natl Acad Sci U S A*, **93,** 15195-202.

BLONDEL, O., TAKEDA, J., JANSSEN, H., SEINO, S. & BELL, G.I. (1993). Sequence and functional characterization of a third inositol trisphosphate receptor subtype, IP3R-3, expressed in pancreatic islets, kidney, gastrointestinal tract, and other tissues. *J Biol Chem*, **268,** 11356-63.

BOCKAMP, E., MARINGER, M., SPANGENBERG, C., FEES, S., FRASER, S., ESHKIND, L., OESCH, F. & ZABEL, B. (2002). Of mice and models: improved animal models for biomedical research. *Physiol Genomics*, **11,** 115-32.

BOKKALA, S. & JOSEPH, S.K. (1997). Angiotensin II-induced down-regulation of inositol trisphosphate receptors in WB rat liver epithelial cells. Evidence for involvement of the proteasome pathway. *J Biol Chem*, **272,** 12454-61.

BOOTMAN, M.D., COLLINS, T.J., PEPPIATT, C.M., PROTHERO, L.S., MACKENZIE, L., DE SMET, P., TRAVERS, M., TOVEY, S.C., SEO, J.T., BERRIDGE, M.J., CICCOLINI, F. & LIPP, P. (2001a). Calcium signalling--an overview. *Semin Cell Dev Biol*, **12,** 3-10.

BOOTMAN, M.D. & LIPP, P. (1999). Ringing changes to the 'bell-shaped curve'. *Curr Biol*, **9,** R876-8.

BOOTMAN, M.D., LIPP, P. & BERRIDGE, M.J. (2001b). The organisation and functions of local Ca(2+) signals. *J Cell Sci*, **114,** 2213-22.

BOS-MIKICH, A., SWANN, K. & WHITTINGHAM, D.G. (1995). Calcium oscillations and protein synthesis inhibition synergistically activate mouse oocytes. *Mol Reprod Dev*, **41,** 84-90.

BREITBART, H., RUBINSTEIN, S. & NASS-ARDEN, L. (1985). The role of calcium and Ca2+-ATPase in maintaining motility in ram spermatozoa. *J Biol Chem*, **260,** 11548-53.

BRIGGS, R. & KING, T.J. (1952). Transplantation of Living Nuclei From Blastula Cells into Enucleated Frogs' Eggs. *Proc Natl Acad Sci U S A*, **38,** 455-63.

BRIND, S., SWANN, K. & CARROLL, J. (2000). Inositol 1,4,5-trisphosphate receptors are downregulated in mouse oocytes in response to sperm or adenophostin A but not to increases in intracellular Ca(2+) or egg activation. *Dev Biol*, **223,** 251-65.

BURGOYNE, R.D. & CLAGUE, M.J. (2003). Calcium and calmodulin in membrane fusion. *Biochim Biophys Acta*, **1641,** 137-43.

BURKHOLDER, J.K., DECKER, J. & YANG, N.S. (1993). Rapid transgene expression in lymphocyte and macrophage primary cultures after particle bombardment-mediated gene transfer. *J Immunol Methods*, **165,** 149-56.

BURNSTOCK, G. (1990). Overview. Purinergic mechanisms. *Ann N Y Acad Sci*, **603,** 1-17; discussion 18.

CALCRAFT, P.J., RUAS, M., PAN, Z., CHENG, X., ARREDOUANI, A., HAO, X., TANG, J., RIETDORF, K., TEBOUL, L., CHUANG, K.T., LIN, P., XIAO, R., WANG, C., ZHU, Y., LIN, Y., WYATT, C.N., PARRINGTON, J., MA, J., EVANS, A.M., GALIONE, A. & ZHU, M.X. (2009). NAADP mobilizes calcium from acidic organelles through two-pore channels. *Nature*, **459,** 596-600.

CAMPBELL, A.K. (1988). *Chemiluminescnece: Principles and Applications in Biology and Medicine*.

CAMPBELL, K. (2007). The relationship between calcium and metabolism in mouse eggs at fertilisation. pp. 262. Cardiff: Cardiff University.

CANCELA, J.M., CHURCHILL, G.C. & GALIONE, A. (1999). Coordination of agonist-induced Ca2+-signalling patterns by NAADP in pancreatic acinar cells. *Nature*, **398,** 74-6.

CANTLEY, L.C. (2002). The phosphoinositide 3-kinase pathway. *Science*, **296,** 1655-7.

CAPECCHI, M.R. (1980). High efficiency transformation by direct microinjection of DNA into cultured mammalian cells. *Cell*, **22,** 479-88.

CARAFOLI, E. (2002). Calcium signaling: a tale for all seasons. *Proc Natl Acad Sci U S A*, **99,** 1115-22.

CARAFOLI, E., SANTELLA, L., BRANCA, D. & BRINI, M. (2001). Generation, control, and processing of cellular calcium signals. *Crit Rev Biochem Mol Biol*, **36,** 107-260.

CARLSON, A.E., WESTENBROEK, R.E., QUILL, T., REN, D., CLAPHAM, D.E., HILLE, B., GARBERS, D.L. & BABCOCK, D.F. (2003). CatSper1 required for evoked Ca2+ entry and control of flagellar function in sperm. *Proc Natl Acad Sci U S A*, **100,** 14864-8.

CARROLL, J. (2001). The initiation and regulation of Ca2+ signalling at fertilization in mammals. *Semin Cell Dev Biol*, **12,** 37-43.

CHALFIE, M., TU, Y., EUSKIRCHEN, G., WARD, W.W. & PRASHER, D.C. (1994). Green fluorescent protein as a marker for gene expression. *Science*, **263,** 802-5.

CHAMBERS, E.L. & DE ARMENDI, J. (1979). Membrane potential, action potential and activation potential of eggs of the sea urchin, Lytechinus variegatus. *Exp Cell Res*, **122,** 203-18.

CHEN, C. & OKAYAMA, H. (1987). High-efficiency transformation of mammalian cells by plasmid DNA. *Mol Cell Biol*, **7,** 2745-52.

CHEN, S.R., LEONG, P., IMREDY, J.P., BARTLETT, C., ZHANG, L. & MACLENNAN, D.H. (1997). Single-channel properties of the recombinant skeletal muscle Ca2+ release channel (ryanodine receptor). *Biophys J*, **73,** 1904-12.

CHENG, H., LEDERER, W.J. & CANNELL, M.B. (1993). Calcium sparks: elementary events underlying excitation-contraction coupling in heart muscle. *Science*, **262,** 740-4.

CHINI, E.N., BEERS, K.W. & DOUSA, T.P. (1995). Nicotinate adenine dinucleotide phosphate (NAADP) triggers a specific calcium release system in sea urchin eggs. *J Biol Chem*, **270,** 3216-23.

CHISHOLM, V. (1995). *High efficiency gene transfer into mammalian cells.* Oxford: Oxford University Press.

CHU, A., FILL, M., STEFANI, E. & ENTMAN, M.L. (1993). Cytoplasmic Ca2+ does not inhibit the cardiac muscle sarcoplasmic reticulum ryanodine receptor Ca2+ channel, although Ca(2+)-induced Ca2+ inactivation of Ca2+ release is observed in native vesicles. *J Membr Biol*, **135,** 49-59.

CHURCHILL, G.C., OKADA, Y., THOMAS, J.M., GENAZZANI, A.A., PATEL, S. & GALIONE, A. (2002). NAADP mobilizes Ca(2+) from reserve granules, lysosome-related organelles, in sea urchin eggs. *Cell*, **111,** 703-8.

CIAPA, B., BORG, B. & WHITAKER, M. (1992). Polyphosphoinositide metabolism during the fertilization wave in sea urchin eggs. *Development*, **115,** 187-95.

CIAPA, B. & CHIRI, S. (2000). Egg activation: upstream of the fertilization calcium signal. *Biol Cell*, **92,** 215-33.

CLAPHAM, D.E. (1995). Calcium signaling. *Cell*, **80,** 259-68.

CLERMONT, Y. (1972). Kinetics of spermatogenesis in mammals: seminiferous epithelium cycle and spermatogonial renewal. *Physiol Rev*, **52,** 198-236.

COAKLEY, W.T. (1997). Ultrasonic separations in analytical biotechnology. *Trends Biotechnol*, **15,** 506-11.

COCKCROFT, S. & THOMAS, G.M. (1992). Inositol-lipid-specific phospholipase C isoenzymes and their differential regulation by receptors. *Biochem J*, **288 (Pt 1),** 1-14.

COHEN, P. (2002). The origins of protein phosphorylation. *Nat Cell Biol*, **4,** E127-30.

COOK, S.P., BROKAW, C.J., MULLER, C.H. & BABCOCK, D.F. (1994). Sperm chemotaxis: egg peptides control cytosolic calcium to regulate flagellar responses. *Dev Biol*, **165,** 10-9.

COPELLO, J.A., BARG, S., ONOUE, H. & FLEISCHER, S. (1997). Heterogeneity of Ca2+ gating of skeletal muscle and cardiac ryanodine receptors. *Biophys J*, **73,** 141-56.

CORMACK, B.P., VALDIVIA, R.H. & FALKOW, S. (1996). FACS-optimized mutants of the green fluorescent protein (GFP). *Gene*, **173,** 33-8.

COWARD, K., CAMPOS-MENDOZA, A., LARMAN, M., HIBBITT, O., MCANDREW, B., BROMAGE, N. & PARRINGTON, J. (2003). Teleost fish spermatozoa contain a cytosolic protein factor that induces calcium release in sea urchin egg homogenates and triggers calcium oscillations when injected into mouse oocytes. *Biochem Biophys Res Commun*, **305,** 299-304.

COWARD, K., KUBOTA, H., HIBBITT, O., MCILHINNEY, J., KOHRI, K. & PARRINGTON, J. (2006). Expression of a fluorescent recombinant form of sperm protein phospholipase C zeta in mouse epididymal sperm by in vivo gene transfer into the testis. *Fertil Steril*, **85 Suppl 1,** 1281-9.

COX, L.J., LARMAN, M.G., SAUNDERS, C.M., HASHIMOTO, K., SWANN, K. & LAI, F.A. (2002). Sperm phospholipase Czeta from humans and cynomolgus monkeys triggers Ca2+ oscillations, activation and development of mouse oocytes. *Reproduction*, **124,** 611-23.

CROSS, N.L. (2004). Reorganization of lipid rafts during capacitation of human sperm. *Biol Reprod*, **71,** 1367-73.

CSORDAS, G., THOMAS, A.P. & HAJNOCZKY, G. (1999). Quasi-synaptic calcium signal transmission between endoplasmic reticulum and mitochondria. *Embo J*, **18,** 96-108.

CUBITT, A.B., HEIM, R., ADAMS, S.R., BOYD, A.E., GROSS, L.A. & TSIEN, R.Y. (1995). Understanding, improving and using green fluorescent proteins. *Trends Biochem Sci*, **20,** 448-55.

CULLEN, P.J., COZIER, G.E., BANTING, G. & MELLOR, H. (2001). Modular phosphoinositide-binding domains--their role in signalling and membrane trafficking. *Curr Biol*, **11,** R882-93.

CUTHBERTSON, K.S. (1983). Parthenogenetic activation of mouse oocytes in vitro with ethanol and benzyl alcohol. *J Exp Zool*, **226,** 311-4.

DARSZON, A., NISHIGAKI, T., WOOD, C., TREVINO, C.L., FELIX, R. & BELTRAN, C. (2005). Calcium channels and Ca2+ fluctuations in sperm physiology. *Int Rev Cytol*, **243,** 79-172.

DAVID, C., HALLIWELL, J. & WHITAKER, M. (1988). Some properties of the membrane currents underlying the fertilization potential in sea urchin eggs. *J Physiol*, **402,** 139-54.

DE BLAS, G., MICHAUT, M., TREVINO, C.L., TOMES, C.N., YUNES, R., DARSZON, A. & MAYORGA, L.S. (2002). The intraacrosomal calcium pool plays a direct role in acrosomal exocytosis. *J Biol Chem*, **277,** 49326-31.

DE CRESCENZO, V., ZHUGE, R., VELAZQUEZ-MARRERO, C., LIFSHITZ, L.M., CUSTER, E., CARMICHAEL, J., LAI, F.A., TUFT, R.A., FOGARTY, K.E., LEMOS, J.R. & WALSH, J.V., JR. (2004). Ca2+ syntillas, miniature Ca2+ release events in terminals of hypothalamic neurons, are increased in frequency by depolarization in the absence of Ca2+ influx. *J Neurosci*, **24,** 1226-35.

DE KONINCK, P. & SCHULMAN, H. (1998). Sensitivity of CaM kinase II to the frequency of Ca2+ oscillations. *Science*, **279,** 227-30.

DE WET, J.R., WOOD, K.V., DELUCA, M., HELINSKI, D.R. & SUBRAMANI, S. (1987). Firefly luciferase gene: structure and expression in mammalian cells. *Mol Cell Biol*, **7,** 725-37.

DE WET, J.R., WOOD, K.V., HELINSKI, D.R. & DELUCA, M. (1985). Cloning of firefly luciferase cDNA and the expression of active luciferase in Escherichia coli. *Proc Natl Acad Sci U S A*, **82,** 7870-3.

DE YOUNG, G.W. & KEIZER, J. (1992). A single-pool inositol 1,4,5-trisphosphate-receptor-based model for agonist-stimulated oscillations in Ca2+ concentration. *Proc Natl Acad Sci U S A*, **89,** 9895-9.

DEGUCHI, R., SHIRAKAWA, H., ODA, S., MOHRI, T. & MIYAZAKI, S. (2000). Spatiotemporal analysis of Ca(2+) waves in relation to the sperm entry site and animal-vegetal axis during Ca(2+) oscillations in fertilized mouse eggs. *Dev Biol*, **218,** 299-313.

DELUCA, M. (1976). Firefly luciferase. *Adv Enzymol Relat Areas Mol Biol*, **44,** 37-68.

DENG, C.X., SIELING, F., PAN, H. & CUI, J. (2004). Ultrasound-induced cell membrane porosity. *Ultrasound Med Biol*, **30,** 519-26.

DESOUZA, N., REIKEN, S., ONDRIAS, K., YANG, Y.M., MATKOVICH, S. & MARKS, A.R. (2002). Protein kinase A and two phosphatases are components of the inositol 1,4,5-trisphosphate receptor macromolecular signaling complex. *J Biol Chem*, **277,** 39397-400.

DIGONNET, C., ALDON, D., LEDUC, N., DUMAS, C. & ROUGIER, M. (1997). First evidence of a calcium transient in flowering plants at fertilization. *Development*, **124,** 2867-74.

DONAHUE, R.P. (1968). Maturation of the mouse oocyte in vitro. I. Sequence and timing of nuclear progression. *J Exp Zool*, **169,** 237-49.

DONG, J.B., TANG, T.S. & SUN, F.Z. (2000). Xenopus and chicken sperm contain a cytosolic soluble protein factor which can trigger calcium oscillations in mouse eggs. *Biochem Biophys Res Commun*, **268,** 947-51.

DORVAL, V., DUFOUR, M. & LECLERC, P. (2002). Regulation of the phosphotyrosine content of human sperm proteins by intracellular Ca2+: role of Ca2+-adenosine triphosphatases. *Biol Reprod*, **67,** 1538-45.

DOUGHMAN, R.L., FIRESTONE, A.J. & ANDERSON, R.A. (2003). Phosphatidylinositol phosphate kinases put PI4,5P(2) in its place. *J Membr Biol*, **194,** 77-89.

DUBYAK, G.R. & EL-MOATASSIM, C. (1993). Signal transduction via P2-purinergic receptors for extracellular ATP and other nucleotides. *Am J Physiol*, **265,** C577-606.

DYM, M. (1994). Spermatogonial stem cells of the testis. *Proc Natl Acad Sci U S A*, **91,** 11287-9.

EDWARDS, R.G. (1965). Maturation in vitro of mouse, sheep, cow, pig, rhesus monkey and human ovarian oocytes. *Nature*, **208,** 349-51.

EISENBACH, M. (1999). Sperm chemotaxis. *Rev Reprod*, **4,** 56-66.

ELLIS, M.V., CARNE, A. & KATAN, M. (1993). Structural requirements of phosphatidylinositol-specific phospholipase C delta 1 for enzyme activity. *Eur J Biochem*, **213,** 339-47.

ELLIS, M.V., JAMES, S.R., PERISIC, O., DOWNES, C.P., WILLIAMS, R.L. & KATAN, M. (1998). Catalytic domain of phosphoinositide-specific phospholipase C (PLC). Mutational analysis of residues within the active site and hydrophobic ridge of plcdelta1. *J Biol Chem*, **273,** 11650-9.

EMORI, Y., HOMMA, Y., SORIMACHI, H., KAWASAKI, H., NAKANISHI, O., SUZUKI, K. & TAKENAWA, T. (1989). A second type of rat phosphoinositide-specific phospholipase C containing a src-related sequence not essential for phosphoinositide-hydrolyzing activity. *J Biol Chem*, **264,** 21885-90.

EVANS, J.P. (2002). The molecular basis of sperm-oocyte membrane interactions during mammalian fertilization. *Hum Reprod Update*, **8,** 297-311.

FECHHEIMER, M., BOYLAN, J.F., PARKER, S., SISKEN, J.E., PATEL, G.L. & ZIMMER, S.G. (1987). Transfection of mammalian cells with plasmid DNA by scrape loading and sonication loading. *Proc Natl Acad Sci U S A*, **84,** 8463-7.

FELGNER, P.L., GADEK, T.R., HOLM, M., ROMAN, R., CHAN, H.W., WENZ, M., NORTHROP, J.P., RINGOLD, G.M. & DANIELSEN, M. (1987). Lipofection: a highly efficient, lipid-mediated DNA-transfection procedure. *Proc Natl Acad Sci U S A*, **84,** 7413-7.

FERGUSON, K.M., LEMMON, M.A., SCHLESSINGER, J. & SIGLER, P.B. (1995). Structure of the high affinity complex of inositol trisphosphate with a phospholipase C pleckstrin homology domain. *Cell*, **83,** 1037-46.

FERRERI-JACOBIA, M., MAK, D.O. & FOSKETT, J.K. (2005). Translational mobility of the type 3 inositol 1,4,5-trisphosphate receptor Ca2+ release channel in endoplasmic reticulum membrane. *J Biol Chem*, **280,** 3824-31.

FERRIS, C.D., HUGANIR, R.L., SUPATTAPONE, S. & SNYDER, S.H. (1989). Purified inositol 1,4,5-trisphosphate receptor mediates calcium flux in reconstituted lipid vesicles. *Nature*, **342,** 87-9.

FESKE, S. (2007). Calcium signalling in lymphocyte activation and disease. *Nat Rev Immunol*, **7,** 690-702.

FILOSA, J.A., BONEV, A.D. & NELSON, M.T. (2004). Calcium dynamics in cortical astrocytes and arterioles during neurovascular coupling. *Circ Res*, **95,** e73-81.

FLEISCHER, S. & INUI, M. (1989). Biochemistry and biophysics of excitation-contraction coupling. *Annu Rev Biophys Biophys Chem*, **18,** 333-64.

FLORMAN, H.M. & DUCIBELLA, T. (2006). *Fertilization in mammals. In: The Physiology of Reproduction*. San Diego: Elsevier Press.

FLUCK, R., ABRAHAM, V., MILLER, A. & GALIONE, A. (1999). Microinjection of cyclic ADP-ribose triggers a regenerative wave of Ca2+ release and exocytosis of cortical alveoli in medaka eggs. *Zygote*, **7,** 285-92.

FOLTZ, K.R. & SHILLING, F.M. (1993). Receptor-mediated signal transduction and egg activation. *Zygote*, **1,** 276-9.

FOSKETT, J.K., WHITE, C., CHEUNG, K.H. & MAK, D.O. (2007). Inositol trisphosphate receptor Ca2+ release channels. *Physiol Rev*, **87,** 593-658.

FRALEY, R., SUBRAMANI, S., BERG, P. & PAPAHADJOPOULOS, D. (1980). Introduction of liposome-encapsulated SV40 DNA into cells. *J Biol Chem*, **255,** 10431-5.

FRANZINI-ARMSTRONG, C. & PROTASI, F. (1997). Ryanodine receptors of striated muscles: a complex channel capable of multiple interactions. *Physiol Rev*, **77,** 699-729.

FRASER, L.R. (1987). Strontium supports capacitation and the acrosome reaction in mouse sperm and rapidly activates mouse eggs. *Gamete Res*, **18,** 363-74.

FREDHOLM, B.B., ARSLAN, G., HALLDNER, L., KULL, B., SCHULTE, G. & WASSERMAN, W. (2000). Structure and function of adenosine receptors and their genes. *Naunyn Schmiedebergs Arch Pharmacol*, **362,** 364-74.

FRY, D. (2008). Modulating intracellular Ca2+ signalling using recombinant fragments of the human cardiac ryanodine receptor (RyR2). pp. 299. Cardiff: Cardiff University.

FUKAMI, K. (2002). Structure, regulation, and function of phospholipase C isozymes. *J Biochem*, **131,** 293-9.

FURUICHI, T., SIMON-CHAZOTTES, D., FUJINO, I., YAMADA, N., HASEGAWA, M., MIYAWAKI, A., YOSHIKAWA, S., GUENET, J.L. & MIKOSHIBA, K. (1993). Widespread expression of inositol 1,4,5-trisphosphate receptor type 1 gene (Insp3r1) in the mouse central nervous system. *Receptors Channels*, **1,** 11-24.

GALANTINO-HOMER, H.L., FLORMAN, H.M., STOREY, B.T., DOBRINSKI, I. & KOPF, G.S. (2004). Bovine sperm capacitation: assessment of phosphodiesterase activity and intracellular alkalinization on capacitation-

associated protein tyrosine phosphorylation. *Mol Reprod Dev*, **67,** 487-500.

GALIONE, A., EVANS, A.M., MA, J., PARRINGTON, J., ARREDOUANI, A., CHENG, X. & ZHU, M.X. (2009). The acid test: the discovery of two-pore channels (TPCs) as NAADP-gated endolysosomal Ca(2+) release channels. *Pflugers Arch*, **458,** 869-76.

GALIONE, A., MCDOUGALL, A., BUSA, W.B., WILLMOTT, N., GILLOT, I. & WHITAKER, M. (1993). Redundant mechanisms of calcium-induced calcium release underlying calcium waves during fertilization of sea urchin eggs. *Science*, **261,** 348-52.

GALIONE, A. & PETERSEN, O.H. (2005). The NAADP receptor: new receptors or new regulation? *Mol Interv*, **5,** 73-9.

GARCIA, P., GUPTA, R., SHAH, S., MORRIS, A.J., RUDGE, S.A., SCARLATA, S., PETROVA, V., MCLAUGHLIN, S. & REBECCHI, M.J. (1995). The pleckstrin homology domain of phospholipase C-delta 1 binds with high affinity to phosphatidylinositol 4,5-bisphosphate in bilayer membranes. *Biochemistry*, **34,** 16228-34.

GENAZZANI, A.A. & GALIONE, A. (1997). A Ca2+ release mechanism gated by the novel pyridine nucleotide, NAADP. *Trends Pharmacol Sci*, **18,** 108-10.

GEORGE, C.H., JUNDI, H., WALTERS, N., THOMAS, N.L., WEST, R.R. & LAI, F.A. (2006). Arrhythmogenic mutation-linked defects in ryanodine receptor autoregulation reveal a novel mechanism of Ca2+ release channel dysfunction. *Circ Res*, **98,** 88-97.

GEORGE, C.H., YIN, C.C. & LAI, F.A. (2005). Toward a molecular understanding of the structure-function of ryanodine receptor Ca2+ release channels: perspectives from recombinant expression systems. *Cell Biochem Biophys*, **42,** 197-222.

GERDES, H.H. & KAETHER, C. (1996). Green fluorescent protein: applications in cell biology. *FEBS Lett*, **389,** 44-7.

GEVER, J.R., COCKAYNE, D.A., DILLON, M.P., BURNSTOCK, G. & FORD, A.P. (2006). Pharmacology of P2X channels. *Pflugers Arch*, **452,** 513-37.

GODI, A., DI CAMPLI, A., KONSTANTAKOPOULOS, A., DI TULLIO, G., ALESSI, D.R., KULAR, G.S., DANIELE, T., MARRA, P., LUCOCQ, J.M. & DE MATTEIS, M.A. (2004). FAPPs control Golgi-to-cell-surface membrane traffic by binding to ARF and PtdIns(4)P. *Nat Cell Biol*, **6,** 393-404.

GONZALEZ GARCIA, J.R. (2008). Studies on the mechanisms regulating sperm phospholipase C Zeta (PLC [zeta]) activity at mammalian fertilization. pp. 239. Cardiff: Cardiff University.

GOZANI, O., KARUMAN, P., JONES, D.R., IVANOV, D., CHA, J., LUGOVSKOY, A.A., BAIRD, C.L., ZHU, H., FIELD, S.J., LESSNICK, S.L., VILLASENOR, J., MEHROTRA, B., CHEN, J., RAO, V.R., BRUGGE, J.S., FERGUSON, C.G., PAYRASTRE, B., MYSZKA, D.G., CANTLEY, L.C., WAGNER, G., DIVECHA, N., PRESTWICH, G.D. & YUAN, J. (2003). The PHD finger of the chromatin-associated protein ING2 functions as a nuclear phosphoinositide receptor. *Cell*, **114,** 99-111.

GRAHAM, F.L. & VAN DER EB, A.J. (1973). A new technique for the assay of infectivity of human adenovirus 5 DNA. *Virology*, **52,** 456-67.

GROSCHE, J., MATYASH, V., MOLLER, T., VERKHRATSKY, A., REICHENBACH, A. & KETTENMANN, H. (1999). Microdomains for neuron-glia interaction: parallel fiber signaling to Bergmann glial cells. *Nat Neurosci*, **2,** 139-43.

GRUNDZINSKAS, J.G. & YOVICH, J.L. (1995). *Gametes: The oocyte*: Cambridge University Press.

GRYNKIEWICZ, G., POENIE, M. & TSIEN, R.Y. (1985). A new generation of Ca2+ indicators with greatly improved fluorescence properties. *J Biol Chem*, **260,** 3440-50.

GWACK, Y., SRIKANTH, S., FESKE, S., CRUZ-GUILLOTY, F., OH-HORA, M., NEEMS, D.S., HOGAN, P.G. & RAO, A. (2007). Biochemical and functional characterization of Orai proteins. *J Biol Chem*, **282,** 16232-43.

HAJNOCZKY, G., ROBB-GASPERS, L.D., SEITZ, M.B. & THOMAS, A.P. (1995). Decoding of cytosolic calcium oscillations in the mitochondria. *Cell*, **82,** 415-24.

HALET, G., TUNWELL, R., BALLA, T., SWANN, K. & CARROLL, J. (2002). The dynamics of plasma membrane PtdIns(4,5)P(2) at fertilization of mouse eggs. *J Cell Sci*, **115,** 2139-49.

HALET, G., TUNWELL, R., PARKINSON, S.J. & CARROLL, J. (2004). Conventional PKCs regulate the temporal pattern of Ca2+ oscillations at fertilization in mouse eggs. *J Cell Biol*, **164,** 1033-44.

HAMADA, K., MIYATA, T., MAYANAGI, K., HIROTA, J. & MIKOSHIBA, K. (2002). Two-state conformational changes in inositol 1,4,5-trisphosphate receptor regulated by calcium. *J Biol Chem*, **277,** 21115-8.

HANAHAN, D. (1983). Studies on transformation of Escherichia coli with plasmids. *J Mol Biol*, **166,** 557-80.

HARDIE, R.C. & MINKE, B. (1993). Novel Ca2+ channels underlying transduction in Drosophila photoreceptors: implications for phosphoinositide-mediated Ca2+ mobilization. *Trends Neurosci*, **16,** 371-6.

HARRIS, N., HILL, M., SHEN, Y., TOWNSEND, R.J., BEEBY, S. & WHITE, N. (2004). A dual frequency, ultrasonic, microengineered particle manipulator. *Ultrasonics*, **42,** 139-44.

HEIM, R., CUBITT, A.B. & TSIEN, R.Y. (1995). Improved green fluorescence. *Nature*, **373,** 663-4.

HEIM, R., PRASHER, D.C. & TSIEN, R.Y. (1994). Wavelength mutations and posttranslational autoxidation of green fluorescent protein. *Proc Natl Acad Sci U S A*, **91,** 12501-4.

HERRICK, S.B., SCHWEISSINGER, D.L., KIM, S.W., BAYAN, K.R., MANN, S. & CARDULLO, R.A. (2005). The acrosomal vesicle of mouse sperm is a calcium store. *J Cell Physiol*, **202,** 663-71.

HO, H.C. & SUAREZ, S.S. (2001). An inositol 1,4,5-trisphosphate receptor-gated intracellular Ca(2+) store is involved in regulating sperm hyperactivated motility. *Biol Reprod*, **65,** 1606-15.

HOMA, S.T. & SWANN, K. (1994). A cytosolic sperm factor triggers calcium oscillations and membrane hyperpolarizations in human oocytes. *Hum Reprod*, **9,** 2356-61.

HOTH, M. & PENNER, R. (1992). Depletion of intracellular calcium stores activates a calcium current in mast cells. *Nature*, **355,** 353-6.

HUBER, P.E. & PFISTERER, P. (2000). In vitro and in vivo transfection of plasmid DNA in the Dunning prostate tumor R3327-AT1 is enhanced by focused ultrasound. *Gene Ther*, **7,** 1516-25.

HWANG, J.I., OH, Y.S., SHIN, K.J., KIM, H., RYU, S.H. & SUH, P.G. (2005). Molecular cloning and characterization of a novel phospholipase C, PLC-eta. *Biochem J*, **389,** 181-6.

INOUYE, S. & TSUJI, F.I. (1994). Aequorea green fluorescent protein. Expression of the gene and fluorescence characteristics of the recombinant protein. *FEBS Lett*, **341,** 277-80.

IREDALE, P.A. & HILL, S.J. (1993). Increases in intracellular calcium via activation of an endogenous P2-purinoceptor in cultured CHO-K1 cells. *Br J Pharmacol*, **110,** 1305-10.

ITO, M., SHIKANO, T., ODA, S., HORIGUCHI, T., TANIMOTO, S., AWAJI, T., MITANI, H. & MIYAZAKI, S. (2008). Difference in Ca2+ oscillation-inducing activity and

nuclear translocation ability of PLCZ1, an egg-activating sperm factor candidate, between mouse, rat, human, and medaka fish. *Biol Reprod*, **78,** 1081-90.

JAFFE, L.A., GIUSTI, A.F., CARROLL, D.J. & FOLTZ, K.R. (2001). Ca2+ signalling during fertilization of echinoderm eggs. *Semin Cell Dev Biol*, **12,** 45-51.

JAFFE, L.F. (1985). *Biology of fertilization. The fertilization response of the egg.*: Academic Press.

JAFFE, L.F. (1991). The path of calcium in cytosolic calcium oscillations: a unifying hypothesis. *Proc Natl Acad Sci U S A*, **88,** 9883-7.

JAFFE, L.F. (1983). Sources of calcium in egg activation: a review and hypothesis. *Dev Biol*, **99,** 265-76.

JAYARAMAN, T. & MARKS, A.R. (1997). T cells deficient in inositol 1,4,5-trisphosphate receptor are resistant to apoptosis. *Mol Cell Biol*, **17,** 3005-12.

JAYARAMAN, T., ONDRIAS, K., ONDRIASOVA, E. & MARKS, A.R. (1996). Regulation of the inositol 1,4,5-trisphosphate receptor by tyrosine phosphorylation. *Science*, **272,** 1492-4.

JELLERETTE, T., HE, C.L., WU, H., PARYS, J.B. & FISSORE, R.A. (2000). Down-regulation of the inositol 1,4,5-trisphosphate receptor in mouse eggs following fertilization or parthenogenetic activation. *Dev Biol*, **223,** 238-50.

JONES, K.T. (1998). Ca2+ oscillations in the activation of the egg and development of the embryo in mammals. *Int J Dev Biol*, **42,** 1-10.

JONES, K.T., CARROLL, J., MERRIMAN, J.A., WHITTINGHAM, D.G. & KONO, T. (1995). Repetitive sperm-induced Ca2+ transients in mouse oocytes are cell cycle dependent. *Development*, **121,** 3259-66.

JONES, K.T., MATSUDA, M., PARRINGTON, J., KATAN, M. & SWANN, K. (2000). Different Ca2+-releasing abilities of sperm extracts compared with tissue extracts and phospholipase C isoforms in sea urchin egg homogenate and mouse eggs. *Biochem J*, **346 Pt 3,** 743-9.

JONES, K.T., SOELLER, C. & CANNELL, M.B. (1998). The passage of Ca2+ and fluorescent markers between the sperm and egg after fusion in the mouse. *Development*, **125,** 4627-35.

KAO, J.P., ALDERTON, J.M., TSIEN, R.Y. & STEINHARDT, R.A. (1990). Active involvement of Ca2+ in mitotic progression of Swiss 3T3 fibroblasts. *J Cell Biol*, **111,** 183-96.

KATAN, M. (1998). Families of phosphoinositide-specific phospholipase C: structure and function. *Biochim Biophys Acta*, **1436,** 5-17.

KELLEY, G.G., KAPROTH-JOSLIN, K.A., REKS, S.E., SMRCKA, A.V. & WOJCIKIEWICZ, R.J. (2006). G-protein-coupled receptor agonists activate endogenous phospholipase Cepsilon and phospholipase Cbeta3 in a temporally distinct manner. *J Biol Chem*, **281,** 2639-48.

KELLEY, G.G., REKS, S.E., ONDRAKO, J.M. & SMRCKA, A.V. (2001). Phospholipase C(epsilon): a novel Ras effector. *Embo J*, **20,** 743-54.

KELLEY, G.G., REKS, S.E. & SMRCKA, A.V. (2004). Hormonal regulation of phospholipase Cepsilon through distinct and overlapping pathways involving G12 and Ras family G-proteins. *Biochem J*, **378,** 129-39.

KHAKH, B.S. (2001). Molecular physiology of P2X receptors and ATP signalling at synapses. *Nat Rev Neurosci*, **2,** 165-74.

KHANNA, S., AMSO, N.N., PAYNTER, S.J. & COAKLEY, W.T. (2003). Contrast agent bubble and erythrocyte behavior in a 1.5-MHz standing ultrasound wave. *Ultrasound Med Biol*, **29,** 1463-70.

KHANNA, S., HUDSON, B., PEPPER, C.J., AMSO, N.N. & COAKLEY, W.T. (2006). Fluorescein isothiocynate-dextran uptake by chinese hamster ovary cells in a 1.5 MHz ultrasonic standing wave in the presence of contrast agent. *Ultrasound Med Biol*, **32,** 289-95.

KIM, H.J., GREENLEAF, J.F., KINNICK, R.R., BRONK, J.T. & BOLANDER, M.E. (1996). Ultrasound-mediated transfection of mammalian cells. *Hum Gene Ther*, **7,** 1339-46.

KIMURA, Y. & YANAGIMACHI, R. (1995a). Development of normal mice from oocytes injected with secondary spermatocyte nuclei. *Biol Reprod*, **53,** 855-62.

KIMURA, Y. & YANAGIMACHI, R. (1995b). Intracytoplasmic sperm injection in the mouse. *Biol Reprod*, **52,** 709-20.

KIMURA, Y. & YANAGIMACHI, R. (1995c). Mouse oocytes injected with testicular spermatozoa or round spermatids can develop into normal offspring. *Development*, **121,** 2397-405.

KIRICHOK, Y., NAVARRO, B. & CLAPHAM, D.E. (2006). Whole-cell patch-clamp measurements of spermatozoa reveal an alkaline-activated Ca2+ channel. *Nature*, **439,** 737-40.

KIRKMAN-BROWN, J.C., PUNT, E.L., BARRATT, C.L. & PUBLICOVER, S.J. (2002). Zona pellucida and progesterone-induced Ca2+ signaling and acrosome reaction in human spermatozoa. *J Androl*, **23,** 306-15.

KLEIN, R.M., WOLF, E.D., WU, R. & SANFORD, J.C. (1992). High-velocity microprojectiles for delivering nucleic acids into living cells. 1987. *Biotechnology*, **24,** 384-6.

KLINE, D. & KLINE, J.T. (1992). Repetitive calcium transients and the role of calcium in exocytosis and cell cycle activation in the mouse egg. *Dev Biol*, **149,** 80-9.

KNOTT, J.G., KUROKAWA, M., FISSORE, R.A., SCHULTZ, R.M. & WILLIAMS, C.J. (2005). Transgenic RNA interference reveals role for mouse sperm phospholipase Czeta in triggering Ca2+ oscillations during fertilization. *Biol Reprod*, **72,** 992-6.

KONO, T., CARROLL, J., SWANN, K. & WHITTINGHAM, D.G. (1995). Nuclei from fertilized mouse embryos have calcium-releasing activity. *Development*, **121,** 1123-8.

KOUCHI, Z., FUKAMI, K., SHIKANO, T., ODA, S., NAKAMURA, Y., TAKENAWA, T. & MIYAZAKI, S. (2004). Recombinant phospholipase Czeta has high Ca2+ sensitivity and induces Ca2+ oscillations in mouse eggs. *J Biol Chem*, **279,** 10408-12.

KREBS, J. & MICHALAK, M. (2007). *Calcium: A Matter of Life or Death*: Elsevier.

KRETSINGER, R.H. & NOCKOLDS, C.E. (1973). Carp muscle calcium-binding protein. II. Structure determination and general description. *J Biol Chem*, **248,** 3313-26.

KUME, S., MUTO, A., ARUGA, J., NAKAGAWA, T., MICHIKAWA, T., FURUICHI, T., NAKADE, S., OKANO, H. & MIKOSHIBA, K. (1993). The Xenopus IP3 receptor: structure, function, and localization in oocytes and eggs. *Cell*, **73,** 555-70.

KUO, R.C., BAXTER, G.T., THOMPSON, S.H., STRICKER, S.A., PATTON, C., BONAVENTURA, J. & EPEL, D. (2000). NO is necessary and sufficient for egg activation at fertilization. *Nature*, **406,** 633-6.

KUPKER, W., DIEDRICH, K. & EDWARDS, R.G. (1998). Principles of mammalian fertilization. *Hum Reprod*, **13 Suppl 1,** 20-32.

KURODA, K., ITO, M., SHIKANO, T., AWAJI, T., YODA, A., TAKEUCHI, H., KINOSHITA, K. & MIYAZAKI, S. (2006). The role of X/Y linker region and N-terminal EF-hand domain in nuclear translocation and Ca2+ oscillation-inducing activities of phospholipase Czeta, a mammalian egg-activating factor. *J Biol Chem*, **281,** 27794-805.

KYOZUKA, K., DEGUCHI, R., MOHRI, T. & MIYAZAKI, S. (1998). Injection of sperm extract mimics spatiotemporal dynamics of Ca2+ responses and progression of meiosis at fertilization of ascidian oocytes. *Development*, **125,** 4099-105.

LAI, F.A., ANDERSON, K., ROUSSEAU, E., LIU, Q.Y. & MEISSNER, G. (1988). Evidence for a Ca2+ channel within the ryanodine receptor complex from cardiac sarcoplasmic reticulum. *Biochem Biophys Res Commun*, **151,** 441-9.

LANGE, A., MILLS, R.E., LANGE, C.J., STEWART, M., DEVINE, S.E. & CORBETT, A.H. (2007). Classical nuclear localization signals: definition, function, and interaction with importin alpha. *J Biol Chem*, **282,** 5101-5.

LARMAN, M.G., SAUNDERS, C.M., CARROLL, J., LAI, F.A. & SWANN, K. (2004). Cell cycle-dependent Ca2+ oscillations in mouse embryos are regulated by nuclear targeting of PLCzeta. *J Cell Sci*, **117,** 2513-21.

LAVER, D.R., RODEN, L.D., AHERN, G.P., EAGER, K.R., JUNANKAR, P.R. & DULHUNTY, A.F. (1995). Cytoplasmic Ca2+ inhibits the ryanodine receptor from cardiac muscle. *J Membr Biol*, **147,** 7-22.

LAWRIE, A., BRISKEN, A.F., FRANCIS, S.E., CUMBERLAND, D.C., CROSSMAN, D.C. & NEWMAN, C.M. (2000). Microbubble-enhanced ultrasound for vascular gene delivery. *Gene Ther*, **7,** 2023-7.

LAX, Y., RUBINSTEIN, S. & BREITBART, H. (1994). Epidermal growth factor induces acrosomal exocytosis in bovine sperm. *FEBS Lett*, **339,** 234-8.

LEE, H.C. & AARHUS, R. (1991). ADP-ribosyl cyclase: an enzyme that cyclizes NAD+ into a calcium-mobilizing metabolite. *Cell Regul*, **2,** 203-9.

LEE, H.C. & AARHUS, R. (1995). A derivative of NADP mobilizes calcium stores insensitive to inositol trisphosphate and cyclic ADP-ribose. *J Biol Chem*, **270,** 2152-7.

LEE, Y.H. & PENG, C.A. (2005). Enhanced retroviral gene delivery in ultrasonic standing wave fields. *Gene Ther*, **12,** 625-33.

LEMMON, M.A. (2003). Phosphoinositide recognition domains. *Traffic*, **4,** 201-13.

LEMMON, M.A. & FERGUSON, K.M. (2000). Signal-dependent membrane targeting by pleckstrin homology (PH) domains. *Biochem J*, **350 Pt 1,** 1-18.

LEMMON, M.A., FERGUSON, K.M., O'BRIEN, R., SIGLER, P.B. & SCHLESSINGER, J. (1995). Specific and high-affinity binding of inositol phosphates to an isolated pleckstrin homology domain. *Proc Natl Acad Sci U S A*, **92,** 10472-6.

LEWIS, R.S. & CAHALAN, M.D. (1989). Mitogen-induced oscillations of cytosolic Ca2+ and transmembrane Ca2+ current in human leukemic T cells. *Cell Regul*, **1,** 99-112.

LI, X., ZIMA, A.V., SHEIKH, F., BLATTER, L.A. & CHEN, J. (2005). Endothelin-1-induced arrhythmogenic Ca2+ signaling is abolished in atrial myocytes of inositol-1,4,5-trisphosphate(IP3)-receptor type 2-deficient mice. *Circ Res*, **96,** 1274-81.

LIANG, H.D., LU, Q.L., XUE, S.A., HALLIWELL, M., KODAMA, T., COSGROVE, D.O., STAUSS, H.J., PARTRIDGE, T.A. & BLOMLEY, M.J. (2004). Optimisation of ultrasound-mediated gene transfer (sonoporation) in skeletal muscle cells. *Ultrasound Med Biol*, **30,** 1523-9.

LIM, D., KYOZUKA, K., GRAGNANIELLO, G., CARAFOLI, E. & SANTELLA, L. (2001). NAADP+ initiates the Ca2+ response during fertilization of starfish oocytes. *Faseb J*, **15,** 2257-67.

LIN, Y., MAHAN, K., LATHROP, W.F., MYLES, D.G. & PRIMAKOFF, P. (1994). A hyaluronidase activity of the sperm plasma membrane protein PH-20 enables sperm to penetrate the cumulus cell layer surrounding the egg. *J Cell Biol*, **125,** 1157-63.

LIOU, J., FIVAZ, M., INOUE, T. & MEYER, T. (2007). Live-cell imaging reveals sequential oligomerization and local plasma membrane targeting of stromal interaction molecule 1 after Ca2+ store depletion. *Proc Natl Acad Sci U S A*, **104,** 9301-6.

LIOU, J., KIM, M.L., HEO, W.D., JONES, J.T., MYERS, J.W., FERRELL, J.E., JR. & MEYER, T. (2005). STIM is a Ca2+ sensor essential for Ca2+-store-depletion-triggered Ca2+ influx. *Curr Biol*, **15,** 1235-41.

LIU, Z., ZHANG, J., SHARMA, M.R., LI, P., CHEN, S.R. & WAGENKNECHT, T. (2001). Three-dimensional reconstruction of the recombinant type 3 ryanodine receptor and localization of its amino terminus. *Proc Natl Acad Sci U S A*, **98,** 6104-9.

LOEB, J. (1921). Further observations on the production of parthenogenetic frogs. *J Gen Physiol*, **3,** 539-545.

MACHATY, Z., BONK, A.J., KUHHOLZER, B. & PRATHER, R.S. (2000). Porcine oocyte activation induced by a cytosolic sperm factor. *Mol Reprod Dev*, **57,** 290-5.

MACKRILL, J.J. (1999). Protein-protein interactions in intracellular Ca2+-release channel function. *Biochem J*, **337 (Pt 3),** 345-61.

MACKRILL, J.J., CHALLISS, R.A., O'CONNELL D, A., LAI, F.A. & NAHORSKI, S.R. (1997). Differential expression and regulation of ryanodine receptor and

myo-inositol 1,4,5-trisphosphate receptor Ca2+ release channels in mammalian tissues and cell lines. *Biochem J*, **327 (Pt 1),** 251-8.

MAEDA, N., KAWASAKI, T., NAKADE, S., YOKOTA, N., TAGUCHI, T., KASAI, M. & MIKOSHIBA, K. (1991). Structural and functional characterization of inositol 1,4,5-trisphosphate receptor channel from mouse cerebellum. *J Biol Chem*, **266,** 1109-16.

MAES, K., MISSIAEN, L., DE SMET, P., VANLINGEN, S., CALLEWAERT, G., PARYS, J.B. & DE SMEDT, H. (2000). Differential modulation of inositol 1,4,5-trisphosphate receptor type 1 and type 3 by ATP. *Cell Calcium*, **27,** 257-67.

MARANGOS, P., FITZHARRIS, G. & CARROLL, J. (2003). Ca2+ oscillations at fertilization in mammals are regulated by the formation of pronuclei. *Development*, **130,** 1461-72.

MARCET, B., CHAPPE, V., DELMAS, P., GOLA, M. & VERRIER, B. (2003). Negative regulation of CFTR activity by extracellular ATP involves P2Y2 receptors in CFTR-expressing CHO cells. *J Membr Biol*, **194,** 21-32.

MARCET, B., CHAPPE, V., DELMAS, P. & VERRIER, B. (2004). Pharmacological and signaling properties of endogenous P2Y1 receptors in cystic fibrosis transmembrane conductance regulator-expressing Chinese hamster ovary cells. *J Pharmacol Exp Ther*, **309,** 533-9.

MATSUDA, Y., SAEGUSA, H., ZONG, S., NODA, T. & TANABE, T. (2001). Mice lacking Ca(v)2.3 (alpha1E) calcium channel exhibit hyperglycemia. *Biochem Biophys Res Commun*, **289,** 791-5.

MATSUMOTO, M., NAKAGAWA, T., INOUE, T., NAGATA, E., TANAKA, K., TAKANO, H., MINOWA, O., KUNO, J., SAKAKIBARA, S., YAMADA, M., YONESHIMA, H., MIYAWAKI, A., FUKUUCHI, Y., FURUICHI, T., OKANO, H., MIKOSHIBA, K. & NODA, T. (1996). Ataxia and epileptic seizures in mice lacking type 1 inositol 1,4,5-trisphosphate receptor. *Nature*, **379,** 168-71.

MATTSON, M.P., GUO, Q., FURUKAWA, K. & PEDERSEN, W.A. (1998). Presenilins, the endoplasmic reticulum, and neuronal apoptosis in Alzheimer's disease. *J Neurochem*, **70,** 1-14.

MCELROY, W.D. (1947). The Energy Source for Bioluminescence in an Isolated System. *Proc Natl Acad Sci U S A*, **33,** 342-5.

MEHLMANN, L.M., CHATTOPADHYAY, A., CARPENTER, G. & JAFFE, L.A. (2001). Evidence that phospholipase C from the sperm is not responsible for initiating Ca(2+) release at fertilization in mouse eggs. *Dev Biol*, **236,** 492-501.

MICHEL, A.D., CHESSELL, I.P., HIBELL, A.D., SIMON, J. & HUMPHREY, P.P. (1998). Identification and characterization of an endogenous P2X7 (P2Z) receptor in CHO-K1 cells. *Br J Pharmacol*, **125,** 1194-201.

MIGNEN, O., THOMPSON, J.L. & SHUTTLEWORTH, T.J. (2007). STIM1 regulates Ca2+ entry via arachidonate-regulated Ca2+-selective (ARC) channels without store depletion or translocation to the plasma membrane. *J Physiol*, **579,** 703-15.

MINTA, A., KAO, J.P. & TSIEN, R.Y. (1989). Fluorescent indicators for cytosolic calcium based on rhodamine and fluorescein chromophores. *J Biol Chem*, **264,** 8171-8.

MISSIAEN, L., RAEYMAEKERS, L., DODE, L., VANOEVELEN, J., VAN BAELEN, K., PARYS, J.B., CALLEWAERT, G., DE SMEDT, H., SEGAERT, S. & WUYTACK, F. (2004a). SPCA1 pumps and Hailey-Hailey disease. *Biochem Biophys Res Commun*, **322,** 1204-13.

MISSIAEN, L., VAN ACKER, K., VAN BAELEN, K., RAEYMAEKERS, L., WUYTACK, F., PARYS, J.B., DE SMEDT, H., VANOEVELEN, J., DODE, L., RIZZUTO, R. & CALLEWAERT, G. (2004b). Calcium release from the Golgi apparatus and the endoplasmic reticulum in HeLa cells stably expressing targeted aequorin to these compartments. *Cell Calcium*, **36,** 479-87.

MIYAZAKI, S. & ITO, M. (2006). Calcium signals for egg activation in mammals. *J Pharmacol Sci*, **100,** 545-52.

MIYAZAKI, S., SHIRAKAWA, H., NAKADA, K. & HONDA, Y. (1993). Essential role of the inositol 1,4,5-trisphosphate receptor/Ca2+ release channel in Ca2+ waves and Ca2+ oscillations at fertilization of mammalian eggs. *Dev Biol*, **158,** 62-78.

MIYAZAKI, S., YUZAKI, M., NAKADA, K., SHIRAKAWA, H., NAKANISHI, S., NAKADE, S. & MIKOSHIBA, K. (1992). Block of Ca2+ wave and Ca2+ oscillation by antibody to the inositol 1,4,5-trisphosphate receptor in fertilized hamster eggs. *Science*, **257,** 251-5.

MYLES, D.G. & PRIMAKOFF, P. (1997). Why did the sperm cross the cumulus? To get to the oocyte. Functions of the sperm surface proteins PH-20 and fertilin in arriving at, and fusing with, the egg. *Biol Reprod*, **56,** 320-7.

NAKAHARA, M., SHIMOZAWA, M., NAKAMURA, Y., IRINO, Y., MORITA, M., KUDO, Y. & FUKAMI, K. (2005). A novel phospholipase C, PLC(eta)2, is a neuron-specific isozyme. *J Biol Chem*, **280,** 29128-34.

NAKANO, Y., SHIRAKAWA, H., MITSUHASHI, N., KUWABARA, Y. & MIYAZAKI, S. (1997). Spatiotemporal dynamics of intracellular calcium in the mouse egg injected with a spermatozoon. *Mol Hum Reprod*, **3,** 1087-93.

NAKASHIMA, S., BANNO, Y., WATANABE, T., NAKAMURA, Y., MIZUTANI, T., SAKAI, H., ZHAO, Y., SUGIMOTO, Y. & NOZAWA, Y. (1995). Deletion and site-directed mutagenesis of EF-hand domain of phospholipase C-delta 1: effects on its activity. *Biochem Biophys Res Commun*, **211,** 365-9.

NISHIGAKI, T., WOOD, C.D., TATSU, Y., YUMOTO, N., FURUTA, T., ELIAS, D., SHIBA, K., BABA, S.A. & DARSZON, A. (2004). A sea urchin egg jelly peptide induces a cGMP-mediated decrease in sperm intracellular Ca(2+) before its increase. *Dev Biol*, **272,** 376-88.

NISWENDER, K.D., BLACKMAN, S.M., ROHDE, L., MAGNUSON, M.A. & PISTON, D.W. (1995). Quantitative imaging of green fluorescent protein in cultured cells: comparison of microscopic techniques, use in fusion proteins and detection limits. *J Microsc*, **180,** 109-16.

NIXON, G.F., MIGNERY, G.A. & SOMLYO, A.V. (1994). Immunogold localization of inositol 1,4,5-trisphosphate receptors and characterization of ultrastructural features of the sarcoplasmic reticulum in phasic and tonic smooth muscle. *J Muscle Res Cell Motil*, **15,** 682-700.

NOMIKOS, M., BLAYNEY, L.M., LARMAN, M.G., CAMPBELL, K., ROSSBACH, A., SAUNDERS, C.M., SWANN, K. & LAI, F.A. (2005). Role of phospholipase C-zeta domains in Ca2+-dependent phosphatidylinositol 4,5-bisphosphate hydrolysis and cytoplasmic Ca2+ oscillations. *J Biol Chem*, **280,** 31011-8.

NOMIKOS, M., MULGREW-NESBITT, A., PALLAVI, P., MIHALYNE, G., ZAITSEVA, I., SWANN, K., LAI, F.A., MURRAY, D. & MCLAUGHLIN, S. (2007). Binding of phosphoinositide-specific phospholipase C-zeta (PLC-zeta) to phospholipid membranes: potential role of an unstructured cluster of basic residues. *J Biol Chem*, **282,** 16644-53.

NORTH, R.A. (2002). Molecular physiology of P2X receptors. *Physiol Rev*, **82,** 1013-67.

NOTTOLA, S.A., MACCHIARELLI, G., FAMILIARI, G., STALLONE, T., SATHANANTHAN, A.H. & MOTTA, P.M. (1998). Egg-sperm interactions in humans: ultrastructural aspects. *Ital J Anat Embryol*, **103,** 85-101.

NUCCITELLI, R. (1991). How do sperm activate eggs? *Curr Top Dev Biol*, **25,** 1-16.

OANCEA, E. & MEYER, T. (1998). Protein kinase C as a molecular machine for decoding calcium and diacylglycerol signals. *Cell*, **95,** 307-18.

OANCEA, E. & MEYER, T. (1996). Reversible desensitization of inositol trisphosphate-induced calcium release provides a mechanism for repetitive calcium spikes. *J Biol Chem*, **271,** 17253-60.

OBENAUER, J.C., CANTLEY, L.C. & YAFFE, M.B. (2003). Scansite 2.0: Proteome-wide prediction of cell signaling interactions using short sequence motifs. *Nucleic Acids Res*, **31,** 3635-41.

OBERDORF, J., WEBSTER, J.M., ZHU, C.C., LUO, S.G. & WOJCIKIEWICZ, R.J. (1999). Down-regulation of types I, II and III inositol 1,4,5-trisphosphate receptors is mediated by the ubiquitin/proteasome pathway. *Biochem J*, **339 (Pt 2),** 453-61.

OGURA, R., MATSUO, N., WAKO, N., TANAKA, T., ONO, S. & HIRATSUKA, K. (2005). Multi-color luciferases as reporters for monitoring transient gene expression in higher plants. *Plant Biotechnol.*, **22,** 151-5.

OKADA, M., FUJII, M., YAMAGA, M., SUGIMOTO, H., SADANO, H., OSUMI, T., KAMATA, H., HIRATA, H. & YAGISAWA, H. (2002). Carboxyl-terminal basic amino acids in the X domain are essential for the nuclear import of phospholipase C delta1. *Genes Cells*, **7,** 985-96.

OTSU, H., YAMAMOTO, A., MAEDA, N., MIKOSHIBA, K. & TASHIRO, Y. (1990). Immunogold localization of inositol 1, 4, 5-trisphosphate (InsP3) receptor in mouse cerebellar Purkinje cells using three monoclonal antibodies. *Cell Struct Funct*, **15,** 163-73.

OZIL, J.P., MARKOULAKI, S., TOTH, S., MATSON, S., BANREZES, B., KNOTT, J.G., SCHULTZ, R.M., HUNEAU, D. & DUCIBELLA, T. (2005). Egg activation events are regulated by the duration of a sustained [Ca2+]cyt signal in the mouse. *Dev Biol*, **282,** 39-54.

OZIL, J.P. & SWANN, K. (1995). Stimulation of repetitive calcium transients in mouse eggs. *J Physiol*, **483 (Pt 2),** 331-46.

PALERMO, G., JORIS, H., DEVROEY, P. & VAN STEIRTEGHEM, A.C. (1992). Pregnancies after intracytoplasmic injection of single spermatozoon into an oocyte. *Lancet*, **340,** 17-8.

PARRINGTON, J., JONES, M.L., TUNWELL, R., DEVADER, C., KATAN, M. & SWANN, K. (2002). Phospholipase C isoforms in mammalian spermatozoa: potential components of the sperm factor that causes Ca2+ release in eggs. *Reproduction*, **123,** 31-9.

PARRINGTON, J., SWANN, K., SHEVCHENKO, V.I., SESAY, A.K. & LAI, F.A. (1996). Calcium oscillations in mammalian eggs triggered by a soluble sperm protein. *Nature*, **379,** 364-8.

PATEL, S., JOSEPH, S.K. & THOMAS, A.P. (1999). Molecular properties of inositol 1,4,5-trisphosphate receptors. *Cell Calcium*, **25,** 247-64.

PATTERSON, R.L., BOEHNING, D. & SNYDER, S.H. (2004). Inositol 1,4,5-trisphosphate receptors as signal integrators. *Annu Rev Biochem*, **73,** 437-65.

PAYRASTRE, B., MISSY, K., GIURIATO, S., BODIN, S., PLANTAVID, M. & GRATACAP, M. (2001). Phosphoinositides: key players in cell signalling, in time and space. *Cell Signal*, **13,** 377-87.

PEMBERTON, L.F. & PASCHAL, B.M. (2005). Mechanisms of receptor-mediated nuclear import and nuclear export. *Traffic*, **6,** 187-98.

PEREZ, P.J., RAMOS-FRANCO, J., FILL, M. & MIGNERY, G.A. (1997). Identification and functional reconstitution of the type 2 inositol 1,4,5-trisphosphate receptor from ventricular cardiac myocytes. *J Biol Chem*, **272,** 23961-9.

PINKERTON, J.H., MC, K.D., ADAMS, E.C. & HERTIG, A.T. (1961). Development of the human ovary--a study using histochemical technics. *Obstet Gynecol*, **18,** 152-81.

PINTON, P., POZZAN, T. & RIZZUTO, R. (1998). The Golgi apparatus is an inositol 1,4,5-trisphosphate-sensitive Ca2+ store, with functional properties distinct from those of the endoplasmic reticulum. *Embo J*, **17,** 5298-308.

PLANK, C., ANTON, M., RUDOLPH, C., ROSENECKER, J. & KROTZ, F. (2003). Enhancing and targeting nucleic acid delivery by magnetic force. *Expert Opin Biol Ther*, **3,** 745-58.

POENIE, M., ALDERTON, J., STEINHARDT, R. & TSIEN, R. (1986). Calcium rises abruptly and briefly throughout the cell at the onset of anaphase. *Science*, **233,** 886-9.

POENIE, M., ALDERTON, J., TSIEN, R.Y. & STEINHARDT, R.A. (1985). Changes of free calcium levels with stages of the cell division cycle. *Nature*, **315,** 147-9.

POGWIZD, S.M., SCHLOTTHAUER, K., LI, L., YUAN, W. & BERS, D.M. (2001). Arrhythmogenesis and contractile dysfunction in heart failure: Roles of sodium-calcium exchange, inward rectifier potassium current, and residual beta-adrenergic responsiveness. *Circ Res*, **88,** 1159-67.

PORTER, T.R., XIE, F., KRICSFELD, A. & KILZER, K. (1995). Noninvasive identification of acute myocardial ischemia and reperfusion with contrast ultrasound using intravenous perfluoropropane-exposed sonicated dextrose albumin. *J Am Coll Cardiol*, **26,** 33-40.

POTIER, M. & TREBAK, M. (2008). New developments in the signaling mechanisms of the store-operated calcium entry pathway. *Pflugers Arch*, **457,** 405-15.

PRASHER, D.C., ECKENRODE, V.K., WARD, W.W., PRENDERGAST, F.G. & CORMIER, M.J. (1992). Primary structure of the Aequorea victoria green-fluorescent protein. *Gene*, **111,** 229-33.

PUCK, T.T., CIECIURA, S.J. & ROBINSON, A. (1958). Genetics of somatic mammalian cells. III. Long-term cultivation of euploid cells from human and animal subjects. *J Exp Med*, **108,** 945-56.

PUTNEY, J.W., JR. & BIRD, G.S. (1993). The inositol phosphate-calcium signaling system in nonexcitable cells. *Endocr Rev*, **14,** 610-31.

RATAN, R.R., SHELANSKI, M.L. & MAXFIELD, F.R. (1986). Transition from metaphase to anaphase is accompanied by local changes in cytoplasmic free calcium in Pt K2 kidney epithelial cells. *Proc Natl Acad Sci U S A*, **83,** 5136-40.

REBECCHI, M.J. & PENTYALA, S.N. (2000). Structure, function, and control of phosphoinositide-specific phospholipase C. *Physiol Rev*, **80,** 1291-335.

REIJO, R., LEE, T.Y., SALO, P., ALAGAPPAN, R., BROWN, L.G., ROSENBERG, M., ROZEN, S., JAFFE, T., STRAUS, D., HOVATTA, O. & ET AL. (1995). Diverse spermatogenic defects in humans caused by Y chromosome deletions encompassing a novel RNA-binding protein gene. *Nat Genet*, **10,** 383-93.

RHEE, S.G. (2001). Regulation of phosphoinositide-specific phospholipase C. *Annu Rev Biochem*, **70,** 281-312.

RHEE, S.G. & BAE, Y.S. (1997). Regulation of phosphoinositide-specific phospholipase C isozymes. *J Biol Chem*, **272,** 15045-8.

RICE, A., PARRINGTON, J., JONES, K.T. & SWANN, K. (2000). Mammalian sperm contain a Ca(2+)-sensitive phospholipase C activity that can generate InsP(3) from PIP(2) associated with intracellular organelles. *Dev Biol*, **228,** 125-35.

RIDGWAY, E.B., GILKEY, J.C. & JAFFE, L.F. (1977). Free calcium increases explosively in activating medaka eggs. *Proc Natl Acad Sci U S A*, **74,** 623-7.

ROBB-GASPERS, L.D., RUTTER, G.A., BURNETT, P., HAJNOCZKY, G., DENTON, R.M. & THOMAS, A.P. (1998). Coupling between cytosolic and mitochondrial calcium oscillations: role in the regulation of hepatic metabolism. *Biochim Biophys Acta*, **1366,** 17-32.

ROOSEN-RUNGE, E.C. (1977). *The process of spermatogenesis in animals*: Cambridge University Press.

ROSS, C.A., MELDOLESI, J., MILNER, T.A., SATOH, T., SUPATTAPONE, S. & SNYDER, S.H. (1989). Inositol 1,4,5-trisphosphate receptor localized to endoplasmic reticulum in cerebellar Purkinje neurons. *Nature*, **339,** 468-70.

RUNFT, L.L., JAFFE, L.A. & MEHLMANN, L.M. (2002). Egg activation at fertilization: where it all begins. *Dev Biol*, **245,** 237-54.

RUSSA, A.D., MAESAWA, C. & SATOH, Y. (2009). Spontaneous [Ca2+]i oscillations in G1/S phase-synchronized cells. *J Electron Microsc (Tokyo)*, **58,** 321-9.

SAKURAI, A., ODA, S., KUWABARA, Y. & MIYAZAKI, S. (1999). Fertilization, embryonic development, and offspring from mouse eggs injected with round spermatids combined with Ca2+ oscillation-inducing sperm factor. *Mol Hum Reprod*, **5,** 132-8.

SALA NEWBY, G.B., KENDALL, J.M., JONES, H., TAYLOR, K.M., BADMINTON, M.N., LLEWELLYN, D.H. & CAMPBELL, A.K. (1999). *Bioluminescent and chemiluminescent indicators for molecular signalling and function in living cells. In: Fluorescent Probes for Biological Function*. London: Academic Press.

SANTELLA, L., KYOZUKA, K., GENAZZANI, A.A., DE RISO, L. & CARAFOLI, E. (2000). Nicotinic acid adenine dinucleotide phosphate-induced Ca(2+) release. Interactions among distinct Ca(2+) mobilizing mechanisms in starfish oocytes. *J Biol Chem*, **275,** 8301-6.

SANTELLA, L., LIM, D. & MOCCIA, F. (2004). Calcium and fertilization: the beginning of life. *Trends Biochem Sci*, **29,** 400-8.

SASAGAWA, I. & YANAGIMACHI, R. (1996). Comparison of methods for activating mouse oocytes for spermatid nucleus transfer. *Zygote*, **4,** 269-74.

SASAKI, T., SASAKI, J., SAKAI, T., TAKASUGA, S. & SUZUKI, A. (2007). The physiology of phosphoinositides. *Biol Pharm Bull*, **30,** 1599-604.

SATO, Y., MIYAZAKI, S., SHIKANO, T., MITSUHASHI, N., TAKEUCHI, H., MIKOSHIBA, K. & KUWABARA, Y. (1998). Adenophostin, a potent agonist of the inositol 1,4,5-trisphosphate receptor, is useful for fertilization of mouse oocytes injected with round spermatids leading to normal offspring. *Biol Reprod*, **58,** 867-73.

SAUNDERS, C.M., LARMAN, M.G., PARRINGTON, J., COX, L.J., ROYSE, J., BLAYNEY, L.M., SWANN, K. & LAI, F.A. (2002). PLC zeta: a sperm-specific trigger of Ca(2+) oscillations in eggs and embryo development. *Development*, **129,** 3533-44.

SCHUEL, H. (1985). *Biology of fertilization. The fertilization response of the egg.*: Academic Press.

SCHULTZ, R.M. & KOPF, G.S. (1995). Molecular basis of mammalian egg activation. *Curr Top Dev Biol*, **30,** 21-62.

SELINGER, Z., DOZA, Y.N. & MINKE, B. (1993). Mechanisms and genetics of photoreceptors desensitization in Drosophila flies. *Biochim Biophys Acta*, **1179,** 283-99.

SETTE, C., BEVILACQUA, A., BIANCHINI, A., MANGIA, F., GEREMIA, R. & ROSSI, P. (1997). Parthenogenetic activation of mouse eggs by microinjection of a truncated c-kit tyrosine kinase present in spermatozoa. *Development*, **124,** 2267-74.

SHARMA, G. & VIJAYARAGHAVAN, S. (2003). Modulation of presynaptic store calcium induces release of glutamate and postsynaptic firing. *Neuron*, **38,** 929-39.

SHEELEY, D.M., MERRILL, B.M. & TAYLOR, L.C. (1997). Characterization of monoclonal antibody glycosylation: comparison of expression systems and identification of terminal alpha-linked galactose. *Anal Biochem*, **247,** 102-10.

SHIBAO, K., HIRATA, K., ROBERT, M.E. & NATHANSON, M.H. (2003). Loss of inositol 1,4,5-trisphosphate receptors from bile duct epithelia is a common event in cholestasis. *Gastroenterology*, **125,** 1175-87.

SHIGEKAWA, K. & DOWER, W.J. (1988). Electroporation of eukaryotes and prokaryotes: a general approach to the introduction of macromolecules into cells. *Biotechniques*, **6,** 742-51.

SIMKUS, C.R. & STRICKER, C. (2002). The contribution of intracellular calcium stores to mEPSCs recorded in layer II neurones of rat barrel cortex. *J Physiol*, **545,** 521-35.

SMYTH, J.T., DEHAVEN, W.I., JONES, B.F., MERCER, J.C., TREBAK, M., VAZQUEZ, G. & PUTNEY, J.W., JR. (2006). Emerging perspectives in store-operated Ca2+ entry: roles of Orai, Stim and TRP. *Biochim Biophys Acta*, **1763,** 1147-60.

SONE, Y., ITO, M., SHIRAKAWA, H., SHIKANO, T., TAKEUCHI, H., KINOSHITA, K. & MIYAZAKI, S. (2005). Nuclear translocation of phospholipase C-zeta, an egg-activating factor, during early embryonic development. *Biochem Biophys Res Commun*, **330,** 690-4.

SONG, C., HU, C.D., MASAGO, M., KARIYAI, K., YAMAWAKI-KATAOKA, Y., SHIBATOHGE, M., WU, D., SATOH, T. & KATAOKA, T. (2001). Regulation of a novel human phospholipase C, PLCepsilon, through membrane targeting by Ras. *J Biol Chem*, **276,** 2752-7.

SPUNGIN, B., MARGALIT, I. & BREITBART, H. (1995). A 70 kDa protein is transferred from the outer acrosomal to the plasma membrane during capacitation. *FEBS Lett*, **357,** 98-102.

STAHELIN, R.V. & CHO, W. (2001). Roles of calcium ions in the membrane binding of C2 domains. *Biochem J*, **359,** 679-85.

STEINHARDT, R. (2006). Three stages (and a dividend) on my personal road to Ca2+ activation at fertilization. *Semin Cell Dev Biol*, **17,** 226-8.

STEINHARDT, R.A. & ALDERTON, J. (1988). Intracellular free calcium rise triggers nuclear envelope breakdown in the sea urchin embryo. *Nature*, **332,** 364-6.

STEINHARDT, R.A. & EPEL, D. (1974a). Activation of sea-urchin eggs by a calcium ionophore. *Proc Natl Acad Sci U S A*, **71,** 1915-9.

STEINHARDT, R.A., EPEL, D., CARROLL, E.J., JR. & YANAGIMACHI, R. (1974b). Is calcium ionophore a universal activator for unfertilised eggs? *Nature*, **252,** 41-3.

STEPHENS, L., WILLIAMS, R. & HAWKINS, P. (2005). Phosphoinositide 3-kinases as drug targets in cancer. *Curr Opin Pharmacol*, **5,** 357-65.

STRICKER, S.A. (1999). Comparative biology of calcium signaling during fertilization and egg activation in animals. *Dev Biol*, **211,** 157-76.

STRICKER, S.A. (1997). Intracellular injections of a soluble sperm factor trigger calcium oscillations and meiotic maturation in unfertilized oocytes of a marine worm. *Dev Biol*, **186,** 185-201.

SUAREZ, S.S. & HO, H.C. (2003). Hyperactivated motility in sperm. *Reprod Domest Anim*, **38,** 119-24.

SUDBRAK, R., BROWN, J., DOBSON-STONE, C., CARTER, S., RAMSER, J., WHITE, J., HEALY, E., DISSANAYAKE, M., LARREGUE, M., PERRUSSEL, M., LEHRACH, H., MUNRO, C.S., STRACHAN, T., BURGE, S., HOVNANIAN, A. & MONACO, A.P. (2000). Hailey-Hailey disease is caused by mutations in ATP2C1 encoding a novel Ca(2+) pump. *Hum Mol Genet*, **9,** 1131-40.

SUH, P.G., PARK, J.I., MANZOLI, L., COCCO, L., PEAK, J.C., KATAN, M., FUKAMI, K., KATAOKA, T., YUN, S. & RYU, S.H. (2008). Multiple roles of phosphoinositide-specific phospholipase C isozymes. *BMB Rep*, **41,** 415-34.

SUNTHARALINGAM, M. & WENTE, S.R. (2003). Peering through the pore: nuclear pore complex structure, assembly, and function. *Dev Cell*, **4,** 775-89.

SWANN, K. (1994). Ca2+ oscillations and sensitization of Ca2+ release in unfertilized mouse eggs injected with a sperm factor. *Cell Calcium*, **15,** 331-9.

SWANN, K. (1990). A cytosolic sperm factor stimulates repetitive calcium increases and mimics fertilization in hamster eggs. *Development*, **110,** 1295-302.

SWANN, K. (1996). Soluble sperm factors and Ca2+ release in eggs at fertilization. *Rev Reprod*, **1,** 33-9.

SWANN, K., CAMPBELL, K., YUANGSONG, Y., SAUNDERS, C.M. & LAI, F.A. (2007). *Use of luciferase chimera to monitor PLCzeta expression in mouse eggs. In: Microinjection, Methods and Applications*. New York: Humana Press.

SWANN, K., LARMAN, M.G., SAUNDERS, C.M. & LAI, F.A. (2004). The cytosolic sperm factor that triggers Ca2+ oscillations and egg activation in mammals is a novel phospholipase C: PLCzeta. *Reproduction*, **127,** 431-9.

SWANN, K. & OZIL, J.P. (1994). Dynamics of the calcium signal that triggers mammalian egg activation. *Int Rev Cytol*, **152,** 183-222.

SWANN, K., PARRINGTON, J. & JONES, K.T. (2001). Potential role of a sperm-derived phospholipase C in triggering the egg-activating Ca2+ signal at fertilization. *Reproduction*, **122,** 839-46.

TAKAHASHI, A., CAMACHO, P., LECHLEITER, J.D. & HERMAN, B. (1999). Measurement of intracellular calcium. *Physiol Rev*, **79,** 1089-125.

TALBOT, P. (1985). Sperm penetration through oocyte investments in mammals. *Am J Anat*, **174,** 331-46.

TANG, M.X., REDEMANN, C.T. & SZOKA, F.C., JR. (1996). In vitro gene delivery by degraded polyamidoamine dendrimers. *Bioconjug Chem*, **7,** 703-14.

TANG, T.S., DONG, J.B., HUANG, X.Y. & SUN, F.Z. (2000). Ca(2+) oscillations induced by a cytosolic sperm protein factor are mediated by a maternal machinery that functions only once in mammalian eggs. *Development*, **127,** 1141-50.

TANG, T.S., TU, H., CHAN, E.Y., MAXIMOV, A., WANG, Z., WELLINGTON, C.L., HAYDEN, M.R. & BEZPROZVANNY, I. (2003). Huntingtin and huntingtin-associated protein 1 influence neuronal calcium signaling mediated by inositol-(1,4,5) triphosphate receptor type 1. *Neuron*, **39,** 227-39.

TANIYAMA, Y., TACHIBANA, K., HIRAOKA, K., AOKI, M., YAMAMOTO, S., MATSUMOTO, K., NAKAMURA, T., OGIHARA, T., KANEDA, Y. & MORISHITA, R. (2002).

Development of safe and efficient novel nonviral gene transfer using ultrasound: enhancement of transfection efficiency of naked plasmid DNA in skeletal muscle. *Gene Ther*, **9,** 372-80.

TAYLOR, C.W., GENAZZANI, A.A. & MORRIS, S.A. (1999). Expression of inositol trisphosphate receptors. *Cell Calcium*, **26,** 237-51.

TESARIK, J., PILKA, L., DRAHORAD, J., CECHOVA, D. & VESELSKY, L. (1988). The role of cumulus cell-secreted proteins in the development of human sperm fertilizing ability: implication in IVF. *Hum Reprod*, **3,** 129-32.

TESARIK, J., SOUSA, M. & TESTART, J. (1994). Human oocyte activation after intracytoplasmic sperm injection. *Hum Reprod*, **9,** 511-8.

THOMAS, D., TOVEY, S.C., COLLINS, T.J., BOOTMAN, M.D., BERRIDGE, M.J. & LIPP, P. (2000). A comparison of fluorescent Ca2+ indicator properties and their use in measuring elementary and global Ca2+ signals. *Cell Calcium*, **28,** 213-23.

THROWER, E.C., HAGAR, R.E. & EHRLICH, B.E. (2001). Regulation of Ins(1,4,5)P3 receptor isoforms by endogenous modulators. *Trends Pharmacol Sci*, **22,** 580-6.

TOSTI, E., PALUMBO, A. & DALE, B. (1993). Inositol tri-phosphate inhuman and ascidian spermatozoa. *Mol Reprod Dev*, **35,** 52-6.

TOWNLEY, I.K., ROUX, M.M. & FOLTZ, K.R. (2006). Signal transduction at fertilization: the Ca2+ release pathway in echinoderms and other invertebrate deuterostomes. *Semin Cell Dev Biol*, **17,** 293-302.

TRAN, E.J. & WENTE, S.R. (2006). Dynamic nuclear pore complexes: life on the edge. *Cell*, **125,** 1041-53.

TSE, A., TSE, F.W., ALMERS, W. & HILLE, B. (1993). Rhythmic exocytosis stimulated by GnRH-induced calcium oscillations in rat gonadotropes. *Science*, **260,** 82-4.

TSIEN, R.Y. (1998). The green fluorescent protein. *Annu Rev Biochem*, **67,** 509-44.

TSIEN, R.Y. (1980). New calcium indicators and buffers with high selectivity against magnesium and protons: design, synthesis, and properties of prototype structures. *Biochemistry*, **19,** 2396-404.

TSIEN, R.Y. (1981). A non-disruptive technique for loading calcium buffers and indicators into cells. *Nature*, **290,** 527-8.

TSIEN, R.Y., POZZAN, T. & RINK, T.J. (1982). Calcium homeostasis in intact lymphocytes: cytoplasmic free calcium monitored with a new, intracellularly trapped fluorescent indicator. *J Cell Biol*, **94,** 325-34.

TURNER, P.R., SHEETZ, M.P. & JAFFE, L.A. (1984). Fertilization increases the polyphosphoinositide content of sea urchin eggs. *Nature*, **310,** 414-5.

UNGER, E.C., HERSH, E., VANNAN, M. & MCCREERY, T. (2001). Gene delivery using ultrasound contrast agents. *Echocardiography*, **18,** 355-61.

VAN BAELEN, K., DODE, L., VANOEVELEN, J., CALLEWAERT, G., DE SMEDT, H., MISSIAEN, L., PARYS, J.B., RAEYMAEKERS, L. & WUYTACK, F. (2004). The Ca2+/Mn2+ pumps in the Golgi apparatus. *Biochim Biophys Acta*, **1742,** 103-12.

VANHAESEBROECK, B., ALI, K., BILANCIO, A., GEERING, B. & FOUKAS, L.C. (2005). Signalling by PI3K isoforms: insights from gene-targeted mice. *Trends Biochem Sci*, **30,** 194-204.

VASSILEV, P.M., GUO, L., CHEN, X.Z., SEGAL, Y., PENG, J.B., BASORA, N., BABAKHANLOU, H., CRUGER, G., KANAZIRSKA, M., YE, C., BROWN, E.M., HEDIGER, M.A. & ZHOU, J. (2001). Polycystin-2 is a novel cation channel implicated in defective intracellular Ca(2+) homeostasis in polycystic kidney disease. *Biochem Biophys Res Commun*, **282,** 341-50.

VASUDEVAN, S.R., GALIONE, A. & CHURCHILL, G.C. (2008). Sperm express a Ca2+-regulated NAADP synthase. *Biochem J*, **411,** 63-70.

VERKHRATSKY, A. (2005). Physiology and pathophysiology of the calcium store in the endoplasmic reticulum of neurons. *Physiol Rev*, **85,** 201-79.

VERMASSEN, E., PARYS, J.B. & MAUGER, J.P. (2004). Subcellular distribution of the inositol 1,4,5-trisphosphate receptors: functional relevance and molecular determinants. *Biol Cell*, **96,** 3-17.

VISCONTI, P.E., GALANTINO-HOMER, H., NING, X., MOORE, G.D., VALENZUELA, J.P., JORGEZ, C.J., ALVAREZ, J.G. & KOPF, G.S. (1999). Cholesterol efflux-mediated signal transduction in mammalian sperm. beta-cyclodextrins initiate transmembrane signaling leading to an increase in protein tyrosine phosphorylation and capacitation. *J Biol Chem*, **274,** 3235-42.

VISCONTI, P.E. & KOPF, G.S. (1998). Regulation of protein phosphorylation during sperm capacitation. *Biol Reprod*, **59,** 1-6.

VISCONTI, P.E., MOORE, G.D., BAILEY, J.L., LECLERC, P., CONNORS, S.A., PAN, D., OLDS-CLARKE, P. & KOPF, G.S. (1995). Capacitation of mouse spermatozoa. II. Protein tyrosine phosphorylation and capacitation are regulated by a cAMP-dependent pathway. *Development*, **121,** 1139-50.

VON KUGELGEN, I. (2006). Pharmacological profiles of cloned mammalian P2Y-receptor subtypes. *Pharmacol Ther*, **110,** 415-32.

VON KUGELGEN, I. & WETTER, A. (2000). Molecular pharmacology of P2Y-receptors. *Naunyn Schmiedebergs Arch Pharmacol*, **362,** 310-23.

WAKAYAMA, T. & YANAGIMACHI, R. (1999). Cloning the laboratory mouse. *Semin Cell Dev Biol*, **10,** 253-8.

WANG, S.Q., SONG, L.S., LAKATTA, E.G. & CHENG, H. (2001). Ca2+ signalling between single L-type Ca2+ channels and ryanodine receptors in heart cells. *Nature*, **410,** 592-6.

WANG, T., PENTYALA, S., ELLIOTT, J.T., DOWAL, L., GUPTA, E., REBECCHI, M.J. & SCARLATA, S. (1999). Selective interaction of the C2 domains of phospholipase C-beta1 and -beta2 with activated Galphaq subunits: an alternative function for C2-signaling modules. *Proc Natl Acad Sci U S A*, **96,** 7843-6.

WANG, Y.J., WANG, J., SUN, H.Q., MARTINEZ, M., SUN, Y.X., MACIA, E., KIRCHHAUSEN, T., ALBANESI, J.P., ROTH, M.G. & YIN, H.L. (2003). Phosphatidylinositol 4 phosphate regulates targeting of clathrin adaptor AP-1 complexes to the Golgi. *Cell*, **114,** 299-310.

WARD, M., WU, J. & CHIU, J.F. (2000). Experimental study of the effects of Optison concentration on sonoporation in vitro. *Ultrasound Med Biol*, **26,** 1169-75.

WASSARMAN, P.M., JOSEFOWICZ, W.J. & LETOURNEAU, G.E. (1976). Meiotic maturation of mouse oocytes in vitro: inhibition of maturation at specific stages of nuclear progression. *J Cell Sci*, **22,** 531-45.

WASSARMAN, P.M., JOVINE, L. & LITSCHER, E.S. (2001). A profile of fertilization in mammals. *Nat Cell Biol*, **3,** E59-64.

WATT, S.A., KULAR, G., FLEMING, I.N., DOWNES, C.P. & LUCOCQ, J.M. (2002). Subcellular localization of phosphatidylinositol 4,5-bisphosphate using the pleckstrin homology domain of phospholipase C delta1. *Biochem J*, **363,** 657-66.

WERNER, R.G., NOE, W., KOPP, K. & SCHLUTER, M. (1998). Appropriate mammalian expression systems for biopharmaceuticals. *Arzneimittelforschung*, **48,** 870-80.

WESTPHAL, L.M., EL DANSASOURI, I., SHIMIZU, S., TADIR, Y. & BERNS, M.W. (1993). Exposure of human spermatozoa to the cumulus oophorus results in increased relative force as measured by a 760 nm laser optical trap. *Hum Reprod*, **8,** 1083-6.

WHITAKER, M., SWANN, K. & CROSSLEY, I. (1989). *What happens during the latent period at fertilisation? in Mechanisms of egg activation.* N.Y.: Plenum Press.

WILLIAMS, C.J. (2002). Signalling mechanisms of mammalian oocyte activation. *Hum Reprod Update*, **8,** 313-21.

WILLIAMS, R.L. (1999). Mammalian phosphoinositide-specific phospholipase C. *Biochim Biophys Acta*, **1441,** 255-67.

WILSON, T. & HASTINGS, J.W. (1998). Bioluminescence. *Annu Rev Cell Dev Biol*, **14,** 197-230.

WOJCIKIEWICZ, R.J. & NAHORSKI, S.R. (1991). Chronic muscarinic stimulation of SH-SY5Y neuroblastoma cells suppresses inositol 1,4,5-trisphosphate action. Parallel inhibition of inositol 1,4,5-trisphosphate-induced Ca2+ mobilization and inositol 1,4,5-trisphosphate binding. *J Biol Chem*, **266,** 22234-41.

WOJCIKIEWICZ, R.J., NAKADE, S., MIKOSHIBA, K. & NAHORSKI, S.R. (1992). Inositol 1,4,5-trisphosphate receptor immunoreactivity in SH-SY5Y human neuroblastoma cells is reduced by chronic muscarinic receptor activation. *J Neurochem*, **59,** 383-6.

WOLNY, Y.M., FISSORE, R.A., WU, H., REIS, M.M., COLOMBERO, L.T., ERGUN, B., ROSENWAKS, Z. & PALERMO, G.D. (1999). Human glucosamine-6-phosphate isomerase, a homologue of hamster oscillin, does not appear to be involved in Ca2+ release in mammalian oocytes. *Mol Reprod Dev*, **52,** 277-87.

WOLOSKER, H., KLINE, D., BIAN, Y., BLACKSHAW, S., CAMERON, A.M., FRALICH, T.J., SCHNAAR, R.L. & SNYDER, S.H. (1998). Molecularly cloned mammalian glucosamine-6-phosphate deaminase localizes to transporting epithelium and lacks oscillin activity. *Faseb J*, **12,** 91-9.

WONG, T.K. & NEUMANN, E. (1982). Electric field mediated gene transfer. *Biochem Biophys Res Commun*, **107,** 584-7.

WOOD, K.V. (1995). The chemical mechanism and evolutionary development of beetle bioluminescence. *Photochem. Photobiol.*, **62,** 662-673.

WU, H., HE, C.L. & FISSORE, R.A. (1997). Injection of a porcine sperm factor triggers calcium oscillations in mouse oocytes and bovine eggs. *Mol Reprod Dev*, **46,** 176-89.

WU, H., HE, C.L., JEHN, B., BLACK, S.J. & FISSORE, R.A. (1998). Partial characterization of the calcium-releasing activity of porcine sperm cytosolic extracts. *Dev Biol*, **203,** 369-81.

WU, M.M., BUCHANAN, J., LUIK, R.M. & LEWIS, R.S. (2006). Ca2+ store depletion causes STIM1 to accumulate in ER regions closely associated with the plasma membrane. *J Cell Biol*, **174,** 803-13.

WURMSER, A.E., GARY, J.D. & EMR, S.D. (1999). Phosphoinositide 3-kinases and their FYVE domain-containing effectors as regulators of vacuolar/lysosomal membrane trafficking pathways. *J Biol Chem*, **274,** 9129-32.

WUYTACK, F., RAEYMAEKERS, L. & MISSIAEN, L. (2003). PMR1/SPCA Ca2+ pumps and the role of the Golgi apparatus as a Ca2+ store. *Pflugers Arch*, **446,** 148-53.

YAMAGA, M., FUJII, M., KAMATA, H., HIRATA, H. & YAGISAWA, H. (1999). Phospholipase C-delta1 contains a functional nuclear export signal sequence. *J Biol Chem*, **274,** 28537-41.

YAMASAKI, M., MASGRAU, R., MORGAN, A.J., CHURCHILL, G.C., PATEL, S., ASHCROFT, S.J. & GALIONE, A. (2004). Organelle selection determines agonist-specific Ca2+ signals in pancreatic acinar and beta cells. *J Biol Chem*, **279,** 7234-40.

YANG, N.S., BURKHOLDER, J., ROBERTS, B., MARTINELL, B. & MCCABE, D. (1990). In vivo and in vitro gene transfer to mammalian somatic cells by particle bombardment. *Proc Natl Acad Sci U S A*, **87,** 9568-72.

YE, G.N., DANIELL, H. & SANFORD, J.C. (1990). Optimization of delivery of foreign DNA into higher-plant chloroplasts. *Plant Mol Biol*, **15,** 809-19.

YODA, A., ODA, S., SHIKANO, T., KOUCHI, Z., AWAJI, T., SHIRAKAWA, H., KINOSHITA, K. & MIYAZAKI, S. (2004). Ca2+ oscillation-inducing phospholipase C zeta expressed in mouse eggs is accumulated to the pronucleus during egg activation. *Dev Biol*, **268,** 245-57.

YOSHIDA, N., AMANAI, M., FUKUI, T., KAJIKAWA, E., BRAHMAJOSYULA, M., IWAHORI, A., NAKANO, Y., SHOJI, S., DIEBOLD, J., HESSEL, H., HUSS, R. & PERRY, A.C. (2007). Broad, ectopic expression of the sperm protein PLCZ1 induces parthenogenesis and ovarian tumours in mice. *Development*, **134,** 3941-52.

YU, Y., HALET, G., LAI, F.A. & SWANN, K. (2008a). Regulation of diacylglycerol production and protein kinase C stimulation during sperm- and PLCzeta-mediated mouse egg activation. *Biol Cell*, **100,** 633-43.

YU, Y., SAUNDERS, C.M., LAI, F.A. & SWANN, K. (2008b). Preimplantation development of mouse oocytes activated by different levels of human phospholipase C zeta. *Hum Reprod*, **23,** 365-73.

ZHANG, G., GURTU, V. & KAIN, S.R. (1996). An enhanced green fluorescent protein allows sensitive detection of gene transfer in mammalian cells. *Biochem Biophys Res Commun*, **227,** 707-11.

ZHANG, Y. & YU, L.C. (2008). Single-cell microinjection technology in cell biology. *Bioessays*, **30,** 606-10.

ZHU, C.C., FURUICHI, T., MIKOSHIBA, K. & WOJCIKIEWICZ, R.J. (1999). Inositol 1,4,5-trisphosphate receptor down-regulation is activated directly by inositol 1,4,5-trisphosphate binding. Studies with binding-defective mutant receptors. *J Biol Chem*, **274,** 3476-84.

ZUCKER, R.S., STEINHARDT, R.A. & WINKLER, M.M. (1978). Intracellular calcium release and the mechanisms of parthenogenetic activation of the sea urchin egg. *Dev Biol*, **65,** 285-95.